ISOLATION AND CHARACTERISATION OF POTENTIAL ANTICANCER COMPOUNDS FROM MEDICINAL PLANTS

THESIS

Submitted for the degree of

DOCTOR OF PHILOSOPHY

Kingston University

By

ABDUL WAHEED

School of Pharmacy and Chemistry
Kingston University London
UNITED KINGDOM

February 2011

Any maps, pages, tables, figures graphs,or photographs, missing from this digital copy, have been excluded at the request of the university.

DECLARATION

This thesis entitled "**Isolation and characterisation of potential anticancer compounds from medicinal plants**" is based upon work conducted by the author in the **School of Pharmacy and Chemistry at Kingston University London** between April 2007 and Feb 2011. All of the work described herein is original unless otherwise acknowledged in the text or by references. None of the work has been submitted for another degree in this or any other university.

Abdul Waheed

ABSTRACT

*The research work presented in this thesis deals with the anticancer activity of four medicinal plants: Caralluma tuberculata (Asclepiadaceae), Fagonia indica (Zygophyllaceae), Solanum surattense (Solanaceae) and Arisaema utile (Araceae) that originate from the North West and Himalayan regions of Pakistan. Through a bioactivity-guided fractionation approach, the crude and resultant organic fractions were tested on cultured breast cancer cells (MCF-7 and MDA MB-468) and colorectal carcinoma cells (Caco-2) in vitro. Five new compounds out of seven in total were isolated from potent fractions of the medicinal plants using repeated flash column chromatography. Structural elucidation was carried out through a series of spectroscopic experiments (1-D and 2-D NMR, GC-MS, LC-MS). Single crystal X-ray structure was determined using X-ray crystallography for the crystalline compounds, which showed a diffraction pattern. The apparent IC_{50} for compounds (**1–6**) were estimated from serial dilutions of eight concentrations (0.78–100 μM) of each compound, tested against breast and colon cancer cell lines, using two cell viability assays (MTT and neutral red uptake assays) for 24 h and 48 h treatments. Two new steroidal glycosides, acylated pregnane (**1**) and acylated androstane (**2**) glycosides, isolated from the ethyl acetate fraction of Caralluma tuberculata showed highly significant ($P<0.001$) percentage growth inhibition in Caco-2 cells (IC_{50} 1.56 – 6.25 μM) and MCF-7 cells (IC_{50} 6.25 – 25 μM), however, oestrogen independent cancer cells (MDA MB-468) were less responsive with IC_{50} 25 – 50 μM. These steroidal glycosides induced apoptosis in cancer cells as measures of cytotoxic activity (NRU, PARP cleavage, DNA ladder) on MCF-7, MDA MB-468 and Caco-2 cells were inhibited by pre-treatment with the pan-caspase inhibitor (Z-VAD-FMK). Another pregnane glycoside (**3**), isolated for the first time from Fagonia indica, was found to be more potent in suppressing cell growth (IC_{50} 6.25 – 25 μM), in oestrogen negative breast cancer cells (MDA MB-468,) as compared to oestrogen positive cancer cells (MCF-7). Although a cleaved PARP (89 kDa) was detected by Western blotting, cytomorphological alterations and in cells pre-treated with a pan-caspase inhibitor (NRU assay), indicated that the necrosis mode of cell death is more likely. Moreover, three esters: hexadecanoic acid ethyl ester (**4**), phthalic acid 1-(1, 1-dimethyl-pentyl) ester 2-(2-ethyl-dec-5-enyl) ester (**5**) from chloroform fraction of Solanum surattense, and 5-Oxo-19-propyl-docosanoic acid methyl ester (**6**) from Arisaema utile, showed a highly significant ($p<0.001$) decrease in cell numbers for MDA MB-468 and Caco-2 cells with apparent IC_{50} 6.25 – 12.5 μM in cell viability assays (MTT and NRU) after 48 h treatment, while MCF-7 cells were less responsive (IC_{50} 25 μM). Compounds **5** and **6** (first report from a natural source) did not restrict the growth inhibition in MCF-7 and Caco-2 cells, pre-treated with Z-VAD-FMK, which indicated less involvement of Caspase-dependent apoptosis, while DAPI staining and Western blots (cleaved-PARP) showed characteristics of apoptosis that suggested the possibility of the aponecrosis phenomenon of cell death. In preliminary screening (Western blot and DNA ladder assays), compounds (**1-6**) were not toxic to normal human cells (HUVEC and U937) and indicated some selectively between malignant and normal cells.*

Dedicated to my parents

Every journey begins with a single step
I took my first step holding your index finger
This journey is for you!

ACKNOWLEDGEMENTS

"In the Name of Allah, the Beneficent, the Merciful"
"All praise belongs to Allah, Lord of the universe"

First praise is to Allah, the Almighty, on whom ultimately we depend for sustenance and guidance. I would like to thank my Director of Studies Dr. James Barker and my co-supervisors Dr. Mark Carew and Dr. Stephen Barton for their constant encouragement and support, while I undertook this research. I appreciate all their contributions of time, ideas and directions to make my Ph.D. experience productive and stimulating at Kingston University. Dr. Barker has been particularly instrumental in the development of central ideas and plan of thesis. Much of the clarity of ideas, motivation and exposition is a result of the demands placed by Dr. Carew during the writing-up phase. The intellectual and technical expertise from Dr. Barton guided me through the set of issues that form the core of the thesis. The joy and perpetual energy from them was contagious and encouraging for me, even during tough times in the Ph.D. pursuit.

I also owe a particular debt to Prof. Sabbir Ahmed, with whom I started my research work at Kingston and who later advised me from University of West of Scotland as external supervisor. I am heartily thankful to him for his guidance and support from the initial to the final level, enabling me to develop an understanding of the subject. I am also thankful to Dr. Caroline Owen for her pharmaceutical advice in suggesting pathways to pursue my research objectives during early stages of the research work.

It was an honour for me to work with Dr. David Watkin and Dr. Amber Thompson, at Oxford University, UK, and I pay special thanks and appreciation for their hospitality and generosity for helping in single-crystal X-ray structure determination of isolated chemical compounds. I benefitted from their critical discussions and helpful suggestions of my work.

I would like to express my humble gratitude to my teachers in Pakistan Prof. Farid Khan, Vice Chancellor and Prof. Gul-Majid Khan, Dean Faculty of Pharmacy, Gomal University;

ACKNOWLEDGEMENTS

Prof. Qazi Najm-us-Saqib Department of Pharmaceutical Sciences, COMSAT, Abbottabad; Dr. Manzoor Hussain, Hazara University, for their continous support, motivation and help in medicinal plants selection and collection process.

In phytochemical investigations for structural elucidation of novel compounds, I remember those hard days of my research work, when every forward step was much shorter and much heavier than the previous one with ambiguities; at that moment Dr. Jean-Marie Peron always gave me essential assistance in reviewing NMR data. I owe my sincere appreciation to him and to Dr. Julian Swinden, Mr. Paul Stovell and Mr. Siamak S. KhanKahdani for untiring technical support on LC-MS, GC-MS and IR.

In my later work on cell culture, I acknowledge the help of Dr. Karen Ball and Mrs. Gillian Rice from School of Pharmacy and Biological Sciences, University of Portsmouth, UK for providing training on handling cancerous cells and setting up cytotoxicity assays. Many thanks also go to Dr. John Peacock and Dr. Andrew Snabaitis, who organised DNA fragmentation and Western blot assays, and I acknowledge their contributions, advice and suggestions on each step.

I gratefully acknowledge the funding sources that made my Ph.D work possible. I specially mention Brother Zakir Rajuwalla and Rashida Appe from Queen's Pharmacy, UK, for kind hospitality and financial support in my 1st year of study. I was honoured with Overseas Research Scholarship (ORS) from Higher Education Funding Council for England (HEFCE) for my 2nd and 3rd year, based on competitive research potential.

My time at Kingston was made enjoyable in large part due to the many friends and groups that became a part of my life. I wish to extend my warmest thanks to other past and present group members that I have had the pleasure to work with: Dr. Imran Shahid, Dr. Anshuman Ghosh, Ms. Ammara Abdullah, Ms. Blerina Ahmetaj, Mr. Naved

Deshmukh, Mr. Iltaf Shah and last, but not least, Mrs. Khatebah Mazloumi. I am grateful for the time spent with friends, for lovely and unforgettable jokes and memorable trips abroad.

My deepest gratitude goes to my family for their unflagging love and support throughout my life; this thesis was simple impossible without them. I am indebted to my deceased father Abdul Rashid (May Allah rest his soul in peace; Ameen), for his care and love. As a typical Asian father, he worked industriously to support the family and spared no effort in providing the best possible environment for us to adopt a disciplined life. He never complained in spite of all the hardships in his life. Although he is no longer with us, he is forever remembered. I am sure, God willing, he shares our joy and happiness in Heaven. I cannot ask for more from my mother, Ammi is simply perfect. I remember many sleepless nights with her accompanying me when I was suffering from fever. I remember her constant support when I encountered difficulties and I remember, most of all her delicious dishes. Ammi, I love you. I feel proud of my brother Khurram and my whole family, specially my youngest sister Nadia for her talent and courage to stand firm in hard times of life.

Lastly, I owe my loving thanks to my wife Farzana and my son Mouiez. They have lost a lot due to my research abroad. Her encouragement, understanding, faithful support from the start until the final stages of my Ph.D. and especially her unconditional love is so appreciated. I now anxiously wait to see them. Thank you.

TABLE OF CONTENTS

TABLE OF CONTENTS

LIST OF ABBREVIATIONS

ACT:	Actinomycin-D
ADMET:	Absorption, distribution, metabolism, excretion and toxicity
ADP:	Adnosine di-phosphate
ANS:	Anastrozole
ATCC:	American type culture collection
ATP:	Adenosone tri-phosphate
AU:	*Arisaema utile*
Caco-2:	Colon adenocarcinoma cancer cells
Cdk:	Cyclin-dependent kinases
CE:	Collision energy
CT:	*Caralluma tuberculata*
DAPI:	4',6-diamidino-2-phenylindole
DEPT:	Distortion enhancement by polarisation transfer
DMEM:	Dulbecco's modified eagle medium
DMSO:	Dimethylsulfoxide
DQF-COSY:	Double quantum filtered ^{1}H-^{1}H correlation spectroscopy
ECCC:	European collection of cell cultures
ECL:	Enhanced chemiluminescence
EGM:	Endothelial cell growth medium
EI:	Electron impact
ESI:	Electrospray ionisation
EtOAc:	Ethyl acetate
FBS:	Fetal bovine serum
FI:	*Fagonia indica*
FT-IR:	Fourier transform infra-red
GC-MS:	Gas chromatography mass spectrometery
HETCOR:	Heteronuclear correlation

HMBC: Heteronuclear multiple bond coherence

HUVEC: Human umbilical vein endothelial cells

ICE: Interleukin-1β converting enzyme

IR: Infra-Red

LC-MS: Liquid chromatography-mass spectrometery

MCDB: Medium for cultivation of human microvascular endothelial cells

MCF-7: Oestrogen positive breast cancer cells

MDA MB-468: Oestrogen negative breast cancer cells

MeOH: Methanol

MTT: (3-(4,5-Dimethylthiazole-2-yl)-2,5-diphenyltetrazolium bromide

NADH: Nicotinamide adenine dinucleotide-reduced

NADPH: Nicotinamide adenine dinucleotide phosphate-reduced

NMR: Nuclear magnetic resonance

NR: Neutral Red

NRU: Neutral red uptake assay

PARP: Poly-ADP ribose polymerase

PBS: Phosphate buffered saline

PVDF: Poly vinylidene difluoride

ROS: Reactive oxygen species

SDS: Sodium dodecyl sulphate

SS: *Solanum surattense*

TAM: Tamoxifen

TEMED: Tetramethylethylenediamine

TLC: Thin layer chromatography

TMS: Tetramethylsilane

TOF: Time of flight

T-TBS: Tris-buffered saline-Tween 20

U937: Human lymphatic monocytes

LIST OF FIGURES

LIST OF FIGURES

LIST OF FIGURES

LIST OF TABLES

1. INTRODUCTION

1.1. Medicinal plants in anticancer drug discovery

Humans have used plants in a multitude of ways in a tradition spanning human evolution. Since early Neanderthal man, plants have been used for healing purposes. Not all of nature's secrets come from dark and sultry rain forests. Rustic lore often hides for years the treasures that nature has secreted in the roots, stem, bark, flowers and seeds of plants, some of them are now world-wide remedies (Buchman *et al.,* 1980).

Plants have been the basis of sophisticated medical systems for many hundreds of years. Knowledge of medicinal plants has its origin in the 4th and 5th centuries B.C. under the patronage of Hippocrates in Greece (Cragg *et al.*, 1997). As the science progressed, the crude dried powdered plants were replaced by their extracts, glanicals, tinctures, poultices and other herbal formulations. The World Health Organization has estimated that 80% of the earth's inhabitants rely on traditional medicines for primary healthcare, and plant products are highly important in the remaining 20% of the population (Farnsworth *et al.,* 1985). For example, in China, traditional medicine is largely based on around 5,000 plants, which are used for treating 40% of urban patients and 90% cent of rural patients (Farnsworth *et al.*, 1997).

Medicinal plants have a long history of use in the treatment of cancer. Hartwell (1982), in his review of "plants used against cancer", lists more than 3000 plant species that have reportedly been used in the treatment of cancer. In many instances, however, the "cancer" is undefined, or reference is made to conditions such as "hard swellings", abscesses, calluses, corns, warts, polyps, or tumours, to name but a few. These symptoms would generally apply to skin, "tangible", or visible conditions, and may indeed sometimes correspond to a cancerous

condition. Some of the claims for efficacy in the treatment of cancer, however, should be viewed with some scepticism because cancer, as a specific disease entity, is likely to be poorly defined in terms of folklore and traditional medicine. This is in contrast to other plant-based therapies used in traditional medicine for the treatment of afflictions such as malaria and pain, which are more easily defined, and where the diseases are often prevalent in the regions where traditional medicine systems are extensively used. However, despite these observations, it is significant that over 60% of currently used anti-cancer agents are derived in one way or another from 25,000 vegetal species and 600 are for oncological use having played, and continue to play, a dominant role in the discovery of leads for the development of conventional drugs (Cragg *et al.*, 1997).

Despite major scientific and technological progress in combinatorial chemistry, anticancer agents derived from medicinal plants still make an enormous contribution to drug discovery. These bioactive products provide a starting point for new synthetic compounds, with diverse structures and often with multiple stereocenters that can be challenging synthetically (Clardy and Walsh, 2004; Nicolaou and Snyder, 2004; Peterson and Overman, 2004; Koehn and Carter, 2005). Many structural features common to natural products (e.g. chiral centers, aromatic rings, complex ring systems, degree of molecule saturation, and number and ratio of heteroatoms) have been shown to be highly relevant to drug discovery efforts (Lee *et al.*, 2001; Feher *et al.*, 2003; Clardy *et al.*, 2004; Koehn *et al.*, 2005).

One of the most significant examples is the vinca alkaloids family (Figure 1.1), isolated from the periwinkle *Catharanthus roseus*, which is found in the rain forests of Madagascar (Noble *et al.*, 1990) and has been used clinically for over 40 years (Van Der Heijden *et al.*, 2004). The introduction of the vinca alkaloid; Vincristine was responsible for an increase in the cure rates for Hodgkin's disease and some forms of leukaemia, whilst Vinblastine is also used in

advanced testicular cancer, breast and lung cancers (Okouneva *et al.*, 2003). These drugs were first discovered during an investigation of the plant as a source of potential oral hypoglycemic agents. While research investigators could not confirm this activity, it was noted that extracts reduced white blood cell counts and caused bone marrow depression in rats, and subsequently, it was found that the treatment of mice bearing a transplantable lymphocytic leukemia caused significant life extension.

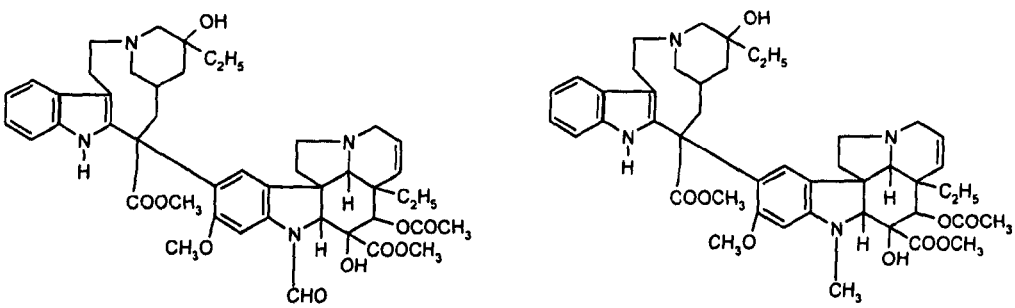

Vincristine Vinblastine

Figure 1.1: Structures of vinca alkaloids from Catharanthus roseus.

This led to the isolation of Vincristine and Vinblastine as the active agents, so their discovery may be indirectly attributed to the observation of an unrelated medicinal use of the source plant (Johnson *et al.*, 1963). The vinca alkaloids and several of their semi-synthetic analogues (Vinorelbine and Vindesine) block mitosis with metaphase arrest by binding specifically to tubulin, resulting in its depolymerisation (Okouneva *et al.*, 2003; Pezzuto, 1997).

Another example of a highly active agent derived from a natural product is etoposide, which has produced high cure rates in testicular cancer when used in combination with bleomycin (also derived from a natural product) and cisplatin (Williams *et al.*, 1987). Etoposide (Figure 1.2) is a epipodophyllotoxin, derived from the mandrake plant *Podophyllum peltatum* and the wild chervil *Podophyllum emodi*. It has also significant activity against small-cell lung carcinoma (Chabner *et al.*, 1991; Harvey *et al.*, 1999). Etoposide is a topoisomerase II inhibitor,

stabilizing enzyme–DNA cleavable complexes leading to DNA breaks (Liu, 1989).

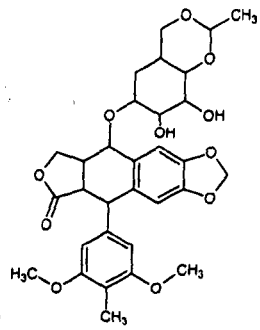

Figure 1.2: Structure of Etoposide

The taxanes paclitaxel originally isolated from the bark of the yew tree *Taxus brevifolia* (Wani *et al.*, 1971), a finite source of the compound. It took some years to develop a semi-synthetic analog (docetaxel) which is derived from a renewable source, the leaves of *Taxus baccata* (Cortes, 1995). Currently, total synthesis has been achieved for both agents and drug supply is no longer a problem.

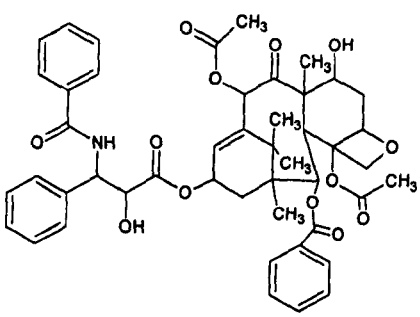

Paclitaxel

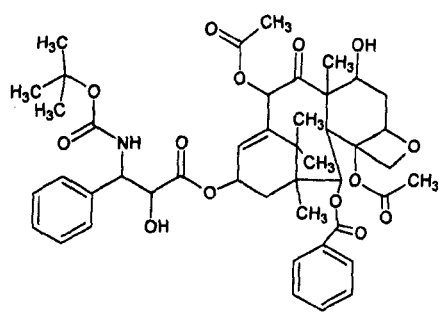

Docetaxel

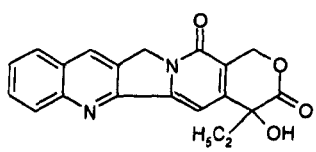

Camptothecin

Figure 1.3: Structures of taxanes and camptothecins.

The taxanes paclitaxel and docetaxel (Figure 1.3) have shown impressive anti-tumour activity against breast, ovarian and other tumour types in the clinic. Paclitaxel stabilises microtubules, leading to mitotic arrest (Andriana *et al.*, 2001; Wani *et al.*, 1971). In addition, the camptothecin (Figure: 3) derivatives irinotecan and topotecan, have shown significant anti-tumour activity against colorectal and ovarian cancer respectively (Bertino, 1997). These compounds were initially obtained from the bark and wood of *Nyssacea Camptotheca accuminata* and act by inhibiting topoisomerase I, which is responsible for changing the degree of supercoiling of DNA by causing single strand breaks and re-ligation. The taxanes and the camptothecins' derivatives have been approved for human use against lung and ovarian cancers in a number of countries (Liu *et al.*, 2000).

Flavopiridol is one of the most exciting plant-based anticancer agents currently in development, representing the first cyclindependent kinase inhibitor to enter the clinic (Kelland, 2000). Flavopiridol is a synthetic flavone derived from the plant alkaloid Rohitukine, which was isolated from the leaves and stems of *Amoora rohituka* and later from *Dysoxylum binectariferum* (Maliaceae) (Cragg *et al.*, 1988, Harmon *et al.*, 1979, Losiewicz *et al.*, 1994, Worland et al. 1993). The mechanism of action of flavopiridol involves interfering with the phosphorylation of cyclin-dependent kinases, hampering their activation and blocking cell-cycle progression at growth phase 1 (G1) or G2 (Worland *et al.*, 1993). In phase I clinical trials with flavopiridol (Senderowicz *et al.*, 1998, Wright *et al.*, 1988), secretory diarrhoea was found to be the dose-limiting toxicity, and encouraging response rates were noted in a variety of solid and hematological malignancies. Currently, flavopiridol is in phase II trials in patients with colorectal, prostate, renal cell and non-small-cell lung carcinoma, as well non-Hodgkin's lymphoma and chronic lymphocytic leukaemia (Kaur *et al.*, 1992).

Overall, the integration of ethnobotanical, pharmacological and phytochemical studies allowed the development of a new approach to the study and the pharmaceutical use of medicinal plants as anticancer medicines, resulting in

herbal remedies being transformed into chemically defined structures. In conclusion, anticancer agents discovered from medicinal plants (and derivates thereof) have provided numerous clinically used medicines. Even with all the challenges facing drug discovery from medicinal plants, natural products isolated from medicinal plants can be predicted to remain an essential component in the search for new anticancer medicines.

1.2. Asclepiadaceae (ethnobotanical aspects)

Asclepiadaceae is a group of perennial herbs and shrubs comprising a significant number of leafless plants with succulent stems. The name "Asclepiadaceae" is derived from the order Apocynales, and was given in honour of Esculapius, or Asklepios whose priests or fabled descendants were known as the Asklepiads or priest-physicians and who served the god of medicine in the ancient sanctuaries at Epidauros, Sikyon, Cos, Achaia and elsewhere (Sundell, 1994).

The Angiosperm Phylogeny Group (APG II), has classified "Asclepiadaceae" as subfamily Asclepiadoideae under the family Apocynaceae (Endress and Bruyns, 2000). According to Hutchison's system of classification (1963), the family Asclepiadaceae contains 175-180 genera and about 2200 species; distributed mainly in the tropical & sub- tropical regions of the world, especially in Africa and South America, represented in Pakistan by 23 genera and 41 species (Ali *et al.*, 1983).

Plants belonging to the family Asclepiadaceae are reported to be a copious source of C_{21} steroidal glycosides: pregnane glycosides from *Boucerosia aucheriana, Caralluma tuberculata, Caralluma russeliana*, *Caralluma dalzielii* and *Hemidesmus indicus* (Abdel-Sattar *et al.*, 2008; Deepak *et al.*, 1997; Qiu *et al.*, 1999); alkaloids: steroidal alkaloids from *Cryptolepis obtusa*, *Tyophora* alkaloids

from various species as anti-tumour agents (Paulo *et al.*, 2000; Rahman *et al.*, 2008); saponins: *Asclepias fruticosa* saponin, 16α- hydroxy-5,6-dehydroasclepin; Cardiac glycosides: cardenolides (cymarin, strophanthidin and strophanthidin glycoside) from the roots of *Parquetina nigrescens* possessing cytotoxic activity (Marks *et al.*, 1975). Similarly Ye *et al.*, 2005 reported seven new C_{21} steroidal glycoside from the roots of *Stephanotis mucronata* (Asclepiadaceae), in which four glycosides namely stemucronatosides A, B, C and F showed immunomodulatory activity, but three glycosides stemucronatosides D, E, G demonstrated immunosuppressive effects.

Asclepiadaceae plants have a wide range of chemical compositions, and a variety of pharmacological effects. Therefore, further in-depth systematic studies into their chemical and pharmacological aspects are essential for a greater scientific and rational development and utilisation of this species.

1.2.1. *Caralluma tuberculata*

Caralluma tuberculata (family: Asclepiadaceae) is a perennial, succulent, fleshy herb of about 15-45 cm height with an erect stem (Figure 1.4). It is almost leafless, but in some cases, in the angle of the stem, spine like leaves are present (Ali *et al.*, 1983).

The genus *Caralluma* contains about 120 species, widely distributed in Mediterranean region, Africa, Spain, Saudi Arabia, Middle East, Pakistan and India (Copra *et al.*, 1956; Ahmad and Shaikh, 1989). In Pakistan, *Caralluma* is represented by two species namely *Caralluma edulis* and *Caralluma tuberculata* (Ali *et al.*, 1983). *Caralluma tuberculata* largely grows wildly and is cultivated as a vegetable in some areas of Pakistan and India from August to September (Copra *et al.*, 1956). *Caralluma* is the synonym of *Boucerosia*, but differs from *Boucerosia* by its habit to possess inflorescences (Stewart, 1972).

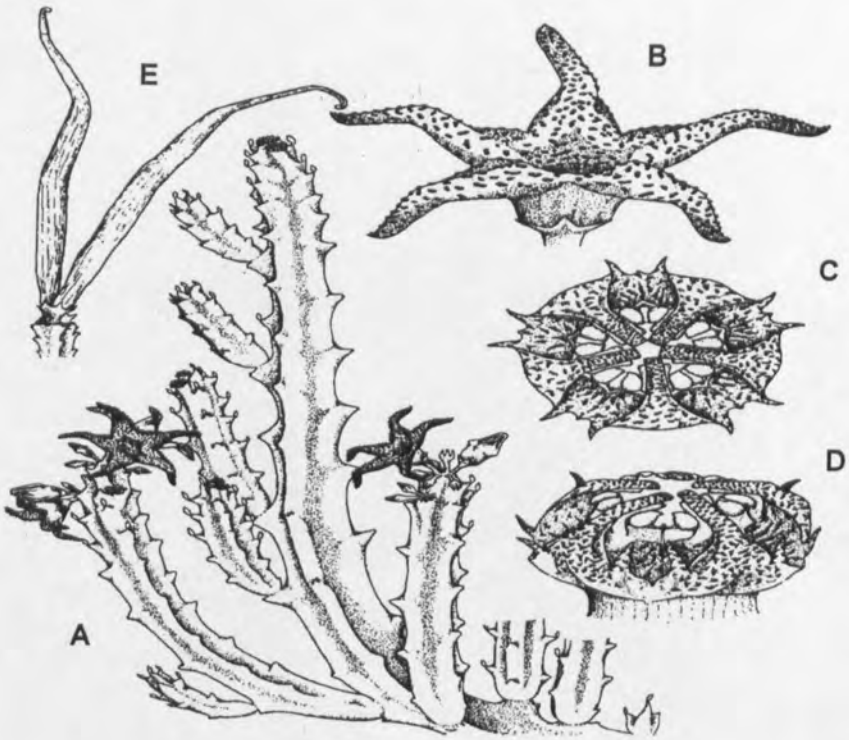

Figure 1.4: Identification features of Caralluma tuberculata [where A: aerial part of plant with flowers; B: flowers; C: crona and gynostegium (top view); D: crona and gynostegium (lateral view); E: fruiting twig].

1.2.2 *Caralluma tuberculata* in folk medicine

Caralluma tuberculata is also known with a vernacular name "*Chung*" in Punjab, Pakistan. This plant is eaten raw or cooked as vegetable (Ali *et al.*, 1983) and is reputed in folkloric medicine for the curing of diabetes, rheumatism, leprosy and in blood disorders (Burkill, 1909; Hoope, 1975). Some reports also indicate the use of this plant as an antipyretic alternative and anthelmintic (Chopra *et al.*, 1956). *Caralluma tuberculata* is also described as a stomachic, carminative and tonic (Kirtikar *et al.*, 1987).

The juice of the stem is bitter in taste and has been shown to possess hypotensive effects. Previous studies show its use in Arabian folk medicine as an antidote for snake and scorpion bites (Al-Yahya *et al.*, 1978). Although there is limited evidence supporting the diverse activities claimed in the folklore, some reports suggested *Caralluma tuberculata* to possess significant antidiabetic, anti-inflammatory and cytotoxic activities (Ahmed *et al.*, 1993; Al-Bekairi *et al.*, 1992).

As previously mentioned, the Asclepiadaceae family is reported to be rich in pregnane glycosides. Deepak *et al.*, 1989 suggested that generally members of Asclepiadaceae produce an abundance of esterified polyoxypregnane glycosides and can therefore be a promising source of antitumour agents. In recent years, pregnane steroids from the genus *Caralluma* has been reported in the isolation of several pregnane glycosides or their esters (Tanaka *et al.*, 1990; Lin *et al.*, 1994; Qui *et al.*, 1999; Abdel-Sattar *et al.*, 2008) with anti-tumour activity. This will be discussed in the next section.

1.2.3 Phytochemical analysis on *Caralluma tuberculata*

A chemical literature review revealed that, in the last twenty years, the genus *Caralluma* has received much attention in the search for novel steroidal anticancer compounds, mainly the abundance of pregnane glycosides in members of the Asclepiadaceae family.

Pregnanes are C_{21} steroidal compounds found in nature either in the free state or as glycosides (Reichstein, 1967). In pregnane glycosides, the sugar moiety is linked to an alcoholic hydroxyl group of the pregnane aglycon, most frequently at C-3 (Hemidescine, Emidine; Chandra *et al.*, 1994), C-20 (Cellobiosides; Palter *et al.*, 1972) or both (bisdesmosidic glycosides: Lasianthoside; Qiu *et al.*, 1999), through an acetyl linkage. However, in some cases, the sugar moiety is linked to hydroxyl functions at C-2 (Toosendanoside; Nakanishi *et al.*, 1988), C-4

(Verruccoside; Kashman *et al.*, 1991) or C-21 (Biondianoside E; Tan *et al.*, 2003). Pregnane glycosides containing one to six sugar units have been isolated from the extracts of different plants parts, i.e. roots, stems, seeds etc (Deepak *et al.*, 1989).

A literature review showed that no phytochemical work had been reported prior to 1967, when Nikaido *et al.*, (1967) reported that the dried whole plant of *Boucerosia aucheriana* (Synonym: *Caralluma tuberculata*) resulted in a mixture of glycosides, Boucerin and Dihydroboucerin. The difference between both compounds lies only in one double bond and after mild hydrolysis, cymarose, sarmentose, oleandrose, and digitoxose were analysed as the sugar components (Figure 1.5).

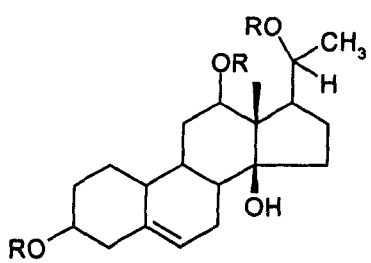

Boucerin

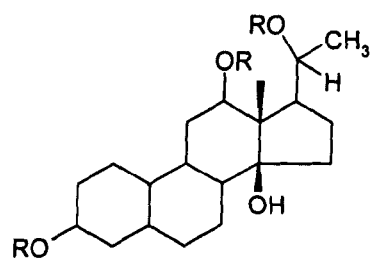

Dihydroboucerin

Figure 1.5: Structures of glycosides from Boucerosia aucheriana [Where: Boucerin R=H, Dihydroboucerin R=H, 5α-H]

In a chemical investigation of medicinal herbs, Khan and co-workers reported the presence of β-sitosterol and lupeol (Figure 1.6) in the ethyl acetate fraction of *Caralluma tuberculata* (Khan *et al.*, 1987).

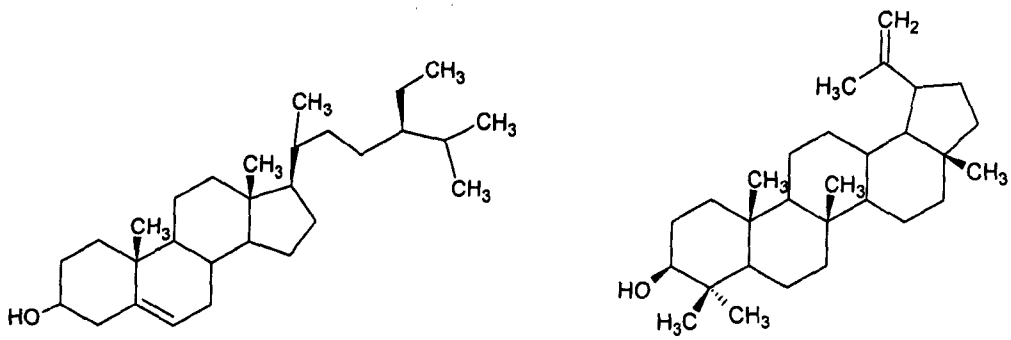

B-sitosterol Lupeol

Figure 1.6: Structures of steroids from Caralluma tuberculata

A year later, Ahmad *et al.*, (1988) isolated two new pregnane glycosides Caratuberoside A and Caratuberoside B as white crystalline compounds from *Caralluma tuberculata* (Figure 1.7). This was the first report of the isolation of pregnane glycoside from *Caralluma tuberculata*, and in 1992, two more Caratuberosides C and D (Figure 1.7) were isolated. Their structures were determined mainly on the basis of NMR spectroscopic data (Rizwani *et al.*, 1992).

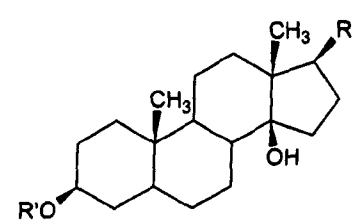

Caratuberoside A
R=CH_3-C=O
R'=3-O-methyl fucose (4←1)-β-D-glucose
Caratuberoside B
R=CH_3-CH-OH
R'=3-O-methyl fucose (4←1)-β-D-glucose
Caratuberoside C
R=CH_3-CH-OH
R'=3-O-methyl fucose (4←1)-β-D-glucose (4←1)-β-D-glucose
Caratuberoside C acetate
R=CH_3-CH-OAc
R'=3-O-methyl fucose (4←1)-β-D-glucose (4←1)-β-D-glucose acetate
Caratuberoside D
R=CH_3-CH-OH
R'=3-O-methyl fucose (4←1)-β-D-glucose (6←1)-β-D-glucose
Caratuberoside D acetate
R=CH_3-CH-OAc
R'=3-O-methyl fucose (4←1)-β-D-glucose (6←1)-β-D-glucose acetate

Figure 1.7: Caratuberosides from Caralluma tuberculata

In 1993 Rizwani *et al.*, reported the isolation of a Caratuberoside A2 (Figure 1.8), showing a sugar (3-O-methyl fucose (4←1)-β-D-glucose) linkage at C-14 which is a rare site of substitution.

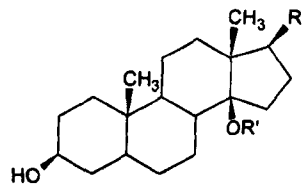

Figure 1.8: Caratuberoside A2 from Caralluma tuberculata
R=CH_3-C=O
R'=3-O-methyl fucose (4←1)-β-D-glucose

Besides pregnane glycosides, *Caralluma tuberculata* also possesses flavonoids. Rizwani *et al.*, in 1990, reported for the first time, three flavone glycosides from the fresh vegetative part of the plant. The structures of these flavons (Figure 1.9) were characterised as:

Luteolin-4'-O-β-D-glucopyranosyl-(2→1)-α-L-rahmnopyranoside **(1)**

Kaemferol-7-O-β-D-glycopyranosyl-(2→1)-α-L-rahmnopyranoside **(2)**

Kaemferol-7-O-β-D-glycopyranosyl-(6→1)-α-L-rahmnopyranoside **(3)**

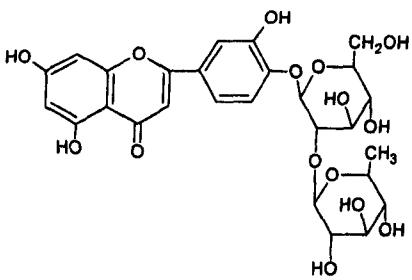

(1)

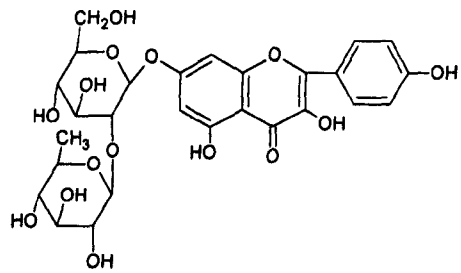

(2)

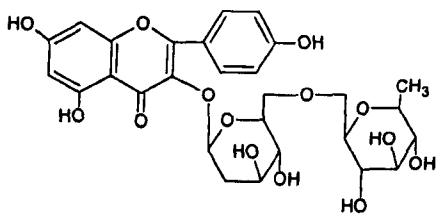

(3)

Figure 1.9: Flavone glycosides from Caralluma tuberculta

The anti-inflammatory activity of many plants has been attributed to their sterol and flavonoid contents. In folk medicine, *Caralluma tuberculata* has been used in the treatment of rheumatism and other inflammatory conditions. This ethnobotanical use is justified from a study in 1993, when Ahmad *et al.* reported that an ethanolic extract of *Caralluma tuberculata* possessed significant anti-inflammatory and analgesic activities in male Wistar rats and male SWR mice (Ahmed *et al.,* 1993). In another study, *Caralluma tuberculata* offered dose-dependent protection against the ulceration caused by ethanol, sodium hydroxide and sodium chloride (Al-Harbi *et al.*, 1994) in male Wistar, albino rats. It was suggested that the cytoprotective and antioxidative effects of *Caralluma tuberculata* can be attributed to the presence of flavonoids and saponins (Rizwani *et al.,* 1990).

Pregnane glycosides can be bisdesmosidic. It is rarely reported that C_{21} steroidal glycosides contain sugar (s) at both C-3 and C-20 positions. A literature review indicated that no bisdesmosidic pregnane glycoside has been isolated so far from the *Caralluma tuberculata* specie. However, Qiu *et al.* have isolated acylated C_{21} sterodial bisdesmosidic glycosides (Figure 1.10) from *Caralluma umbellata* with acyl groups bound to the sugars, rather than the steroidal parent skeletons, usually to the C-11, C-12 and C-20 hydroxyl groups. This may be of some significance for the biosynthesis of pregnane steroidal glycosides and also the chemotaxonomy of the title plant (Qiu *et al.*, 1997).

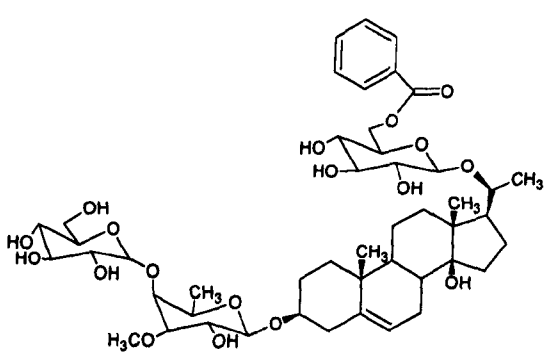

Figure 1.10: Acylated C_{21} steroidal bisdesmosidic glycosides from Caralluma umbellata

Recently, in 2008, in a biologically-guided fractionation approach, the methanolic extract of *Caralluma tuberculata* as well as, petroleum ether, chloroform and n-butanol fractions were tested for their antiprotozoal activity against malaria and cytotoxic activity against a human diploid embryonic cell line (MRC5) using MTT assay. It was reported (for the antimalarial activity), only the petroleum ether soluble fraction demonstrated moderate inhibitory effects (IC_{50} 7.94 µg/ml) and this fraction showed high cytotoxicity on MRC5 (IC_{50} 0.8 µg/ml). As for the antitrypanosomal activity, the methanolic extract was inactive, while the petroleum ether soluble fraction showed potent cytotoxic activity (IC_{50} 0.5 µg/ml). On the other hand, the chloroform soluble fraction was moderately active (IC_{50} 3.5 µg/ml). Five new acylated pregnane glycosides (Figure 1.11) were isolated from chloroform soluble fraction of *Caralluma tuberculata*. These acylated pregnanes **(1-5)** were isolated for the first time from nature and their structures were elucidated by the analysis of data from NMR and FAB-MS. These compounds showed *in vitro* weak antimalarial and cytotoxic activities (Abdel-Sattar *et al.*, 2008).

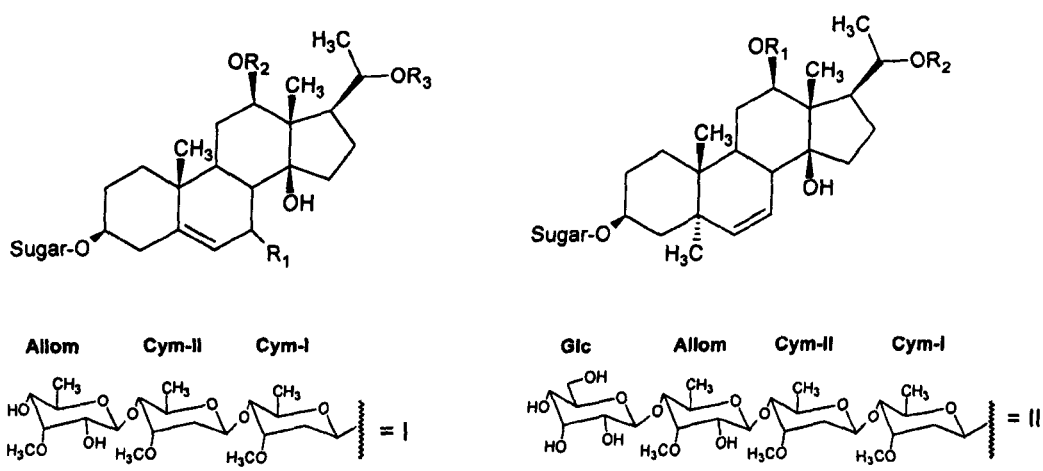

1: Sugar=I, R_1=H, R_2=Benzoyl, R_3= Acetyl

2: Sugar=I, R_1=-OH, R_2=Benzoyl, R_3= Acetyl

3: Sugar=I, R_1=Benzoyl, R_2= Acetyl

4 Sugar=II, R_1=Benzoyl, R_3= Acetyl

5: Sugar=II, R_1=H, R_2= R_3=Benzoyl

Figure 1.11: Acylated pregnane glycoside from Caralluma tuberculata

Overall, from the reported data so far, it can be summarised that Pregnane glycosides in *Caralluma tuberculata* may be totally or partially responsible for diverse biological activities as demonstrated in traditional folk medicine. Thus, there is an urgent need to evaluate these activities *in vitro* and particularly the mechanism by which the active constituents of *Caralluma tuberculata* may exhibit anticancer activity in different cell lines.

1.3. Zygophyllaceae (ethnobotanical aspects)

Zygophyllaceae is a family of annual or perennial herbs, consisting of about 25 genera and 240 species (Mabberley, 1987). Plants are distributed in tropical, subtropical and warm, temperate climates, often in the hyper-arid and arid zones. Zygophyllaceae are also known as the bean-caper or caltrop family of flowering plants having pinnate leaves and capsules as fruits. In Pakistan, it is represented by 8 genera and 22 species (Ghafoor, 1974). The main genera of the family are *Fagonia, Zygophyllum, Gauiacum* and *Tribulusversity.*

The genus *Fagonia* contains about 45 species and is confined to warm and arid areas in deserts from S.W. Asia to the Indo-Pakistan sub-continent, Mediterranean region, western Asia including Lebanon, Turkey, and the Arabian Peninsula east to Afghanistan, Africa, Chile, Mexico, and S. W. United States (Chopra *et al.,* 1956; Saeed, 1969). The plants included are mostly shrubs with free spinescent or pointed stipules, pink or purple petals, and an obconical, more or less pubescent capsule, often with persisting sepals. Most species of *Fagonia* have three-foliolate leaves, but there are also several species that are one-foliolate. The free stipules and the pubescent, obconical capsules are particularly important in the circumscription of *Fagonia* (Ghafoor, 1974).

In an ethnobotanical context, aqueous decoctions of the plants included in Zygophyllaceae are popular in indigenous systems of medicine for their ability to

treat early-stage cancers; especially from the genus *Fagonia* and for the treatment of various digestive and blood vascular system disorders (Saeed, 1969). The aerial parts, including flowers of various *Fagonia* species were investigated mainly for glycosides linked to aglycon moieties such as flavonoids, terpenoids, triterpenoids or steroidal saponins (Atta *et al.,* 1982; Ansari *et al.,* 1987; El-Hadidi *et al.,* 1988).

1.3.1. *Fagonia indica*

Fagonia indica is a small annual to perennial, densely glandular, spiny, well-branched shrub, (Figure 1.12), which grows up to 60 cm. Its stem has a woody base, which may be erect or prostate. Leaves are small, petiolate, three lobed and up to 8-15 mm long. The flowers are small, about 12 mm in diameter and are pinkish-purple in colour. The fruit grows as a capsule 3-5 mm long, 2-5 mm wide with flat, rounded seeds that are brown in colour. It grows in deserts and dry areas throughout India, Afghanistan, Iran, Aden, Eritrea, Ethiopia, Sudan, United Arab Emirates, Somalia, Kenya, America and Pakistan (Ghafoor *et al.,* 1974; Hooker, 1975).

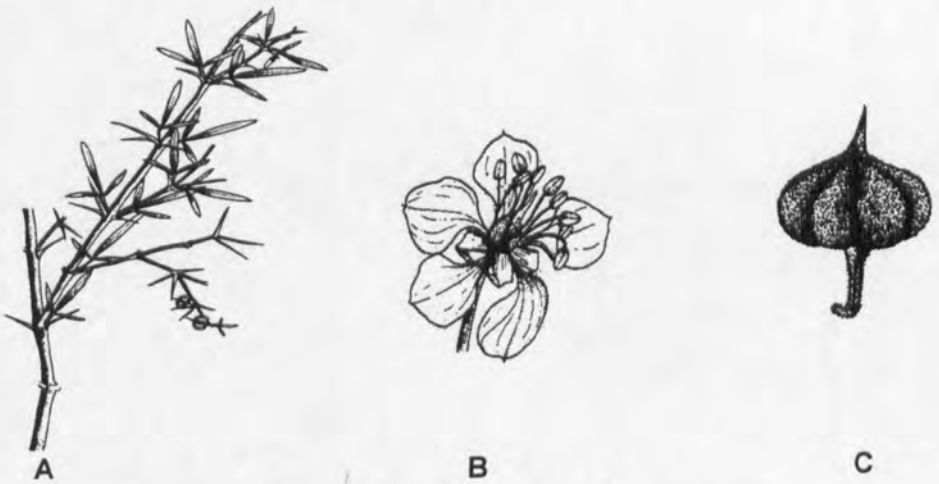

Figure 1.12: Identification features of Fagonia indica
(A: fruiting twigs, B: flower, C: fruit)

1.3.2. *Fagonia indica* in folk medicine

Fagonia indica is a reputed medicinal plant in scientific and folkloric literature and its medicinal values are well documented (Chopra *et al.,* 1965; Saeed, 1969). Fagonia has been used as astringent, febrifuge and as prophylactic agent against smallpox. It has also been reported that the paste may be applied topically on tumours, sores and other swellings of the body. Leaves and twigs have also been reported to have been used as an antidote for snakebite (Atta *et al.,* 1982).

On account of the prickly nature of the plant, it is called in Sanskrit language "Dusparsha" meaning "Painful to touch". *Fagonia indica* has been extensively used as a suppurative in case of abscess from thorns and it is also used as a cooling agent in stomatitis. The juice is thought to prevent suppression when applied to open wounds (Sharma *et al.,* 2010).

An ethnobotanical survey revealed that the Thari people of the Nara Desert, Sindh, Pakistan have used *Fagonia indica* as a remedy for fever areas, whilst the aqueous decoction of leaves has been used for itching and other skin lesions (Qureshi *et al.,* 2008). In folklore medicine, *Fagonia* is used for asthma, vomiting, dysentery, urinary discharges, typhoid, and for blood disorders. The plant is believed to have a vital role as a treatment in hepatotoxicity, chronic bronchitis, ophthalmology and toothache. The bark has also been used in the treatment of scabies (Saeed, 1969).

In Barmer district of Rajasthan in India, the natives prepare a powder of this plant mixing it with fruits of *Terminalia chebula* and leaves of *Casisa italica* (Goral, Gharawal). It is orally taken to cure abdominal pain and as a tonic against weakness (Singh *et al.,* 1998). The plant is used as a bitter astringent, tonic and febrifuge. It is employed in the preparation of *Kumari Asava,* an indigenous

medicinal preparation known for its stimulative and laxative properties. The plant has antiseptic properties and the twigs are used as tooth brushes (Chakre, 2000).

1.3.3. Phytochemical analysis of *Fagonia indica*

Although folkloric, medicinal literature claimed aqueous decoctions of leaves and twigs of *Fagonia indica* as an effective remedy for tumours in the early stages, there was still no scientific evidence until 1982, when Ansari *et al.,* reported the isolation and structural elucidation of new saponins from the aerial parts of *Fagonia indica* (Ansari *et al.,* 1982; Graham *et al.,* 2000).

Saponins are generally known as non-volatile, surface active compounds that are widely distributed in nature, primarily in the plant kingdom (Oleszek, 2002; Hostettmann and Marston, 2005). The name 'saponin' is derived from the Latin word sapo, which means 'soap', because saponin molecules form soap-like foams when shaken with water. They are structurally diverse molecules that are chemically referred to as triterpene and steroid glycosides. They consist of non-polar aglycones coupled with one or more monosaccharide moieties (Oleszek, 2002). This combination of polar and non-polar structural elements in their molecules explains their soap-like behaviour in aqueous solutions. Saponins are often subdivided into two main classes, the triterpenoids and the steroid saponins (Abe *et al.,* 1993), which are both derived from the 30 carbon atoms containing precursor oxidosqualene (Haralampidis *et al.,* 2002). The difference between the two classes lies in the fact that the steroid saponins have three methyl groups removed (i.e. they are molecules with 27 C-atoms), whereas in the triterpenoid saponins all 30 C-atoms are retained. A structure-activity investigation of saponins revealed that the cytotoxic effect is due to their ability to stimulate the apoptotic process in tumour cells, usually through its intrinsic pathway. Moreover, non-apoptotic processes are also involved in saponin cytotoxic activity, such as

cell cycle arrestment, autophagic cell death stimulation, inhibiting of metastasis and cytoskeleton disintegration (Podolak *et al.*, 2010).

A phytochemical literature review indicated that the first report concerning the chemical constituents of *Fagonia indica* described the isolation of β-siosterol, n-triacentanol and ceryl alcohol (long chain fatty acid alcohol) (Tiwari *et al.*, 1966).

Rimlper *et al.*, (1969) reported the isolation of a new triterpene after acid hydrolysis of *Fagonia indica* extract followed by column chromatography. The fraction eluted with benzene-methanol (99:1), and was a mixture of two components, one of which was crystallised to yield oleanolic acid (Figure 1.13).

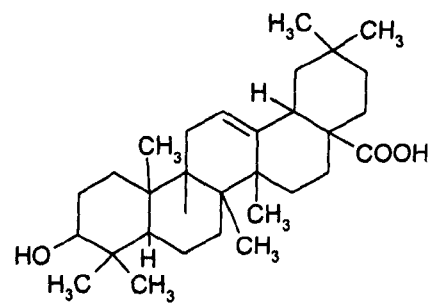

Figure 1.13: Chemical structure of oleanolic acid from Fagonia indica

Further work on the genus *Fagonia* resulted in the isolation of betulinic acid (Figure 1.14), which was isolated by thin layer chromatography from a defatted, entire Fagonia indica plant (Rizk *et al.*, 1972).

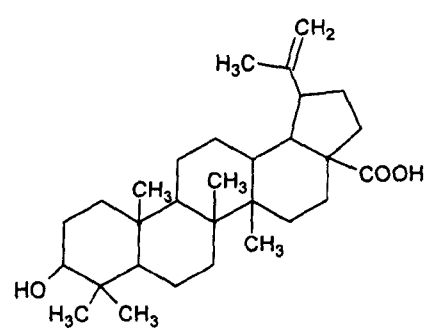

Figure 1.14: Chemical structure of betulinic acid from Fagonia indica

Recently, the anticancer properties of betulinic acid were found to be linked to its ability to induce apoptotic cell death in cancer cells by triggering the mitochondrial pathway of apoptosis, in contrast to its action against normal cells and tissues, which are relatively resistant to, thus pointing to a therapeutic window (Fluda, 2008).

Atta *et al.*, (1982, 1984) reported the isolation of new sapogenins: Nahagenin and Hederagenin, as well as two known compounds Ursolic acid and Pinatol from *Fagonia indica* (Figure 1.15) by hydrolysing the crude saponin with 20% alcoholic hydrochloric acid, followed by column chromatography. The structures of these compounds were elucidated by high resolution mass spectrometry and NMR spectroscopic experiments.

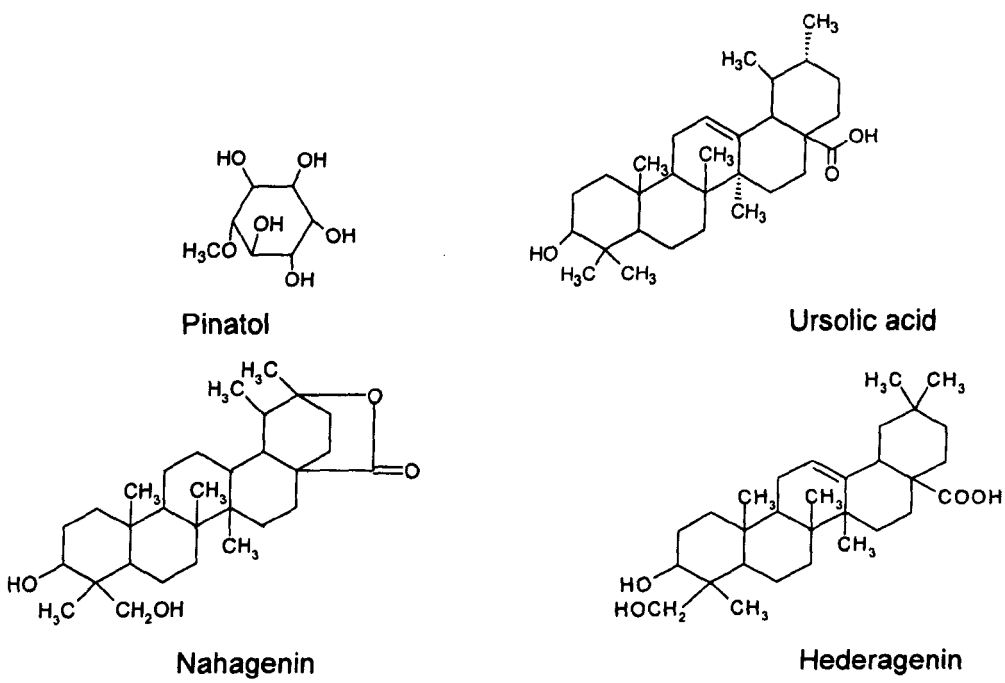

Figure 1.15: Chemical structures of pinatol, ursolic acid and sapogenins.

In 1987, Ansari *et al.*, further isolated two new bisglycosidic triterpenoid saponins from ethanolic extract of *Fagonia indica*. They were characterised as 23,28-di-O-

β-D-glucopysanosyl-taraxer-20-en-28-oic-acid and 3β,28-di-O-β-D-glucopyransoyl 23-hydroxytaraxer-20-en-28-oic acid. Furthermore, conversion of the aglycon to Nahagenin during the acid hydrolysis of the new saponins was also observed (Figure 1.16).

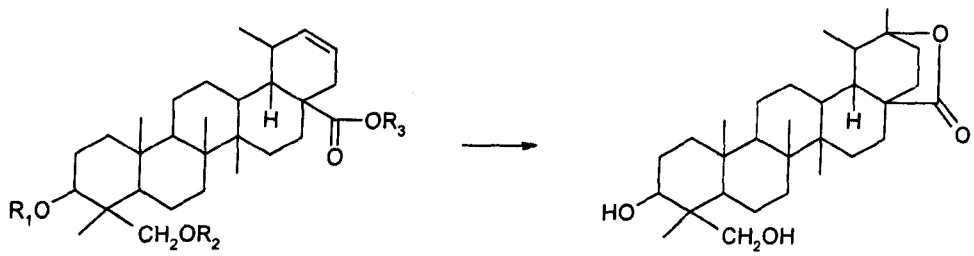

Compounds	R_1	R_2	R_3
Saponin A	H	β-D-Glcp	β-D-Glcp
Saponin B	β-D-Glcp	H	β-D-Glcp
Prosepogenin from Saponin B	β-D-Glcp	H	H

Figure 1.16: Conversion of aglycons to nahagenin

In 1988, Ansari *et al.*, obtained a trierpenoid saponin mixture from the ethanolic extract of the aerial parts of *Fagonia indica*. The Saponin C isolated was characterised as 21, 22-β-epoxy-23-O-β-D-glucopysan-osyl–nahagenin. After β-O-acetylation, the aglycon was found to be transformed to Sapogenin (dihydroxy form of Nahagenin) during acid hydrolysis (Figure 1.17).

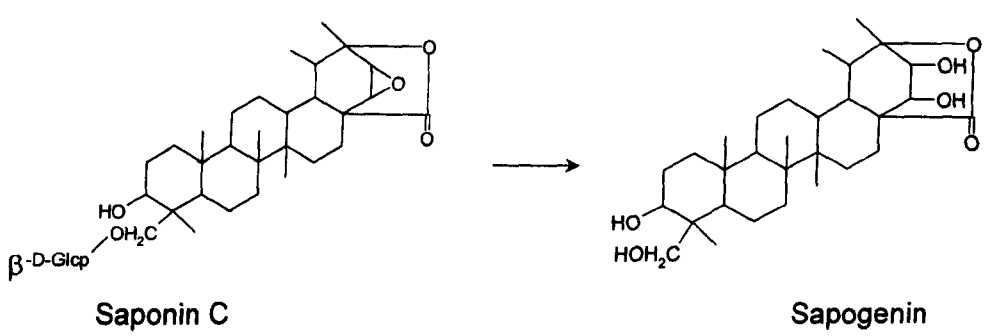

Figure 1.17: Conversion of saponin C to sapogenin

Within the framework of a continuing search for triterpenoid saponins and to investigate the plant constituents of *Fagonia indica* from Egypt, Shaker and co-workers in 1999 were productive in isolating two new triterpenoid saponins (Figure 1.18) along with the already reported ursolic and oleanolic acids. The butanol fractions from the methanolic crude extract of the whole, dried powdered *Fagonia indica* resulted in a crude saponin mixture. The crude saponins were subjected to column chromatography on silica gel followed by preparative HPLC on RP-18 material. Structural elucidations for Indicasaponins A and B were carried out on the basis of 1 and 2D NMR and mass spectroscopic data (Shaker *et al.*, 1999)

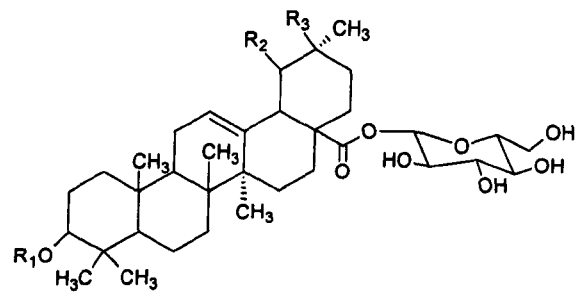

	R_1	R_2	R_3
Ursolic acid	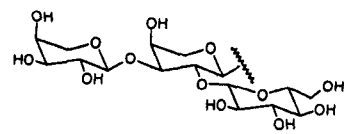	CH_3	H
Indicasaponin A	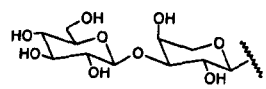	CH_3	H
Oleanolic acid	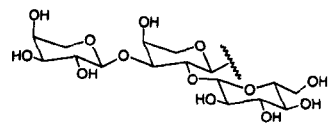	H	CH_3
Indicasaponin B	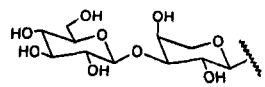	H	CH_3

Figure 1.18: Ursolic acid, indicasaponin A, oleanolic acid and indicasaponin B

1.4. Solanaceae (ethnobotanical aspects)

Solanacea is a family of flowering plants comprising of 84 genera and about 3000 species, nearly half of which belong to a single genus, *Solanum*. The name of the family comes from the Latin word *Solanum* "the nightshade plant" (Edwards, 1990).

Solanum is one of the major genera of this cosmopolitan family, which are distributed throughout the world. They occur in greater concentrations in tropical and warm temperate regions with centres of diversity occurring in the Southern Hemisphere, particularly in South America. Other centres of speciation occur in Australia and Africa, with relative few and less diverse species being found in Europe and Asia (Symon 1981; D'Arcy 1991; Hawkes *et al.*, 1992). Represented in Pakistan by 14 genera and 52 species of which 27 species are native, 6 naturalised and the others exclusivley cultivated or found occasionally as escapes (Nasir, 1985).

Ethnobotanically, the Solanaceae family is extensively used by humans as a source of food and for the presence of a variety of natural products of medicinal significance. Many species are rich in alkaloids and are reported to be toxic to humans and animals in low concentrations. Some key members included are *Datura* (Jimson weed), *Belladonna* (deadly nightshade), *Capsicum* (Paprika, chili pepper), *Solanum* (potato, tomato, aubergine) and *Nicotiana* (tobacco) (Jennifer *et al.*, 1997).

1.4.1 *Solanum surattense*

Solanum surattense is a suffrutescent perennial shrub, which grows in waste lands in Northern India and Pakistan (Rawalpindi, Hazara, Lahore, Karachi, Quetta), often in dry and sunny places, on roadsides and in open scrublands

(Stewart, 1972; Nasir, 1985). It is widely distributed throughout Nepal, Southeast Asia, Australia, Africa and America (Manandhar *et al.*, 2002; Symon, 1981).

The young shoots are densely covered with minute star-shaped hairs (Figure 1.19). The zigzag branches, spread close to the ground are covered with yellow, sharp, shining prickles, about 1.5 cm long. The leaves are up to 10 cm in length, their midribs and other nerves with sharp yellow prickles. The flowers are pretty purple in colour, about 2 cm long, a few together in small bunch opposite the leaves, appear between April and October. The fruits are glabrous, globular drooping berries, 1.5 - 2cm, yellow or pale with green veins (Stewart, 1972; Nasir, 1985).

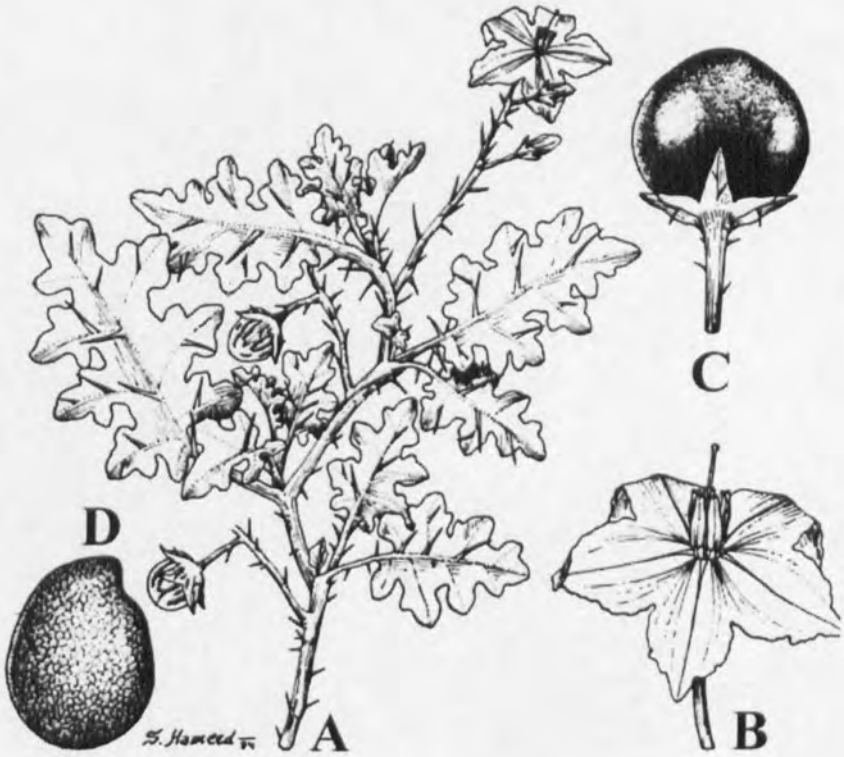

Figure 1.19: Identification features of Solanum surattense (A: portion of shoot, B: flower, C: fruit, D: seed)

1.4.2 *Solanum surattense* in folk medicine

Solanum surattense commonly known as Kanteli, Yellow-berried nightshade, Kantakari, Kandiari. In traditional herbal medicine, the plant has been claimed as valuable for its leaves, fruits, roots or as the whole plant against a wide variety of diseases (Mohan, 2002). Indian Materia Medica describes the use of leaves of *Solanum surattense* as an anthelmintic, anti-inflammatory, antipyretic, carminative and as an appetizer (Vaidyaratnam, 1994). The stem and flowers are prescribed for relief of burning sensations in the feet, accompanied by vesicular eruptions (Chopra, 1982).The hot aqueous extract of dried fruits with honey is used for treating cough, fever, and heart diseases (Saived, 1963). The fruit paste is applied externally to the affected area for treating tumours, pimples and on swollen and painful joints in arthritis. (Jain *et al.*, 1984; Natarajan *et al.*, 2010). Traditionally, the juice of the leaves is used for the treatment of rheumatism and in autoimmune disorders (Rahman *et al.*, 2003).

In Ayuredic medicine, *Solanum surattense* is reported as a vegetable and has proved beneficial as an anti- gonorrhoeal treatment, in patients with idiopathic infertility and has been shown to increase libido in men and used for women with irregular menstruation and dysmenorrheal (Devi *et al.*, 2004; Swamy *et al.*, 2005; Hamayun, 2007). The crude plant extract is beneficial in bronchial asthma and has showen very significant results in diabetes and in skin tumours in south Indian traditional medicine. (Sheeba, 2009).

Despite diverse pharamacological activities of the family solanaceae and especially the genus *Solanum*, Solanaceous plants are widely distributed in the world and used as traditional drugs for anticancer and anti-herpes as well as foodstuff for prevention of cancer (Chi, 1980). In December 1967, Hartwell published the first of a series of articles in Lloydia on the use of plants by humans against cancer (Hartwell, 1967). A survey of plants used ethno-medically against

cancer was undertaken, using the NAPRALERT database. Over 350 species which are reported to be used against cancer are not universally well referenced, "Plants used against cancer" (Graham *et al.*, 2000). In 1979, El Kheir *et al.*, reported the use of fruit from *Solanum dubium* to treat tumours. Similarly *Solanum hispidum and Solanum lyratum* have been used to treat skin cancers (Yu *et al.*, 1994; Lee *et al.*, 1997).

In China, leaves are used as a febrifugal or detoxicant drug. Medicinally used preparations consist of dried aerial parts of plants, which are used as a diuretic, antihypertensive, anticancer agent, for infections of the urinary system, hypertension and for cancer of the digestive system (Schilling *et al.* 1992). Fresh leaves are also used to treat wounds.

1.4.3 Phytochemical analysis of *Solanum surattense*

The Solanaceae family comprises a number of plants widely known for the presence of a variety of natural products of medicinal significance, mainly steroidal lactones, glycosides, alkaloids and flavanoids. *Solanum surattense* in the genus solanum has potential medical and economic importance, because its roots are a rich source of Solasodine (Heiser, 1969; Yousaf 2009), a steroidal alkaloid (Figure 1.20) used in the commercial production of sex hormones (Dulberger *et al.*, 1981).

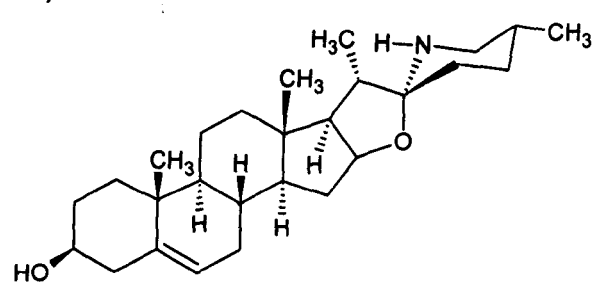

Figure 1.20: Solasodine from Solanum surattense

In the majority of solanaceous plants, solasodine occurs as the aglycone part of glycoalkloids, which are nitrogen analogues to sapogenins (Pawar *et al.*, 2008). Solasodine, can readily be converted to 16-dehydropregnenolone a key intermediate in the synthesis of steroidal drugs e.g. Progesterone, Cortisone etc (Mann *et al.*, 1978).

In Japan, Saijo *et al.*, (1982) observed that immature fruits of *Solanum nigrum* contain steroidal glycosides which show considerable anticancer activity. These glycosides could be solasonine, solamargine, diosgenin and solasodine. Later in 2003, Ikeda *et al.*, reported the cytotoxic activities of steroidal glycosides against PC-12 (human lung cancer) and HCT-116 (human colon cancer) cell lines of twenty-one samples, with spirostane, spirosolane, furostane, and pregnane type steroids obtained from mainly *Solanum* plants, and discussed their structure-activity relationships. The cytotoxic activity of the aglycon part was in the order of spirostane > furostane > pregnane type steroids, suggesting the E ring of the spirostane skeleton (Figure 1.21) should be essential for anticancer activity.

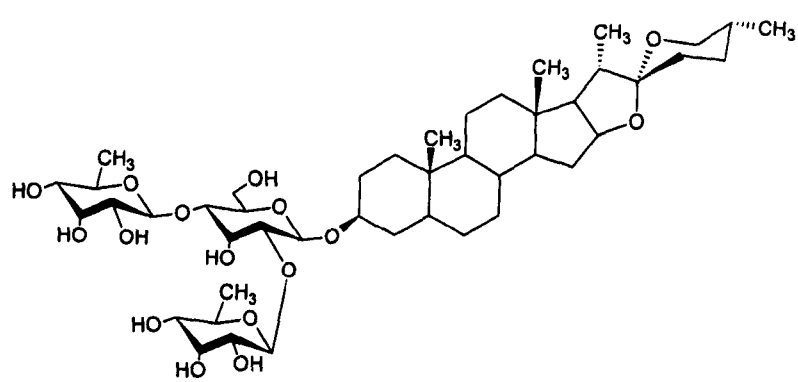

Figure 1.21: Spirostane –Type Glycoside (Dioscin)

Most of these bioactive substances exert their cancer chemotherapeutic activity by blocking cell cycle progression and triggering apoptotic cell death. Therefore, induction of apoptosis in tumour cells has become an indicator of the tumour

treatment response in employing a plant derived-bioactive substance to reduce and control human mortality due to cancer (Smets, 1994; Paschka *et al.*, 1998). In 2003, South Korean researchers reported the crude ethanolic extract of ripe fruit of *Solanum nigrum* showed highly significant antiproliferative activity against MCF-7 (human oestrogen dependent breast cancer) cells. The crude extract mediated suppression of cell growth was verified to be apoptotic based on the appearance of DNA laddering, increase in DNA fragmentation and low fluorescence intensity in nuclei after propidium iodide staining of the cells (Son *et al.*, 2003).

Spirosolane – Type Glycoside "Solamargine" isolated from *Solanum incanum* herb, displayed a superior cytotoxicity in four human lung cancer cell lines. The half-inhibitory concentrations (IC_{50}), of the cell viability assay for H441 (human adenocarcinoma), H520 (squamous cell lung carcinoma), H661 (large cell lung cancer) and H69 (small cell lung cancer) cells were 3, 6.7, 7.2 and 5.8 μM, respectively. Solamargine (Figure 1.22) induced apoptosis of these cells by phosphatidylserine externalisation in a dose-dependent manner and an increased sub-G1 fraction was observed (Liu *et al.*, 2004).

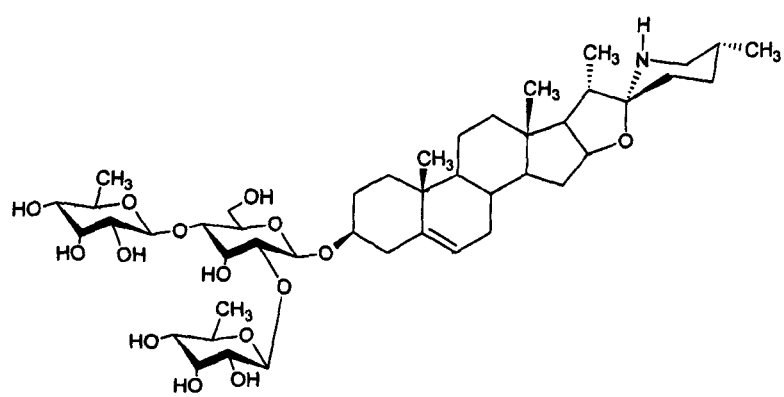

Figure 1.22: Spirosolane – Type Glycoside "Solamargine"

Tumour promotion is an important process in carcinogenesis. Particularly, 12-O-tetradecanoyl phorbol-13-acetate (TPA) is one of the tumour promoters in

several cell lines. In 2004, Heo *et al.*, isolated a glycoprotein (150 kDa) from an ethanolic extract of *Solanum nigrum*. It was observed that the glycoprotein has the capacity to modulate TPA-induced DNA-binding activities of transcription factors and nitric oxide production, which play a critical role with respect to cytotoxicity in MCF-7 cells. Therefore, it was suggested the glycoprotein might be one of the agents that blocks TPA-mediated signal responses in tumour cells (Heo *et al.*, 2004). In 2006, Lee *et al.*, investigated that the glycoprotein from *Solanum nigrum* consisted of carbohydrate content (69.74%) and protein content (30.26%), which contained more than 50% hydrophobic amino acids, such as glycine and proline. The glycoprotein showed remarkable cytotoxic and apoptotic effects at 40 µg/ml, in just 4 h in HCT-116 (human colorectal carcinoma) cells. The results showed that the glycoprotein has a stimulatory effect on caspase-3 activation and PARP cleavage in HCT-116 cells (Lee *et al.*, 2006).

Polyphenols from fruits and vegetables exhibit anticancer properties both *in vitro* and *in vivo* and speciality (coloured) potatoes (*Solanum tuberosum*) from the family Solanaceae are an excellent source of dietary polyphenols, including phenolic acids and anthocyanins. In 2007, Reddivari, investigated the effects of speciality potato phenolics and their fractions on LNCaP (androgen dependent) and PC-3 (androgen independent) prostate cancer cells. This was the first report showing that the cytotoxic activities of potato extracts in cancer cells were due to activation of caspase-independent apoptosis (Reddivari *et al.*, 2007).

In Chinese traditional medicine, the nightshade (*Solanum nigrum* Linn.) has been widely used as a remedy for the treatment of digestive system cancer. The anti-tumour activity of solanine (Figure 1.23), a steroid alkaloid isolated from the nightshade has been explored to evaluate the IC_{50} on the three digestive system tumour cell lines HepG2 (human hepatocarcinoma), SGC-7901 (human gastric carcinoma) and LS-174 (human large intestine cancer). The expression of Bcl-2 (an anti-apoptosis gene) protein was measured by Western blotting. The results

showed the target of solanine in inducing apoptosis in HepG2 cells seems to be mediated by the inhibition in the expression of Bcl-2 protein (Ji *et al.*, 2008).

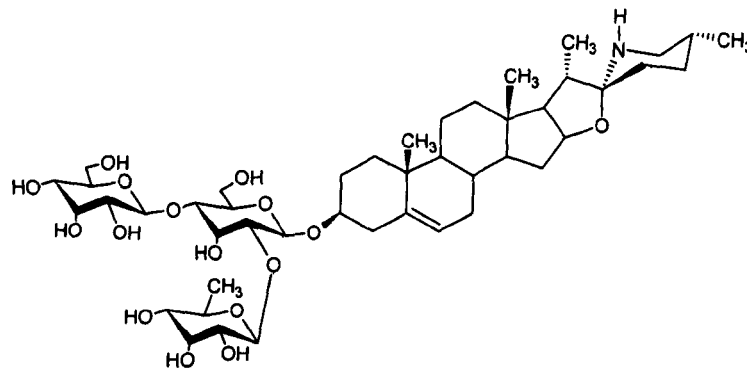

Figure 1.23: The molecular structure of Solasonine from Solanum nigrum

A phytochemical and phytopharmacological literature search showed that not much research work has been carried out on the anticancer activity of *Solanum surattense* in the last decade. Most recent reports emphasised on the significance of the ethanolic extract in the evaluation of antibacterial (Sheeba, 2010), antimalarial (Ramazani *et al.*, 2010) and anthelmintic (Nayak *et al.*, 2009) activities as well as the antihyperglycaemic, antilipidperoxidative, hepatoprotective and antioxidant potential in diabetic rats (Sridevi *et al.*, 2007).

1.5. Araceae (ethnobotanical aspects)

The aroids or family Araceae are abundantly found on the forest floor in tropical rainforests. The Araceae, comprising nine subfamilies, 115 genera and about 2000 species, is mainly tropical and is distributed worldwide (Nasir, 1985). Ecologically, aroids can be found in streams, ponds and canals, terrestrial habitats, tidal mud, swamps and wasteland. Araceae are best characterised by the inflorescence, a fleshy cylindric or ovoid, unbranched spadix subtended or surrounded by a spathe. Rhizomes are vertical or horizontal, creeping at or near surface, sometimes branched (Renner *et al.,* 2004). *Arisaema* is one of the important genus of the family Araceae and consists of 150 species, distributed throughout in Asia (including Arabian Peninsula), North East Africa, North America to Mexico, primarily in tropical regions. According to Flora of Pakistan, only 6 species are reported in the Pakistani habitat and are often called Cobra Lilies (Nasir, 1985).

Araceae plants contain crystals of calcium oxalate, which are often cited as causing the intense irritation experienced when handling or consuming the raw plant tissue of many genera in the family. This supposition is contradicted by some biological studies, which demonstrated that a proteolytic enzyme, is responsible for the severe irritation caused by this plant and that raphides of calcium oxalate do not play a major role (Arditti and Rodriguez, 1982). Whether irritation is caused by enzymes or crystals, this aspect of Araceae has resulted in aroid genera being included in many lists of poisonous plants (Lampe and McCann, 1985; Mulligan and Munro, 1990).

Despite the toxic effects of Araceae, species of several genera are cultivated as food plants, mainly as subsistence crops in tropical areas. The major edible Araceae are *Colocasia esculenta* and several species of *Xanthosoma* are grown primarily for their corms and sometimes for their leaves. Most North American

species of Araceae were historically used by Native Americans, as both food and medicine (Plowman, 1969).

Aroid species such as *Arisaema consanguineum, Arisaema erubescens, Arisaema lobatum, Homalomena sagittifolia, Homalomena coerulescens*, and *Typhonium flagelliforme* have shown promising results in fighting cancer (Graham *et al.*, 2000; Choo *et al.*, 2001).

1.5.1. *Arisaema utile*

Arisaema utile is a perennial tuberous herb about 16.5-33 cm tall, commonly known as "Cobra Lily" with broad conspicuous foliage (Figure 1.24). Three broad,

Figure 1.24: Identification features of Ariseama utile: A- Aerial part with rhizome, B-Portion of male spadix, C- Berry, D- Immature berry, E- Seeds

leaflets held above dark purple spathe. This plant is ornamental with distinctive striping and has long, thin, spadix extension. *Arisaema* are grown in part to full shade in well-drained fertile, evenly moist soils. The plants emerge in spring and die back to the ground in winter. *Arisaema utile* is fairly common in rich; moist forests at elevations of 2300-3300 m in the Himalayas from Himachal Pradesh, India to Bhutan, south-east to China and Japan.

1.5.2 *Arisaema utile* in folk medicine

An ethnobotanical literature review revealed that not much work has been reported on *Arisaema utile*, as compared to folklore use of other species in the genus *Arisaema*. *Arisaema* has been used in Chinese herbal medicine for thousands of years and is especially valued for its beneficial effects upon the chest. When prescribed internally, it is always used dried and in conjunction with fresh ginger root (Hu, 1993). The root is an acrid, irritant herb that is antibacterial, antifungal, antiphlogistic, antirheumatic, anticancer, antispasmodic and antitumor (Duke *et al.*, 1985; Zheng *et al.*, 1991). The dried root is used internally in the treatment of coughs with profuse phlegm as an expectorant, tumours, cervical cancer, epilepsy, tetanus and complaints involving muscular spasms (Hatfield, 2004). In North America, the fresh root is applied externally as a poultice to ulcers and other skin complaints. As for *Arisaema flavum,* the rhizome is mixed in oil and applied to eczema lesion (Hu, 1993).

In 2000, Graham *et al.*, in a survey of plants used ethnomedically against cancer has highlighted the importance of the family Araceae and the use of "*Arisaema consanguineum*" in Chinese herbal medicine as the entire plant or roots. *Pinellia, arisaema, acorus,* and *typhonium* are Chinese herbs that all come from the Araceae family. The underground portions (a corm-like rhizome) of each of the herbs are the parts used in medicine (Duke *et al.*, 1985). As with pinellia, little is known about the active constituents of arisaema, although saponins have been

found. The root decoction of *Arisaema* also reveals a sedative action and an anticonvulsant effect in epilepsy (Zhang, 1988).

1.5.3. Phytochemical analysis of *Aisaema utile*

In the flora of Pakistan, plants from the family Araceae are classified as poisonous plants. Previous studies on toxic plants were focused on their chemical compositions and pharmacological effects (e.g., Farnsworth 1966; Rios and Waterman 1998; Vetter 2000). However, little is known about the relationships between the therapeutic uses of *Arisaema utile* and their taxonomic and phytochemical composition in different ethnic groups. Different ethnic groups may have their own knowledge and experiences of using plant resources, even if they inhabit the same environments, and scientific evidence on the basis of phytochemical and biological screening is vital. A phytochemical literature search revealed that aroids are rich source of plant "Lectins".

Lectins are the carbohydrate-binding proteins or glycoproteins of non-immune origin capable of specific recognition of, and reversible binding to carbohydrates, without altering their covalent structure (Dixon, 1981). On the basis of recent advances in molecular structure and biological specificities of lectins, a new definition has been proposed as proteins possessing at least one non-catalytic domain, which binds reversibly to a specific mono- or oligosaccharide (Peumans, 1995).

Lectin-carbohydrate interactions occur in the molecular events underlying the immune response. Lectins are therefore used as polyclonal reagents to investigate the molecular basis and control of lymphocyte activation and proliferation, to identify and fractionate cells of the immune system, and as drugs. One of the most dramatic effects of the interaction of lectins with the cells is mitogenicity, i.e., the triggering of quiescent, non-dividing lymphocytes into a

state of growth and proliferation. The first mitogenic agent to be described was PHA, the lectin from red kidney bean (*Phaseolus vulgaris*) by Nowell in 1960.

Plant lectins have been shown to possess antitumor activity (i.e., an inhibitory effect on tumour growth) and anticarcinogenic activity (i.e., an inhibitory effect on the induction of cancer by carcinogens). Like antitumor drugs which trigger apoptotic death of tumour cells (Lenartz *et al.*, 1996; Werner *et al.*, 1996), plant lectins have also shown cytotoxic effects mediated via apoptosis (Abdullaev *et al.*, 1997). During the last two decades, there has been a growing interest in lectins, which exhibit anticancer activities.

In 1995, Shangary *et al.*, reported the purification of four monocot lectins from the tubers of araceaeous plants namely, *Arisaema consanguineum*, *Arisaema curvatum* and *Sauromatum guttatum*. The lectins agglutinate rabbit, rat and sheep red blood cells (RBCs), but are inactive towards human ABO erythrocytes (Shangary *et al.*, 1995).

Numerous diacylglycerylgalactosides have been isolated from algae and higher plants. However, in most cases they were not reported as single components; neither have the sequence of their acyl moieties been determined. Another interesting specie, *Arisaema amurense* resulted in isolation of a series of diacylglycerylgalactosides previously undescribed as single components. In this report, the sequence of acyl moieties of each compound was determined by regio-selective enzymic hydrolysis (Jung *et al.*, 1996a).

The search for bio-active compounds from *Arisaema amurense* led to isolation and structure elucidation of four new cerebrosides (1, 2, 4 and 5 Figure 1.25), along with a known cerebroside (3) (Jung *et al.*, 1996b).

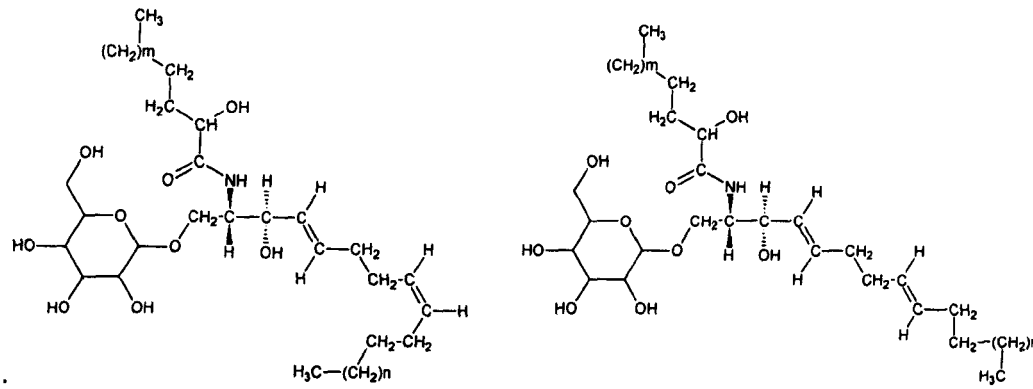

1	m=15, n=6	4	m=15, n=6
2	m=13, n=6	5	m=13, n=6
3	m=11, n=6		

Figure 1.25: Cerebrosides from Arisaema amurense

A series of homologous, phenylalkanoic acids (Figure 1.26) and phenylalkenoic acids were isolated from seed lipids of various genera of the subfamily Aroideae or Araceae (the Jack-in-the-Pulpit family). It was observed that the genera divide into two groups: one that has a sizable amount (5–16%) of 13-phenyltridecanoic acid (such as genus *Arisaema*; fatty acids from the seeds of *Arisaema utile*) and the other which has none (Meija *et al.*, 2004).

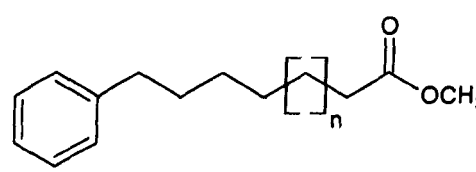

Figure 1.26: Structure of the phenylalkanoic acid methylester identified in seed oil of Arisaema utile where n=7

The search for more glycoprotein resulted in isolation of a novel lectin having specificity towards a complex glycoprotein asialofetuin, which was purified from tubers of *Arisaema flavum* (Schott.) by affinity chromatography on asialofetuin-

linked amino-activated silica beads. *Arisaema flavum* lectin gave a single peak on HPLC size exclusion and a single band on non-denatured PAGE (Polyacrylamide gel electrophoresis) at pH 4.5. The molecular mass of the lectin, as determined by gel filtration chromatography, was 56 kDa and showed significant *in vitro* antiproliferative activity towards J774 and P388D1 murine (macrophage) cancer cell lines (Singh *et al.*, 2004).

Lectins, have elicited much attention in view of their unique ability to bind reversibly to specific carbohydrate ligands without any chemical alteration (Dixon, 1981). Owing to their fine specificity, lectins have been employed for various applications in biomedical sciences, including cancer research. A variety of alternations in carbohydrate structure have been observed in cancer cells. These may involve increased sialylation or increased branching of complex carbohydrates (Abdullaev *et al.*, 1997). Lectins can serve as an excellent probe to study these altered glycosylation patterns.

In 2006, Kaur *et al.*, reported an anti-cancer lectin, isolated from *Arisaema helleborifolium Schott* by affinity chromatography using asialofetuin-linked amino activated silica beads. The lectin was found to inhibit *in vitro* proliferation of some well established human cancer cell lines HOP-62 (lung, 95%), HCT-15 (colon, 92%), HEP-2 (liver, 66%), HT-29 (colon, 68%), PC-3 (prostate, 39.4%), and A-549 (lung, 20.7%).

Recently, in 2010, Dhuna *et al.*, investigated the anti-proliferative activity of a N-acetyl-D-lactosamine binding lectin from tubers of the Cobra Lily (*Arisaema utile*). Results showed that 50% growth inhibition was achieved in six cancer cell lines, SW-620 (colon), HCT-15(colon), SK-N-SH (CNS), IMR-32 (Neuroblastoma), Colo-205 (Colon), HT-29 (Colon) at 38, 42, 43, 49, 50 and 89 µg/ml, respectively (Dhuna *et al.*, 2010).

1.6. Cancer

Among the oldest of the world's writings mentioning both benign and malignant tumours are several Egyptian papyrus scrolls, dating from approximately 1600 BC. Hippocrates, an ancient Greek physician, the "father of modern medicine", first gave the name *karkinos* and *karkinoma* (the ancient Greek words for "crab") to a group of diseases that are now known as cancer. He thought the disease spread out from a tiny spot like a crab and eventually took over the whole body.

Cancer is an abnormal state in which uncontrolled proliferation of one or more cell populations interferes with normal biological functioning. The hallmarks of malignant neoplastic tissue are unregulated cell proliferation, invasiveness and metastasis to distant sites in the body. The proliferative changes are usually accompanied by other changes in cellular properties, including reversion to a less differentiated, more developmentally primitive state (McKinnell *et al.*, 1998). A cancer is said to be benign when the growth is localised to the site of origin within a tissue, with no invasion. Although cancer is a generic term encompassing many different diseases, a unifying feature of many tumours is the uncontrolled proliferation of their cells (Vogelstein and Kinzler, 2002). As they proliferate, cancer cells disrupt the normal function of surrounding tissues (or distant tissues in the case of metastases), leading to eventual organ failure and death. There are more than 200 types of cancer, each with different causes, symptoms and treatments (Trichopoulos *et al.*, 1996).

According to GLOBOCAN (WHO project for estimation of incidences and mortalities globally from major cancer types), an estimated 12.7 million new cancer cases and 7.6 million deaths occurred across the world in 2008 (Figure 1.27). The most commonly diagnosed cancers worldwide are lung (1.61 million, 12.7% of the total), breast (1.38 million, 10.9%) and colorectal cancers (1.23 million, 9.7%). There are big variations in cancer incidence across the world. The highest incidence rates are seen in the more developed regions of the world,

Figure 1.27: Golobocan 2008, cancer incidence and mortality worldwide

such as Australia/New Zealand and the lowest rates in the less developed regions, such as Africa and Central America. An estimated 6.6 million men were diagnosed with cancer worldwide in 2008 . In the UK, colorectal cancer (14%) is projected as the second most common cancer after prostate cancer (24%) in men. While in women, 6 million were diagnosed with cancer worldwide in 2008; breast cancer, the most common one, accounts for almost a third (31%) of the cancer burden, then colorectal cancer (12%). GLOBOCAN also provides cancer incidence and mortality projections for the next twenty years. Based on "GLOBOCAN 2008" projects that by 2030, there will be almost 21.4 million new cases diagnosed annually and that there will be over 13.2 million deaths from cancer (Ferlay *et al.*, 2010).

The primary causes of cancer are through avoidable means, in about 90-95 % cases, reflecting lifestyle and environmental factors, while about 5-10% are due to genetics alone (Anand *et al.*, 2008). The most common environmental factors leading to cancer death include: unbalanced diet and obesity (30-35%), smoking tobacco, 25-30%), infectious conditions (T-cell leukemia, 15-20%), radiation (UV light, ionising radiations), stress level, lack of physical activity, environmental pollutants etc. These environmental factors cause abnormalities in the genetic material of cells. Typically, serious damage of DNA leads to programmed cell death, but if the cell cannot repair itself or the programmed cell death pathway is damaged, then it becomes a cancerous cell (Vogelstein and Kinzler, 2002).

Cancer arises because of mutations in the genome of somatic cells as a result of hereditary deficiencies in DNA, inaccuracies in DNA replication, or chromosomal rearrangement at mitosis over a certain period of time: The Somatic Cell Theory of cancer states that: "if a result of the mutation is loss of control over cell growth and division, the mutant cell divides more rapidly (tumourigenesis) than the surrounding tissues to form clone daughter tumour cells". Tumourigenesis is a complex process and requires more than one somatic mutation before full

transformation of the cell occurs. Such a multistage process may occur over a period of years, with contributory mutations being accumulated over many generations of cell (Polinsky, 2007).

Genetic abnormalities found in cancer cells typically affect two general classes of genes. Cancer-promoting "oncogenes" are typically activated in cancer cells, giving these cells new properties, such as hyperactive growth and division, protection against programmed cell death, loss of respect for normal tissue boundaries and the ability to become established in diverse tissue environments. The proteins encoded by oncogenes are related to the products on non-oncogenic cellular genes, termed proto-oncogenes (Norman *et al.,* 2007). These potentially oncogenic genes have important functions in normal cells, either in signalling and/or the regulation of cell differentiation, and potentially arise from their ability to mimic signal pathway components or transcription factors, which ultimately lead to a modified control of key regulatory genes. The second class "tumor suppressor genes" are then inactivated in cancer cells e.g. proteins of PARP 1 (poly-ADP ribose polymerase 1), resulting in the loss of normal functions in these cells, such as accurate DNA replication control over the cell cycle, orientation and adhesion within tissues and interaction with protective cells of the immune system (Polinsky, 2007).

1.6.1. Cell Cycle

The process of cell division is cyclical and unidirectional, in which a cell grows, replicates its DNA and then divides to give two daughter cells. The period between successive cell divisions is termed as interphase. This process is divided into four sequential phases (Figure 1.28). It is often considered that the two most important of these are S phase, when DNA replication occurs and M phase "mitosis", when the cell undergoes division to give two daughter cells. The cell moves between these phases growing, replicating its DNA, ensuring the

DNA is replicated completely and not damaged and then dividing. In fact a key concept of the cell cycle is that the S phase must always follow the M phase and that the M phase must not start until the S phase has been completed. In other words, DNA replication must not commence until mitosis is complete and mitosis must not begin until the previous round of DNA replication has ended. Entry and exit from the phases is highly regulated, leading to ordered progression through the phases thus, the integrity of the genome is maintained (Norman *et al.*, 2007).

Figure 1.28: The complete series of events from one cell division to the next. Cyclical cell division and the action of the mammalian Cdk-cyclin complexes during the cell cycle. Cyclins: G_1/S (activate cyclin-dependent kinases (Cdks) in the late G_1, S cyclins (stimulate the chromosome duplication), M cyclins (activate Cdks that stimulate entry into mitosis at the G_2/M checkpoint.Cyclin-dependent kinase (Cdks): G_1 Cdk (Cdk-4 and Cdk-6), S Cdk (Cdk-2), M-Cdk (Cdk-1)

In-between S and M phases are two gaps G_1 and G_2. G_1 follows on from mitosis and is a time during the cell cycle when the cell is responsive to both positive and negative growth signals. G_2 is the gap after the S phase, when the cell prepares

for entry into mitosis. Finally, there is a fifth state, G_0 (also known as quiescence) into which the cell may reversibly exit from G_1, if it is deprived of the appropriate growth-promoting signals (Elledge, 1996). Proliferation of quiescent cells (transition from G_0 to G_1) can be induced by mitogens, leading to the expression of responsive genes and progression of the cell through the G_1 phase and past a "restriction point" (mammalian cells). Once past the restriction point, cells become committed to a complete division cycle and no longer require the presence of growth factors (Madine *et al.*, 1995).

1.6.1.1. Cell cycle check points

Regulation of a typical somatic cell can be complex and is regulated in a phase-specific manner. In the event of damaged or unreplicated DNA, the cell pauses during the cell cycle, once at G_1, just prior to the S phase (Moreno and Nurse, 1994; Zeng *et al.*, 1998), and again at G_2, just prior to the M phase (Kumagai *et al.*, 1998). The cell pauses again at metaphase prior to anaphase in mitosis, if the mitotic spindle is not correctly assembled (Minshull *et al.*, 1994). These pauses in the cell cycle are called checkpoints, and the checkpoints ensure that the cellular components have been properly maintained in the cell, otherwise inappropriate proliferation can occur – the hallmark of cancer.

1.6.1.2 Control of the cell division cycle

At the core of the mammalian cell division cycle is the cyclin-dependent kinase (Cdk) family of serine/threonine kinases (Morgan, 1997). The name Cdk describes the fact that the full activity of each of these kinases is dependent on its association with a regulatory subunit known as a cyclin. In mammalian cells, different Cdks are active and required at different phases of the cell cycle (Figure 1.28). The expression of the Cdk subunit is generally constant throughout the cell cycle; the expression of each cyclin (of which there is a whole family) tends to be

cell cycle dependent, so that a specific Cdk will have full activity when its cyclin partner is expressed. The role of the Cdks is to control cell cycle progression through phosphorylation of proteins that function at specific cell cycle stages (Taya *et al.,* 1997). For example, the product of the retinoblastoma tumour suppressor gene, pRb is a key regulator of the G_1 phase by inhibiting the cell cycle progression until a cell is ready for division. It regulates the starting point of cell division by stopping the transcription of genes required for cell division, as well as sequestering the proteins that regulate DNA replication. Lack of or absence of the pRb gene causes many common types of cancer, such as lung, breast and bladder cancer (Harbour *et al.,* 2000).

1.6.2. Cell death

The number of cells in an organ is determined by the rates of cell immigration, cell division, and cell death (Raff, 1996). Cell death is a critical process in development and homeostasis of normal organisms. All cells are equipped with a genetic program for self-destruction that plays an important role in balancing cell proliferation with cell death and many other physiological processes. The cell death in multi-cellular organisms is subject to genetic control (Ellis *et al.,* 1986; Vaux *et al.,* 1988) and abnormalities in cell death regulation can cause diseases such as cancer (Strasser *et al.,* 1990).

The naturally-occurring turnover of cells in the body is referred to as "programmed cell death". This cell death that occurs in a predictable "programmed" form in physiological conditions was first recognised in the neuronal system of developing toad embryos and the phrase "programmed cell death" (PCD) was coined to describe cell death (Lockshin *et al.,* 1965). Kerr and colleagues used a new term "apoptosis" for cell death with distinct morphology – whether it occurs in response to physiologic or pathologic stimuli (Kerr *et al.,* 1972).

1.6.2.1 Apoptosis

Apoptosis is a genetically encoded, ubiquitous pathway enabling cells to undergo highly regulated death in response to pro-death signalling. Apoptosis is characterised by a number of unique distinguishing features (Figure 1.29) including cytoplasmic shrinkage, membrane blebbing, nuclear fragmentation, intranucleosomal DNA fragmentation, phosphatidylserine exposure and, finally, fragmentation into membrane-enclosed apoptotic bodies sequestered by macrophages or other engulfing cells (Wyllie *et al.*, 1980).

Figure 1.29: Hallmarks of the apoptotic and necrotic cell death process. *Apoptosis includes cellular shrinking, chromatin condensation and margination at the nuclear periphery with the eventual formation of membrane-bound apoptotic bodies that contain organelles, cytosol and nuclear fragments and are phagocytosed without triggering inflammatory processes. The necrotic cell swells, becomes leaky and finally is disrupted and releases its contents into the surrounding tissue resulting in inflammation.*

Apoptosis is critical for the maintenance of normal homeostasis, on par with other important processes like proliferation and differentiation. The dysregulation of such a powerful process can lead to disastrous consequences, and is involved in

many diseases such as cancer, autoimmunity and neurodegeneration. Apoptosis occurs under normal physiological conditions and is an active process requiring energy. The apoptotic cascade can be initiated via two major pathways, involving either the release of *cytochrome-c* from the mitochondria (mitochondrial pathway), or activation of death receptors in response to ligand binding (death receptor pathway; Ashkenazi *et al.,* 1998). Upon triggering of either pathway, a specific family of cysteine proteases, the caspases, is activated to execute the cell's fate in a programmed fashion, leading to the typical morphologic changes (Degterev *et al.,* 2003). Biochemical hallmarks of apoptosis such as activation of caspases are usually absent in necrotic cells (Hengartner, 2000).

1.6.2.2. Necrosis

Necrotic cell death is an unregulated process resulting from severe damage, such as ATP depletion, hypoxia, various toxins and hyperthermia and characterised by (Figure 1.29) cell swelling, lysis, and the release of intracellular contents associated with pathological tissue injury (Wyllie *et al.,* 1980; Hirsch *et al.,* 1997). Necrosis is associated with release of lysosomal proteases, which causes proteolysis of nuclear histones, leaving "naked" stretches of DNA, not protected by histones. In addition, necrotic cells enhance pro-inflammatory responses of activated macrophages, whereas apoptotic cells profoundly inhibit these (Cocco and Ucker, 2001).

1.6.2.3. Factors determining apoptosis or necrosis in a cell

Despite the numerous models proposed to categorize PCD, exclusive definitions are difficult to make and are probably artificial due to the overlap and shared signalling pathways between the different death programs. It has been shown that apoptotic and necrotic death markers can concomitantly be present in the same cell after cerebral ischemia, indicating that more than one death program

may be activated at the same time (Unal-Cevik *et al.*, 2004). In addition, a cell may switch back and forth between different death pathways as shown in neuronal cell death that exhibited elements of autophagic degeneration.

Mitochondria constitute an important component of the cell death machinery. The mitochondrial permeability transition (MPT) is a common pathway leading to both necrotic and apoptotic cell death (Kim *et al.*, 2003). Signals that trigger or switch cell death pathways are ATP, reactive oxygen species (ROS) and apoptotic/necrotic factors.

Apoptosis is an energy-dependent process and decrement of ATP levels may cause the shift from apoptosis to necrosis (Eguchi *et al.*, 1997). Oxygen radicals are created under different physiological and toxic conditions and may induce cell death by selectively altering the structure and the function of the plasma membrane. Free radicals interact with lipids, proteins and other cellular constituents, leading to cell death (Halliwell, 2000). Cell death induced by free radicals may have characteristics of apoptosis or necrosis (Kane *et al.*, 1993). Hydrogen peroxide (H_2O_2) causes apoptosis or necrosis, depending on the intracellular concentrations (Troyano *et al.*, 2003) and the depletion of intracellular glutathione (GSH) diverts the mode of death from apoptosis to necrosis in drug treated cells (Troyano *et al.*, 2001).

Different intracellular mediators (Figure 1.30) and their receptors, TNF (tumour necrosis factor), TRAIL (TNF- related apoptosis inducing ligand), and induction of ROS have been found to be major factors in both apoptosis and necrosis (Lin *et al.*, 2004). The enzyme poly (ADP-ribose) polymerase (PARP) is a nuclear enzyme involved in DNA repair and activated by DNA damage. Strong activation of PARP activity can cause depletion of NAD^+, and consequently ATP depletion, leading to a shift from apoptosis to necrosis (Lazebnik *et al.*, 1994).

Figure 1.30: Apoptotic and necrotic pathways in mammalian cells (Lazebnik et al., 1994)

1.6.2.4. Caspases

Apoptosis is mediated by a specific group of cysteine proteases, the "caspases ". These enzymes are typically activated in the early stages of apoptosis by processing from its inactive precursor (zymogen) and are involved in both initiation and execution of apoptosis (Thornberry *et al.,* 1998). Once caspases are activated they can often activate other pro-caspases, allowing initiation of a protease cascade. Some pro-caspases can also aggregate and auto-activate.

Thus, a proteolytic cascade in which one caspase can activate other caspases amplifies the apoptotic signalling pathway and thus leads to rapid cell death. Caspases have proteolytic activity and are able to cleave proteins at aspartic acid residues, although different caspases have different specificities involving recognition of neighbouring amino acids. Once caspases are initially activated, there seems to be an irreversible commitment towards cell death. So far, ten major caspases have been identified and broadly categorised into:

a- Initiators (caspase-2,-8,-9,-10)
b- Effectors or executioners (caspase-3,-6,-7)
c- Inflammatory caspases (caspase-1,-4,-5)

The other caspases that have been identified include caspase-11, which is reported to regulate apoptosis and cytokine maturation during septic shock; caspase-12, which mediates endoplasmic-specific apoptosis and cytotoxicity by amyloid-β; caspase-13, which is suggested to be a bovine gene and caspase-14, which is highly expressed in embryonic tissues but not in adult tissues (Cohen, 1997; Koenig *et al.*, 2001; Kang *et al.*, 2002).

1.6.3 Mechanism of Apoptosis

The mechanisms of apoptosis are highly complex and sophisticated, involving an energy-dependent cascade of molecular events. There are two main apoptotic pathways: the extrinsic or death receptor pathway and the intrinsic or mitochondrial pathway (Figure 1.31). However, there is now evidence that the two pathways are linked and that molecules in one pathway can influence the other (Igney and Krammer, 2002). There is an additional pathway that involves T-cell mediated cytotoxicity and perforin-granzyme-dependent killing of the cell. The perforin/granzyme pathway can induce apoptosis via either granzyme B or granzyme A. The extrinsic, intrinsic, and granzyme B pathways converge on the same terminal or execution pathway. The granzyme A pathway activates a

parallel, caspase-independent cell death pathway via single stranded DNA damage (Martinvalet *et al.*, 2005).

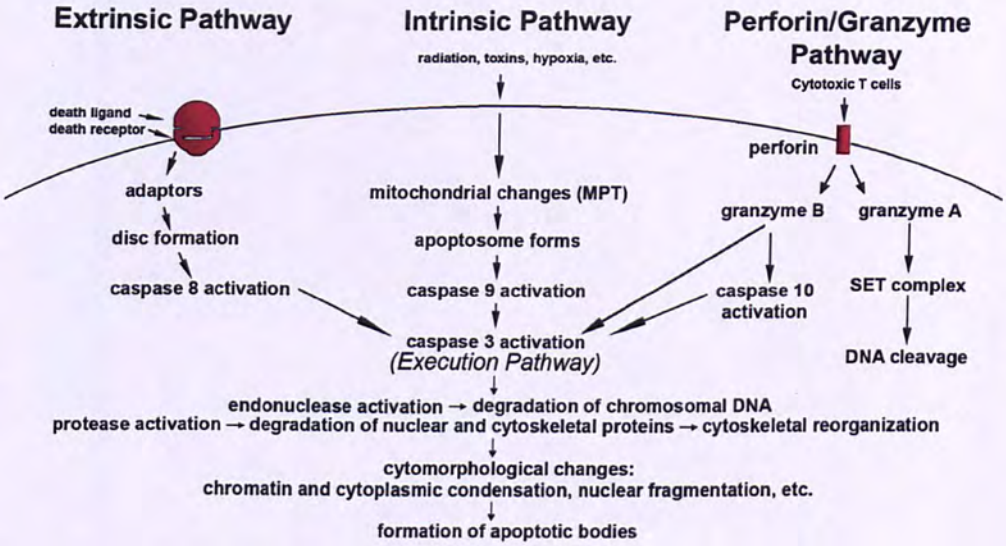

Figure 1.31: Schematic representation of apoptotic events.
The two main pathways of apoptosis are extrinsic and intrinsic, as well as a perforin/granzyme pathway. Each requires specific triggering signals to begin an energy-dependent cascade of molecular events. Each pathway activates its own initiator caspase (8, 9, and 10), which in turn will activate the executioner caspase-3. However, granzyme A works in a caspase-independent fashion. The execution pathway results in characteristic cytomorphological features including cell shrinkage, chromatin condensation, formation of cytoplasmic blebs and apoptotic bodies and finally phagocytosis of the apoptotic bodies by adjacent parenchymal cells, neoplastic cells or macrophages.

1.6.3.1. The extrinsic pathway

The extrinsic signalling pathways that initiate apoptosis involve trans-membrane receptor-mediated interactions (Figure 1.31). These involve death receptors that are members of the tumour necrosis factor (TNF) receptor gene super family (Locksley *et al.*, 2001). Members of the TNF receptor family share similar cyteine-rich extracellular domains and have a cytoplasmic domain of about 80 amino acids called the "death domain" (Ashkenazi *et al.*, 1998). This death

domain plays a critical role in transmitting the death signal from the cell surface to the intracellular signalling pathways. To date, the best-characterized ligands and corresponding death receptors include FasL/FasR, TNF-α/TNFR1, Apo3L/DR3, Apo2L/DR4 and Apo2L/DR5 (Rubio-Moscardo *et al.*, 2005).

1.6.3.2. The intrinsic pathway

The intrinsic signalling pathways that initiate apoptosis involve a diverse array of non-receptor mediated stimuli that produce intracellular signals that act directly on targets within the cell and are mitochondrial initiated events (Figure 1.31). The stimuli that initiate the intrinsic pathway produce intracellular signals that may act in either a positive or negative fashion. Negative signals involve the absence of certain growth factors, hormones and cytokines that can lead to failure of suppression of death programs, thereby triggering apoptosis. In other words, there is the withdrawal of factors, loss of apoptotic suppression, and subsequent activation of apoptosis.

Other stimuli that act in a positive fashion include, but are not limited to, radiation, toxins, hypoxia, hyperthermia, viral infections and free radicals. All of these stimuli cause changes in the inner mitochondrial membrane that result in an opening of the mitochondrial permeability transition (MPT) pore, loss of the mitochondrial trans-membrane potential and release of two main groups of normally sequestered pro-apoptotic proteins from the inter membrane space into the cytosol (Saelens *et al.*, 2004).

1.7. Cancer Chemotherapy

There are three main approaches in treating established cancer: surgical excision, irradiation and chemotherapy. The role of each of these depends on the type of tumour and the stage of its development. Chemotherapy is the treatment of cancer with drugs by killing cells that divide rapidly, one of the main properties of most cancer cells. Classically, anticancer drugs were grouped as chemotherapy, hormonal therapy and immunotherapy. Ideally, chemotherapeutic drugs should specifically target only neoplastic cells and should decrease tumour burden by inducing cytotoxic and / or cytostatic effects with minimal "collateral damage" to normal cells. Chemotherapy includes a number of families defined by both their chemical structure and mechanism of action. Some of the currently used anticancer drugs are listed below.

1.7.1. Microtubule interactive agents (MIAs)

Microtubules are protein polymers that are responsible for various aspects of cellular shape and movement. The major component of microtubules is tubulin, a protein containing two non-identical subunits (α and β). MIAs act by affecting the equilibrium between free tubulin dimers and assembled polymers (Jordan, 2002). Vinca alkaloids are large molecules produced by the leaves of the periwinkle plant *Catharanthus roseus*. There are slight structural differences between the different alkaloids, which lead to significant variation in therapeutic uses and toxicity. These agents act by binding to tubulin and inhibit its polymerisation in cells undergoing mitosis, leading to arrest at metaphase (Okouneva *et al.*, 2003).

Taxanes are derivatives of yew tree bark and act on microtubules, stabilising them in a polymerised state. Taxanes have significant activity against ovarian cancer, breast cancer and head and neck carcinoma. Resistance to taxanes and vinca alkaloids is due to decreased drug accumulation and results from overexpression of P-glycoprotein (Andriana *et al.*, 2001).

1.7.2. Topoisomerase inhibitors

Etoposide is derived from the mandrake root and inhibits DNA synthesis by inhibiting the enzyme topoisomerase II, which unwinds DNA, and by doing so causes DNA strands to break (Liu, 1989). Cancer cells are less able to repair this damage than healthy cells. Etoposide is a drug of choice in combination with cisplatin in the treatment of small cell lung carcinoma. The camptotecins are a new class of chemotherapeutic agents with a novel mechanism of action targeting the nuclear enzyme topoisomerase I and are effective in colorectal cancers (Bertino, 1997).

1.7.3. DNA interacting agents

The alkylating agents form strong electrophiles through the formation of carbonium ion intermediates. This results in the formation of covalent linkages by alkylation of various nucleophile moieties. The chemotherapeutic and cytotoxic effects are directly related to the alkylation of DNA. The nucleophilic groups of proteins and RNA can also be subject to attack by the alkylating agents although the exact results of these interactions are not known. The alkylating agents are generally considered to be non-specific to the cell cycle base and are known to be most cytotoxic to rapidly proliferating cells. The main alkylating agents are nitrogen mustards, busulphan and nitrosourease (Kaina *et al.*, 1990).

Cisplatin is one of a number of platinum complexes with antitumour activity and is the most frequently used anticancer drug. The platinum compounds are DNA cross-linking agents similar to but not identical to the alkylating agents (Li, *et al.*, 2010). The Bleomycins are a group of antitumour agents isolated from *streptmyces vercillus*. Bleomycin is metal-binding, water-soluble glycopeptide antibiotic. It has been reported to profoundly inhibit DNA synthesis, while RNA and protein synthesis are much less affected (Hall *et al.*, 1996).

1.7.4. Antimetabolites

Antimetabolites block cellular, metabolic pathways involved in DNA synthesis. This class includes folate antagonists, pyrimidine and purine analogues. The main folate antagonist is methotrexate. It is responsible for inhibiting dihydrofolate reductase, preventing the production of tetrahydrofolate, which results in interference with thymidylate synthesis. Pyrimidine analogues such as fluorouracil interfere with thymidylate synthesis, therefore inhibiting DNA synthesis. Purine analogues such as mercaptopurine are converted into nucleotides that cannot be used for RNA and DNA synthesis (Hatse *et al.*, 1999).

1.7.5. Hormonal Therapy

Hormonal therapy is one of the major modalities which involves the manipulation of the endocrine system through exogenous administration of specific hormones, particularly steroid hormones, or drugs which inhibit the production or activity of such hormones (hormone antagonists). Because steroid hormones are powerful drivers of gene expression in certain cancer cells, changing the levels or activity of certain hormones can cause certain cancers to cease growing, or even undergo cell death. These include aromatase inhibitors (Anastrozole, Letrozole) for treating breast cancer in postmenopausal women. The hormone receptor antagonist (Tamoxifen) is used for premenopausal women with breast cancer etc. (Vincent *et al.*, 2005).

1.8. Human Cells as *in vitro* model

Cancer cell lines are of great value in cancer research and cancer drug discovery activities. Investigating the potential anticancer activity of novel compounds on a well-established and reliable cancer cell line is a critically important step in determining the therapeutic characteristics and possible pathways involved in

cytostatic or cytotoxic modes of action. Among other criteria, a stably maintained ability for rapid spontaneous growth is an important and highly appreciated feature of a cancer cell line.

1.8.1. Human cancer cells:

1.8.1.1. Breast oestrogen-dependent cancer cells (MCF-7)

MCF-7 cells are human breast cancer cells derived from the pleural effusion of a 69-year-old Caucasian woman suffering from metastatic breast cancer in 1970. MCF-7 is the acronym of Michigan Cancer Foundation–7, referring to the institute in Detroit (USA) where the cell line was established in 1973 by Herbert Soule and co-workers (Soule *et al.*, 1973).

The MCF-7 cell line is the first hormone-responsive breast cancer cell line and retains several characteristics of differentiated mammary epithelium including the ability to process estradiol via cytoplasmic oestrogen receptors and the capability of forming domes. It also has differential sensitivities to oestrogens and anti-oestrogens, differential expression of oestrogen receptor (ER), ER mRNA, and progesterone receptor, and differences in tumourigenicity and proliferation rates (Levenson *et al.*, 1997). The addition of estradiol, which is one of the fractions of oestrogen, to the medium of MCF-7 cells induces a proliferative response. The characteristics of MCF-7 cells such as the estradiol dependence for growth and low metastatic potential have led to the assumption that they represent an early epithelial breast adenocarcinoma. Growth of MCF-7 cells is inhibited by the tumour necrosis factor alpha (TNF alpha). Secretion of Insulin-like Growth Factor Binding Proteins (IGFBP's) can be modulated by treatment with anti-oestrogens (Chen *et al.*, 2008).

MCF-7 cells have been shown to possess the ability to go through DNA fragmentation and therefore are also an excellent *in vitro* model for studying the

cell death phenomenon because of their susceptibility to apoptosis. These apoptotic responses of MCF-7 cell lines are profoundly exhibited by the apoptosis-inducing agents like Actinomycin-D (McConkey *et al.,* 1996). Moreover, the MCF-7 cell line is a perfect model to study the pathway of malignant progression as it can be subjected to appropriate endocrinologic and physiologic selective pressures for the derivation of variants with more progressed phenotypes (Lacroix *et al.,* 2004).

1.8.1.2. Breast oestrogen-independent cancer cells (MDA MB-468)

The MDA-MB-468 cell line was isolated in 1977 from a pleural effusion of a 51 year old Black female patient with metastatic adenocarcinoma of the breast. Morphologically, these cells are from epithelial tissues of mammary glands and grow as an adherent monolayer in growth medium.

Most human breast cancer cell lines express epidermal growth factor receptor (EGFR) at a level that is inversely proportional to the level of expression of the oestrogen receptor ER (Fitzpatrick *et al.,* 1984). MDA MB-468 human breast cancer cells do not express ER, contrary to MCF-7 cells and are also known as oestrogen independent or ER negative cell lines. Characteristically, MDA MB-468 over-expresses the EGFR as a result of gene amplification (Filmus *et al.,* 1985). While EGF and TGF-α, the natural ligands for the EGFR, have potent growth-promoting effects in many tissues including mammary epithelium (Taketani *et al.,* 1983), MD-MB-468 cells, which express ~ 2 x 10^6 oestrogen growth factor (EGF) binding sites per cell, are growth inhibited by EGF (Filmus *et al.,* 1985). There is generally an inverse relationship between EGFR number and EGF-induced mitogenesis such that a relatively low expression of EGFR is associated with growth stimulation by EGF, while high EGFR expression, as in MDA-MB 468 cells, is associated with growth inhibition by EGF (Ennis *et al.,* 1989). The mechanism of this EGF-induced growth inhibition is not clear.

1.8.1.3. Colorectal cancer cells (Caco-2)

Caco-2 cells are intestinal cell lines derived from colorectal adrenocarcinoma in a 72 years old Caucasian man in 1977, with the aim of performing studies on cancer mechanisms and related cytostatic therapies (Fog *et al.*, 1975). These cells are heterogeneous in characteristics and undergo spontaneous differentiation under standard culture conditions leading to the formation of a cell monolayer, that expresses several morphological and functional characteristics of the mature enterocyte (Pinto *et al.*, 1983).

The epidermal growth factor receptor (EGFR) was reported to be over-expressed in colon cancer (Mendelsohn, 2002). The activation of this receptor in Caco-2 cells plays an important role in the regulation of tumour growth (Spano *et al.*, 2005).

1.8.2. Normal human cells

There are only a few biochemical differences between cancer cells and normal cells and for this reason the efficacy of many anticancer drugs is limited by their toxicity to normal rapidly-growing cells.

1.8.2.1. Human umbilical vein endothelial cells (HUVEC)

Human Umbilical Vein Endothelial Cells (HUVEC) are isolated from normal human umbilical vein. They are cryo-preserved at the end of primary culture and can be cultured and propagated at least 16 population doublings. HUVEC are responsive to cytokine stimulation in the expression of cell adhesion molecules. These cell systems are commonly used for physiological and pharmacological investigations, such as macromolecule transport, blood coagulation, and fibrinolysis (Furie *et al.*, 1988; Weiss *et al.*, 1990).

The HUVECs are established to grow as an *in vitro* monolayer. Endothelial cells form a non-thrombogenic interface between blood and tissues. They function in normal processes including angiogenesis and wound repair and have a role in the pathogenesis of thrombosis and atherogenesis (Folkman 1983). Endothelial cells synthesise, process and regulate the local concentration of bioactive molecules (Broudy *et al.*, 1986). In addition, they transport insulin (King *et al.*, 1985) and perhaps other hormones from intravascular to extravascular sites. Thus, these cells can regulate the levels of hormones, factors and proteins in adjacent tissues. Factors that may modify endothelial cell growth or function include interleukin-1, tumour necrosis factor, β- transforming factor, thrombin, insulin-like growth factors I and II, and the vasoactive hormones, angiotensin I and II, bradykinin, and vasopressin (Brock *et al.*, 1986).

1.8.2.2. Human lymphatic monocytes (U937)

U937 is a human cell line established from a 37 year old male patient (Sundstrom and Nilsson, 1974). This cell line is one of the few cell lines displaying many monocytic characteristics and has thus served as a model for the differentiation of monocytes and macrophages *in vitro* in biomedical research.

Morphologically, as monocytes, U937 cells grow as a suspension in the medium. The granulocyte-macrophage colony stimulating factor (GM-CSF) inhibits the colony growth of these cells in agar culture and induces cell death by apoptosis, due to the induction of secretion of TNF-alpha (Okuma *et al.*, 2000). Proliferation of U937 cells has been shown to be inhibited by VEGI - Vascular Endothelial Growth Inhibitor (Haridas *et al.*, 1999). As shown by Defacque *et al.*, (1999), Vitamin D and retinoids co-operate to inhibit the proliferation and induce differentiation of U937 cells by a mechanism involving the production of the Tumour Growth Factor (TGF-β).

1.9. Aims and objectives of the present investigation

Within the sphere of cancer chemotherapy, many commercialised drugs have been obtained by the synthesis of new compounds, from natural sources or by structural modification of natural products. The objective of cancer chemotherapy is to kill cancer cells with as little damage as possible to normal cells. Therefore, any discovery of anticancer agents must be related to novel molecular targets; *i.e.* they should be effective against specific types of cancer cells but less toxic to normal cells, or have a unique mechanism of action for specific types of cancer (Sawyers, 2004; Zimmermann *et al.,* 2007). Our knowledge about the total physiological functions of target molecules is limited and drugs hardly ever target just the desired molecule (Yamanaka *et al.,* 2006) so consequently, some approved drugs are now being abandoned for their unexpectedly low-response rates or unpredictable adverse effects.

An alternative source of anticancer drugs are natural products, which frequently seem to be more effective and/or less toxic. Screening of medicinal plants on the basis of their folklore or traditional use in the treatment of tumours has revealed some remarkable discoveries in the past. However, some of the claims for the efficacy of such treatments are viewed with some scepticism because cancer, as a specific disease entity, was poorly defined in terms of folklore and traditional medicine.

Hence, ethno-botanical and ethno-pharmacological knowledge is crucial in the discovery and development of drugs from natural sources. The information about the identification of plant specie, part of plant used, preparation and dosage form of a folk remedy, traditional use, and preservation of medicinal plants dramatically facilitates the search for new drugs, and the time needed for drug development programs (Chabner *et al.,* 2005).

"The aims of the present investigation was to evaluate the anticancer activity of four medicinal plants, based on their folklore use in the treatment of different types of tumours and inflammatory conditions, and to explore and identify the potent chemical constituents from these plants responsible for antiproliferative activity against human cancer cells"

These medicinal plants: *Caralluma tuberculata* (Asclepiadaceae), *Fagonia indica* (Zygophyllaceae), *Solanum surattense* (Solanaceae), *Arisaema utile* (Araceae) belong to the North West and Himalayan region of Pakistan and are, or have been used as a source of food.

The selection and identification of these medicinal plants were accomplished after consultation with a practice medicinal botanist Dr. Manzoor Hussain, about their traditional use and a literature search for the main class of chemical constituents have been reported from them. In each case, there was moderate to good evidence of use as a part of the local culture's medical system. In addition, each plant had previously been known to yield interesting classes of compounds with *in vitro* anti-cancer use; *Caralluma tuberculata* (steroidal glycosides, pregnane), *Fagonia indica* (saponin, triterpenoids), *Solanum surattense* (steroidal alkaloids), *Arisaema utile* (lectins: glycoproteins, fatty acids: phenylalkanoic and phenylalkenoic acids).

The next objective was to adopt a bioactivity-guided fractionation approach to explore the most potent fraction with anti-proliferative effects in the crude extract and resultant organic fractions against three cultured cancer cell lines. As in most of the reported work, the studies were just limited to the isolation and identification of compounds from a particular plant specie, and further biological activities could not be investigated due to low yield of isolated compounds, "a common restriction with natural products". In phytochemical analysis, structural elucidation of the isolated compounds from the bioactive fraction utilised advanced spectroscopic and X-ray crystallographic experiments.

Compounds which inhibit oestrogen biosynthesis have been shown to lead to tumour regression, and therefore a reduction in tumour mass. It was hypothesised that the pregnane backbone may have an antiproliferative effect on hormone-dependent cancer cells through the disruption of the steroidal cascade, and therefore sex-steroid biosynthesis (in particular, oestrogen biosynthesis). Therefore, another objective was to characterise the effects of isolated moieties on the growth of certain cancer cells.

Human breast cancer cells (MCF-7, oestrogen-dependent cancer cells) were chosen in the case of pregnane and other steroidal glycosides, because of the structural similarity to the natural androgens. In addition, to study the drug-receptor action, it was therefore sensible to investigate the oestrogen-independent cancer (MDA MB-468) cell line as well. Other cell lines were also tested: the commonly used Caco-2 colon cancer cells.

Isolated compounds were also evaluated for toxic effects against normal, non-malignant cells (HUVECs, U937 cells). Another key objective in cancer drug discovery is the mechanism of cell death, as necrosis causes a generalised inflammatory response, whereas apoptosis is a programmed form of cell death, and of interest in anti-cancer studies.

There were some limitations. Application of crude extracts or even pure chemicals isolated from plants does not reflect the changes caused to these chemicals by the usual ADME parameters e.g. metabolism and the bioavailability of the active chemicals remains unknown.

2. MATERIALS AND METHODS

2.1. Plant material collection:

A- *Caralluma tuberculata* (Asclepiadaceae)

Caralluma tuberculata (local name: *Chungan*) was purchased from the vegetable market of Mansehra Valley, Pakistan, in September 2007. The plant (Figure 2.1-A) was identified by Dr. Manzoor Hussain, Department of Botany, Hazara University, Mansehra, Khyber Pakhtunkhwa, (previously known as NWFP) Pakistan. A voucher specimen (HU-2761A-07) was deposited in the Herbarium of Department of Botany, Hazara University, Mansehra, Pakistan.

B- *Fagonia indica* (Zygophyllaceae)

The aerial parts of *Fagonia indica* (in flowering) were collected from a rocky habitat near the Indus river bank, about one kilometre from Gomal University Campus, Dera Ismail Khan, Khyber Pakhtunkhwa, Pakistan in March 2007. The prickly herb (Figure 2.1-B) locally known as *Damhan* was identified by Prof. Qazi Najm-us-Saqib, Gomal University, D.I. Khan, Pakistan. A voucher specimen (GPharm-148-07) was deposited in the Herbarium of Department of Pharmacognosy, Faculty of Pharmacy, Gomal University, D.I.Khan Pakistan.

C- *Solanum surattense* (Solanaceae)

The leaves of *Solanum surattense* (Yellow-Berried Nightshade) were collected from the Siran Valley, Mansehra district, Pakistan in June 2007. The young shoots with minute star-shaped hairs, attached to the leaves (locally known as Kindiari (Figure 2.1-C), were identified by Dr. Manzoor Hussain, Hazara University, Pakistan and submitted as voucher specimen (HU-2762A-07) in the Herbarium of Department of Botany, Hazara University, Mansehra, Pakistan.

D- *Arisaema utile* (Araceae)

A perennial tuberous herb *Arisaema utile*, locally known as Surganda or Sanp Ki Booti (Hindko), Indian turnip (English), was collected in July 2007, at an altitude of about 2700 m above sea level, from the Siran Valley, district Mansehra, Pakistan. The Cobra Lily plant (Figure 2.1-D) was identified by Dr. Manzoor Hussain, Hazara University, Pakistan and submitted as a voucher specimen (HU-2763A-07) in the Herbarium of Department of Botany, Hazara University, Mansehra, Pakistan.

Figures 2.1-A,-B,-C,-D: Medicinal plants used in the present investigation,
A. *Caralluma tuberculata*, B. *Fagonia indica*, C. *Solanum surattense*, D. *Arisaema utile*

2.2. Chemicals used:

All the organic solvents for compounds isolation were purchased from Fisher (Fisher Scientific UK Ltd., Leicestershire, UK), unless otherwise stated.

Silica gel 60 F_{254} precoated aluminium cards (0.2 mm thickness) for Thin Layer Chromatography (TLC) were ordered from Merck Ltd., Germany.

Silica gel 60738 for column chromatography (0.035 – 0.070 mm) was purchased from Sigma-Aldrich Company Ltd., Dorset, UK.

Silica gel 90 RP-C18 (60757) for column chromatography-reversed phase was purchased from Fluka Analytical, Switzerland.

D-glucopyranose (158968) was purchased from Sigma Aldrich (Sigma Aldrich Company Ltd., Dorset, UK), allopyranose (7283-09-2) from Carbosynth Limited (Berkshire, UK), D-cymarose (10366) and ribopyranose from A-Chem Technologies Co. Ltd. (Suzhou industrial park, China).

Formic acid (94318) ~98% (Fluka) for mass spectroscopy was purchased from Sigma-Aldrich Company Ltd., Dorset, UK.

Wilomonds 5mm Precision NMR tubes (527-PP-8) were ordered from Gross Scientific Instruments Ltd. Cheshire UK.

Deutrated NMR solvents chloroform-D 99.8% (DLM-7-MS), methanol-D3 99.5% (DLM-598) were purchased from Gross Scientific Instruments Ltd. Cheshire UK.

2.3. Extraction

2.3.1. Preparation of plant material for extraction

All the four plants: *Caralluma tuberculata*-CT (10 kg), *Fagonia indica*-FI (4 kg), *Solanum surattense*-SS (6 kg), *Arisaema utile*-AU (5.5 kg), were washed under tap water to remove any sand or any dust. Parts of the plants used in current study, CT: whole plant, FI: aerial parts, SS: young shoots with leaves and AU: underground rhizome part, were chopped into small pieces, then dried in the relatively dark well ventilated area for about 14 days to completely dry the plant materials. The dried plant materials were then powdered separately in a meat grinder in order to facilitate the extraction process.

2.3.2. Extraction of crude ethanolic extract

The precise mode of extraction naturally depends on the texture of the plant material being extracted and on the type of chemical constituents that is being isolated. As pregnane glycosides in *Caralluma tuberculata* have been previously reported to be relatively unstable (Ghazala *et al.*, 1995) and *Arisaema utile* grows in a habitat of 6-10°C, a cold extraction (maceration) technique was used with powdered plant material (CT: 1.5 kg, AU: 800 g) for extraction. However, *Fagonia indica* (200 g) and *Solanum surattense* (250 g) were extracted using a hot extraction method (Soxhlet apparatus).

2.3.2.1. Maceration

The powdered plant material was macerated in ethanol (1000 ml) in a closed glass container, stored at room temperature for one week, followed by vacuum filtration. This procedure was repeated three times and the extract was filtered under vacuum. The combined ethanolic filtrates were concentrated after evaporating ethanol under reduced pressure on a rotary evaporator at 40°C; the

semi-solid residues yielded crude extracts of *Caralluma* and *Arisaema*, approximately 200 g and 75 g respectively.

2.3.2.2. Soxhlet extraction

The powdered plant material was filled in a Soxhlet thimble. This method is very useful when working with powdered plant material on the gram scale. Ethanol (500 mL) was used as extraction solvent to maximise the complete extraction. The combined filtrates were concentrated as mentioned previously, which resulted in crude extract for *Fagonia indica* (50 g) and *Solanum surattense* (55 g).

2.4. Fractionation

The crude extract from each medicinal plants was divided into four organic and an aqueous fraction according to the chemical constiuents solubilities in the respective solvent system.

2.4.1. Fractionation of crude ethanolic extract

The concentrated ethanolic crude extract was dispersed in H_2O (1000 ml), partitioned into four organic fractions starting in turn with hexane (3 x 300 ml), chloroform ($CHCl_3$: 3 x 500 ml) and Ethyl acetate (EtOAc: 3 x 500 ml) respectively. The methanol (MeOH: 3 x 300 ml) fraction was separated from the insoluble residue after evaporating the remaining aqueous layer. This procedure was repeated for all four crude extracts from the medicinal plants. The resulting fractions were concentrated under reduced pressure at 40°C on a rotary evaporator. The fractionation process is summarised in Figure 2.2.

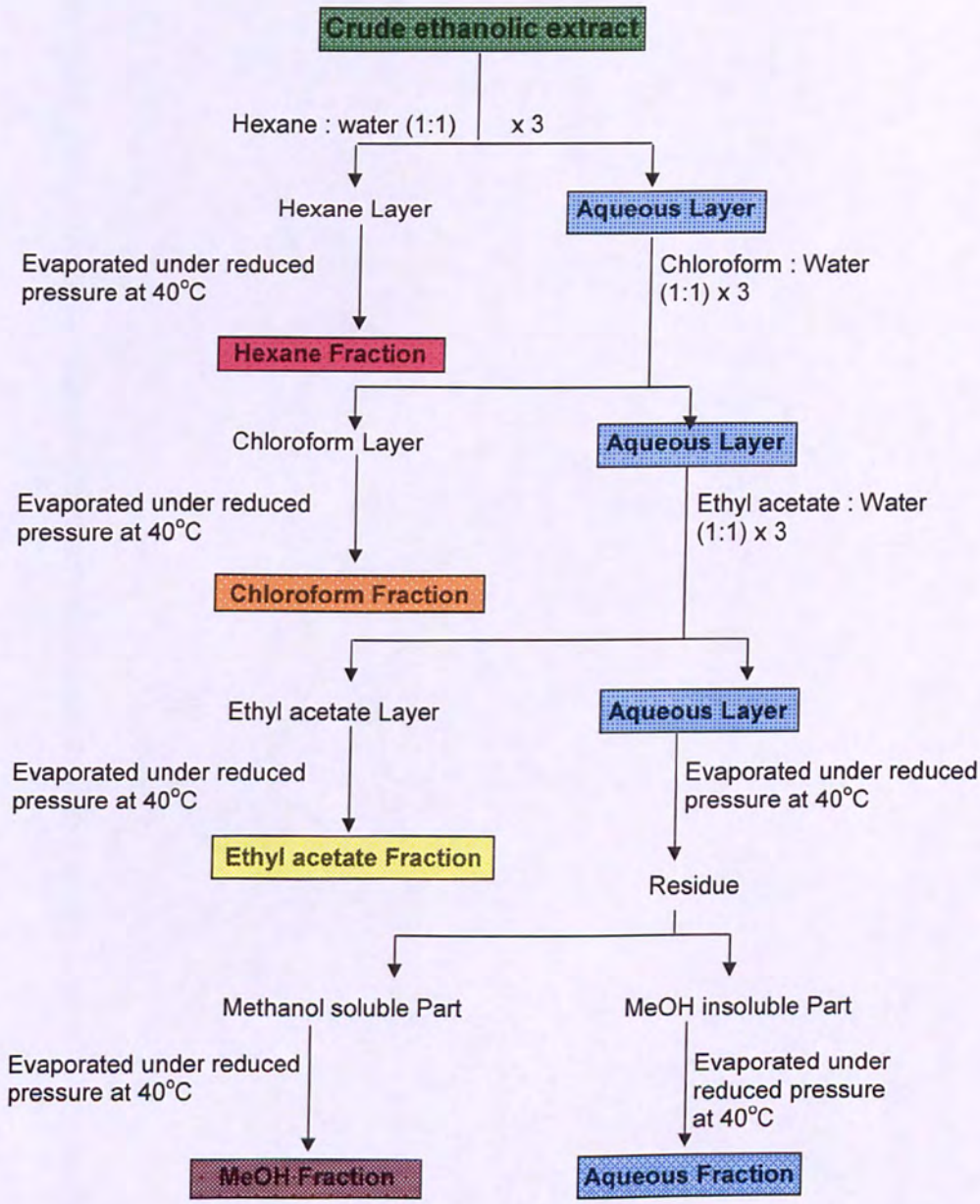

Figure 2.2: Fractionation of crude ethanolic extract into four organic and an aqueous fractions

2.5. Phytochemical analysis:*Caralluma tuberculata*

The crude ethanolic extract of *Caralluma tuberculata,* along with organic and aqueous fractions were screened for cytotoxic activity against human breast cancer cells (MCF-7 and MDA MB-468) and colon cancer cells (Caco-2). Based on cell viability assays, the ethyl acetate fraction was found to be the most potent fraction and was selected for further phytochemical analysis.

2.5.1. Isolation of Compounds 1 and 2

Flash column chromatography was performed on silica gel 60 (2 kg) for column (glass column, 100 cm x 12 cm) adsorption chromatography, manually packed in $CHCl_3$. After the column was cooled to the touch, a volume of the $CHCl_3$ was passed through the silica to remove any remaining air and to equilibrate the column. The EtOAc fraction was loaded (12 g) as adsorbed slurry on silica on the top of the packed column. Stepwise elution was carried out using a $CHCl_3$-MeOH gradient solvent system (1:0, 20:1, 10:1, 8:1, 5:1, 3:1, 2:1, and 0:1; 2.0 L for each step). Fractions of 200 ml were collected and concentrated; TLC was carried out for all the eluted fractions and visualised under UV lamp (254 nm). Fractions possessing similar R_f values were combined together and this resulted in 25 major fractions. Fraction 18 (352 mg) showed a mixture of two compounds on TLC with EtOAc : MeOH (4:1). The fraction was chromatographed on a silica gel column (500 g, 3.5 cm x 60 cm) and eluted with EtOAc : MeOH (5:1, 4:1 1 L each eluent). Repeated adsorption column chromatography of Fraction 18 resulted in three sub-fractions. Sub-fraction I yielded Compound **1** (62 mg) while Sub-fractions II and III were further purified through Reverse Phase Column Chromatography. Sub-fractions I and II were combined together and were loaded on RP-C18 silica (100 g) packed in a glass column (40 cm x 3 cm) with MeOH : H_2O (80:20, 0.5 L) to give Compound **2** (75 mg).

2.5.2. Physico-chemical characteristics of compounds 1 and 2

Compounds **1** and **2** were obtained as amorphous powders. Melting points were determined on a Gallenkamp (Sanyo) melting point instrument and are uncorrected. Optical rotations were measured in MeOH solutions on a Optical Activity AA-10 automatic polarimeter.

To determine the steroidal nature of the compounds, the EtOAc fraction and the isolated Compounds **1** and **2** were analysed by Liebermann-Burchard test (Burke *et al.,* 1974; Halim & Khalil 1996). Among the many colour reactions for steroids, the Liebermann-Burchard procedure is perhaps the most widely used test. Liebermann- Burchard colour reactions for steroids have oxidative mechanisms, yielding oxidation products. This reaction was described initially by Liebermann in 1885 and applied to cholesterol analysis shortly after by Burchard. Chloroform was used as a solvent in the early studies, but the Liebermann-Burchard (L-B) reaction, as performed today, is carried out in an acetic acid, sulphuric acid and acetic anhydride medium (Halim and Khalil 1996).

About 10 drops of 1% solution of the EtOAc fraction in chloroform were added to a dry test tube. Then acetic anhydride, (about 5 drops) were added to the test tube and the solution was mixed well. Then 3 drops of concentrated sulphuric acid was added and the solution was mixed well again. Any colour change was recorded and then the test tube was allowed to stand for 5 minutes. A further change in colour of the solution was observed and recorded. A similar procedure was repeated for compounds **1** and **2**, in order to check the presence of a steroidal skeleton.

2.5.2.1. Acid Hydrolysis of Compounds 1 and 2

In order to determine sugar moieties, Compounds **1** and **2** were hydrolysed according to the method reported by Halim and Khalil (1996). Each compound [**1**

(20 mg) and **2** (24 mg)] was added to a solution (25 ml) containing 0.05 N H_2SO_4 in 50% MeOH at 70°C. After 1 h, a further 5 ml of H_2O was added and the temperature maintained for a further 30 min. The solution was allowed to cool down to room temperature and fractioned with $CHCl_3$ to separate the aglycon portion from the sugar moieties. The aqueous layer was concentrated and TLC was performed against the authentic samples using a mobile phase of $CHCl_3$-MeOH-H_2O (18:3:1). The R_f values revealed that in the case of Compound **1**, the glycoside is comprised of two sugar moieties that are glucopyranose (0.52) and ribopyranose (0.65) while Compound **2** contained three sugars glucopyranose (0.52), allopyranose (0.62) and cymarose (0.7).

The $CHCl_3$ layer was further investigated for the aglycon moiety. After evaporating on the rotary evaporator at 35°C under reduced pressure, the amorphous white powder (6 mg) was loaded on a glass column (20 cm x 2 cm), using isocratic elution with mobile phase $CHCl_3$: EtOAc (90:10). Ten fractions (10 ml each) were collected. The fractions were kept overnight at room temperature and the solvents allowed to evaporate. Fractions 6 and 7 showed some crystals at the bottom of the vials. Crystals were collected and re-crystallised in 1 ml aqueous methanol (50:50) and kept at room temperature. After 48 hours, needle like colourless crystals were observed in the aqueous alcoholic solution.

The crystals were further analysed by X-ray crystallography to elucidate the structure of the hydrolysed form of steroids present in the glycosides.

2.5.3. Structure elucidation of Compounds 1 and 2 - Spectroscopy

Spectroscopy is the study of the absorption and emission of radiation by matter. In physical and analytical chemistry, spectrometry is often used in the identification of substances through the spectrum emitted from or absorbed by them.

2.5.3.1. Infra-Red spectroscopy

Infra-red (IR) spectroscopy provides a way of finding the functional groups in a molecule, because it detects the stretching and bending vibrations of bonds. It is particularly good at detecting the stretching of unsymmetrical bonds of the kind found in functional groups such as OH, C=O, NH_2, and NO_2. Fourier Transform infra-red (FT-IR) spectra for Compounds **1** and **2** were recorded on a PerkinElmer Spectrum 100FT-IR spectrometer with Spectrum Express software on sodium chloride discs.

2.5.3.2. Liquid Chromatography- Mass Spectrometry (LC-MS)

To determine the molecular weight of Compounds **1** and **2**, high resolution (HR) mass spectra were recorded on a Water's LCT Mass Spectrometer with Time-of-Flight (TOF), using electro spray ionisation (ESI +ve mode) connected to an Alliance auto-sampler injection system. The analyte was prepared in MeOH-H_2O (80:20) with 0.1% formic acid to enhance protonation and increase sensitivity. At a flow rate of 20 µl/min analyte, a mass spectrum was recorded relating to their mass to charge (*m/z*) at a capillary potential of 3,500 V. N_2 was used as nebuliser gas. The ESI-MS (+ve mode) fragmentation pattern was recorded on LC-MS/MS TSQ Quantum Access (Thermo electronic corporation UK) with ACCELA auto-sampler. Ionisation of the analytes were carried out at sheath gas (N_2) pressure 10 bars, auxiliary gas (N_2) pressure 5 bars, capillary temperature 350°C and collision energy (CE) 35 eV.

2.5.3.3. Nuclear Magnetic Resonance (NMR) spectroscopy

Nuclear Magnetic Resonance (NMR) spectrometry is basically another form of absorption spectroscopy which is used as a powerful tool in structure elucidation of unknown compounds. Under appropriate conditions in magnetic field, a sample can absorb electromagnetic radiation in the radio frequency (rf) region at

the frequencies governed by the characteristics of the sample. Absorption is a function of certain nuclei in the molecule. A plot of the peak intensities of the absorption peaks versus frequencies constitutes an NMR spectrum.

Samples of Compounds 1 and 2 were prepared in MeOH-D_3 (CD_3OD). Both one-dimensional Proton (^1H), Carbon (^{13}C), DEPT (Distortion Enhancement by Polarisation Transfer), edited DEPT NMR and two-dimensional HETCOR (Heteronuclear Corelation), DQF-COSY (Double Quantum Filtered ^1H-^1H Correlation spectroscopy) and HMBC (Heteronuclear Mutiple Bond Coherence) NMR spectra were recorded using a JEOL Eclipse 400 NMR spectrometer with JEOL Delta version 7.2 control and processing software. Where peak positions were quoted on the chemical shift (δ) scale in ppm (parts per million) relative to an internal standard. Tetramethylsilane (TMS) was used as a reference sample.

2.6. Phytochemical analysis: *Fagonia indica*

In an activity guided fractionation approach, the *Fagonia indica* EtOAc fraction out of the four organic fractions was found to possess significant cytotoxic activity in cell viability assays and subjected to further phytochemical analysis in a search for bioactive compounds from this fraction.

2.6.1. Isolation of Compound 3

Flash column chromatography was performed on the EtOAc fraction of *Fagonia indica* (as described previously for *Caralluma tuberculata* section: Isolation). EtOAc fraction (2 g) was loaded on silica gel 60 (800 g) manually packed in glass column using $CHCl_3$ as solvent. Normal phase adsorption chromatography was carried out with gradient elution using mixture of chloroform, EtOAc and MeOH in an increased polarity order. TLC was carried out for all the eluted fractions and visualised under UV lamp (254 nm). Fractions possessing similar R_f values were combined together and this resulted in 6 groups (A-F). Group **D** was further

purified with reverse phase column chromatography using gradient system of elution. Sub-group (**D-4**) was found pure on TLC in EtOAc: MeOH (40:60) with some non polar impurities. Sub-group (**D-4**) was finally passed through silica gel again with normal phase column chromatography in an isocratic mobile phase EtOAc: MeOH (50:50). Compound **3** was visualised under a UV lamp on a developed TLC plate as single compound. Various concentrations of mobile phase used during isolation are summarised in Table 2.1

Normal Phase: Gradient System			
Mobile phase(Column)	*Fractions*	*Mobile Phase (TLC)*	*Groups*
Chloroform	1-8	Chloroform	A
Chloroform : EtOAc (50:50)	9-26	Chloroform: EtOAc (50:50)	B
EtOAc	27-40	EtOAc: MeOH (95:5)	C
EtOAc : MeOH (50:50)	**41-56**	**EtOAc: MeOH (40:60)**	**D**
EtOAc : MeOH (30:70)	57-84	EtOAc : MeOH (20:80)	E
MeOH	85-105	MeOH	F
Reverse Phase (group-D): Gradient System			
MeOH: Water (20:80)	1-15	EtOAc: MeOH (40:60)	D1
MeOH: Water (30:70)	16-21	EtOAc: MeOH (40:60)	D2
MeOH: Water (40:60)	22-28	EtOAc: MeOH (40:60)	D3
MeOH: Water (50:50)	**29-85**	**EtOAc: MeOH (40:60)**	**D4**
MeOH: Water (60:40)	86-95	EtOAc: MeOH (40:60)	D5
Normal phase (D4): Isocratic System			
EtOAc : MeOH (50:50)	1-8	EtOAc: MeOH (40:60)	Mixture
EtOAc : MeOH (50:50)	**9-18**	**EtOAc: MeOH (40:60)**	**3**
EtOAc : MeOH (50:50)	19-28	EtOAc: MeOH (40:60)	Mixture

Table 2.1:Mobile phases for gradient and isocratic elution systems for the isolation of compound 3 from ethyl acetate fraction of Fagonia indica

2.6.2. Physico-chemical characteristics of Compound 3

The melting point and optical rotation values were determined as described in experimental section for *Caralluma tuberculata*. Compound **3**, as a white amorphous powder was analysed for its steroidal nature following the Liebermann-Burchard test method (Burke *et al.*, 1974; Halim & Khalil 1996), as described previously.

2.6.2.1. Acid hydrolysis of Compound 3

To investigate the type of sugar moieties present in the molecule; Compound **3** (20 mg) was hydrolysed as described in detail for Compounds **1** & **2**, according to the method reported by Halim and Khalil (1996). The concentrated aqueous layer was analysed on TLC against the authentic samples using a mobile phase of $CHCl_3$:MeOH:H_2O (18:3:1). The R_f values indicated that Compound **3** was comprised of two sugar moieties allopyranose (0.65) and cymarose (0.78).

2.6.3. Structure elucidation of Compound 3 - Spectroscopy

To elucidate the structure, Compound **3** was analysed through a series of spectroscopic experiments as described previously in detail for Compounds **1** and **2**.

2.6.3.1. Infra-Red spectroscopy

Fourier Transform Infra-Red (FT-IR) spectra for Compound **3** was recorded on a PerkinElmer Spectrum 100FT-IR spectrometer with Spectrum Express software on sodium chloride discs.

2.6.3.2. Liquid Chromatography-Mass Spectrometry (LC-MS)

The molecular weight was measured by high resolution (HR) mass spectrometryon a Water's LCT mass spectrometer with time-of-flight (TOF) using electro-spray ionisation (ESI +ve mode). The sample was prepared in MeOH-H_2O (80:20) with 0.1% formic acid to enhance protonation and increase sensitivity. At a flow rate of 30 µl/min analyte, a mass spectrum for molecular ions was recorded relating to their mass to charge (*m/z*) at a capillary potential of 3,300 V. A ESI-MS (+ve mode) fragmentation pattern for daughter ions was recorded on the LC-MS/MS at a collision energy (CE) 38 eV and capillary temperature 350°C.

2.6.3.3. Nuclear Magnetic Resonance (NMR) spectroscopy

A series of one-dimensional ^1H, ^{13}C, DEPT, edited DEPT NMR and two-dimensional HETCOR , DQF-COSY and HMBC NMR experiments were carried out on Compound **3** using JEOL Eclipse 400 NMR spectrometer. Vapours of Tetramethylsilane (TMS) were used as a reference; samples were prepared in MeOH-D_3 (CD_3OD).

2.7. Phytochemical analysis: *Solanum surattense*

The chloroform fraction of *Solanum surattense* was selected for isolation of bioactive compounds on the basis of the initial screening results for cytotoxic activity against three cancer cell lines (MCF-7, MDA MB-468 and Caco-2).

2.7.1. Isolation of Compounds 4 and 5

The chloroform fraction (2 g) from *Solanum surattense* was loaded on a normal phase silica gel 60 (850 g) for flash adsorption column chromatography. A glass

column was packed manually using hexane as starting mobile phase for elution. Step-wise elution was carried out at various ratios of hexane, chloroform, ethyl acetate and methanol. A total of 133 fractions were collected and were combined into 11 groups (A-K) according to their R_f values. Groups **D** and **G** were selected for possessing good quantity and showed good separation results on the TLC.

Normal Phase: Gradient System			
Mobile phase(Column)	*Fractions*	*Mobile Phase (TLC)*	*Groups*
Hexane	1-8	Hexane : Chloroform (50:50)	A
Hexane : Chloroform (50:50)	9-20	Hexane : Chloroform (30:70)	B
Chloroform	21-28	Chloroform : EtOAc (90:10)	C
Chloroform : EtOAc (90:10)	**29-56**	**Chloroform : EtOAc (80:20)**	**D**
Chloroform : EtOAc (80:20)	55-62	Chloroform : EtOAc (70:30)	E
Chloroform : EtOAc (70:30)	63-74	Chloroform : EtOAc (50:50)	F
Chloroform : EtOAc (50:50)	**75-101**	**Chloroform : EtOAc (30:70)**	**G**
Chloroform : EtOAc (30:70)	102-114	Chloroform : EtOAc (10:90)	H
EtOAc	115-126	EtOAc: MeOH (98:02)	I
EtOAc: MeOH (50:50)	127-132	EtOAc: MeOH (40:60)	J
MeOH	133	MeOH	K
Normal Phase (group-D): Isocratic System			
Chloroform : EtOAc (90:10)	1-9	Chloroform : EtOAc (80:20)	Mixture
Chloroform : EtOAc (90:10)	**10-37**	**Chloroform : EtOAc (80:20)**	**4**
Chloroform : EtOAc (90:10)	38-45	Chloroform : EtOAc (80:20)	Mixture
EtOAc	46-50	Chloroform : EtOAc (80:20)	Mixture
Normal phase (group-G): Isocratic System			
Chloroform : EtOAc (50:50)	1-12	Chloroform : EtOAc (30:70)	Mixture
Chloroform : EtOAc (50:50)	**13-42**	**Chloroform : EtOAc (30:70)**	**5**
Chloroform : EtOAc (50:50)	43-48	Chloroform : EtOAc (30:70)	Mixture
EtOAc	49-55	Chloroform : EtOAc (30:70)	Mixture

Table 2.2: Mobile phases for gradient and isocratic elution systems for the isolation of Compounds 4 and 5 from chloroform fraction of Solanum surattense

Both groups **D** and **G** were further purified by normal phase column chromatography separately, using isocratic system of elution, which resulted in isolation of Compounds **4** and **5**. Various ratios of mobile phases used during isolation process are summarised in Table 2.2.

2.7.2. Physico-chemical characteristics of Compounds 4 and 5

Physically, both Compounds **4** and **5** were oily or waxy in appearance and were not suitable to determine the melting points. However, both compounds were analysed for steroidal characteristics using the Liebermann-Burchard test method (Burke *et al.*, 1974; Halim and Khalil, 1996), as described previously.

2.7.3. Structure elucidation of Compounds 4 and 5 - Spectroscopy

Both Compounds **4** and **5** were studied through various spectroscopic techniques, to elucidate the possible structures of compounds present in the chloroform fraction of *Solanum surattense.*

2.7.3.1. Infra-Red spectroscopy

IR spectra were recorded as described previously on sodium chloride discs on a PerkinElmer Spectrum 100FT-IR spectrometer.

2.7.3.2. Gas Chromatography-Mass Spectrometry (GC-MS)

Gas chromatography and mass spectrometry are highly compatible techniques. In both techniques, the sample is in the vapour phase, and both techniques deal with about the same amount of sample. It is widely used in identification and quantification of volatile and semi-volatile organic compounds in complex mixtures and for structural determination of unknown organic compounds in

complex mixtures. The GC–MS study was conducted on a Shimadzu GCMS-QP5050A instrument with a BPX-5 column of length 30 m, an inner diameter of 0.25 mm and 0.25 μm film thickness. The temperature programmes were as follows: Initial column temperature of 50°C for 1 min, raised to 150°C with 5 min hold time at a rate of 5°C / min and finally 250°C for 2 min at a rate of 10°C / min. The carrier gas was helium with a flow-rate of 1.5 ml / min. The inlet temperature was 250°C. All mass spectra were acquired in the electron impact (EI) mode with mass range was 50-500 m/z. The interface to the mass spectrometer was heated to 280°C. Samples of Compounds **4** were prepared in chloroform. Ionisation was switched off during the first 3 min, to avoid solvent overloading. The injection volume was 1 μl and the analysis was performed in full scan mode.

2.7.3.3. Liquid Chromatography-Mass Spectrometry (LC-MS)

Samples of Compounds **4** & **5** were prepared in MeOH. Molecular weights were determined on a high resolution (HR) Water's LCT mass spectrophotometer with Time-of-Flight (TOF) using electro-spray ionisation (ESI +ve mode). Analyte flow rate was 50 μl/min. The mass spectrum was recorded according to mass to charge ratio (*m/z*) at a capillary potential 3,500 V. ESI-MS (+ve mode) fragmentation pattern for daughter ions was recorded on LC-MS/MS at collision energy (CE) 40 eV and capillary temperature 350°C.

2.7.3.4. Nuclear Magnetic Resonance (NMR) spectroscopy

Tetramethylsilane (TMS) vapours were used as a reference; samples of Compounds **4** & **5** were prepared in $CDCl_3$. A number of one-dimensional ^1H, ^{13}C, DEPT, edited DEPT NMR and two-dimensional HETCOR, DQF-COSY and HMBC NMR experiments were conducted on a JEOL Eclipse 400 NMR spectrometer.

2.8. Phytochemical analysis: *Arisaema utile*

In a bioactivity guided fractionation approach, *Arisaema utile* crude extract and the resultant organic and aqueous fractions were found to be cytotoxic against breast and colon cancer cells. The chloroform fraction showed maximum percentage growth inhibition, as compared to the rest of the fractions and was selected for further phytochemical analysis.

2.8.1. Isolation of Compounds 6 and 7

The chloroform fraction (1.5 g) was adsorbed on silica gel 60 and poured on top of a silica bed in a glass column manually packed with silica gel 60 (700 g) for normal phase flash column chromatography.

Normal Phase: Gradient System			
Mobile phase(Column)	*Fractions*	*Mobile Phase (TLC)*	*Groups*
Hexane	1-12	Hexane : Chloroform (50:50)	A
Hexane : Chloroform (50:50)	13-27	Hexane : Chloroform (30:70)	B
Chloroform	**28-30**	**Chloroform : EtOAc (90:10)**	**C**
Chloroform	31-39	Chloroform : EtOAc (90:10)	D
Chloroform : EtOAc (90:10)	40-46	Chloroform : EtOAc (80:20)	E
Chloroform : EtOAc (80:20)	47-54	Chloroform : EtOAc (70:30)	F
Chloroform : EtOAc (70:30)	**55-89**	**Chloroform : EtOAc (50:50)**	**G**
Chloroform : EtOAc (50:50)	90-108	Chloroform : EtOAc (30:70)	H
Chloroform : EtOAc (30:70)	109-118	Chloroform : EtOAc (10:90)	I
EtOAc	119-125	EtOAc: MeOH (98:02)	J
Normal Phase (group-G): Isocratic System			
Chloroform : EtOAc (70:30)	1-12	Chloroform : EtOAc (50:50)	Mixture
Chloroform : EtOAc (70:30)	**13-45**	**Chloroform : EtOAc (50:50)**	**6**
Chloroform : EtOAc (70:30)	46-58	Chloroform : EtOAc (50:50)	Mixture
Chloroform : EtOAc (70:30)	59-65	Chloroform : EtOAc (50:50)	Mixture

Table 2.3: Mobile phase ratios for isolation of Compounds 6 and 7 from chloroform fraction of Arisaema utile.

A gradient system of elution was used at various ratios of hexane, chloroform and ethyl acetate in an increased polarity mode. In total, 125 fractions were collected and were combined into 10 groups (A-J) according to their R_f values on TLC. Group **G** was further purified by normal phase adsorption column chromatography, using isocratic system of elution, which resulted in the isolation of Compound **6**. Various ratios of mobile phases used during isolation process are summarised in Table 2.3.

Group **C** was found to crystallise when left overnight at room temperature. On TLC, group **C** showed only one spot under a UV lamp (254 nm). The crystals from group C were dissolved in 1 ml aqueous methanol (50:50) and kept at room temperature for re-crystallisation. After 48 hours, needle-like colourless crystals (Compound **7**) were observed in the aqueous alcoholic solution. Unfortunately, yield was very low and only 2.5 mg of crystals could be recovered.

2.8.2. Physico-chemical characteristics of Compounds 6 and 7

Physically, compound 6 was oily in appearance and was not suitable to determine the melting point. However, compound 7 was obtained as colourless tiny needle like crystals. Melting point was determined on a Gallenkamp (Sanyo) melting point instrument and are uncorrected.

2.8.3. Structure elucidation of Compounds 6 – Spectroscopy

Compound **6** was analysed through various spectroscopic techniques, to elucidate the possible structures of compounds present in chloroform fraction of *Arisaema utile*.

2.8.3.1. Infra-Red spectroscopy

IR spectra were recoreded as described previuosly on sodium chloride discs on PerkinElmer Spectrum 100FT-IR spectrometer.

2.8.3.2. Gas Chromatography-Mass Spectrometry (GC-MS)

A sample of Compound **6** was prepared in $CHCl_3$. GC–MS spectra were recorded on a Shimadzu GCMS-QP5050A instrument with the column and the temperature programmes specification, as described earlier. Ionisation was switched off during the first 3 min, to avoid solvent overloading. The injection volume was 1 µl and the analysis was performed in full scan mode. The mass spectra were acquired in the electron impact (EI) mode with mass range 50-500 m/z. The interface to the mass spectrometer was heated to 280°C.

2.8.3.3. Liquid Chromatography-Mass Spectrometry (LC-MS)

High resolution mass (HR) mass spectra of Compound **6** were recorded on a Water's LCT mass spectrometer with Time-of-Flight (TOF) using electro-spray ionisation (ESI). Samples were prepared in MeOH and at a flow rate of 50 µl/min, the mass spectrum was recorded according to mass to charge ratio (*m/z*) at a capillary potential 3,400 V. Compound **6** was not ionising in ESI positive mode but showed a molecular ion peak in ESI negative mode. The fragmentation pattern of the molecule was studied on LC-MS/MS; the daughter ions were produced at a collision energy (CE) 38 eV and capillary temperature was 350°C.

2.8.3.4. Nuclear Magnetic Resonance (NMR) spectroscopy

The NMR sample of Compound **6** was prepared in $CDCl_3$, and Tetramethylsilane (TMS) vapours were used as a reference. Both one-dimensional ^{1}H, ^{13}C, DEPT, edited DEPT NMR and two-dimensional HETCOR, DQF-COSY and HMBC NMR experiments were carried out on JEOL Eclipse 400 NMR spectrometer.

2.9. X-Ray Crystallography

Crystallography is the study of crystals. More precisely, it is the science of deducing the positions of atoms within these crystals, as well as their element types and the bonding arrangements between them.

X-ray crystallography involves the production of a diffraction pattern (also known as a 'scattering pattern') from parameterised X-ray exposure of a crystal. These patterns are analysed mathematically and compared with patterns generated from a predicted chemical model. Such models undergo iterative refinement – i.e. they are repeatedly modified to account for differences observed between predicted (model) data and observed (X-ray) data. The ultimate goal is to produce a chemical model whose predicted properties match those derived from the diffraction pattern.

2.9.1. Single crystal

A crystal is a solid, within which atoms are arranged in an ordered configuration, which itself is periodic in three dimensions. This sequence of identical neighbourhoods can be represented as a lattice of points in three dimensions, known as the direct lattice, where each point lies at the same arbitrary position within each neighbourhood. This lattice may inherently be described using three linearly-independent basis vectors $\underline{a}$, $\underline{b}$, $\underline{c}$, and these vectors describe a parallelepiped known as the unit cell (Figure: 33). The angles relating these vectors are conventionally defined as α, β, γ. One unit cell may contain one or more than one molecule. Although the number of molecules per unit cell is always the same for the entire unit cells of a single crystal, it may vary between different crystal forms. By definition, a unit cell must be able to tile with itself in three dimensions (without gaps). This restriction adds certain constraints to the unit cell parameters. A unit cell therefore lies within one of seven crystal systems, as summarised in Figure 2.3 (Clegg, 1998).

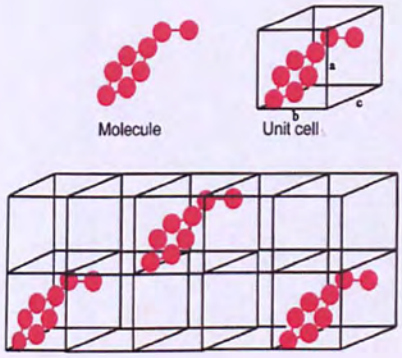

Crystal System	vector constraints (length)	Basis vector constraints (angle)
Triclinic	-	-
Monoclinic	-	$\alpha = \gamma = 90°$
Orthorhombic	-	$\alpha = \beta = \gamma = 90°$
Tetragonal	$a = b$	$\alpha = \beta = \gamma = 90°$
Rhombohedral	$a = b = c$	$\alpha = \beta = \gamma$ ($\neq 90°$)
Hexagonal	$a = b$	$\alpha = \beta = 90°$, $\gamma = 120°$
Isometric/Cubic	$a = b = c$	$\alpha = \beta = \gamma = 90°$

Figure 2.3: A unit cell of a molecule in 3-D lattice and seven crystal systems

2.9.2. Apparatus

The creation of X-rays, handling of a crystal sample during X-ray exposure and detection of diffracted rays are all handled by a single machine: an X-ray diffractometer (Figure 2.4-A). The formation of diffraction patterns via prolonged X-ray exposure is the safest and most convenient method of crystal structure determination.

2.9.2.1. X-Ray Source

The X-ray source, an X-ray tube, generates electrons by passing an electrical current through a wire filament in an evacuated enclosure. The electrons bombard a water-cooled metal block, with a small proportion generating collimated X-rays by interaction with the metal atoms. The wavelength of resultant X-rays differs according to the metal used; copper and molybdenum are typical choices, and produce wavelengths of ~1.54 Å and ~0.71 Å respectively. Detection of these X-rays, after diffraction by the crystal, is made possible by a charge-coupled device (CCD) with a photoactive layer to convert between the analogue X-rays and digital information output by the diffractometer.

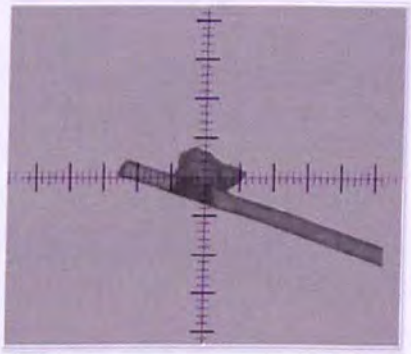

A B

Figures 2.4-A Nonius Kappa CCD diffractometer (Chem cryst, X-ray crystallography, University of Oxford, Oxford, UK), 2.4-B: Crystal's aligment and crystal's size measument.

2.9.2.2. Crystal's alignment

Transformation of a crystal's alignment (Figure 2.4-B) relative to the X-ray source is made possible by a goniometer within the diffractometer, onto which the crystal sample is mounted. The goniometer typically has three degrees of freedom, in the form of three rotational axes.

2.9.2.3. Crystal environment

Temperature within the crystal environment is controlled to produce valid data. Thermal expansion of the unit cell at higher temperatures will distort lattice parameters, in general producing larger unit cell dimensions. Commonly, a temperature of 150 K is recorded for published results.

2.9.2.4. Exposure time

The exposure time varies according to the intensity of the source X-rays, and the compound under analysis. Crystals containing lighter elements (i.e. no heavy metals) will produce weaker scattering of the rays, and will require a longer duration. In such cases, using an intense X-ray source (such as a synchrotron) will greatly reduce the necessary exposure time.

2.9.3. X-Ray analysis and spectroscopy

X-ray structure analysis is rather different from other spectroscopic analytical methods, it gives a clearer picture about the connectivity between atoms. With IR, NMR or Mass Spectroscopy, the experiment yields a relatively small amount of data, sometimes only a one-dimensional spectrum.

With single crystal X-ray diffraction, the experiment yields a massive number of independent observations, the diffraction pattern (Figure 2.5-A). Because diffraction is an interference phenomenon, each diffracted beam of X-rays has a magnitude and a phase. The probable phase values can be estimated from statistical processes called "Direct Methods". If both of these could be measured, it would be possible to perform an analytically correct computation which would yield an image of the crystal structure. That's the main reason, X-ray crystallography has moved from being a laborious and expensive technique into becoming an analytical method that should be first-choice if the material readily forms crystals (Hammond, 2001).

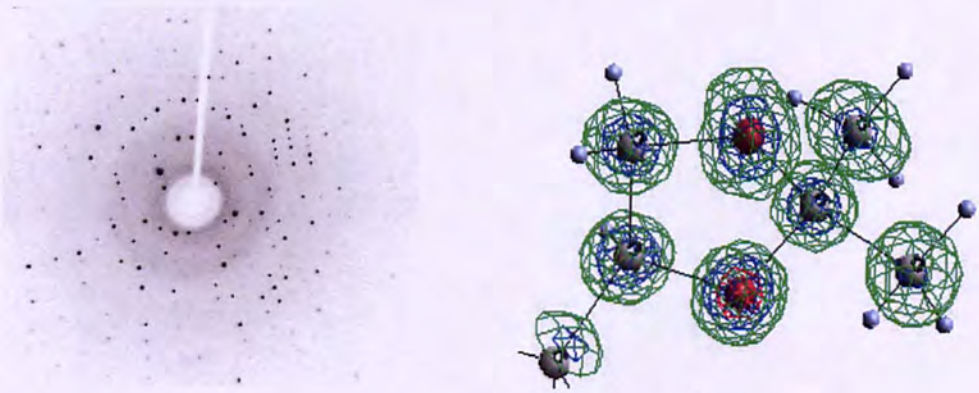

A- B-

Figure 2.5-A Diffraction pattern from a small sugar, 2.5-B The electron density around each nucleus is clearly resolved.

In structure elucidation, the difference between crystallography and spectroscopic methods is that in spectroscopy, the proposed structure is based

on the spectral observations, while in crystallography the analyst (or a program) has to postulate phases. Because there are no intuitive values for the phases, this greatly reduces the possibility of introducing user-bias into the analysis. Crystallography does not directly reveal the types of atoms in a structure (Figure 2.5-B), but it does give connectivity and electron density (Julian, 2008).

An additional and important difference is that X-ray analysis reveals the absolute relationships between all the atoms in the structure and analysis is also generally very reliable and unambiguous. This is because of the high observation: variable ratio (Vainsthein, 1996).

In the computations, all the observed data contribute to all the atoms, and there is no bit of the data that refers specifically to a small structural fragment. However, once the positions of all the atoms have been found, it is possible to compute geometrical relationships (*e.g.* distances, angles, planarity), and perhaps more importantly, produce diagrams (Figure 2.6) of the whole structure (Julian, 2008; Clegg, 1998).

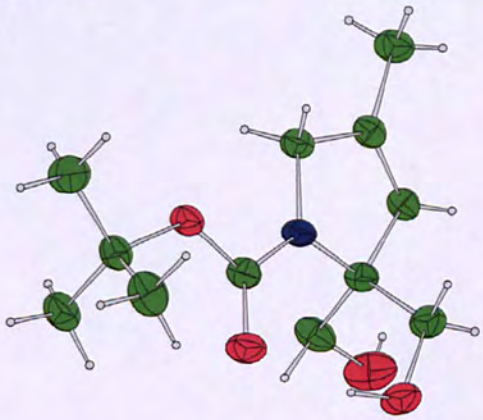

Figure 2.6: Chemical structure of a sugar moiety from X-ray crystallography

2.9.3. X-Ray Crystallography of Compound 7

X-ray crystallography studies were conducted on a Nonius Kappa CCD diffractometer (Chem cryst, X-ray crystallography, University of Oxford, Oxford, UK) equipped with Mo*K*α radiation (λ=0.71073 Å). Single, colourless, plate shaped crystals 0.10 x 0.40 x 0.60 mm in size (Figure 2.7-A), were carefully selected under a dissecting microscope. Then, the selected crystal was mounted on a glass fibre with traces of viscous oil. The fibre loop was fixed on a goniometer head. The crystal was aligned relative to the X-ray source by making adjustments in the goniometer within the diffractometer. Ten frames of data (Figure 2.7-B) were collected at 150±1 K with an oscillation range of 1°/frame and an exposure time of 0.99 min/frame (Nonius, 1998).

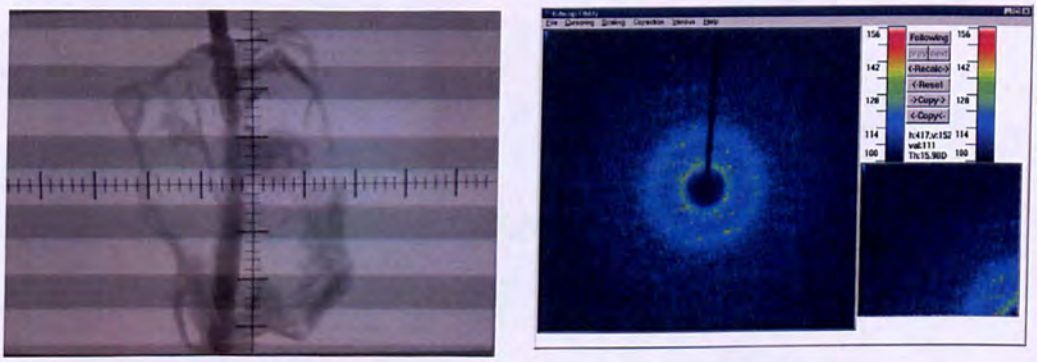

A B

Figures 2.7-A: Alignment of crystal and size measurments of compound 7, 2.7-B: The diffraction pattern from compound 7

A combination of direct methods and heavy atom methods were employed using SIR 97 (Altomare *et al.,* 1997). All of the non-hydrogen atoms were refined with anisotropic displacement coefficients. Hydrogen atoms were located and refined isotropically using SHELXL97 and allowed to ride on their parent atoms (Sheldrick, 1997). Structural figures were prepared using ORTEP3 for windows (Farrugia, 1997).

2.9.4. X-Ray Crystallography of aglycon from Compounds 1 and 2

The aglycone moieties were obtained as shinny colourless tiny needle like crystals, as a results of acid hydrolysis of compounds **1** and **2** isolated from the ethyl acetate farction of *Craralluma tuberculata*.

Structure elucidation was carried on a "Oxford Diffraction Gemini" single crystal diffractometer (Figure 2.8-A). The Gemini diffractometer incorporates two independent high voltage X-ray generators (Copper-Cu & Molybdenum-Mo). The instrument is equipped with Oxford Diffraction's 4-circle kappa goniometer which provides extremely high angular resolution Mo and Cu data. Under a microscopic view a suitable crystal 0.10 x 0.20 x 0.70 mm in size (Figure 2.8-B) was slected and mounted on a glass fiber loop with traces of vicous oil. After fixing the fiber loop on a goniometer, the crystal was aligned to X-ray source. In total 20 frames of data were collected at 293 K with an oscillation range of 1°/frame and an exposure time of 1 min/frame.

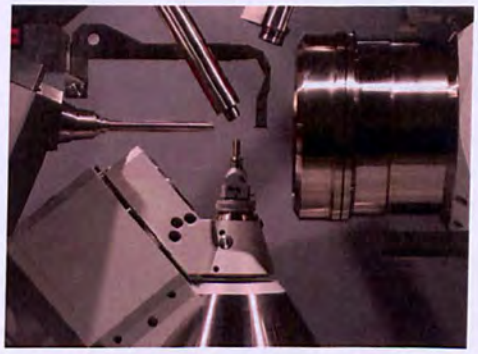

A

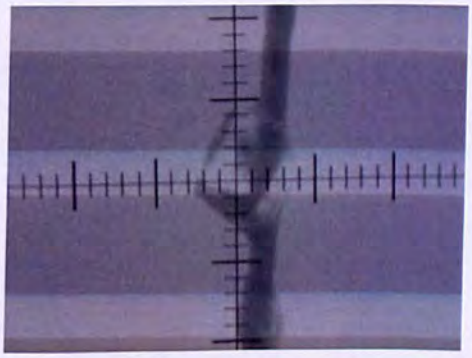

B

Figures 2.8-A: Oxford Diffraction Gemini single crystal diffractometer, 2.8-B: Alignment and size measurments of crystal from aglycon moiety of compound 1 & 2

A "Direct Method" program was attempted to compute phase angles for the reflections, followed by extraction of an atomic model.

3. Materials and Methods (Anticancer studies)

3.1. Human cell lines collection

Breast oestrogen-dependent cancer cells (MCF-7)

MCF-7 (human breast oestrogen-dependent adenocarcinoma) cells were purchased from ATCC (American Type Culture Collection, USA) through an authorised distributor, LGC Standards, Teddington, UK (Product Code HTB-22). Cells were grown in DMEM supplemented with 15% heat inactivated foetal bovine serum (FBS), Gentamycin (40 μg/ml), Penicillin (100 units/ml) and Streptomycin (1040 μg/ml).

Breast oestrogen-independent cancer cells (MDA MB-468)

MDA-MB-468 (human breast oestrogen-independent adenocarcinoma) cells were obtained from ATCC (American Type Culture Collection) through an authorised distributor, LGC Standards, Teddington, UK (Product Code HTB-132). Cells were grown in DMEM supplemented with 15% heat inactivated foetal bovine serum (FBS), Gentamycin (40 μg/ml), Penicillin (100 units/ml) and Streptomycin (1040 μg/ml).

Colorectal cancer cells (Caco-2)

The Caco-2 (human colon adenocarcinoma) cell line was obtained from the ECCC (European Collection of Cell Cultures) through Health Protection Agency, Salisbury, UK (Catalogue No. 86010202). Cells were grown in complete growth medium: DMEM containing 10% v/v FBS, 2 mM L-glutamine, Gentamycin (40 μg/ml), Penicillin (100 units/ml) and Streptomycin (1040 μg/ml).

Human umbilical vein endothelial cells (HUVEC)

HUVEC (human umbilical vein endothelial cells) were isolated from umbilical cords (kindly donated by Dr Anshuman Ghosh, School of Life Sciences, Kingston

University, UK) by enzymatic detachment using collagenase, as previously described (Bernhard *et al.*, 2003). HUVEC Cells were routinely passaged in 0.2% gelatine-coated (Sigma, Steinheim, Germany) polystyrene culture flasks (Becton Dickinson, Meylan Cedex, France) in MCDB 131 growth media (Invitrogen Ltd. Paisley UK) supplemented with EGM (Endothelial Cell Growth Medium) supplements and growth factors purchased from Invitrogen Ltd. (UK).

Human lymphatic monocytes (U937)

U937 cells were obtained from ATCC (American Type Culture Collection) through an authorised distributor, LGC Standards, Teddington, UK (Product Code CRL-1593.2) and were grown in RPMI-1640 Medium supplemented with FBS to a final concentration of 10%, Gentamycin (40 µg/ml), Penicillin (100 units/ml) and Streptomycin (1040 µg/ml).

3.2. Chemicals used

Foetal bovine serum (FBS), Penicillin/Streptomycin-L-Glutamine, Dulbeccos Modified Eagles Medium (DMEM), Trypsin-EDTA, Phosphate buffer saline (PBS), were purchased from Fisher (Fisher Scientific Ltd., Leicestershire, UK). Positive controls: Actinomycin-D (A1410, ~ 98%), Tamoxifen (T5648, ≥ 99%), Anastrozole (A2736, ≥ 98%), RPMI medium (acronym RPMI: Roswell Park Memorial Institute, New York USA), 1640 medium without phenol red, MTT Dye (Tetrazolium bromide 98%), Neutral red (N4638), Trypane blue solution 0.4% (T8154) were purchased from Sigma Aldrich (Sigma Aldrich Company Ltd. Dorset, UK).

Z-VAD-FMK Caspase family inhibitor (fluoro-methyl ketone) was purchased from Enzo Life Sciences Ltd. (Exeter UK). Vectashield Hard set mounting medium with DAPI stain (H-1500) was supplied from Vector Laboratories Ltd.

(Peterborough, UK). Precision-Standards blue stain molecular markers (610373) for PARP detection were purchased from Bio-Rad Laboratories Ltd. (Herts, UK). ECL blotting detection reagents was purchased from Fisher Scientific UK (Leicestershire UK). Ribonuclease A (from bovine pancreas) and Tergitol solution (NP-40) were purchased from Sigma Aldrich UK.

3.3. Cell culture

All cell lines were grown in a humidified incubator at 37°C in an atmosphere containing 5% CO_2. Cells were passaged routinely and an identification number was assigned to each passage for an individual cell line. Cells were in the logarithmic phase of growth at the time of cytotoxicity assays. Overall general protocols for cell culture are as follows:

3.3.1. Growth medium preparation

DMEM (Dulbecco's Modified Eagles Medium), Foetal bovine serum (FBS) and Penicillin/Streptomycin-L-Glutamine were warmed at 37°C before making up a complete media. Penicillin/Streptomycin with L-glutamine (5 ml) and 50 ml of FBS (for 10%) were added into 500 ml of DMEM in a sterilised environment. The media was mixed and stored in a fridge at 2-8°C.

3.3.2. Defrosting cells

Growth media was pre-warmed at 37°C. The cryovial was removed from liquid nitrogen and the exterior of the vial was sprayed with 70% IMS. The cell vial was then placed in an incubator at 37°C. When the cells were completely thawed, the contents were transferred from the vial to a sterile centrifugation tube. The volume was made up to 8-10 ml by adding DMEM. Cells were centrifuged for 5 min at 1000 rpm. The supernatant was removed and pellet suspended in about 5

ml (for T-25 flask) of media. The cell suspension was transferred into a 25 ml cell culture flask. The flask was labelled with cell type, date, initials and passage number and was incubated overnight. After 24 hrs, the media was removed, cells were washed with PBS (5 ml) twice and the flask was replenished with fresh media.

3.3.3. Passage (splitting cells)

When cells were 80-100% confluent, they were divided into two portions. Firstly, the media was removed from the flasks and cells were washed with PBS (5-8 ml) twice to remove the metabolites and to partially remove the dead cells, as they are non-adherent to the flask surface. Pre-warmed trypsin-EDTA (2 ml/ T-25 flask) was added and incubated for 1-3 mins at 37°C. The flasks were tapped gently to dislodge the cells and were visualised under a microscope.

After the cells were completely disassociated from the flask, the growth media (complete; 8ml) was added into the flask. The media was pipetted up and down several times to break up any cell lumps. The cell suspension was divided into two fresh flasks. The growth media was topped up to 5 ml in each flask. Flasks were labelled with new passage number and kept in an incubator at 37°C. After 24 hrs, the old media containing Trypsin was removed from each flask and cells were replenished with fresh media.

3.3.4. Freezing and storing cells

Cells can be maintained for short periods of time by repeated passaging. However, they will start to deteriorate and may start to loose some of their characteristics after a certain number of passages, depending on the type of cell line. Cells are therefore regularly frozen and stored in liquid nitrogen to provide a long term means of storage.

After cell splitting (as described previously), the portion of cells that needs to be stored were re-suspended in a centrifuge tube for 1 min at 1000 rpm. The supernatant was removed and to the pellet, a mixture containing 90% FBS and 10% DMSO (as cryopreservative agent) was added. The cell suspension was transferred to a cryovial tube marked with the initials, cell line name, passage number and date. The cryovial tubes were kept overnight at -80°C. After 24 hrs, the cells were transferred into liquid nitrogen.

3.3.5. Cell counting

There are a number of different ways to assess the number of viable cells in a population growing in a flask. In the present study, the trypan blue method using a haemocytometer was selected as it is a quick and efficient method and is useful for determining cell numbers for setting up assays. Cells were trypsinised (as described earlier in cell passage), DMEM was added and cells were centrifuged in Falcon tube for 1 min at 1000 rpm.

The supernatant was removed and pellet was re-suspended in 1 ml of DMEM. Cell suspension (10 µl) and 90 µL of trypan blue were mixed by pipetting up and down for few times. Cell suspension (10 µl) was added to the haemocytometer slide. Viable cells are typically round and refractile and exclude the stain, whilst non-viable cells are stained dark blue and are larger in size, crenated and non-refractile. The dead or injured cells take up the stain due to their leaky/porous cell membranes. The viable cells were counted in each of 5 squares and the mean was calculated.

Total viable cells were calculated using the following equation:

$$\text{Total viable cells / ml} = \text{Mean of cells} \times 10^4 \times 10 \text{ (dilution factor)}$$

3.4. Cytotoxicity of crude ethanolic extracts

Crude extracts of the four medicinal plants (*Caralluma tuberculata, Fagonia indica, Solanum surattense, Arisaema utile*) were tested for cell cytotoxicity against three cancer cell lines (MCF-7, MDA MB-468, Caco-2). A series of eight dilutions (10, 25, 50, 100, 200, 300, 400 and 500 µg of final concentration) of each plant crude extract were prepared in the medium (100 µl) containing DMSO (Dimethyl sulfoxide, maximum: 0.01%).

Cells were seeded into 96-well cell culture plates at a density of $1x10^4$ cells per well in 100 µl aliquots of medium. The cells were allowed to attach for 24 h at 37°C, 5% CO_2 in air in a humidified atmosphere. The next day, the dilutions of plant extracts were added to the desired final concentrations. Vehicle control groups received the same amount of DMSO. After a 24 h exposure period, the toxic endpoints were determined using two colorimetric assays; namely the MTT assay and neutral red uptake assay.

3.4.1. Cytotoxicity assays

Cellular damage will inevitably result in a loss of the ability of the cell to maintain and provide energy for metabolic cell function and growth. A number of methods have been developed to study cell viability and proliferation in cell populations. One parameter used as the basis for colorimetric assays is the metabolic activity of viable cells. Both qualitative and quantitative cell viability assays have been developed in a microplate format (96-well plates).

3.4.1.1. MTT assay

Mitochondria are the cells' main energy producers and are therefore essential for cellular life; however, recent research has shown that these organelles play a key role in cell death when their membranes become permeabilized (Green & Kroemer, 2004). The methyl-thiazolyl tertrazolium (MTT) assay measures the mitochondrial function activity of mitochondrial dehydrogenases. MTT is a yellow coloured dye [3-(4,5-dimethyl- 2- thiazolyl)-2,5-diphenyl-2H-tetrazolium bromide],

which converts to a purple insoluble product formazan at the expense of the reduction reaction with concomitant oxidation of NADH (Nicotinamide adenine dinucleotide-reduced) and NADPH (nicotinamide adenine dinucleotide phosphate-reduced) through the ability of the mitochondrial succinic dehydrogenase enzyme in living cells (Twentyman and Luscombe, 1987).

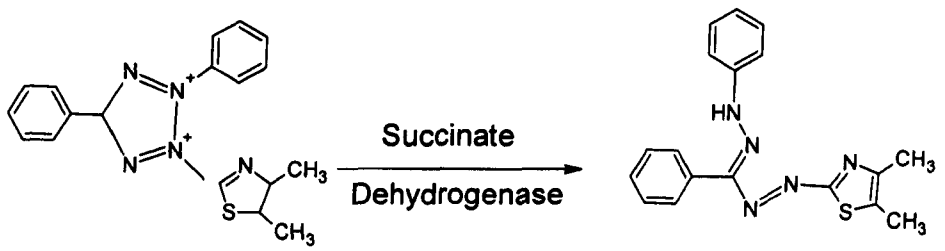

Yellow coloured tetrazolium salt *Purple coloured formazan*

Figure 3.1: Reduction of MTT to formazan due to succinate dehydrogenase enzyme present in the mitocondria of viable cells.

According to the method described by Borenfreund *et al.*, (1988), growth of cancer cells was quantified. Following a 24 h exposure period of drugs, cells were washed twice with PBS, and a 10 µl of MTT reagent (5 mg/ml in PBS) was added to each well including the blanks, which contained medium only. The plates were returned to the incubator for 4 h at 37°C. Subsequently, cells were washed twice with PBS, and 100 µl/well DMSO was added in each well as solvent to dissolve the insoluble crystalline formazan products. The effect of plant extracts on cancer cells was quantified as the percentage of control absorbance of reduced dye at 550 nm on microplate reader (Labtech LT-4000MS, Labtech International Ltd., East Sussex, and UK). For each treatment, five replicate wells were examined, and each experiment was repeated three times (n = 3). Mean and strandard deviation were calculated between three experiments. Results were calculated as percentage growth inhibition, untreated (control) cells versus treated cells according to the following formula:

$$\% \text{ Growth inhibition} = \frac{(\text{Control} - \text{Actual absorbance})}{\text{Control}} \times 100$$

Where: Control = absorbance of untreated cells after substracting absorbance of media
Actual absorbance = absorbance of treated cells at a particular concentration of testing sample after substracting the absorbance of media

3.4.1.2. Neutral Red uptake (NRU) assay

The neutral red (NR) metabolic impairment assay works simply on the principle that this dye accumulates in the lysosomes of viable cells by a combination of active endocytosis and pinocytosis until a stable equilibrium is reached. Alterations of the cell surface or the sensitive lysosomal membrane lead to lysosomal fragility and other changes that gradually become irreversible. Such changes produced by toxic substances cause decreased uptake and binding of NR, making it possible to distinguish between viable, healthy and damaged or dead cells. Metabolically inactive cells lose their ability to accumulate and retain NR (Borenfreund and Puerner, 1985). However, this loss does not occur until late in the apoptotic process, when membrane integrity is compromised.

The neutral red uptake assay was performed according to the method of Borenfreund and Puerner (1985) by removal of the medium after dosing cells and 200 µl of neutral red solution (40 µg/ml) was added to each well (including the blanks, which contained medium only). After incubation for 2.5 hours, the neutral red was removed, cells were carefully rinsed with pre-warmed PBS, and 200 µl of ethanol/acetic acid (1% glacial acetic acid in 5% ethanol) was added to all wells.

The plates were covered in foil and placed on a plate shaker for 30 minutes to extract neutral red from the cells and form a homogeneous solution. Absorbance of the wells was measured at 540 nm in a microplate reader within 60 minutes. For each treatment, five replicate wells were examined and each experiment was repeated three times (n = 3). Results were calculated as percentage growth inhibition, untreated (control) cells versus treated cells according to the formula as described previously (MTT assay, section: 3.4.1.1.). Mean and strandard deviation were calculated between three experiments.

3.5. Cytotoxicity of fractions from crude ethanolic extracts

As all the four medicinal plants showed moderate to good cytotoxic activity, the next objective was to find out the most potent fraction of the crude extract. Four organic fractions (hexane, chloroform, ethyl acetate and methanol) and an aqueous fraction of each plant were tested for antiproliferative activity on three cancer cell lines (MCF-7, MDA MB-468, Caco-2). For each fraction, a final concentration of 200 µg per well was prepared in the medium (100 µl) containing DMSO (Dimethyl sulfoxide, maximum: 0.01%).

Cells were seeded into 96-well cell culture plates at a density of $1x10^4$ cells per well in 100 µl aliquots of medium. After 24 h of incubation, prepared samples of the fractions were added to the cells. Vehicle control groups received the same amount of DMSO. After a 24 h drug exposure period, the antiproliferative activity was determined using MTT and Neutral red uptake assays under the same protocol conditions as described earlier in cytotoxicity of crude extracts.

3.6. Anticancer activity of isolated compounds 1-6

Preliminary screening of organic fractions against three cancer cell lines revealed the most potent cytotoxic fraction for each medicinal plant. Phytochemical analysis of these potent fractions highlighted the relation of these isolated compounds to some key classes (steroidal glycosides and long chain fatty acids) having significant anticancer activity.

3.6.1. Cytotoxicity assays (MTT and NRU)

Compounds **1–6** were evaluated for antiproliferative activity against three cancer cell lines (MCF-7, MDA MB-468 and Caco-2). In this study, eight serial dilutions (0.78, 1.56, 3.12, 6.25, 12.5, 25, 50, 100 µM) of each compound containing

DMSO (maximum: 0.01%) were prepared in 200 µl media as a final concentration in the well. Antiproliferative activity of compounds **1-6** was evaluated at 24 h and 48 h in order to establish a time dependent as well as concentration dependent cytotoxic effect. Actinomycin-D (4 µM), Tamoxifen (5 µM) and Anastrozole (5 µM) were used as positive controls. For each cell line, a density of $1x10^4$ cells per well in 100 µl aliquots of medium were seeded into 96-well cell culture plates. The cells were allowed to attach for 24 h at 37°C, 5% CO_2 in air in a humidified atmosphere. The next day, the serial dilutions of compounds **1-6** were added. Vehicle control groups received the same amount of DMSO (maximum: 0.01%). After a 24h and 48h drug exposure time, the toxic endpoints were determined using MTT and Neutral red uptake assays under the same protocol conditions as described earlier (cell cytotoxicity of crude extracts) in detail for crude extracts. For each treatment, five replicate wells were examined, and each experiment was repeated three times (n = 3). During these cytotoxicity assays there was a change in plate reader used to determine absorbance for initial experiments, which may account for variation. Results were calculated as percentage growth inhibition, untreated (control) cells versus treated cells according to the formula as described previously (MTT assay, section: 3.4.1.1.). Mean and strandard deviation were calculated between three experiments.

3.6.2. Cytomorphological alterations (DAPI staining)

"Cytomorphology" the study of the structures contained within cells. DAPI (4', 6-diamidino-2-phenylindole) is a DNA-specific probe which forms a fluorescent complex by attaching in the minor grove of A-T rich sequences of DNA. Binding of DAPI to DNA produces a ~20-fold fluorescence enhancement, apparently due to the displacement of water molecules from both DAPI and the minor groove (Kapuscinski, 1995). The blue-fluorescent DAPI nucleic acid stain preferentially stains DNA and is used to study the morphological condition of cancer cells, especially as a marker for apoptosis in the cells. DAPI produces a blue

fluorescence when bound to DNA with excitation at about 360 nm and emission at 460 nm.

In the present study, DAPI was used to assess morphological changes in nuclei of treated cells. Cells were seeded at $1x10^4$ cells/well in 500 µl of medium on sterilised glass coverslips in 12 well plates for 24 h. The three cancer cell lines (MCF-7, MDA MB-468, Caco-2) were treated with negative control (culture medium), positive control Actinomycin-D (4 µM), Tamoxifen (5 µM) and Anastrozole (5 µM) along with six isolated compounds (compounds **1–6**) according to their specific IC_{50} values for a particular cell line. The plates were incubated at 37°C, 5% CO_2 in air in a humidified atmosphere for 24 hours. After treatment, cells were briefly equilibrated with PBS, fixed with 4% paraformaldehyde for 15 min, permeabilised with methanol for 5 min, and mounted in a DAPI-containing medium (VectorShield, Vector Labs, Peterborough, UK). The morphology of the nuclei was observed using a confocal fluorescence microscope, Leica SP2 AOBS confocal microscope (Leica Microsystems, Mannheim, Germany) with excitation at 350 nm and emission 460 nm under a 40 x oil objective.

3.6.3. Inhibition of apoptosis (caspase inhibitor Z-VAD-FMK)

The process of cell death, "apoptosis" is mediated by a specific group of cysteine proteases, the "caspases". Caspases exhibit catalytic and substrate recognition motifs that have been highly conserved. These characteristic amino acid sequences allow caspases to interact with both positive and negative regulators of their activity (Cryns *et al.*, 1998). Mammalian interleukin-1β converting enzyme (ICE) a member of the caspase gene family (cysteine proteases) with a marked specificity for aspartic acid in the P_1 position, play significant roles in both inflammation and apoptosis (Steller, 1995). Over expression of these proteases results in apoptosis (Munday, 1995).

The substrate preferences or specificities of individual caspases have been exploited for the development of peptides that successfully compete for caspase binding (Garcia-Calvo *et al.*, 1998). The caspases inhibitor binds to the active site of activated proteases. It is possible to generate reversible or irreversible inhibitors of caspase activation by coupling caspase-specific peptides to certain aldehyde, nitrile or ketone compounds. These caspases inhibitors can successfully inhibit the induction of apoptosis in various tumor cell lines as well as normal cells (Gastman *et al.*, 1999).

Caspase inhibitors are important tools in the investigation of apoptosis, utilising whole cells, cell lysates, and *in vivo* systems. Z-VAD-FMK is a synthetic inhibitor that has been widely used to examine the roles of caspases in regulating cellular processes. Benzyloxycarbonyl-Val-Ala-Asp(OMe) fluoro methyl ketone (Z-VAD-FMK), is an irreversible inhibitor of ICE-like proteases with no added cytotoxic effects (Figure 3.2). It is synthesised with a benzyloxycarbonyl group (also known as BOC or Z) at the N-terminus and O-methyl side chains exhibit enhanced cellular permeability, thus facilitating their use in both *in vitro* cell culture as well as *in vivo* animal studies (Zhu *et al.*, 1995).

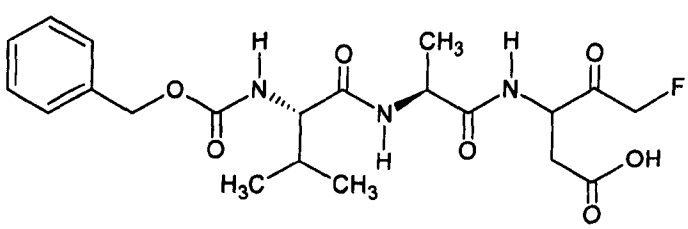

Figure 3.2: Chemical structure of Z-VAD-FMK

Cells that are induced to undergo apoptosis can be cultured in the presence or absence of the caspase inhibitor. Treated cells can then be assayed for evidence of apoptosis inhibition by examining either whole cells or cell lysates using standard apoptosis assays (MTT, NRU etc.).

Methodology

The inhibition of apoptosis was assessed by use of the pan-caspase inhibitor Z-VAD-FMK in three human cancer cell (MCF-7, MDA MB-468, Caco-2) lines. Cells were seeded into 96-wells, cell culture plates at a density of $1x10^4$ cells per well in 100 µl aliquots of medium. The cells were allowed to attach for 24 h at 37°C, 5% CO_2 in air in a humidified atmosphere. The next day, one hour before dosing the cells with isolated compounds, cells were pre-treated with caspase inhibitor Z-VAD-FMK at 50 µM of final concentration in the wells. Stock solution of Z-VAD-FMK was prepared in DMSO and diluted with growth medium to the required final concentration (50 µM), for each dose per well. After pre-treatment with caspase inhibitor, the desired concentrations of isolated compounds **1-6** (according to their IC_{50} for specific cell lines) and positive control, Actinomycin-D (4 µM) was added and cells were allowed to incubate under above mentioned conditions for further 24 h. Vehicle control groups received the same amount of DMSO (maximum: 0.01%). As a comparison cells were treated with isolated compounds **1-6** and positive controls in the absence of caspase inhibitor and cell treated with Z-VAD-FMK (50 µM) alone.

After a 24 h treatment, the percentage of growth inhibition was determined using colorimetric assay "Neutral red uptake assay", as described in detailed earlier (under cytotoxicity of crude extracts).

The effect of caspase inhibitor was also assessed using Western blots and DNA ladder assay. Cancer cells (MCF-7, MDA MB-468, Caco-2) and normal cells (HUVEC, U937) were seeded and received doses in the presence and absence of caspase inhibitor along with isolated compounds **1-6** and positive controls as described above. After 24h incubation, cell protein lysates were prepared and were resolved electrophoretically for PARP detection and DNA ladder, according to the respective protocol for each assay, as described in detail in next coming sections (under Western blot and DNA ladder assays).

3.6.4. Poly (ADP-ribose) polymerase (PARP) cleavage (Western blot)

The DNA-repair and protein-modifying enzyme PARP, which is also called poly (ADP-ribose) synthetase and poly (ADP-ribose) transferase, is an abundant nuclear protein that is involved in the DNA-base-excision-repair system. The PARP family includes PARP-1, PARP-2, PARP-3 (Smith S, 2001). Each member of the PARP's family shares homology on the C-terminal catalytic domain of PARP. On average, approximately one molecule of PARP is present per 1000 bp of DNA. In response to DNA damage, PARP activity is rapidly increased up to 500-fold upon binding to DNA strand nicks and breaks. PARP transfers 50–200 residues of PAR to itself and to acceptor proteins such as histones, DNA polymerases, topoisomerases, DNA ligase-2, high-mobility-group proteins and transcription factors (Smulson, 2000).

Figure 3.3: DNA repairing enzyme PARP

taken from: www.astrazenecaoncology.com/oncology-research/ (dated 23/08/2010)

The synthesis and turnover of ADP-ribose polymers is a dynamic cellular response to DNA damage (Figure 3.3). PARP enzymatic activity increases in response to various cellular stresses (Kraus, 2008). The intensity of PARP activation might be a key factor that regulates whether cells either die or survive following DNA damage. As a nick sensor, activation of PARP regulates cellular repair, transcription and replication of DNA, cytoskeletal organization, protein degradation and other cellular activities through ADP-ribosylation of PARP substrates. However, excessive DNA damage generates large branched-chained PAR polymers, which leads to the activation of a unique cell-death program (Virag *et al.,* 2002).

The primary structure of the PARP-1 enzyme (Figure 3.4) is highly conserved between species. It is a 116-kDa protein that contains three main functional domains: an N-terminal, DNA-binding domain (42 kDa) that contains a nuclear localisation signal; a central automodification domain (16 kDa); and a C-terminal, catalytic domain (55 kDa) [Murcia *et al.,* 1994].

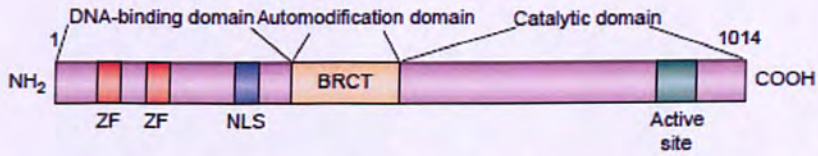

Figure:3.4 Primary structure of Poly (ADP-ribose) polymerase (PARP)

Given the central role of PARPs in vital cellular processes as well as disease states, chemical inhibitors of PARP have been explored as therapeutic agents for a wide variety of diseases, including cancer (Tong *et al.,* 2008).

Methodology

According to a modified protocol by Kim *et al.,* (2010), a confluent monolayer of cancer cells (MCF-7, MDA MB-468, Caco-2) and normal cells (HUVEC, U937) were incubated in a 6 well plate for 24 hours in DMEM (complete) media. After dosing cells with positive controls (Actinomycin-D 4 μM, Tamoxifen 5 μM,

Anastrazole 5 μM), along with isolated compounds (compounds **1-6**) from the four plants according to their specific IC_{50} values for a particular cell line, the plates were incubated for a further 24 h in an incubator at 37°C, 5% CO_2 in air in humidified atmosphere. Incubations were terminated by rapid aspiration of the cell supernatant followed by washing with cold PBS. The cells were lysed with 1×Laemmli lysis buffer (2.4 M glycerol, 0.14 M Tris, pH 6.8, 0.21 M sodium dodecyl sulphate, 0.3 mM bromophenol blue) mixed with β-mecaptoethanol (91:9) and boiled for 5 minutes.

An assembly of spacer plate (1 mm space) and short plate, size 7.5 cm x 8.5 cm was used for preparing 10.5% denaturing SDS-polyacrylamide gel. Resolving gel (10 ml) was prepared by adding 2.5 ml of running buffer X 4, 3.5 ml 30% Acrylamide, 100μl of 10% Ammonium persulfate and 3.89 ml of deionised water and mixed gently. Then finally a 10 μl of TEMED (Tetramethylethylenediamine) was added and then after mixing, quickly poured between the plates, which were fixed in the assembly stand (Bio-Rad). Resolving gel was allowed to settle down for approximately 15 min. A solution of stacking gel (10 ml) was prepared by adding 2.5 ml of stacking buffer X 4, 1.16 ml 30% Acrylamide, 100μl of 10% Ammonium persulfate and 6.23 ml of deionised water and mixed gently. Then finally by adding 10 μl of TEMED, solution was mixed and quickly poured onto the settled resolving gel. For well formation, a 10 lane comb with 1 mm thickness was placed and allowed the gel to settle for 20 min approximately.

The samples of protein lysates (10 μl per well) loaded along with Precision-Standards blue stain molecular markers (10 μl) for PARP detection on 10.5% denaturing SDS-polyacrylamide gel and were resolved electrophoretically (Bio-Rad electrophoresis apparatus frequency 50/60 Hz with Bio-Rad Mini-Protean Tetra cell reservoir, Singapore) at 200 V. After resolving the protein lysate, the pattern was transferred to nitrocellulose membranes (Hybond-C Extra, GE Health Care, UK) by preparing sandwiche of membrane using Wattman blotting paper in

transfer buffer. Sandwiches were soaked in transfer buffer and placed in ECL semi-dry transfer unit connected to 45 amp (for one membrane) current for 2 h.

After blotting, membranes were blocked with Tris-buffered saline - Tween 20 (T-TBS, 0.1% Tween 20) containing 5% skimmed dried milk for 1 h at room temperature, then membranes were washed twice with T-TBS. Then each membrane was cut through between 75 and 50 kDa indicated by the molecular marker. The upper half of the membrane was incubated with 10 µl PARP rabbit primary antibody (Cell signalling technology, product code 9542, Danvers USA), while the lower half was incubated with 10 µl goat polyclonal IgG primary antibody (SC-1616, Santa Cruz Biotechnology, USA) in 1% Milk in TBS-T (10 ml) for overnight at 4 °C. Then membranes were washed three times with TBS-T for 30 min.

For detection of intact or cleaved PARP, the upper half of the membrane was incubated with 10 µl Anti-rabbit IgG from Donkey secondary antibody (product code NA 9340, Amersham Biosciences, UK), while lower half of the membrane was incubated with 10 µl Donkey anti goat IgG-HRP secondary antibody, in 1% Milk in TBS-T (10 ml) for 2 h at room temperature. After incubation, the membranes were given a good wash with TBS-T for 2 h. Bands were detected by soaking the membranes in 10 ml ECL-Enhanced Chemiluminescence reagent [by mixing solution A (5ml) and solution B(5 ml)] for 1 min. Band intensities were captured using the ECL system on X-ray film (GE Healthcare, UK). The signals were visualised through Kodak film developer using develper (40% v/v) and fixer (30% v/v).

3.6.5. DNA fragmentation assay (DNA ladder)

During apoptosis, a series of well defined morphological and biochemical changes occur within the cell (Wyllie, 1992). The process includes nuclear

membrane breakdown, cytoskeletal reorganisation, plasma membrane blebbing, and loss of adhesion. The most noticeable changes take place in the nucleus: shrinkage of the nucleus is observed, the chromatin condenses, and the nuclear material collapses into patches and dissociates into many lobes. Associated with the loss of the integrity of the nucleus is digestion of the genomic DNA by an endonuclease (Compton, 1992).

In cells of hematopoietic origin, cells undergo extensive DNA degradation, typically generating a ladder of small fragments of double-stranded DNA, as detected in nondenaturing agarose gel electrophoresis. The fragments are multiples of approximately 180 bp, reflecting the preferential accessibility of internucleosomal linker DNA to endonucleases (Arends *et al.,* 1990).

DNA fragmentation into high molecular weight fragments is a hallmark of apoptosis (Brown *et al.,* 1992; Huang *et al.,* 1995). In epithelial and endothelial cells undergoing apoptotic cell death, the nucleosomal fragments are often absent; analysis of the DNA on denaturing sucrose density gradients, however, reveals that infrequent single-strand nicks are generated (Gromkowski *et al.,* 1986).

Methodology

DNA fragmentation assay was conducted using the procedure of Wu *et al.,* (2005) and Gilbert *et al.,* (2007) with some modifications. All three cancer (MCF-7, MDA MB-468, Caco-2) and two normal (HUVEC and U937) cell lines were cultured at a density of $5x10^5$ per well in the presence or absence of isolated compounds (compounds **1-6**), according to their estimated IC_{50} for a specific cell line for 48 h. Actinomycin-D (4 μM), tamoxifen (5 μM) and anastrozole (5 μM) were used as positive controls. Cells were collected and washed with PBS. The pellet was homogenized in 450 μl of lysis buffer (20 mM Tris-HCl, pH 8.0, 10 mM EDTA, pH 8.0, 0.2% Triton X-100) by repeated pipetting in a microtube and incubated for 10 min on ice.

The lysates were centrifuged for 15 min at 13,000 x g and to the supernatants, 5 µl of 10% SDS solution was added. Then the samples were incubated at 50°C for 2 h after treating with 5 µl RNase A (1 mg/ml). A further 5 µl proteinase K (2 mg/ml) was added and incubated for 2 h at 37°C. DNA was precipitated with two volumes of 100% ice cold ethanol and 0.1 volume of 10 M ammonium acetate for 2 h at -70 °C. DNA was pelleted at 12,000×*g* for 15 min and washed twice with 70% ice cold ethanol and air-dried for 10 min at room temperature. The DNA pellet was dissolved in 30 µl of TE (Tris : EDTA) loading Buffer at 37 °C, and analyzed by electrophoresis.

A 1.5% agarose gel was made by dissolving 1.5 % w/v agarose (cat. 15510-027, Invitrogen, UK) solution in 1×TAE buffer (2 M Tris, 1 N glacial acetic acid and 0.05 M EDTA, pH 8), supplemented with 5 µl of GelRed (Biotium Hayward, UK). The solid gel was placed in a tank containing 1× TAE buffer. After solidification, isolated DNA was injected into the wells with Amplisize molecular marker (50-2,000 bp, Cat. 170-8200, Bio-Rad, UK) and a 100 V current applied for 45 min. After electrophoresis, the gel was visualised using the GelDoc system and was photographed through a digital camera.

3.7. Data presentation and statistical analysis

All data were compiled from a minimum of three experiments. Data for statistical analysis were expressed as the mean ± standard deviation, n (number of experiments). One-way ANOVA with Dunnett's or Tukey's post test, as specified, was performed using GraphPad Prism version 5.00 for Windows, GraphPad Software, San Diego California USA.

4. Results and Discussion

Medicinal Plants have a long history of use in the treatment of cancer. Plants have formed the basis for traditional medicine systems, which have been used for thousand of years in countries such as China (Chang *et al.*, 1986), India and Pakistan (Kapoor, 1990; Rehman *et al.*, 1982). Hartwell, in his review of plants used against cancer, lists more than 3000 plant species that have reportedly been used in the treatment of cancer (Hartwell, 1982). An impressive number of anticancer drugs have been isolated or derived from medicinal plants, are currently in clinical practice, based on their folklore use (Cragg *et al.*, 2001). Cancer chemotherapy plays a significant role in the treatment of many malignancies, either curative or palliative care, depending upon the specific tumour condition (Carter, 1982). The main objective of any cancer chemotherapy is to kill cancer cells with as little damage as possible to normal cells (Halliwell *et al.*, 1988). In the present study, four medicinal plants were selected from the Himalayan region of Pakistan, where these plants are used or claimed to be effective in the treatment of cancer based on folklore or traditional remedies.

4.1 Cytotoxicity of crude ethanolic extracts

The crude ethanolic extracts of four medicinal plants *Caralluma tuberculata, Fagonia indica, Solanum surattense* and *Arisaema utile* were investigated for anticancer activity against three cancer cell lines MCF-7 (Breast oestrogen dependent cancer cells), MDA MB-468 (Breast oestrogen independent cancer cells) and Caco-2 (Colorectal carcinoma cells). A series of eight dilutions of each crude extract (10–500 µg/ml) were used to determine the concentration-dependent anti-proliferative effect on cancer cells after 24 h treatment, using two cytotoxicity assays; MTT and Neutral Red uptake (NRU) assays. The results for percentage growth inhibition are summarised in Table 4.1 (MTT assay) and Table 4.2 (NRU assay) and the detailed calculations of absorbance for treated verses untreated cells (n=3, Mean ± STD) are enclosed in appendices (1-8).

Conc. (µg/ml)	Percentage growth inhibition of cancer cells (Mean ± Std. Dev.)											
	Caralluma tuberculata			*Fagonia indica*			*Solanum surattense*			*Arisaema utile*		
	MCF-7 cells	MDA MB-468 cells	Caco-2 cells	MCF-7 cells	MDA MB-468 cells	Caco-2 cells	MCF-7 cells	MDA MB-468 cells	Caco-2 cells	MCF-7 cells	MDA MB-468 cells	Caco-2 cells
10	22.19* (±5.94)	2.25 (±0.73)	12.50* (±4.62)	17.46* (±4.41)	15.96* (±6.82)	23.44* (±5.55)	21.58* (±3.27)	9.47 (±4.95)	10.87 (±5.67)	19.26* (±6.66)	10.15 (±2.91)	9.87 (±3.65)
25	24.78* (±7.19)	6.05 (±3.09)	23.75* (±5.34)	36.58** (±1.10)	27.97* (±2.18)	28.28* (±4.64)	37.50** (±415)	15.81* (±5.44)	16.76* (±6.90)	31.55** (±6.63)	13.32* (±3.24)	12.72* (±3.08)
50	41.65** (±3.87)	14.42* (±4.15)	31.79** (±4.23)	40.80 ** (±3.24)	49.25 ** (±5.00)	42.04** (±4.14)	35.45** (±8.67)	38.47** (±6.35)	37.98** (±3.83)	38.84** (±6.28)	23.80* (±2.86)	22.78* (±1.98)
100	40.04** (±3.48)	28.14 * (±6.32)	37.59** (±7.42)	37.18** (±5.75)	53.93*** (±4.00)	49.16** (±5.05)	35.22** (±5.17)	46.25** (±1.87)	44.74** (±4.94)	48.60** (±6.94)	40.53** (±3.72)	38.90** (±3.91)
200	48.41** (±4.26)	39.89** (±3.65)	55.14*** (±7.42)	49.76** (±4.36)	64.95*** (±4.24)	60.42*** (±7.19)	58.28*** (±4.85)	61.62*** (±7.33)	56.95*** (±3.92)	54.86*** (±5.12)	58.86*** (±3.76)	57.26*** (±4.48)
300	67.65*** (±3.00)	60.19 *** (±3.82)	68.23*** (±6.07)	47.20 ** (±8.90)	75.60*** (±8.56)	71.65*** (±7.12)	65.74*** (±7.85)	70.05*** (±4.73)	72.32*** (±7.44)	72.28*** (±4.52)	65.18*** (±3.39)	69.48*** (±4.79)
400	70.03*** (±6.52)	65.60*** (±3.48)	85.47 *** (±8.93)	61.23*** (±6.45)	88.90*** (±5.88)	76.28*** (±3.49)	73.70*** (±10.25)	74.82*** (±3.74)	81.68*** (±2.06)	81.72*** (±4.56)	81.56*** (±4.19)	85.15*** (±2.84)
500	82.36*** (±3.96)	76.18*** (±1.59)	93.18*** (±9.68)	84.51*** (±7.52)	94.24*** (±4.32)	82.99*** (±2.51)	95.88*** (±6.01)	85.04*** (±6.44)	85.95*** (±1.25)	91.32*** (±9.70)	86.89*** (±6.62)	90.54*** (±6.86)
Vehicle Control	1.11 (±4.43)	-1.39 (±4.05)	-0.01 (±6.15)	-7.51 (±3.03)	-2.10 (±4.26)	0.88 (±3.69)	2.87 (±8.63)	-1.63 (±5.20)	5.67 (±0.89)	-0.62 (±6.58)	1.73 (±9.33)	4.92 (±2.91)

Table 4.1: Cytotoxic activity of crude extract of four medicinal plants using MTT assay with apparent IC_{50} about 200 µg/ml after 24 hours treatment. Where statistically (Dunnett's multiple comparison test)
** = Significant (P<0.05), ** = Highly significant (P<0.01), *** = Very highly significant (P<0.001)*

Conc. (µg/ml)	Percentage growth inhibition of cancer cells (Mean ± Std. Dev.)											
	Caralluma tuberculata			*Fagonia indica*			*Solanum surattense*			*Arisaema utile*		
	MCF-7 cells	MDA MB-468 cells	Caco-2 cells	MCF-7 cells	MDA MB-468 cells	Caco-2 cells	MCF-7 cells	MDA MB-468 cells	Caco-2 cells	MCF-7 cells	MDA MB-468 cells	Caco-2 cells
10	30.12** (±3.02)	14.89 * (±7.84)	22.80* (±8.12)	29.00* (±6.12)	16.02* (±7.56)	30.13** (±3.93)	25.76* (±2.18)	13.98* (±3.97)	21.58* (±9.58)	16.76* (±3.49)	16.30* (±6.52)	19.43* (±8.35)
25	43.92** (±3.02)	29.89** (±9.29)	38.42** (±2.65)	33.05** (±6.12)	27.89* (±6.18)	41.77** (±4.63)	26.60* (±4.23)	29.60* (±3.97)	29.12* (±9.58)	29.69* (±3.49)	22.26* (±4.79)	25.87* (±6.06)
50	46.06** (±3.02)	46.06** (±3.57)	41.89** (±5.78)	44.17** (±6.12)	46.82** (±6.10)	56.89*** (±3.73)	30.52** (±4.32)	39.31** (±3.97)	36.34** (±9.58)	43.06** (±3.49)	37.25** (±7.02)	41.53** (±8.93)
100	53.36*** (±3.02)	49.48** (±5.00)	58.28*** (±4.55)	50.76*** (±6.12)	58.08*** (±7.16)	60.74*** (±7.43)	42.99** (±3.36)	53.53*** (±3.97)	45.72** (±9.58)	64.51** * (±3.49)	50.59*** (±7.39)	48.11** (±5.05)
200	52.69*** (±3.02)	56.11*** (±3.18)	68.74*** (±2.70)	51.50*** (±6.12)	58.75*** (±4.08)	65.06*** (±2.96)	59.78*** (±6.73)	55.75*** (±3.97)	62.49*** (±9.58)	84.23** * (±3.49)	65.02*** (±6.31)	66.37*** (±7.66)
300	73.72*** (±3.02)	62.32*** (±2.72)	75.80*** (±7.48)	58.09*** (±6.12)	71.62*** (±4.87)	76.97*** (±5.61)	72.47*** (±5.63)	66.62*** (±3.97)	79.29*** (±9.58)	94.82** * (±3.49)	73.18*** (±12.58)	72.50*** (±7.14)
400	87.20*** (±3.02)	72.69*** (±7.27)	92.47*** (±3.32)	81.68*** (±6.12)	80.89*** (±6.24)	89.64*** (±6.62)	91.78*** (±3.63)	73.72*** (±3.97)	87.80*** (±9.58)	98.39** * (±3.49)	82.10*** (±5.11)	90.14*** (±10.00)
500	93.87*** (±3.02)	81.34*** (±6.53)	96.52*** (±1.33)	96.15*** (±6.12)	86.18*** (±4.68)	94.97*** (±3.80)	96.86*** (±2.95)	93.29*** (±3.97)	91.13*** (±9.58)	98.08** * (±3.49)	86.67*** (±1.59)	93.30*** (±9.97)
Vehicle Control	4.03 (±3.02)	-1.82 (±4.23)	-2.70 (±6.69)	-1.61 (±6.12)	-1.49 (±6.05)	6.93 (±2.10)	-3.45 (±7.82)	1.38 (±3.97)	1.43 (±9.58)	-5.51 (±3.49)	0.29 (±10.14)	4.30 (±8.05)

Table 4.2: Cytotoxic activity of crude extract of four medicinal plants using neutral red uptake assay with apparent IC_{50} 100 µg/ml after 24 h treatment. Where statistically (Dunnett's multiple comparison test)
** = Significant (P<0.05), ** = Highly significant (P<0.01), *** = Very highly significant (P<0.001)*

These results indicate all the four plants possess very highly significant ($P<0.001$) concentration-dependent growth inhibition (up to 95%) activity in the malignant cells, with the apparent IC_{50} values ranging between 100 µg/ml (NRU assay) - 200 µg/ml (MTT assay) as shown in Tables 4.1 and 4.2.

The difference in the apparent IC_{50} values can be justified by the physiological mechanisms on which these assays are based. As in the MTT assay, tetrazolium salts are reduced to formazan by mitochondrial succinate dehydrogenase, an enzyme which is active only in viable cells with an intact respiratory chain (Green & Kroemer, 2004).

The uptake of neutral red depends on the lysosomal capacity to maintain pH gradients, through the production of ATP (Winckler *et al.,* 974). The weakly cationic dye penetrates cell membranes by non-ionic passive diffusion enabling a proton gradient to maintain a pH lower than that of cytoplasm. Thus, the dye becomes charged and retained inside the lysosomes of metabolically active cells, characterising the neutral red uptake assay as a more sensitive technique, differentiating between the dead and metabolically active cells that have a tendency to proliferate in the cultured cell population (Repetto *et al.,* 2008).

This preliminary screening data revealed that these four medicinal plants contain chemical constituents capable of cytotoxic activity against rapidly growing cancer cells and this needs further investigation.

4.2. Cytotoxicity of fractions from crude ethanolic extract

In a biologically activity-guided fractionation approach, the crude extract of each plant was partitioned into hexane, $CHCl_3$, EtOAc, MeOH and aqueous fractions. All the fractions were tested against MCF-7, MDA-MB-468 and Caco-2 cells at a concentration of 200 µg/ml, using MTT and neutral red uptake assays for 24 hours.

Fractions (200 µg/ml)	Percentage growth inhibition of cancer cells (Mean ± Std. Dev.)											
	Caralluma tuberculata			*Fagonia indica*			*Solanum surattense*			*Arisaema utile*		
	MCF-7 cells	MDA MB-468 cells	Caco-2 cells	MCF-7 cells	MDA MB-468 cells	Caco-2 cells	MCF-7 cells	MDA MB-468 cells	Caco-2 cells	MCF-7 cells	MDA MB-468 cells	Caco-2 cells
Hexane Frac.	50.62*** (±5.38)	5.29 (±3.51)	21.25* (±4.5)	69.36*** (±8.02)	11.61 (±4.37)	17.41 (±5.86)	49.08** (±5.21)	9.43 (±3.82)	7.77 (±4.83)	48.58** (±7.36)	8.62 (±5.08)	7.40 (±4.74)
Chloroform Frac.	79.69*** (±7.45)	21.38* (±5.11)	63.88*** (±5.99)	76.93*** (±6.84)	71.14*** (±5.58)	69.74*** (±7.92)	85.33*** (±3.41)	94.59*** (±3.00)	95.25*** (±4.35)	71.19*** (±2.76)	88.86*** (±5.29)	93.59*** (±5.00)
Ethyl acetate Frac.	95.00*** (±2.64)	38.47** (±6.42)	93.44*** (±3.89)	93.88*** (±3.31)	94.02*** (±5.23)	89.89*** (±3.45)	68.62*** (±2.48)	61.82*** (±4.07)	66.43*** (±3.24)	45.96** (±10.67)	43.26** (±3.73)	42.62** (±4.42)
Methanol Frac.	75.88*** (±8.41)	26.88* (±4.88)	46.84** (±6.22)	42.01** (±6.67)	47.15** (±3.30)	42.39** (±7.62)	49.20** (±4.76)	35.96** (±5.63)	42.19** (±4.27)	80.77*** (±8.38)	70.86*** (±3.61)	71.56*** (±3.76)
Aqueous Frac.	54.33*** (±1.89)	17.10 (±7.15)	26.74* (±3.64)	65.37*** (±3.34)	42.13** (±2.11)	19.73 (±4.71)	14.09 (±3.76)	26.19* (±3.44)	5.85 (±2.93)	9.14 (±3.01)	15.96 (±7.66)	31.58** (±3.47)
Vehicle Control	3.17 (±5.67)	-1.31 (±7.44)	-2.51 (±4.57)	3.32 (±5.94)	-1.31 (±7.44)	-3.28 (±5.13)	3.43 (±6.80)	0.20 (±2.34)	2.92 (±3.20)	4.23 (±7.80)	0.25 (±2.39)	2.86 (±3.14)

Table 4.3: Cytotoxic activity of fractions (200 µg/ml) from four medicinal plants using MTT assay indicating the most potent fraction after 24 h treatment. Where statistically (Dunnett's multiple comparison test)
** = Significant (P<0.05), ** = Highly significant (P<0.01), *** = Very highly significant (P<0.001)*

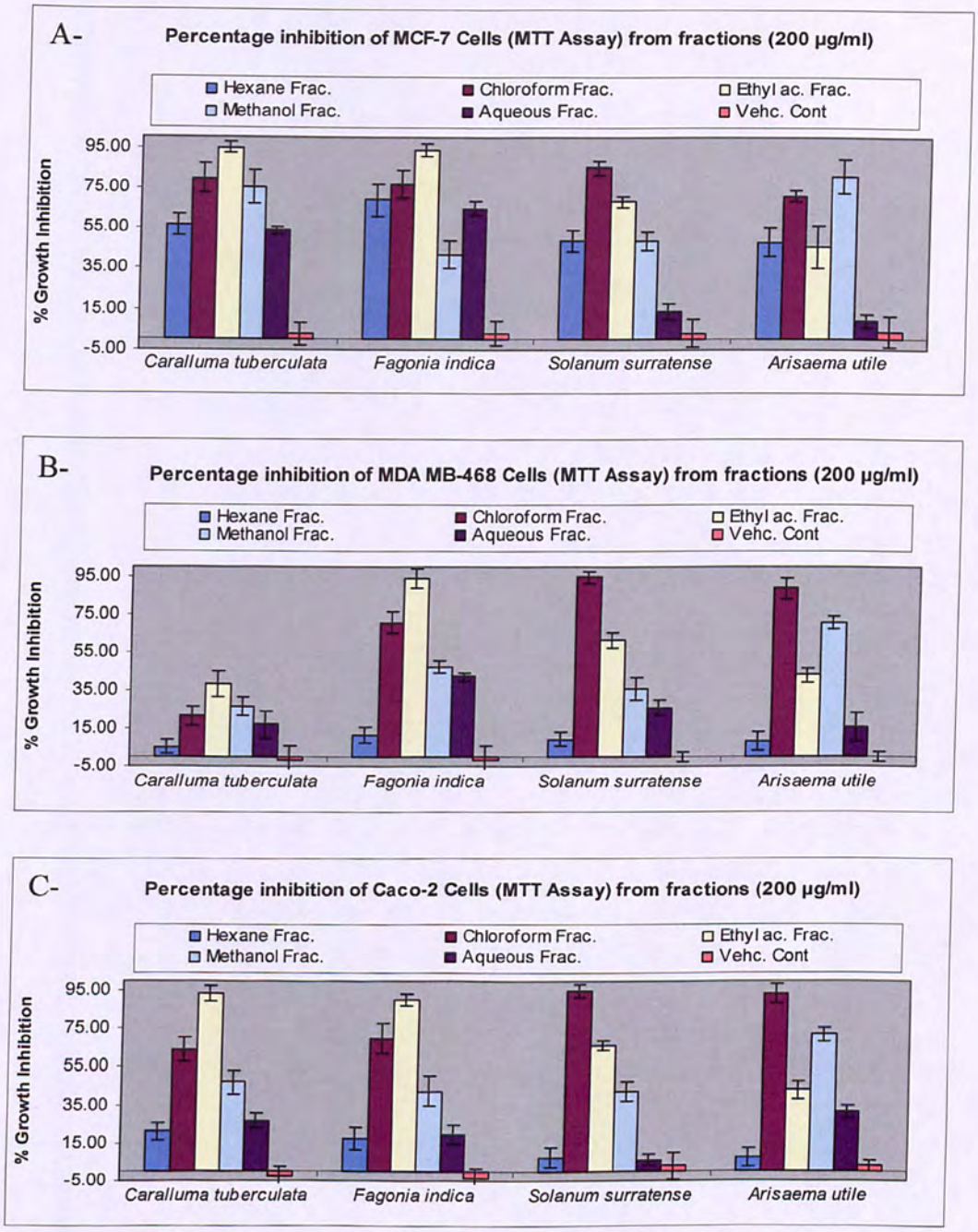

Figure 4.1: MTT assay results: showing percentage growth inhibition of cancer cells with fractions from four medicinal plants after 24 h treatment A- MCF-7 cells, B- MDA MB-468 cells, C- Caco-2 cells

Percentage growth inhibition of cancer cells (Mean ± STD, n=3) and levels of statistically significance (based on Dunnet's Test) are summarised in Table 4.3 (MTT assay) and Table 4.4 (NRU assay); the detailed calculations of absorbance for treated verses untreated cells (n=3, Mean ± STD) are enclosed in appendices (9-16).

Results showed in *Caralluma tuberculata*, that the anti-proliferative activity was significantly concentrated in three fractions: chloroform, ethyl acetate and methanol fractions against MCF-7, MDA MB-468 and Caco-2 cells. Overall in this plant, the ethyl acetate fraction was found to be the most potent fraction reducing the growth by 95.00 % (±2.64) in MCF-7 (Figure 4.1-A), 93.44 % (±3.89) in Caco-2 (Figure 4.1-C). MDA MB-468 cells (Figure 4.1-B) were less sensitive to each of the fractions from *Caralluma tuberculata,* but the EtOAc fraction was still the most potent fraction, with only 38.47% (±6.42) inhibition (Table 4.3). These results were further verified with the neutral red uptake assay, where the activity was similar to that observed in the MTT assay. Again the EtOAc fraction showed maximum inhibition 96.00% (±7.65) in Caco-2 (Figure 4.2-B), 94.13% (±4.01) in MCF-7 (Figure 4.2-A) and 45.55% (±2.83) in MDA MB-468 cells (Figure 4.2-C) after 24 h treatment (Table 4.4).

In *Fagonia indica*, a similar pattern of growth inhibition was observed in fractions as *Caralluma tuberculata* (Table 4.3). In the MTT assay, the EtOAc fraction again showed maximum cytotoxicity in the three cancer cell lines exhibiting 93.88 % (±3.31) in oestrogen dependent (Figure 4.1-A) and 94.02 % (±5.23) in oestrogen independent breast cancer cells (Figure 4.1-B), while for colorectal cancer cells the results were also very promising and showed 89.89% (±3.45) inhibition (Figure 4.1-C). The EtOAc fraction of *Fagonia indica* in comparison to *Caralluma tuberculata* was more responsive to MDA MB-468 cells (Figure 4.1-B) and antiproliferative activity was further in support from neutral red uptake assay where 92.04% (±3.80) reduction in growth was observed. Furthermore, the results from the neutral red uptake assay revealed that only 3-6% of

metabolically active cells could survive in Caco-2 and MCF-7 cell lines, where growth was reduced to 97.94% (±2.83) and 93.81% (±2.32) respectively (Table 4.4).

In contrast to *Caralluma* and *Fagonia*, the chloroform fraction of *Solanum surattense* showed maximum cytotoxic activity against cancer cells as compared to hexane, ethyl acetate, methanol and aqueous fractions. Cell viability in the MTT assay (Table 4.3) was greatly reduced to 3-6% in the three cell lines where the calculated inhibition was 85.33% (±3.41) in MCF-7 (Figure 4.1-A), 94.59% (±3.00) in MDA-MB 468 (Figure 4.1-B) and 95.25% (±4.35) in Caco-2 cells (Figure 4.1-C). Neutral red uptake assay (Table 4.4) also exhibited almost the same cell viability results in chloroform fractions where antiproliferative activity climbed up to 97.29% (±3.14) in MCF-7 (Figure 4.2-A), 97.42% (±1.70) in MDA MB-468 (Figure 4.2-B) and 93.27% (±2.88) in Caco-2 (Figure 4.2-C). A significant to moderate growth inhibition (70-45%) was also observed in ethyl acetate and methanol fractions, while hexane and aqueous fractions did not show any promising results.

Four organic and one aqueous fractions of *Arisaema utile* were also evaluated for cytotoxicity studies, where most cytotoxic constituents were observed to concentrate in the chloroform fraction, based on MTT and neutral red uptake assays.In the MTT assay (Table 4.3), a highly significant reduction in cell proliferation was marked with a percentage inhibition for Caco-2 cells (Figure 4.1-C) of 93.59% (±5.00), followed by 88.86 % (±5.29) and 71.19 % (±2.76) for MDA MB-468 (Figure 4.1-B) and MCF-7 Cells (Figure 4.1-A) respectively. Neutral red uptake assay (Table 4.4) retained this remarkable activity and showed an increased potency in the chloroform fraction. The results showed only 3-10% of metabolically active cells could survive and the percentage growth inhibition jumped to 95.53% (±6.62) for MCF-7 (Figure 4.2-A), 97.41% (±3.33) for MDA MB-468 (Figure 4.2-B) and 90.38% (±6.05) for Caco-2 cells (Figure 4.2-C).

Fractions (200 µg/ml)	Percentage growth inhibition of cancer cells (Mean ± Std. Dev.)											
	Caralluma tuberculata			*Fagonia indica*			*Solanum surattense*			*Arisaema utile*		
	MCF-7 cells	MDA MB-468 cells	Caco-2 cells	MCF-7 cells	MDA MB-468 cells	Caco-2 cells	MCF-7 cells	MDA MB-468 cells	Caco-2 cells	MCF-7 cells	MDA MB-468 cells	Caco-2 cells
Hexane Frac.	29.57* (±3.87)	13.65 (±1.46)	28.79* (±7.77)	53.16*** (±3.31)	21.39* (±5.17)	31.80** (±8.46)	21.44* (±1.54)	20.48* (±8.08)	13.28 (±5.49)	23.45* (±0.82)	23.91* (±7.68)	14.61 (±3.91)
Chloroform Frac.	57.05*** (±1.42)	39.47** (±8.05)	62.68*** (±3.33)	81.67*** (±4.15)	77.92*** (±8.42)	81.16*** ±9.03)	97.29*** (±3.14)	97.42*** (±1.70)	93.27*** (±2.88)	95.53*** (±6.62)	97.41*** (±3.33)	90.38*** (±6.05)
Ethyl acetate Frac.	94.13*** (±4.01)	45.55** (±2.83)	96.00*** (±7.65)	93.81*** (±2.32)	92.04*** (±3.80)	97.94*** (±2.83)	73.32*** (±7.16)	76.40*** (±5.91)	67.47*** (±8.57)	34.36** (±1.90)	61.35*** (±14.88)	44.25** (±3.32)
Methanol Frac.	75.18*** (±6.32)	36.37** (±4.64)	52.14*** (±10.53)	36.76** (±3.05)	56.26*** (±1.54)	49.35** (±5.57)	37.47** (±2.49)	51.11*** (±7.29)	44.53** (±7.27)	69.58*** (±2.17)	87.29*** (±2.88)	66.99*** (±5.53)
Aqueous Frac.	59.84*** (±4.19)	19.82 (±10.85)	56.59*** (±7.02)	46.04** (±2.26)	40.52** (±10.89)	38.25** (±10.11)	20.31* (±3.42)	34.70** (±10.83)	36.76** (±12.87)	24.45* (±1.00)	21.72* (±3.43)	50.99*** (±11.29)
Vehicle Control	-0.19 (±2.68)	5.97 (±4.38)	4.57 (±9.23)	-0.19 (±2.68)	5.97 (±4.38)	4.57 (±9.23)	4.08 (±4.16)	-2.01 (±4.79)	2.13 (±0.93)	4.08 (±4.16)	-2.01 (±4.79)	2.13 (±0.93)

Table 4.4: Cytotoxic activity of fractions (200 µg/ml) from four medicinal plants using neutral red uptake assay indicating the most potent fraction after 24 h treatment. Where statistically (Dunnett's multiple comparison test)
** = Significant (P<0.05), ** = Highly significant (P<0.01), *** = Very highly significant (P<0.001)*

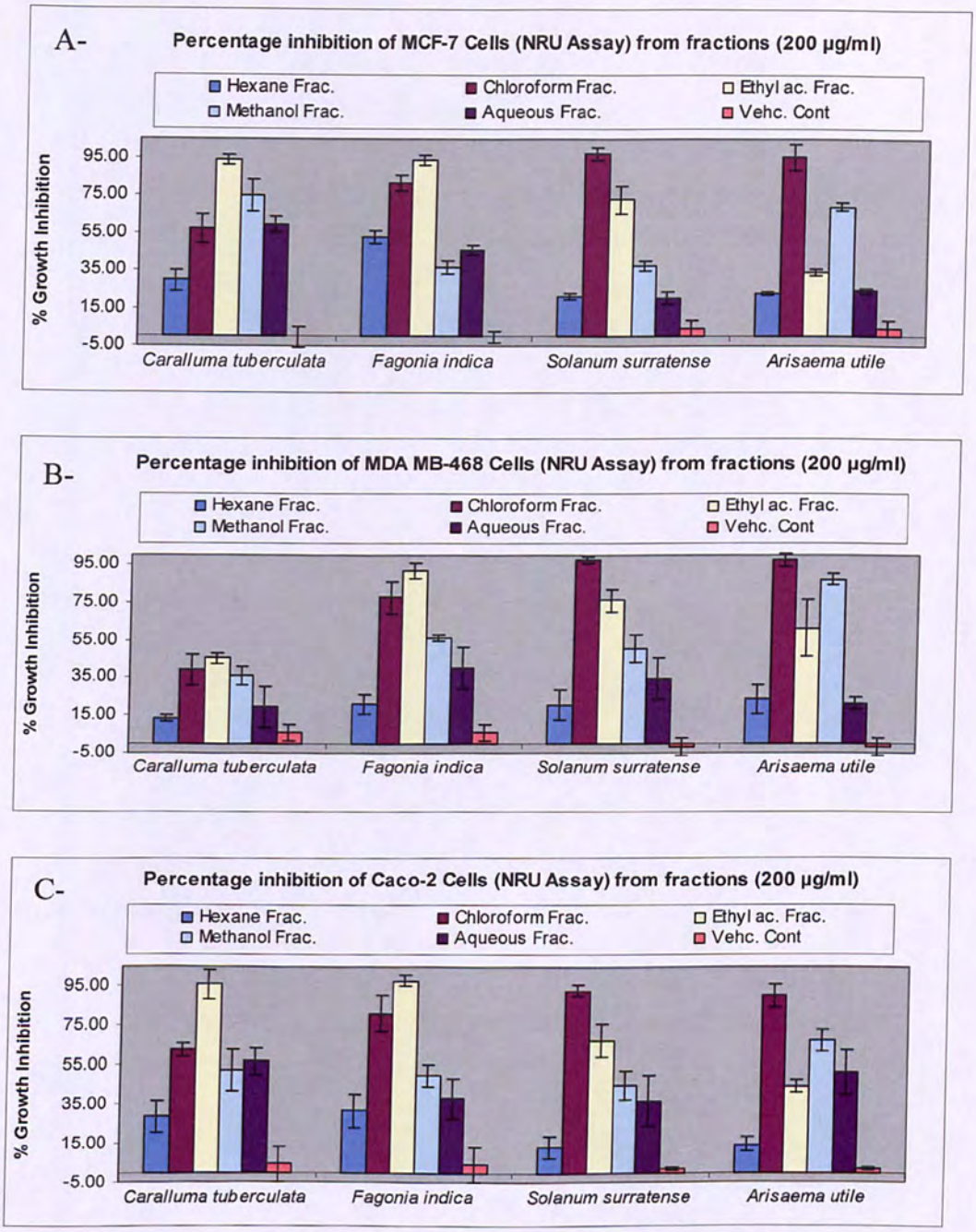

Figure 4.2: Neutral red uptake assay results: showing percentage growth inhibition of cancer cells with fractions from four medicinal plants after 24 h treatment A- MCF-7 cells, B- MDA MB-468 cells, C- Caco-2 cells

Moreover, the methanol fraction also showed significant cytotoxicity in three cancer cell lines, where percentage growth inhibition rose to 87.29% (±2.88) for the MDA MB-468 (in NRU assay), while a very highly significant ($P<0.001$) increase of 80.77% (±8.38) in MCF-7 was observed in the MTT assay.

4.3 Phytochemical analysis: *Caralluma tuberculata*

The cytotoxicity screening of four organic (hexane, chloroform, ethyl acetate, methanol) and an aqueous fraction from *Caralluma tuberculata* against the breast cancer cells (MCF-7 and MDA-MB-468) and colorectal carcinoma cells (Caco-2) showed that the ethyl acetate fraction is the most potent fraction and this was selected for further phytochemical analysis. A series of chromatographic experiments (normal and reverse phase flash column chromatography) resulted in the isolation of two acylated steroidal glycosides Compounds **1** and **2** from the potent fraction.

4.3.1 Compound 1 (Acylated Pregnane Glycoside)

Compound **1** was analysed through different physico-chemical means and a series of spectroscopic techniques (IR, LC-MS, NMR) including X-ray crystallography in order to identify and elucidate the molecular structure.

4.3.1.1. *Physico-chemical characteristics*

Compound **1** was isolated as a light-yellowish white amorphous powder (yield 62 mg), with melting point ranging 206-208°C. Optical rotation was calculated as: $[\alpha]_D^{20} = +4.0°$, (*c* 0.012, MeOH).

The Lieberman-Burchard test gave a positive result, indicated by the appearance of a dark green colour, when acetic anhydride and concentrated sulphuric acid were added to a chloroform solution of Compound **1** and demonstrated that the

isolated compound may have a steroidal skeleton. The change in colour is due to the hydroxyl group (-OH) of the steroid reacting with the reagents (acetic acid and sulphuric acid) and increasing the conjugation of the un-saturation in the adjacent fused rings in a steroidal skeleton (Burke *et al.,* 1974; Halim *et al.,* 1996).

4.3.1.2. Infra-Red spectroscopy of Compound 1

The IR spectrum showed a broad absorption band at 3444 cm^{-1} due to the hydroxyl (-OH) group, 2949, 2922, 2852 cm^{-1} bands represented the asymmetric and symmetric stretch vibrations of ($-CH_3$) and ($-CH_2$) groups. Aliphatic ester (C=O) stretch vibrations were observed at 1713 cm^{-1} while a medium intensity band at 1275 cm^{-1} represented the (C–O) group of an ester.

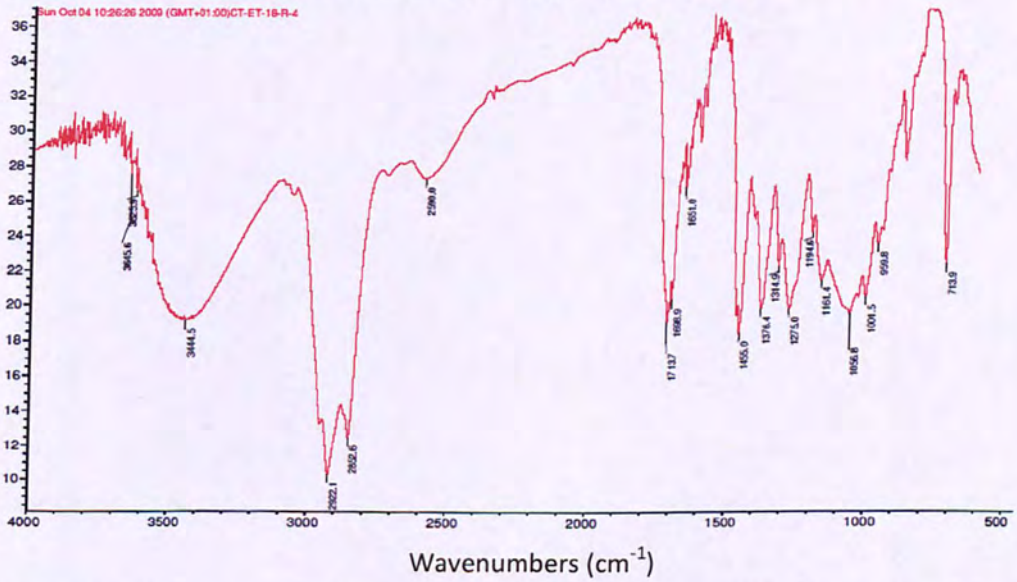

Figure 4.3: IR spectrum of Compound 1 showing absorption bands of functional groups corresponds to % Transmittance versus Wavenumber (cm^{-1}).

4.3.1.3. Nuclear Magnetic Resonance (NMR) spectroscopy

The ^1H- and ^{13}C-NMR (CD_3OD, 400 and 100 MHz) data is presented in Table 4.5. The analysis of ^1H and ^{13}C-NMR data for aglycon moiety indicated the

No.	δ_H	δ_C	No.	δ_H	δ_C
1	1.14(2H, m, H-1α, H-1β)	36.8, t	12	4.91(1H, m, H-12α)	79.1, d
2	1.79(2H, m, H-2α, H-2β)	29.1, t	13	----------	52.0, s
3	3.83(1H, m, H-3β)	77.1, d	14	OH-14β	85.8, s
4	1.58(2H, m, H-4α, H-4β)	35.5, t	15	2.05(2H, m, H-15α, H-15β)	34.3, t
5	1.29 (1H, m, H-5α)	48.6, d	16	1.92(2H, m, H-16α, H-16β)	28.6, t
6	1.10(2H, m, H-6α, H-6β)	26.1, t	17	3.02(1H, m, , H-17α)	49.9, d
7	1.14(2H, m, H-7α, H-7β)	31.1, t	18	1.05(3H, s, H-18β)	9.0, q
8	1.70(1H, m, H-8β)	40.1, d	19	0.81(3H, s, H-19β)	18.2, q
9	1.36(1H, m, H-9α)	44.3, d	20	3.59(1H, m, H-20 β)	73.9, d
10	----------	35.7, s	21	1.09(3H, d, *J* = 6.2 Hz, H-21)	18.8, q
11	1.93(2H, m, H-11α, H-11β)	27.5, t	---	----------	---------
Benzoyl					
1	----------	166.5, s	4,6	7.49(2H, t, *J* = 7.6 Hz, H-4, 6)	128.6, d 128.3, d
2	----------	130.7, s	5	7.61(1H, *dd*, *J* = 7.3, H-5)	133.1, d
3,7	8.09(2H, *dd*, *J* = 6.9 Hz, H-3, 7)	129.4, d 129.1, d	---	----------	---------
Acetyl					
-CH_3	1.91 (3H, s)	20.5, q	-C=O	----------	171.1, s

Table 4.5: ^{1}H- and ^{13}C-NMR data (ppm) of aglycon moiety of Compound 1*

**Multiplicity of assigned peaks were determined by edited DEPT experiments (s= quaternary, d = methine, t = methylene, q = methyl), (TMS as internal standard)*

presence of one acetyl (methyl at δ_H 1.91 as singlet for 3H and -C=O at δ_C 171.1) and one benzoyl (-C=O at δ_C 166.5, C quaternary at δ_C 130.7 and five methine groups at δ_C 129.4, 128.6, 133.1, 128.3, 129.1) moieties (Table 4.5). In the 2D-NMR (HMBC) spectrum, the strong long-range correlation between the carbonyl group at δ_C 171.1 and hydrogen at C-20 (δ_H 3.59), and carbonyl group at δ_C 166.5 and hydrogen at C-12 (δ_H 4.91) confirmed the position of acetylation at C-20 and benzoylation at C-12. The α-configuration of hydrogen at C-17 was suggested on the basis of a lack of evidence of spatial correlation between hydrogen at C-17 and CH_3-18.

No	Glucopyranose I		Glucopyranose II		Ribopyranose	
	δ_H	δ_C	δ_H	δ_C	δ_H	δ_C
1	4.55, d, *J* = 8.2	102.7, d	4.71, d, *J* = 8.2	102.1, d	4.79, d, *J* = 9.5	100.9, d
2	3.18, t, *J* = 9.3	71.9, d	3.28, t, *J* = 9.3	72.3, d	3.41, t , *J* = 1.8	73.8, d
3	3.32, t, *J* = 9.5	77.2, d	3.32, t, *J* = 9.5	77.1, d	3.59, t, *J* = 10.8	82.5, d
4	3.23, t, *J* = 8.6	69.8, d	3.26, t, *J* = 8.6	68.5, d	3.65, m	82.8, d
5	3.26, m	77.4, d	3.26, m	77.4, d	3.39, d, *J* = 5.1	68.5, t
6a	3.60, dd, *J* = 10.5	61.4, d	3.60, dd, *J* = 10.5	61.4, t	---------	---------
6b	3.80, m, *J* = 10.8	---------	3.80, m, *J* = 10.8	---------	---------	---------
OCH_3	---------	---------	---------	---------	3.33, s	59.8, q

Table 4.6: ^1H- and ^{13}C-NMR data (ppm) of sugar moieties of Compound 1*
** Multiplicity of assigned peaks were determined by edited Dept experiments*
(s = quaternary, d = methine, t = methylene, q = methyl), (TMS as internal standard)

Moreover, cross peak signals in DQF-COSY experiments (Figure 4.4) were observed between hydrogen at C-17 to hydrogen at C-20. Signals for protons of the methyl group at position 18 and hydrogen at position 20 strongly suggest the

stereochemistry as β of C-20, which is further supported from the absence of any correlation between 3 protons at C-21 and 3 protons at C-18 is in relation to the reported data (Abdel-Sattar *et al.,* 2008). The ^{1}H-NMR spectrum of Compound **1** displayed three anomeric protons (Table 4.6), which all appear as doublets at δ 4.79 (J = 9.5 Hz) , 4.71 (J = 8.2 Hz), 4.55 (J = 8.2 Hz) with the large coupling constant between 8.2 - 9.5 Hz, diagnostic of the axial orientations for all three sugar moieties (Agrawal, 1992).

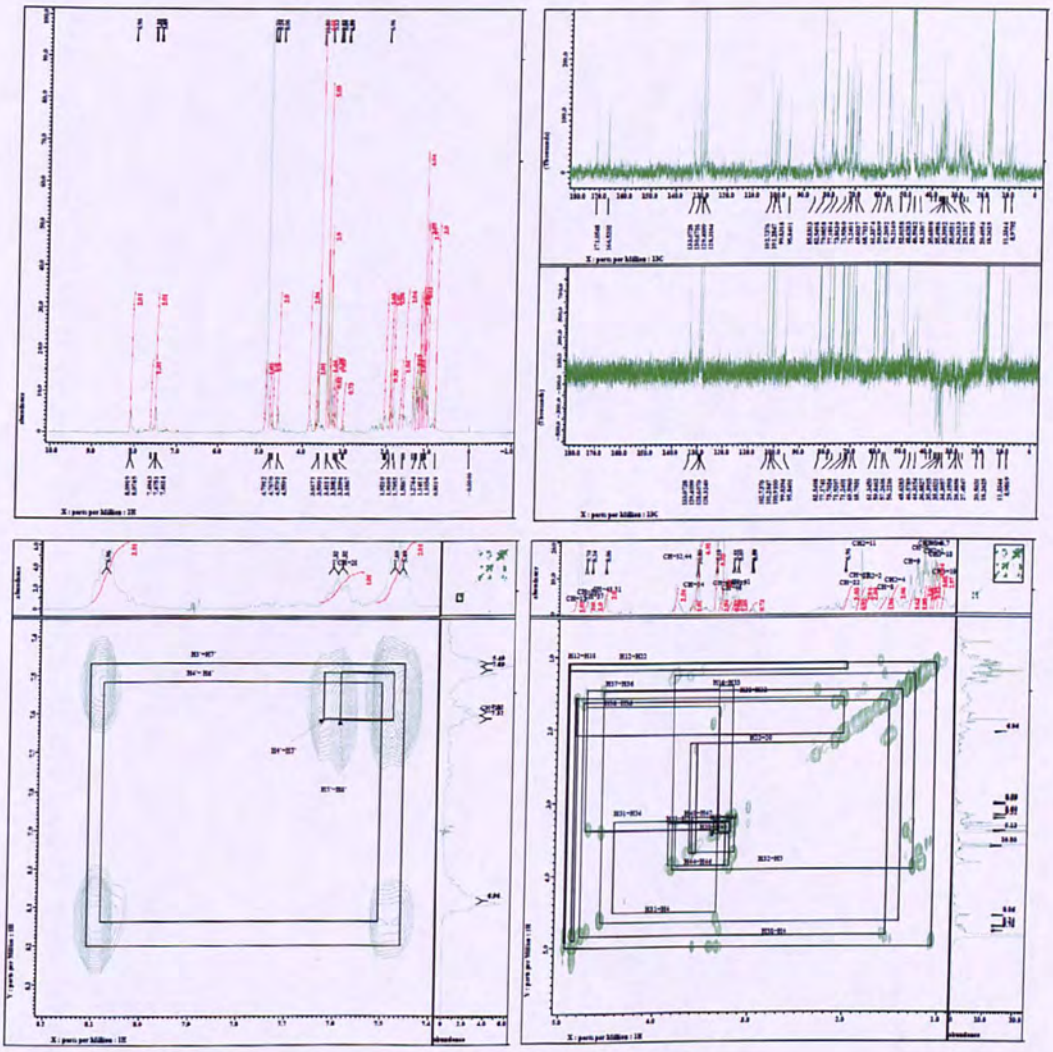

Figure 4.4: 1D (^{1}H, ^{13}C, DEPT) NMR and 2D (DQF-COSY) NMR spectra of Compound 1

The sequence of sugar moieties and their linkage sites in-between and with the aglycon part were determined from HMBC and DQF-COSY spectral data, which showed correlation peaks between H-1_{Ribopy} – C-3, H-$1_{Glucopy}$ – C-4_{Ribopy}, H-$1_{Glucopy}$ – C-$4_{Glucopy}$. The ^{1}H-NMR signal for one methoxy group at C-3 of ribopyranoside was observed at δ_H 3.33 as a singlet and in ^{13}C-NMR at δ_C 59.8 (Table 4.6), whereas the protons of the methylene group at C-5 was found at δ_H 3.39 as a doublet (J = 5.1 Hz) and δ_C 68.5 ppm, supporting the presence of the 3-methoxy-β-D-ribopyranosyl moiety.

The ^{13}C-NMR and edited DEPT (Dept-45, Dept-90, Dept-135) experiments revealed a total of 48 carbon signals, of which five methyl carbons, eleven methylene carbons, twenty-six methine carbons, and six quaternary carbons, corresponding to an acylated pregnane glycoside ($C_{48}H_{72}O_{20}$) carrying three sugar moieties.

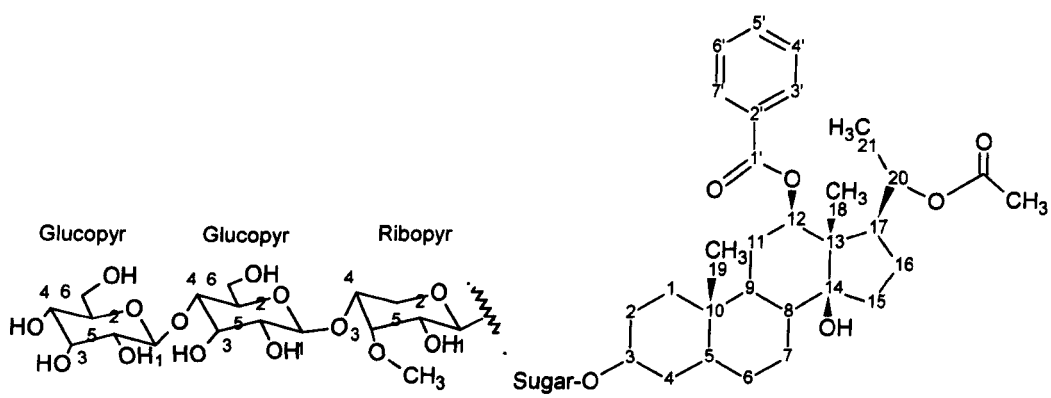

Figure 4.5: Proposed structure of Compound 1 identified as acylated pregnane glycoside from the ethyl acetate fraction of Caralluma tuberculata

In the steroidal skeleton, the NMR (^{1}H, ^{13}C and edited DEPT) spectral data clearly implied the absence of olefinic carbon atoms, indicating that there is no double bond in the compound. This is further supported by data from IR spectrum.

Therefore, based on the present studies and reported data, the structure of Compound **1** was established as 12-*O*-benzoyl-20-*O*-acetyl-3β,12β,14β,20β-tetrahydroxy-(20S)-pregnan-3-yl-*O*-β-D-glucopyranosyl-(1→4)-β-D-glucopyranosyl-(1→4)-3-methoxy-β-D-ribopyranoside (Figure 4.5).

4.3.1.4. Liquid Chromatography- Mass Spectrometry (LC-MS)

Based on the data analysis from NMR and IR studies, the molecular formula for Compound **1** (acylated pregnane glycoside) was determined as $C_{48}H_{72}O_{20}$ with calculated monoisotopic mass 968.4617. High resolution (HR) mass spectra (Figure 4.6) were recorded on a LCT Mass Spectrometer with Time-of-Flight (TOF), using electro spray ionisation (ESI +ve mode) and this showed *m/z*: 969.4681 (calculated for $C_{48}H_{72}O_{20}$ $[M+H]^+$: 969.4687).

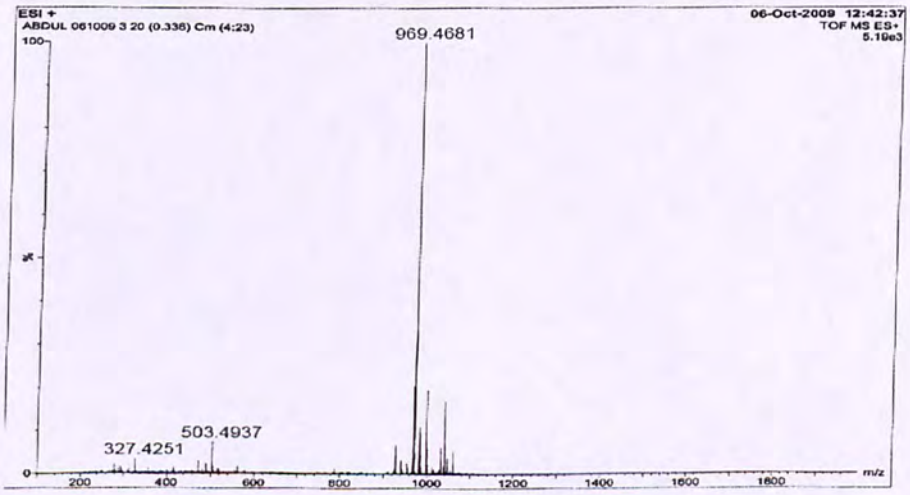

Figure 4.6: High resolution mass spectrum of Compound 1 on LCT Mass spectrometer with TOF in ESI +ve mode.

LC-MS/MS ESI (+ve mode) data showed molecular ion peak at *m/z* 969.30, $[M+H]^+$ which corresponded to a calculated *m/z*: 969.4687. The fragmentation pattern exhibited a daughter ion peak at *m/z* 847 showing loss of a fragment that may be a benzoyl group ($C_7H_6O_2$, nominal mass 122), which upon further loss of

a nominal mass 60 (two CH-OH groups) yielded the daughter ion peak at *m/z* 787 providing further supporting evidence.

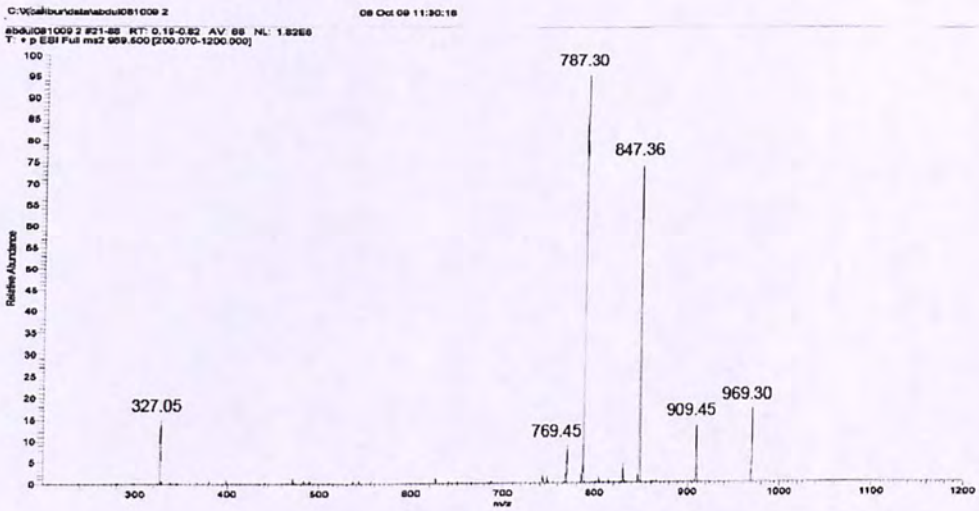

Figure 4.7: Daughter ion peaks correspond to molecular ion of Compound 1 on LC-MS/MS in ESI +ve mode.

4.3.2 Compound 2 (Acylated Androstane Glycoside)

The identification and structure elucidation of Compound **2** was carried through different physico-chemical means and a number of advanced spectroscopic techniques (IR, LC-MS, NMR), including X-ray crystallography.

4.3.2.1. Physico-chemical characteristics

Compound **2** was also isolated as an amorphous powder (yield 75 mg), light-yellowish white in colour, with a melting point ranging 219-221°C. Optical rotation was calculated as: $[\alpha]_D^{20}$= +4.5°, (*c* 0.015, MeOH).

The steroidal nature of Compound **2** was indicated by the appearance of dark green colour, when acetic anhydride and concentrated sulphuric acid were added to a chloroform solution in the Lieberman-Burchard test. The positive result may

suggest an increase in the conjugation of the un-saturation in the adjacent fused rings in a steroidal skeleton, as described earlier for Compound **1** (Burke *et al.*, 1974; Halim *et al.*, 1996).

4.3.2.2. Infra-Red spectroscopy of compound 2

The IR spectrum showed a broad absorption band at 3426 cm^{-1} for the hydroxyl (–OH) group; the asymmetric and symmetric stretch vibrations of ($-CH_3$) and ($-CH_2$) groups are represented as 2953, 2923, 2853 cm^{-1} bands. Aliphatic ester (C=O) stretch vibrations were observed at 1713 cm^{-1}. A medium intensity band at 1456 cm^{-1} indicates ($-CH_3$) asymmetric deformation vibration, while a weak intensity band at 1275 cm^{-1} represented the (C-O) group of an ester.

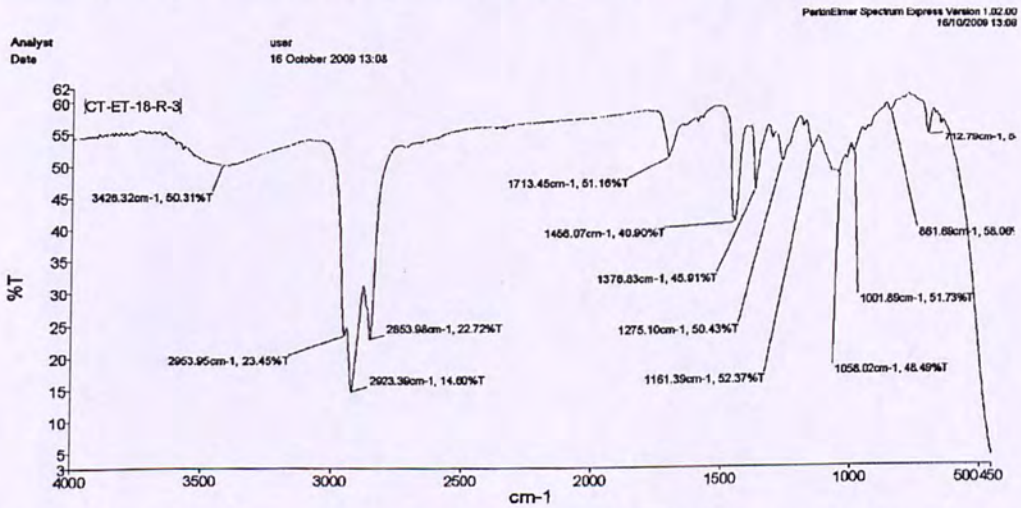

Figure 4.8: IR spectrum of Compound 2 showing absorption bands of functional groups corresponds to % Transmittance versus Wavenumber (cm^{-1}).

4.3.2.3. Nuclear Magnetic Resonance (NMR) spectroscopy

^{1}H, ^{13}C-NMR, DEPT and DQF-COSY NMR experiments (Figure 4.9) showed many similarities, as observed in elucidating the structure of the aglycon moiety

No.	δ_H	δ_C	No.	δ_H	δ_C
1	1.15(1H, m, H-1α, H-1β)	36.9, t	12	4.89(1H, m, H-12α)	82.4, d
2	1.81(2H, m, H-2α, H-2β)	29.1, t	13	----------	52.0, s
3	3.85(1H, m, H-3β)	77.1, d	14	OH-14β	85.8, s
4	1.57(2H, m, H-4α, H-4β)	35.6, t	15	2.10 (1H, m, H-15β)	36.3, t
5	1.40(1H, m, H-5α)	43.3, d	16	2.32(2H, m, H-16α, H-16β)	28.6, t
6	1.68,(2H, m, H-6α, H-6β)	34.5, t	17	3.17(1H, m, H-17α)	46.1, d
7	3.52(1H, m, H-7α)	71.4, d	18	1.26(3H, s, H-18β)	9.1, q
8	2.16(1H, m, H-8β)	40.2, d	19	0.81(3H, s, H-19β)	19.7, q
9	1.89 (1H, m, H-9α)	44.3, d	20	3.30(1H, m, H-20)	73.6, d
10	----------	35.7, s	21	1.30(2H, q, *J* = 5.8 Hz, H-21)	27.5, t
11	1.93(2H, m, H-11α, H-11β)	26.1, t	---	----------	---------
Benzoyl at C-12					
1'	----------	166.4,	4',6'	7.50(2H, t, *J* = 7.1 Hz, H-4, 6)	128.3, d
2'	----------	130.7,	5'	7.61(1H, *dd*, *J* = 7.1, 6.9 Hz, H-5)	133.0,
3',7'	8.09(2H, *dd*, *J* = 7.14, 6.9Hz, H-3, 7)	129.4, d 129.1,d	---	----------	---------
Acetyl at C-20					
$-CH_3$	1.89 (3H, s)	17.8,q	-C=O	----------	170.9,s
Acetyl at C-7					
$-CH_3$	2.01 (3H, s)	18.3, q	-C=O	----------	171.6, s
Isopropyl at C-21					
$-CH_3$	1.26 (6H, m)	11.4, q 12.3, q	-CH	2.12 (1H, m)	20.6, d

Table 4.7: ^{1}H- and ^{13}C-NMR data (ppm) of aglycon moiety of Compound 2*

**Multiplicity of assigned peaks were determined by edited DEPT experiments (s= quaternary, d = methine, t = methylene, q = methyl), (TMS as internal standard)*

of Compound **1** (Table 4.5). By comparing the spectral data (Table 4.7), Compound **2**, in the DQF-COSY experiment also showed the presence of an acetyl group at C-20 and a benzoyl group at C-12 (Figure 4.9), however, two differences were observed in the spectral data of the aglycon part.

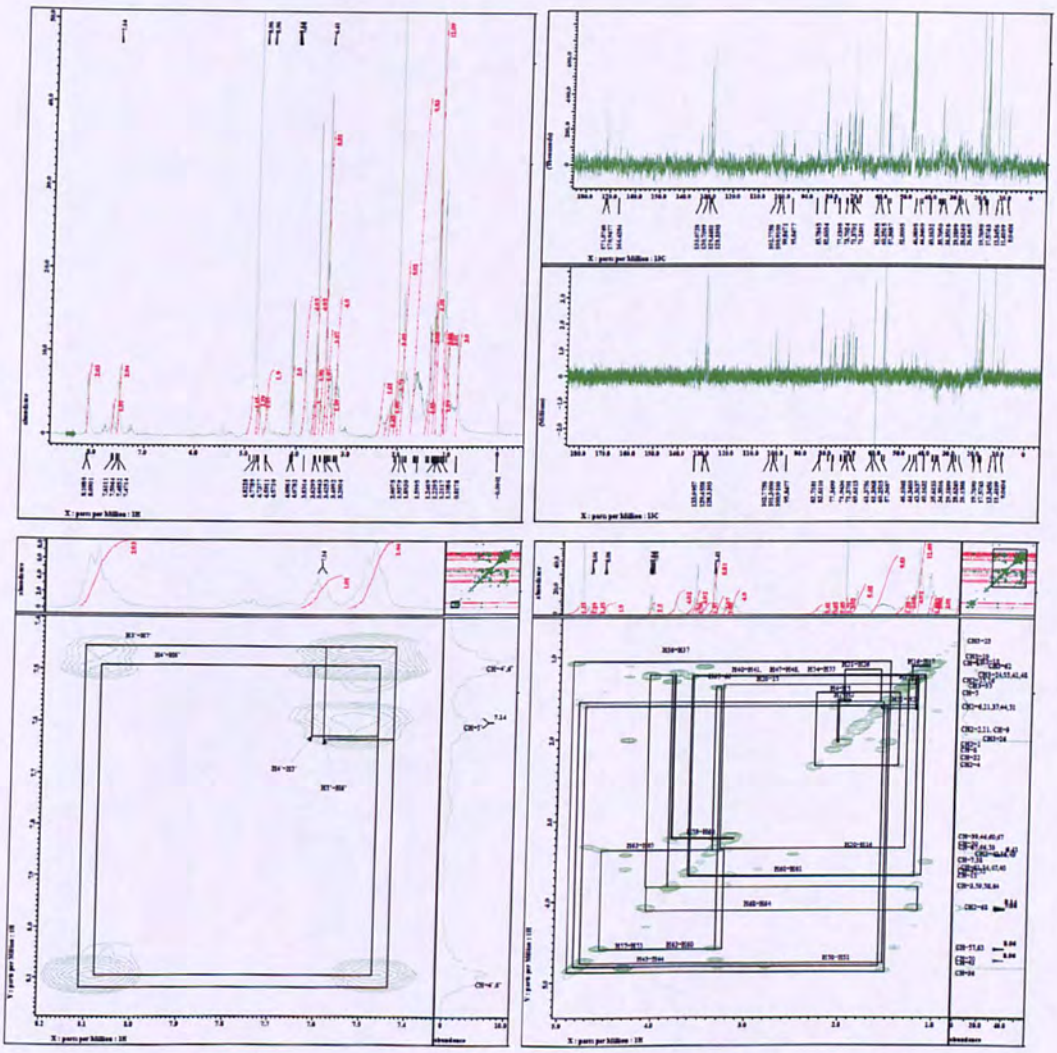

Figure 4.9: 1D (^1H, ^{13}C, DEPT) NMR and 2D (DQF-COSY) NMR spectra of Compound 2 (Acylated androstane glycoside)

Firstly, a ^{1}H-NMR signal was observed for the hydrogen attached to C-7 at δ_H 3.52 as a multiplet. According to the ^{13}C-NMR spectrum, a methine signal at δ_C

71.4 was observed, in contrast to the methylene signal found in Compound **1** (Table 4.7).This was confirmed with DEPT-NMR experiments. In the ^{1}H-NMR, the three protons of the methyl group of the acetyl moiety were observed at δ_H 2.01 as a singlet. In ^{13}C-NMR, the methyl group appeared at δ_C 18.3 and quaternary (C=O) at δ_C 171.6.

From the 2D-NMR (HMBC) spectrum, it may be suggested that C-7 is attached to an acetyl group, which is further supported by long range coupling correlations between the hydrogen of the methyl group and the hydrogen at C-6 and C-8. In addition, from this ^{1}H-^{1}H long range coupling correlations, the β stereochemical characterisation of the acetyl group at C-7 can be supported (Abdel Sattar *et al.*, 2008; Nomura *et al.*, 1979; Li *et al.*, 1999).

Secondly, the ^{1}H-NMR signal was observed for hydrogen at C-21 at δ_H 1.30 for 2H as a quartet (J = 5.8); moreover in ^{13}C and the edited Dept NMR data, a signal at δ_C 27.5 indicated the presence of a methylene group. In ^{1}H-NMR, at δ_H 2.12 (1H, m), 1.26 (6H, m) and in ^{13}C-NMR, at δ_C 20.6 (-CH), 12.3 (-CH_3), 11.4 (-CH_3) exhibit the attachment of side chain as an isopropyl group.

The ^{1}H and ^{13}C-NMR spectra displayed five anomeric protons (Table 4.8) instead of three in Compound **1**, which appeared at δ_H 4.89 (dd, J = 2, 9.52 Hz), 4.82 (dd, J = 2, 9.5 Hz), 4.77 (dd, J = 2, 9.5 Hz), 4.73 (d, J = 8.0 Hz), 4.57 (d, J = 8.0 Hz) and corresponding anomeric carbons occurred at δ_C 98.0, 99.2, 100.6, 101.3, 102.8 respectively (Table 4.9). The stereochemistry of anomeric protons of all five sugars was established on the basis of their large coupling constants (8.0 – 9.5 Hz). Signals in ^{1}H-NMR for three methyl at δ_H 1.18 (d, J = 6.0 Hz), 1.21 (d, J = 6.0 Hz), 1.24 (d, J = 6.0 Hz) and for three methoxyl δ_H 3.40 (s), 3.42 (s), 3.60 (s) along with three methylenes in ^{13}C-NMR at δ_C 35.6, 35.4, 35.3 respectively suggested the presence of three 2, 6 dideoxy-3-*O*-methylhexose moieties.

No.	Glucopyranose (δ_H)	Allopyranose (δ_H)	Cymaropyranose (δ_H)		
			I	II	III
1	4.57, d, *J* = 8.0	4.73, d, *J* = 8.0	4.77, dd, *J* = 2.0, 9.5	4.82, dd, *J* = 2.0, 9.5	4.89, dd, *J* =2.0, 9.5
2	3.18, t, *J* = 9.3	3.42, t, *J* = 6.4	1.57, m	1.62, m	1.65, m
3	3.30, t, *J* = 9.5	3.62, t, *J* = 9.3	3.82, m	3.82, m	3.82, m
4	3.22, t, *J* = 8.6	3.22, dd, *J* = 9.5	3.34, m	3.35, m	3.37, m
5	3.30, m	3.83, m	3.83, brd	3.83, brd	3.83, brd
6	3.62, dd, *J* = 10.2	1.24, d, *J* = 6.0	1.18, d, *J* = 6.0	1.21, d, *J* = 6.0	1.24, d, *J* = 6.0
OCH_3	----------	----------	3.40, s	3.42, s	3.60, s

Table 4.8: ^{1}H-NMR data (ppm) of sugar moieties of Compound 2 (Androstane glycoside)

No.	Glucopyranose (δ_C)	Allopyranose (δ_C)	Cymaropyranose (δ_C)		
			I	II	III
1	102.8, d	101.3, d	100.6, d	99.2, d	98.0, d
2	72.2, d	77.2, d	35.6, t	35.4, t	35.3, t
3	77.1, d	82.4, d	73.8, d	73.8, d	73.8, d
4	69.9, d	82.6, d	82.7, d	82.7, d	82.7, d
5	77.3, d	71.2, d	68.7, d	68.7, d	68.7, d
6	60.2, d	17.5, d	17.2, t	17.2, t	17.2, t
OCH_3	----------	----------	57.4, t	57.4, t	57.4, t

Table 4.9: ^{13}C-NMR data (ppm) of sugar moieties of Compound 2 (Androstane glycoside)*

**Multiplicity of assigned peaks were determined by edited Dept experiments (s = quaternary, d = methine, t = methylene, q = methyl), (TMS as internal standard)*

Acid hydrolysis of Compound **2** yielded three sugar moieties identified as cymarpyranose, allopyranose and glucopyranose (Table 4.8). Interglycosidic linkages, sequence and points of attachment of the saccharide chain to aglycon were established by HMBC experiments. From the ^{13}C-NMR data, it is observed that the C-1 (δ_C 98.0) of cymarose (cym-III) moiety is attached to C-3 of aglycon part which resonates upfield as compared to C-1 (δ_C 99.2) of cymarose (cym-II) attached to cymarose (cym-III). Similarly, another sequence was observed for C-1 (δ_C 100.6) of cymarose (cym-I), C-1 (δ_C 101.3) of allopyranose and C-1 (δ_C 102.8) of glucopyranose (Figure 4.9).

As observed in Compound **1**, the ^{13}C-NMR and edited DEPT exhibited the absence of olefinic carbon atoms, indicating that there is no double bond between carbons in Compound **2**, which is further evident from the IR spectrum.

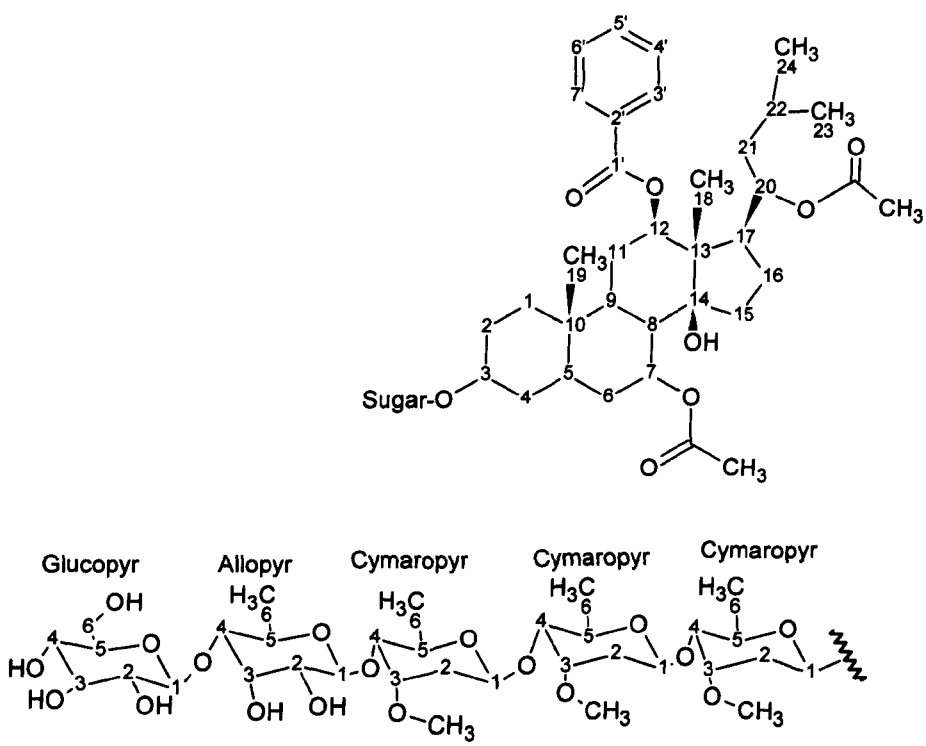

Figure 4.10: Proposed structure of Compound 2 identified as acylated androstane glycoside from the ethyl acetate fraction of Caralluma tuberculata.

The ^{13}C and DEPT-NMR experiments revealed a total of 68 carbon signals, of which 13 corresponded to methyl carbons, 12 to methylene carbons, 36 to methine carbons, and 7 to quaternary carbons, corresponding to a androstan glycoside carrying five sugar moieties with molecular formula represented as $C_{68}H_{106}O_{26}$.

From the aforementioned data, the structure of Compound **2** was established as 7-*O*-acetyl-12-*O*-benzoyl-3β,7β,12β,14β-tetrahydroxy-17β-(3-methylbutyl-*O*-acetyl-1-yl)-androstan-3-yl*O*-β-D-glucopyranosyl-(1→4)-6-deoxy-β-D-allopyranosyl-(1→4)-β-D-cymaropyranosyl-(1→4)-β-D-cymapyranosyl-(1→4)-β-D-cymaropyranoside (Figure 4.10).

4.3.1.4. Liquid Chromatography- Mass Spectrometry (LC-MS)

High resolution (HR) mass spectra (Figure 4.11) were recorded on a LCT Mass Spectrometer with Time-of-Flight (TOF), using electro spray ionisation (ESI +ve mode) showed *m/z*: 1339.7016 (calculated for $[M+H]^+$: 1339.7042) representing the molecular weight of $C_{68}H_{106}O_{26}$ 1338.6946 (calculated monoisotopic mass 1338.6972).

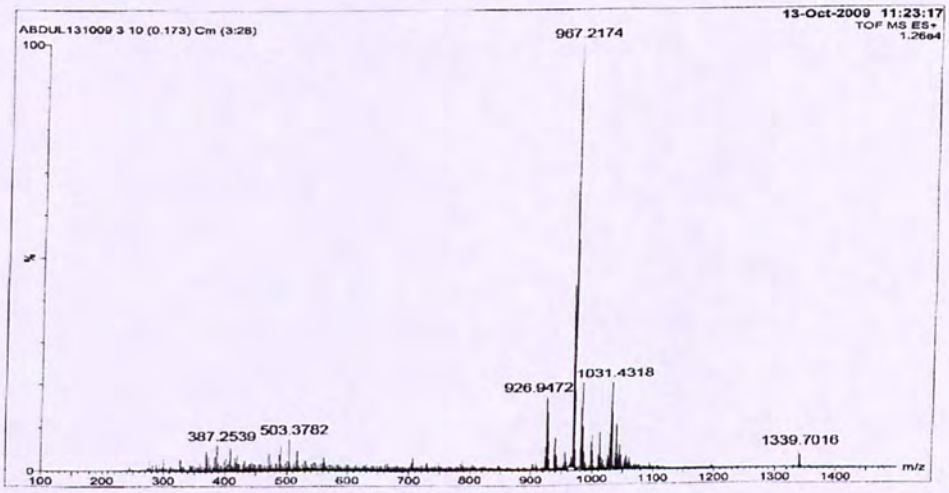

*Figure 4.11: High resolution mass spectrum of Compound **2** on LCT Mass spectrometer with TOF in ESI +ve mode.*

The mass spectroscopic data showed a molecular ion peak at *m/z* 1339.9 $[M+H]^+$ ascribable to a calculated *m/z* 1339.7042. A daughter ion peak observed at nominal *m/z* 1308 may be loss of CH_2OH group $[M+H-31]^+$. Another signal appeared at nominal *m/z* 1280 representing removal of an acetyl group from the parent molecular ion fragment $[M+H-59]^+$. Product ions m/z (relative abundance): 905 (85%), 800(40%), 513(70%) were also observed.

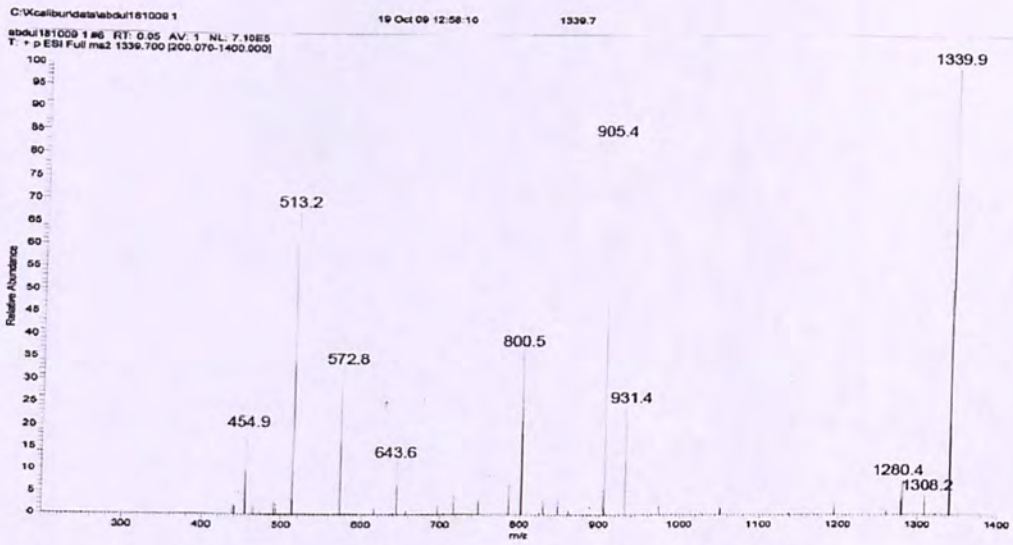

Figure 4.12: Daughter ion peaks corresponds to molecular ion of Compound 2 on LC-MS/MS in ESI +ve mode.

4.3.3. X-ray crystallography of Compound 1 and 2

Compound **1** (Acylated pregnane glycoside) and Compound **2** (Acylated androstane glycoside) were isolated as amorphous powders. Crystallisation was attempted in solvent systems comprising of ethyl acetate and methanol (90:10) at room temperature. Yellow, transparent cubes (approx. 0.5 x 0.8 x 0.6 mm) were observed, but these did not show any diffraction pattern on a Nonius Kappa CCD (Oxford Cryosystems, Oxford, UK) diffractometer; Figure 4.13, and were

classified as "glassy" in nature. Unfortunately, this form was not suitable for further X-ray crystallographic analysis.

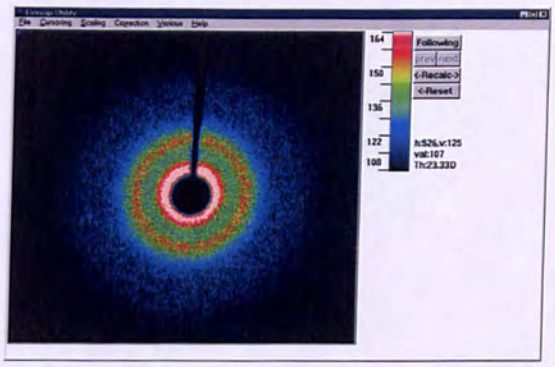

Figure 4.13: X-ray crystallography of Compound 1 and 2 (as intact glycosides) showing no signs of X-ray diffraction, defined as "glass"

However, the crystals obtained from the acid hydrolysis of Compound **1** & **2** after concentrating the chloroform layer (as described in materials and methods), were studied for elucidation of molecular structure of aglycon moieties. The single crystals of these hydrolysed compounds revealed a steroidal skeleton (Figure 4.14) present in the isolated pregnane and androstane glycosides. The hydrogen atom positions were geometrically idealised and allowed to ride on their parent atoms.

Based on 6346 reflections used, the indexing and unit cell refinement showed a monoclinic plane lattice. Post refinement of the unit cell gave a=71.13(11) Å, b=7.654(12) Å, c=10.227(15) Å, $\alpha=90^{o}$, $\beta=90.476(3)^{o}$, and $\gamma=90^{o}$, Volume= 5567(15) $Å^3$. Structural figures were prepared using ORTEP3 for Windows (Farrugia, 1997).

The crystal structure showed that after acid hydrolysis, the sugar moiety attached at C-1 and acetyl group at C-20 were replaced with hydroxyl groups (Figure

4.14), while the methine group at C-12 was converted to a methylene group due to the loss of a benzoyl group as benzoic acid.

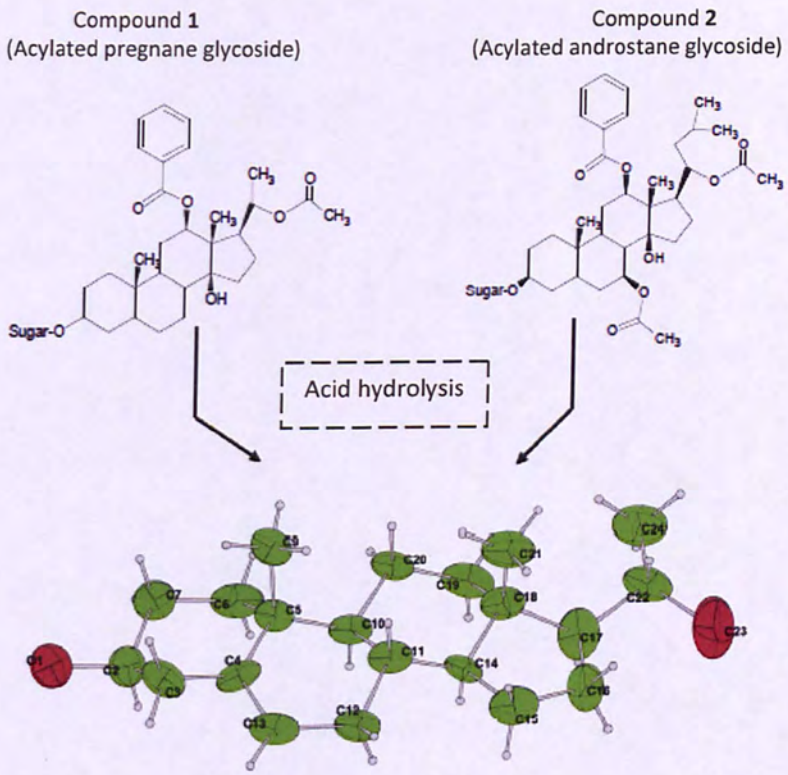

Figure 4.14: Single crystal structure of aglycon of Compound 1 & 2 after hydrolysis

4.4. Phytochemical analysis: *Fagonia indica*

Based on the cytotoxicity results of organic (hexane, ethyl acetate, methanol) and aqueous fractions of Fagonia indica on three cancer cell lines (MCF-7, MDA MB-468, Caco-2), the ethyl acetate fraction (200 µg/ml) was found to possess maximum antiproliferative activity. This potent fraction was selected for further investigation in order to isolate compound(s) which is/are active against rapidly growing cancer cells.

4.4.1. Compound 3 (Pregnane Glycoside)

Identification and structure elucidation of Compound **3** was conducted based on its physical and chemical characteristics, and combination of spectroscopic experiments including (^{1}H, ^{13}C, DEPT, HETCOR, DQF-COSY) NMR, LC-MS and IR.

4.4.1.1. Physico-chemical characteristics

Compound **3** was isolated as a light-greenish white amorphous powder (yield 42 mg), with a melting point ranging 212–215°C. Optical rotation was calculated as: $[\alpha]_D^{20}$= +2.5°, (*c* 0.010, MeOH). Positive Lieberman-Burchard test was indicated by the appearance of a dark green colour in the chloroform solution of Compound **3** in the presence of acetic anhydride and concentrated sulphuric acid, thus demonstrating the steroidal nature of the compound, as described earlier for Compound **1** & **2** (Burke *et al.*, 1974; Halim *et al.*, 1996).

4.4.1.2. Infra-Red spectroscopy of Compound 3

The IR spectrum showed a broad absorption band at 3370 cm^{-1} ascribable to the hydroxyl (–OH) group. Bands at 2927, 2881 cm^{-1} represent the asymmetric and symmetric stretch vibrations of ($-CH_3$) and ($-CH_2$) groups. Stretch vibrations in

alkene (C=C) was observed at 1686 cm^{-1}, while medium intensity bands at 1712 and 1223 cm^{-1} represented the (C=O) and (C–O) in aliphatic ester respectively. Asymmetric deformation of ($-CH_3$) was observed at 1387 cm^{-1}. A medium to strong intensity band near 1023 cm^{-1} indicated the presence of tri-substituted alkene groups in the molecule.

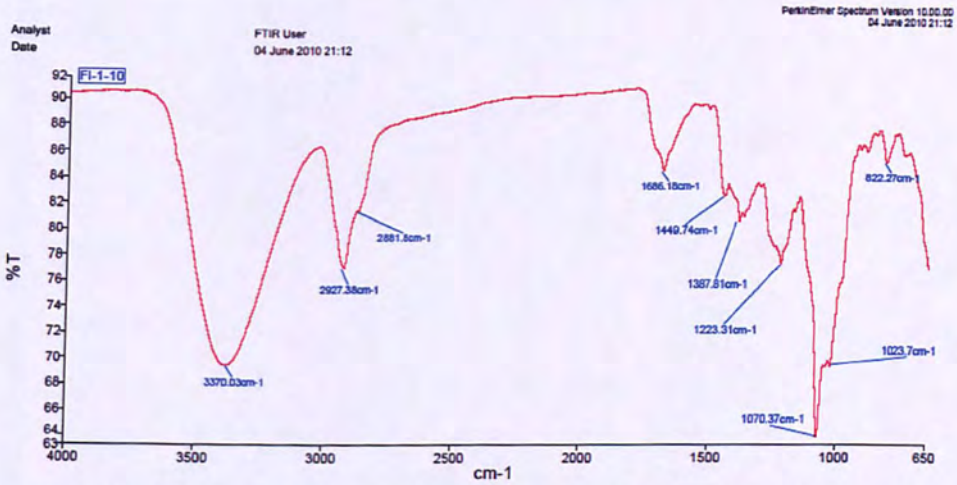

Figure 4.15: IR spectrum of Compound 3 showing absorption bands of functional groups corresponds to % Transmittance versus Wavenumber (cm^{-1}).

4.4.2.3. Nuclear Magnetic Resonance (NMR) spectroscopy

^1H-, ^{13}C-, DEPT- and HMBC-NMR experiments (Figure 4.16) demonstrated that Compound **3** comprised of a steroidal skeleton in the aglycon moiety. Based on the peak assignments data, Compound **3** showed some resemblance in chemical shift values of ^1H (δ_H) and ^{13}C (δ_C), which are in agreement with the reported data for pregnane glycosides (Halim *et al.,* 1996; Abdel Sattar *et al.,* 2008) and for Compound **1** and **2** as listed earlier in Tables 4.5 and 4.7. The complete set of ^1H- and ^{13}C-NMR data for the aglycon part of Compound **3** are summarised in Table 4.10.

No.	δ_H	δ_C	No.	δ_H	δ_C
1	1.23(2H, m, H-1α, H-1β)	36.7, t	12	3.13(1H,m, H-12α)	89.1, d
2	1.49(2H, m, H-2α, H-2β)	29.8, t	13	----------	56.0, s
3	3.13(1H, m, H-3 α)	74.3, d	14	2.26(1H, m, H-14α)	54.0, d
4	1.74(2H, m, H-4α, H-4β)	38.6, t	15	1.49(2H, m, H-15α, H-15β)	18.0, t
5	1.23 (1H, m, H-5α)	55.5, d	16	1.90(2H, m, H-16α, H-16β)	22.5, t
6	1.72(2H, m, H-6α, H-6β)	25.7, t	17	2.26(1H, m, H-17α)	54.0, d
7	1.22(2H, m, H-7α, H-7β)	30.0, t	18	0.83(3H, s, H-18β)	15.7, q
8	1.68(1H, m, H-8β)	39.1, d	19	0.95(3H, s, H-19β)	17.9, q
9	1.23(1H, m, H-9α)	48.6, d	20	3.33(1H, m, H-20)	72.7, d
10	----------	36.5, s	21	1.04(3H, d, *J* = 7.51 Hz, H-21)	27.2, q
11	2.05(2H, m, H-11α, H-11β)	24.5, t	----	----------	-------
Side chain "a" at C-20			**Side chain "b" at C-12**		
1a	----------	176.6,s	1b	----------	178.0, s
2a	3.67(2H,dd, *J* = 12.63.12.36 Hz H-2a)	61.2,t	2b	3.84(2H, dd, *J* = 12.63.12.36 Hz, H-2b	61.4, t
3a	5.60(1H, m, H-3a)	128.9,d	3b	5.60(1H, m, H-3b)	129.5, d
4a	----------	131.9,s	4b	----------	132.7, s
5a	0.88(3H, m, H-5a)	16.9,q	5b	0.88(3H, m, H-5b)	17.0, q
6a	0.91(3H, m, H-6a)	20.3,q	6b	0.91(3H, m, H-6b)	20.2, q

Table 4.10: ^{1}H- and ^{13}C-NMR data (ppm) of the aglycon moiety of Compound 3*

**Multiplicity of assigned peaks were determined by edited DEPT experiments (s= quaternary, d = methine, t = methylene, q = methyl), (TMS as internal standard)*

The ^{1}H- and ^{13}C-NMR spectra showed the presence of two side chains "a & b" as 4-methyl-pent-3enoyloxy groups. Each side chain consists of two quaternary carbons (δ_C 176.6 and 131.9), one methine (δ_H 5.6; δ_C 128.9), one methylene (δ_H 3.67; δ_C 61.2) and two methyl groups (δ_H 0.88, 0.91; δ_C 16.9, 20.3) with unsaturated double bonds between C-3 and C-4, which is further evident from their high chemical shift values in ^{1}H- and ^{13}C-NMR spectra, as listed in table 4.10.

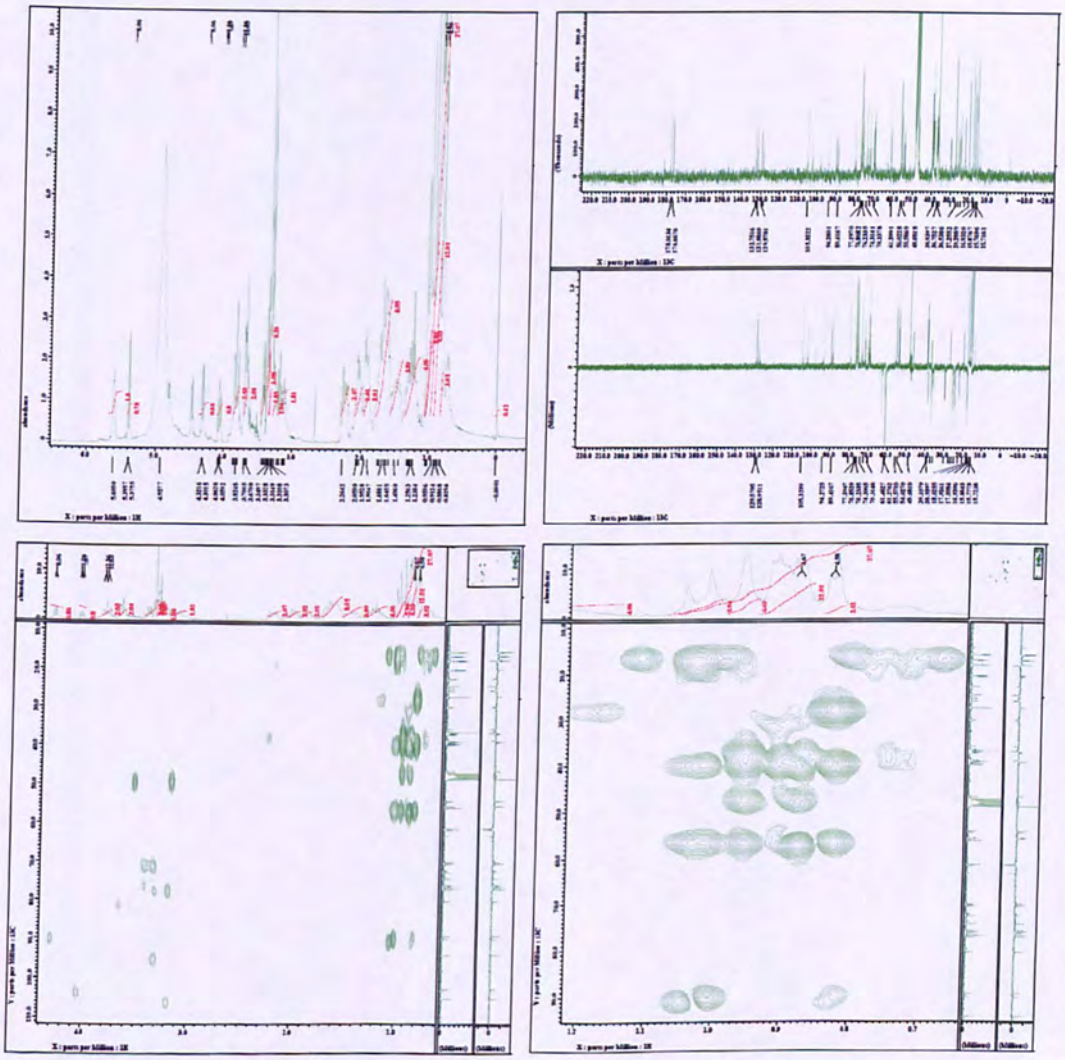

Figure 4.16: 1D (^{1}H, ^{13}C, DEPT) NMR and 2D (HMBC) NMR spectra of Compound 3 (Pregnane glycoside) from Fagonia indica.

The attachment of these two side chains were observed in a ^{1}H and ^{13}C plot through HMBC spectra (Figure 4.16).

The ^{1}H-^{1}H long range coupling correlations between methylene (δ_H 3.67; δ_C 61.2) at C-2a and methine (δ_H 3.33; δ_C 72.7) at C-20 suggest the attachment of side chain "a" at C-20. Similarly, cross peak signals between methylene (δ_H 3.84; δ_C 61.4) at C-2b and methine (δ_H 3.13; δ_C 89.1) C-12 refer to side chain "b" at C-12.

	Allopyranose			Cymaropyranose	
No.	δ_H	δ_C	No.	δ_H	δ_C
1*	4.32, d, *J* = 8.06	105.3, d	1'	5.38 d, *J* = 8.06	94.2, d
2*	3.33, m	77.2, d	2'	1.72, m	35.7, t
3*	4.05, t, *J* = 7.87	80.3, d	3'	3.26, m	75.7, d
4*	3.40, m,	76.8, d	4'	3.43, t, *J* = 9.06	76.3, d
5*	3.41, m	76.3, d	5'	3.39, m	38.9, d
6*	1.04, dd, *J* = 7.51	15.7, q	6'	1.01, dd, *J* = 10.25	15.8, q
OCH_3*	3.34, s	69.9, q	OCH_3'	3.34, s	70.3, q

Table 4.11: ^{1}H- and ^{13}C-NMR† data (ppm) of sugar moieties of Compound 3, †Multiplicity of assigned peaks were determined by edited Dept experiments (s = quaternary, d = methine, t = methylene, q = methyl), (TMS as internal standard)

Two anomeric protons signals were detected in the ^{1}H and ^{13}C-NMR spectra, which appeared at δ_H 4.32 (d, *J* = 8.06 Hz), 5.38 (d, *J* = 8.06 Hz) and correspond to anomeric carbons at δ_C 105.3, 94.2 respectively (Table 4.11) suggesting the presence of two sugar moieties in the chemical structure of the pregnane glycoside. The stereochemistry of anomeric protons was established on the basis of their large coupling constants (8.06 Hz). The chemical shift values of ^{1}H- and

^{13}C-NMR data for the glycon part of Compound **3** are summarised in Table 4.11. Based on these observed signals and the reported data for acylated pregnane glycosides from *Caralluma russeliana* (Abdel-Sattar *et al.,* 2007), it is suggested that the pregnane glycoside (Compound **3**) from *Fagonia indica* contains allopyranose and cymaropyranose as sugar moieties.

Interglycosidic linkages and points of attachment of the saccharide chain to aglycon were established by HMBC experiments. From HMBC-NMR spectral data, the ^{1}H-^{1}H long range coupling correlations between methine (δ_H 5.38; δ_C 94.2) at C-1' and methine (δ_H 3.13; δ_C 74.3) at C-3, while as such no cross signal was observed between the methine at C-1* and C-3 of the aglycon part, suggesting that the cymaropyranoside sugar moiety is attached to the aglycon part of the pregnane glycoside.

The ^{13}C and DEPT experiments exhibited a total of 47 carbon signals, of which 11 corresponded to methyl carbons, 11 to methylene carbons, 19 to methine carbons, and 6 to quaternary carbons, corresponding to a pregnane glycoside carrying two sugar moieties with molecular formula represented as $C_{47}H_{76}O_{12}$.

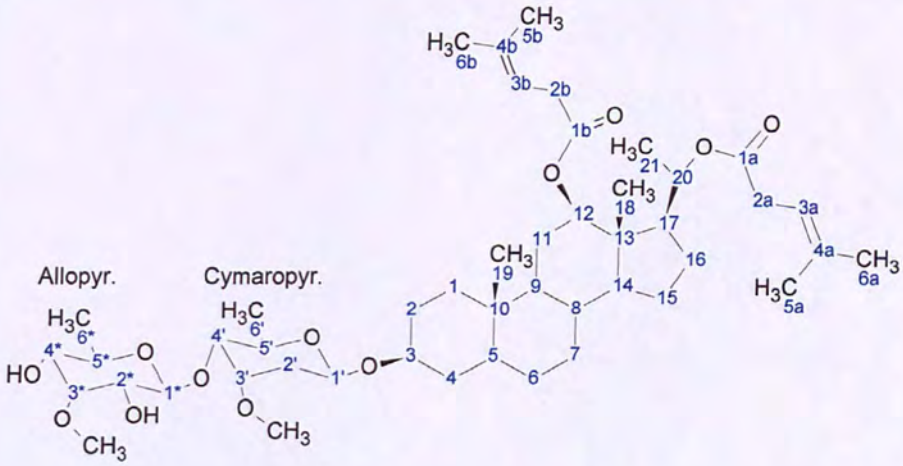

Figure 4.17: Proposed structure of Compound 3 identified as pregnane glycoside from the ethyl acetate fraction of Fagonia indica.

From the aforementioned data, the structure of Compound **3** was established as: 12-(4-methyl-pent-3enoyloxy)-20-(4-methyl-pent-3enoyloxy)-3β,12β,20β-trihydroxy -pregnan-3-yl*O*-β-D-cymapyranosyl-(1→4)-3-methoxy-6-deoxy-β-D-glucopyrano-side (Figure 4.17).

4.4.1.4. Liquid Chromatography- Mass Spectrometry (LC-MS)

Data from NMR peak assignments and absorption bands from IR studies revealed that Compound **3** ($C_{47}H_{76}O_{12}$) has a calculated monoisotopic mass of m/z 832.5337. High resolution (HR) mass spectra (Figure 4.18) were recorded on a LCT Mass Spectrometer with Time-of-Flight (TOF), using electro spray ionisation (ESI +ve mode) showed *m/z*: 833.5423 (calculated for $[M+H]^+$: 833.5407). A daughter ion at m/z 803.5568 represented the loss of two methyl groups $[M+H-30]^+$ from the parent ion. Daughter ions at m/z 603.28, 439.25 and 366.286 were also observed. Compound **3** was not enough in quantity to further investigate for fragmentation pattern on LC-MS/MS and studies were focused towards biological aspects to evaluate this pregnane glycoside for cytotoxicity in cancer cells.

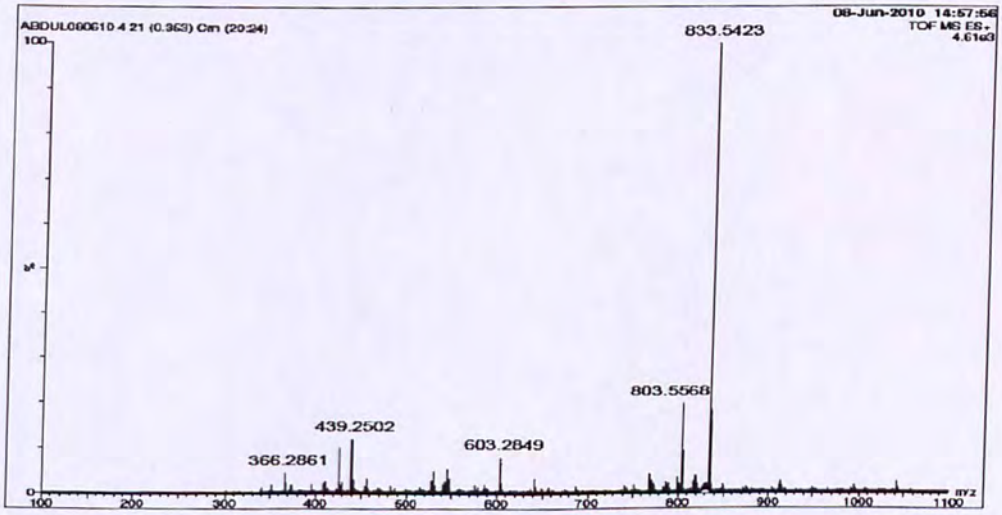

Figure 4.18: High resolution mass spectrum of Compound 3 on LCT Mass spectrometer with TOF in ESI +ve mode.

4.5. Phytochemical analysis: *Solanum surattense*

Polyphenols including phenolic acids, and fatty acids exhibit significant anticancer activity both *in vitro* and *in vivo* and especially member of Solanaceae family like *Solanum tuberosum* (potatoes) are an excellent source of dietary polyphenols (Reddivari *et al.*, 2007). In the present study, the chloroform fraction of Solanum surattense showed highly significant cytotoxicity activity against three cancer cell lines (MCF-7, MDA MB-468 and Caco-2). Phytochemical analysis resulted in the isolation of two compounds from this potent fraction.

4.5.1. Compound 4 (Hexadecanoic acid ethyl ester)

Physically Compound **4** was oily and waxy in appearance at room temperature and the approximate yield was 64 mg. The negative result of the Liebermann-Burchard test was indicated by no change in colour of the chloroform solution of Compound **4** in the presence of acetic anhydride and concentrated sulphuric acid. This suggested that the compound does not belong to a steroidal class (Burke *et al.*, 1974). Further identification and structure elucidation of the Compound **4** were established through a series of spectroscopic experiments including IR, NMR (^{1}H, ^{13}C, DEPT and HMBC), GC-MS and LC-MS.

4.5.1.1. Infra-Red spectroscopy of Compound 4

The plot of percentage transmittance versus wavenumber (cm^{-1}) in the IR spectrum (Figure 4.19) showed absorption bands of very strong intensities at 2922, 2851 cm^{-1}. These represent the asymmetric and symmetric stretch vibrations of ($-CH_3$) and ($-CH_2$) groups. Another strong intensity band was observed at 1738 cm^{-1} demonstrating the stretching vibration due to the (C=O) functional group in aliphatic esters. A medium intensity band at 1461 cm^{-1} indicates the antisymmetric ($-CH_3$) deformation and the bending vibrations of

($-CH_2$) groups in aliphatic compounds. The antisymmetric C–O–C stretching mode in esters gives rise to a slightly broader band (1100-1300 cm^{-1}) in esters. An absorption band at 1179 cm^{-1} represents the C–O–C stretching vibration in Compound **4**.

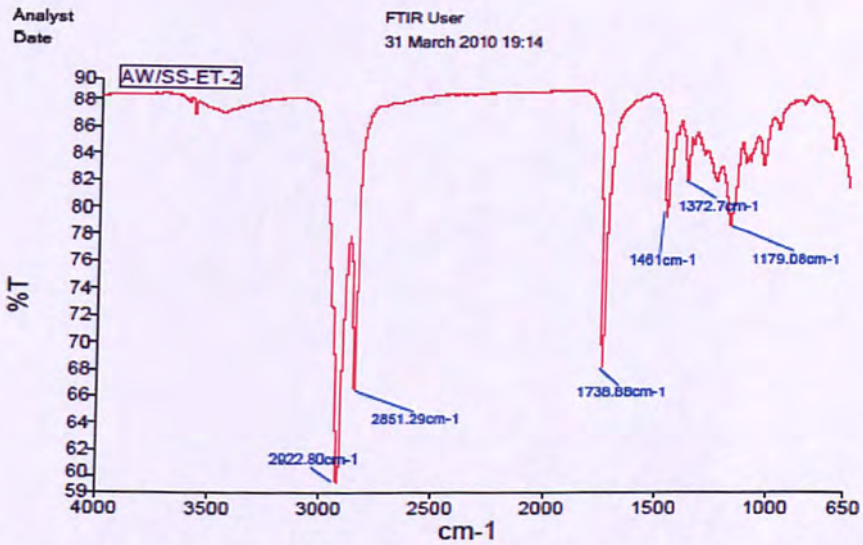

*Figure 4.19: IR spectrum of Compound **4** showing absorption bands of functional groups corresponds to % Transmittance versus Wavenumber (cm^{-1}).*

4.5.1.2. Gas Chromatography-Mass Spectrometry (GC-MS)

Compound **4** was volatile in nature, hence was suitable for analysis on GC-MS. A chloroform solution of Compound **4** (1 µl) was injected and temperature programme (as described in material and methods section: 2.7.3.2.) was used for 20 min each run. A single peak was observed on the chromatogram (Figure 4.20) at a retention time (RT) 14.79 min. Mass spectra were acquired in the electron impact (EI) mode with mass range was 50-500 m/z. A C-13 molecular ion peak at m/z 285 was observed along with C-12 m/z 284 (Calculated mass: 284.2715) in the mass spectrum. Fragments ions at m/z 269, 255, 241, 227, 213, 199, 185, 171, 157, 143, 129, 115, 101 represent the loss of a methyl ($-CH_2$) group from

molecular ion $[M+H-14]^+$ and from each respective daughter ion. A fragment ion at m/z 88 with maximum abundance (600,000) suggests the fragment of an ethyl acetate ion $[C_4H_7OO]^+$.

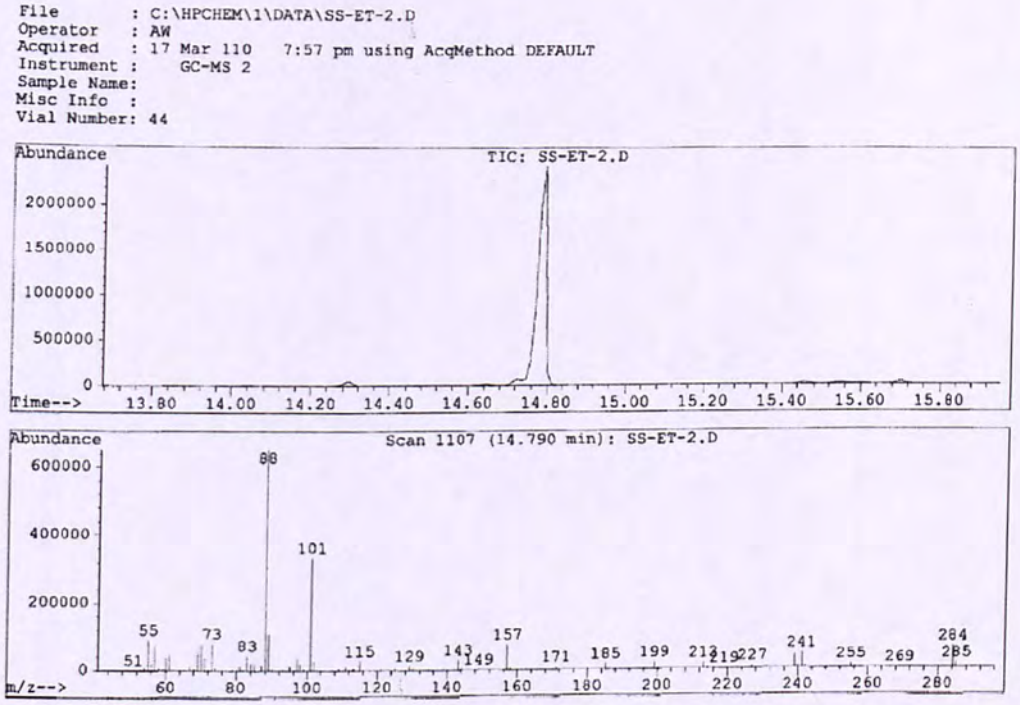

Figure 4.20: Chromatogram of Compound 4 along with mass spectrum on GC-MS showing retention time (RT 14.79 min) and molecular ion peak (m/z 285).

4.5.1.3. Nuclear Magnetic Resonance (NMR) spectroscopy

The analysis of ^{1}H- and ^{13}C-NMR signals (Table 4.12) revealed that the Compound **4** belongs to a class of long chain fatty acids. In ^{1}H-NMR, a signal upfield (δ_H 0.88) as a triplet (J = 6.50, 7.05 Hz) represents the terminal methyl group at C-16 while in ^{13}C-NMR, it is identified at δ_C 14.1. Signals appeared as a broad multiplet (δ_H 1.23-1.27) with an integration of 22 protons in ^{1}H-NMR, thus describing the long chain of 11 methylene ($-CH_2$) groups, positioned between C-4 and C-14, as shown in figure 4.22. This chain of methylene groups was observed in ^{13}C-NMR (δ_C 29.1 - 31.9), as listed in table 4.12.

A further downfield (δ_H 4.11) signal, as a quartet (J = 7.14, 7.14 Hz) in ^{1}H-NMR indicated a methylene group (at C-1*) attached to an electronegative group (acetyl), as observed at δ_H 4.11. This methylene group (δ_C 15.7) is linked with the terminal methyl group (C-2*), ending the long chain on the other side as a multiplet (δ_H 1.32). Two methylene groups at (C-2) and (C-3) were configured as a triplet (δ_H 2.28, J = 7.51, 7.60 Hz) and multiplet (δ_H 1.59) in ^{1}H-NMR and appeared in ^{13}C-NMR at δ_C 34.4 and δ_C 24.9 respectively.

No.	δ_H	δ_C	No.	δ_H	δ_C
1	----------	173.9, s	9	1.25(2H, broad m, H-9)	29.4, t
2	2.28(2H, t, J = 7.51, 7.60 Hz, H-2)	34.4, t	10	1.25(2H, broad m, H-10)	29.6, t
3	1.59(2H, m, H-3)	24.9, t	11	1.25(2H, broad m, H-11)	29.6, t
4	1.25(2H, broad m, H-4)	29.1, t	12	1.25(2H, broad m, H-12)	29.6, t
5	1.25(2H, broad m, H-5)	29.1, t	13	1.25(2H, broad m, H-13)	29.7, t
6	1.25(2H, broad m, H-6)	29.7, t	14	1.25(2H, broad m, H-14)	31.9, t
7	1.25(2H, broad m, H-7)	29.1, t	15	1.29(2H, m, H-15)	22.7, t
8	1.25(2H, broad m, H-8)	29.3, t	16	0.88(3H, t, J = 6.50, 7.05 Hz, H-16)	14.1, q
Ethyl Ester at C-1					
1*	4.11(2H, q, J = 7.14, 7.14 Hz, H-1*)	25.7, t	2*	1.32(3H, m, H-2*)	15.7, q

Table 4.12: ^{1}H- and ^{13}C-NMR† data (ppm) of Compound 4 (Hexadecanoic acid ethyl ester), †Multiplicity of assigned peaks were determined by edited DEPT experiments (s=quaternary, d = methine, t = methylene, q = methyl), (TMS as internal standard)

In two dimensional (2D), Heteronuclear Single Quantum Correlation (HSQC) NMR experiments, cross peak signals were observed for protons attached to corresponding carbon atoms in a plot of ^{1}H- and ^{13}C-NMR spectra (Figure 4.21).

A weak signal for (C=O) at C-1, which was not detected in ^{13}C- and DEPT-NMR experiments, showed a cross peak signal for the methylene group at C-2 (δ_H 2.28) and carbonyl at C-1 (δ_C 173.9). Similarly, cross peak signals between methylene groups at C-2 and C-4, methylene at C-15 and methyl at C-16 were also established (Figure 4.21).

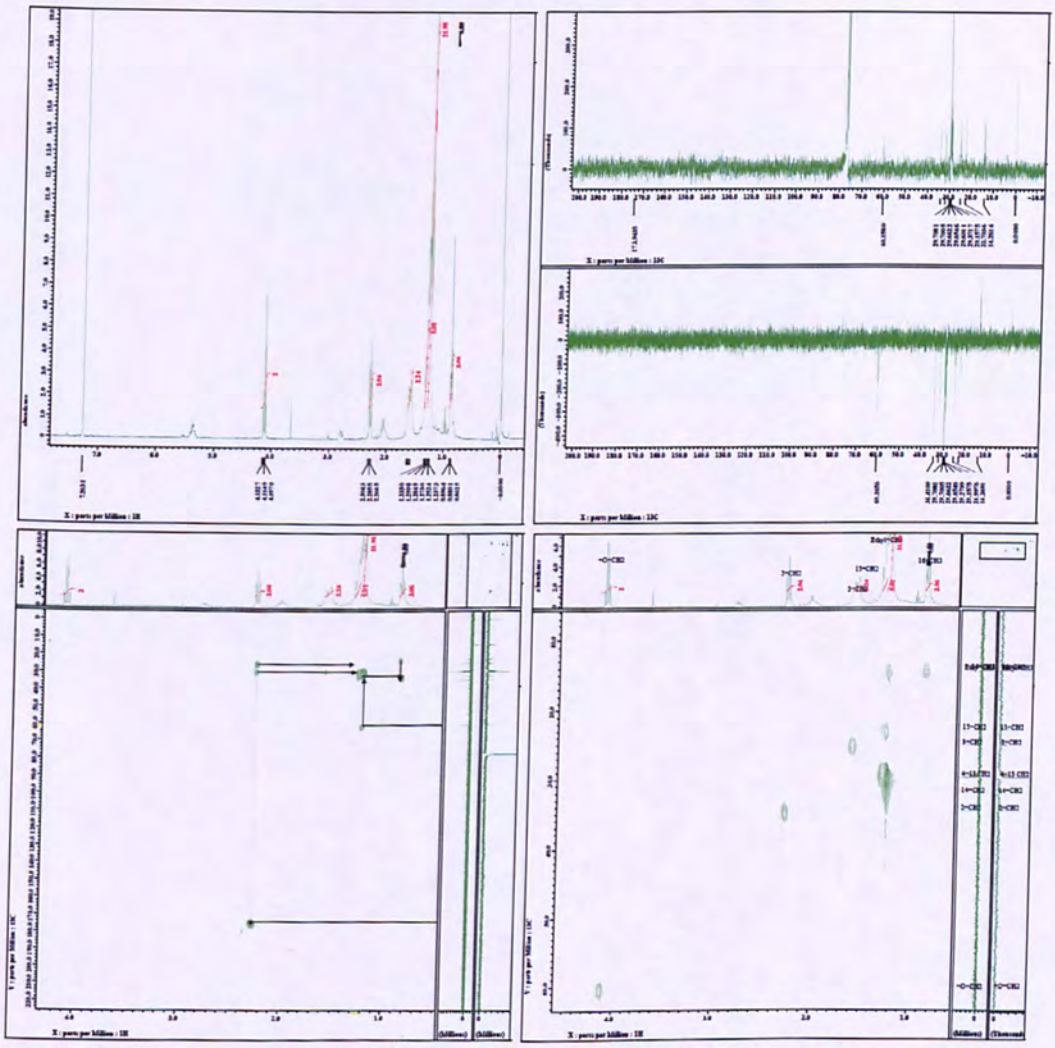

*Figure 4.21: 1D (^1H, ^{13}C, DEPT) NMR and 2D (HMBC, HSQC) NMR spectra of Compound **4** (Hexadecanoic acid ethyl ester) from Solanum surattense.*

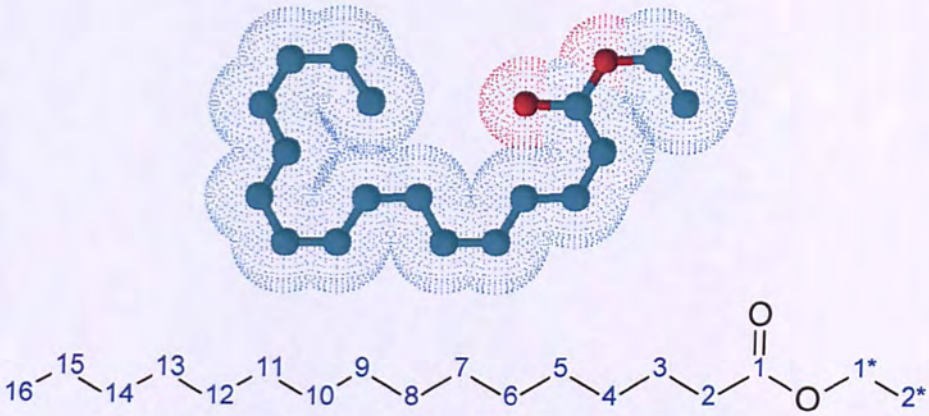

*Figure 4.22: Proposed structure of Compound **4** identified as hexadecanoic acid ethyl ester from the chloroform fraction of Solanum surattense.*

The ^{13}C and DEPT-NMR experiments showed a total of 18 carbon signals, of which 2 corresponded to methyl carbons, 15 to methylene carbons and one to quaternary carbons, suggesting that Compound **4** is hexadecanoic acid ethyl ester (Figure 4.22) with molecular formula represented as $C_{18}H_{36}O_2$.

4.5.1.4. Liquid Chromatography-Mass Spectrometry (LC-MS)

According to GC-MS data, Compound **4** showed a molecular ion peak at m/z 285 in the electron impact (EI) mode. In order to determine the exact molecular weight of the compound, a high resolution (HR) mass spectrum (Figure 4.23)

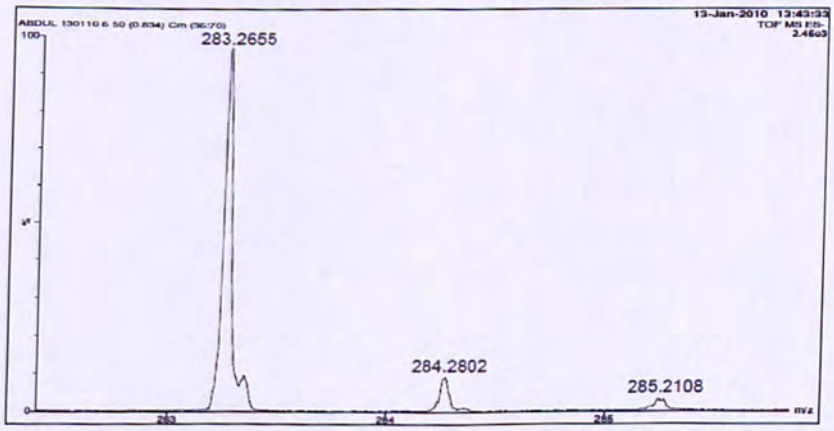

*Figure 4.23: High resolution mass spectrum of Compound **4** on LCT Mass spectrometer with TOF in ESI negative (-ve) mode.*

was recorded on a LCT mass spectrometer with time-of-flight (TOF). Using electro spray ionisation negative (ESI -ve) mode, the mass spectrum showed *m/z*: 283.2655 (calculated for $[M-H]^+$: 283.2645) representing the molecular weight of Compound **4** (Hexadecanoic acid ethyl ester) to be 284.2725 with respect to a calculated monoisotopic mass 284.2715 for $C_{18}H_{36}O_2$.

4.5.2. Compound 5 (Phthalic acid ester)

Compound **5** was isolated as pale yellow amorphous powder; yield was 37 mg. The Liebermann-Burchard test gave negative results, which indicated that the compound is not a steroid. The identification and structure elucidation of the Compound **5** was attempted through a series of spectroscopic experiments including IR, NMR (^1H, ^{13}C, DEPT, HMBC, HETCOR and DQF-COSY) and LC-MS.

4.5.2.1. Infra-Red spectroscopy of Compound 5

The IR spectrum of Compound **5** shows strong intensity absorption bands at 2959, 2928, 2858 cm^{-1} representing the asymmetric and symmetric stretch vibrations of ($-CH_3$) and ($-CH_2$) groups. The stretching vibration of (C=O) functional group in the ester was observed at 1729 cm^{-1}. A weak intensity band at 1644 cm^{-1} appeared due to the (C=C) stretching vibration in alkenes. Further down, a medium intensity band at 1461 cm^{-1} indicates the antisymmetric ($-CH_3$) deformation and the bending vibrations of ($-CH_2$) groups in aliphatic compounds and 1378 cm^{-1} represents the (C–H) methyl rocking vibrations. The strong intensity band (slightly broader) at 1272 cm^{-1}, indicates the antisymmetric (O–C=O) stretching mode of ester in benzoates, while a medium intensity band at 1123 cm^{-1} shows (C–O) stretch vibrations in the molecule. Overall, IR spectra of Compound **5** indicated the presence of a phthalyl group with an unsaturated alkyl chain. This was further investigated with 1D and 2D NMR spectroscopy.

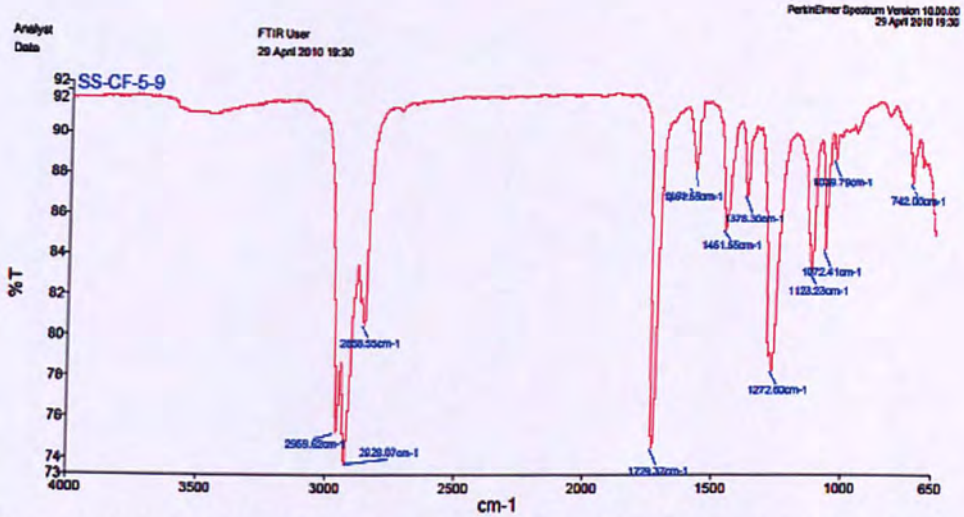

*Figure 4.24 IR spectrum of Compound **5** showing absorption bands of functional groups corresponds to % Transmittance versus Wavenumber (cm^{-1}).*

4.5.2.2. Nuclear Magnetic Resonance (NMR) spectroscopy

The ^{1}H and ^{13}C-NMR data for Compound **5** with signal configurations are listed in Table 4.13. Analysis by ^{1}H-NMR showed two downfield signals at δ_H 7.71 and 7.53 as a double of doublets (J = 3.30, 2.38, 3.39 Hz and J = 3.30, 2.38, 3.30 Hz) showing four aromatic protons, typically representing the aromaticity of the benzene ring in the phthalic acid. The spin spin coupling and peak splitting in the aromatic proton was further investigated in DQF-COSY (Figure 4.25) and HMBC experiments, where cross peak signals were observed for the neighbouring proton in the benzene ring. The presence of only four carbon signals for the phthalyl moiety clearly demonstrates that both the carboxylic groups were esterified. The signals for methine groups in ^{13}C- and DEPT-NMR at δc 128.88 (C-3), 130.96 (C-4), 130.97 (C-5), 128.89 (C-6), and for quaternary carbons at δc 167.8 (C-1), 132.5 (C-2), 132.5 (C-7), 167.8 (C-8) were observed (Table 4.13). The presence of only four carbon signals for the phthalyl moiety clearly demonstrates that both the carboxylic groups were esterified.

No.	δ_H	δ_C	No.	δ_H	δ_C
Phthalic acid group					
1	----------	167.8, s	5	7.53(1H,dd, *J* = 3.30, 2.38,3.30 Hz)	130.9, d
2	----------	132.5, s	6	7.71(1H,dd, *J* = 3.30, 2.38,3.39 Hz)	128.8, d
3	7.71(1H,dd, *J* = 3.30, 2.38,3.39 Hz)	128.8, d	7	----------	132.5, s
4	7.53(1H,dd, *J* = 3.30, 2.38,3.30 Hz)	130.9, d	8	----------	167.8, s
1,1-Dimethyl-pentyl group at –OC-1					
1*	----------	77.3, s	4*	1.39(2H, m)	23.0, t
2*	1.98(2H,m)	39.8, t	5*	0.92(3H, t, *J* = 7.41, 7.51 Hz)	14.1, q
3*	1.42(2H, m)	23.8, t	2(CH_3)	1.59(3H, s), 1.68(3H,s)	23.5, q 23.5, q
2-Ethyl-dec-5-enyl group at –OC-8					
1'	4.21(1H,m)	68.2, t	7'	2.04(2H,m)	32.2, t
2'	1.65(1H,m)	38.7, d	8'	1.31(2H, m)	29.0, t
3'	1.25(2H,m)	29.7, t	9'	1.29(2H, m)	23.0, t
4'	2.04(2H,m)	26.4, t	10'	0.89(3H, t, *J* = 6.96, 6.22)	14.1, q
5'	5.12(1H, m)	125.0, d	-CH_2	1.36(2H,m)	30.4, t
6'	5.12(1H, m)	125.1, d	-CH_3	0.92(3H, t, *J* = 7.41, 7.51)	11.0, q

Table 4.13: ^{1}H- and ^{13}C-NMR† data (ppm) of Compound 5 (Phthalic acid ester)

†Multiplicity of assigned peaks were determined by edited DEPT experiments (s=quaternary, d = methine, t = methylene, q = methyl), (TMS as internal standard)

In ^{1}H-NMR, two signals at δ_H 1.59 and 1.68, each as a singlet indicated the attachment of two methyl groups to a quaternary carbon, δc 77.3 at (C-1*), which is linked to an ester of phthalic group. The alkyl chain of 3 methylene groups at δ_H 1.98 (C-2*), 1.42 (C-3*), 1.39 (C-4*) as a multiplet and a terminal methyl group δ_H 0.92 as a triplet (J = 7.41, 7.51 Hz) were also observed. The proton assignment for the corresponding carbons was carried out according to the cross

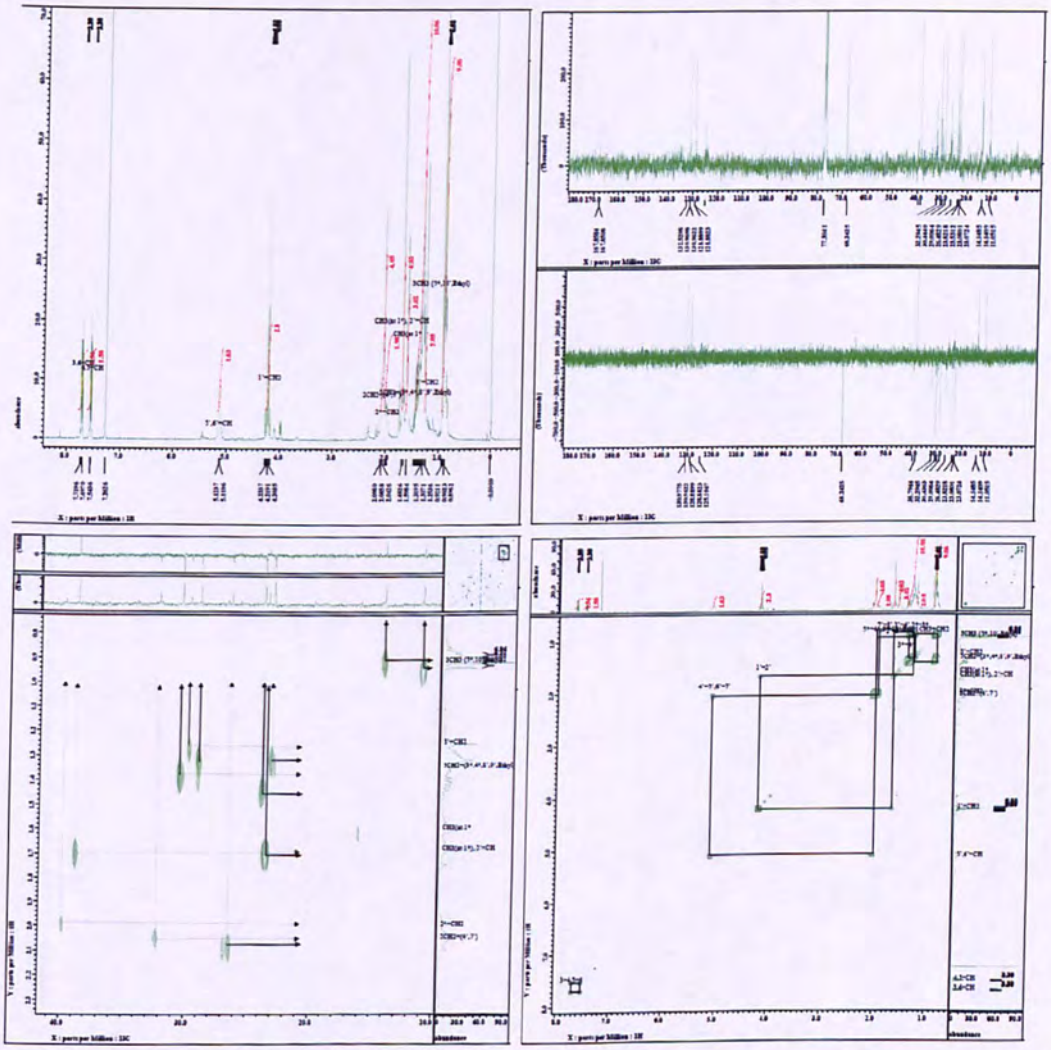

*Figure 4.25: 1D (^{1}H, ^{13}C, DEPT) NMR and 2D (HETCOR, DQF-COSY) NMR spectra of Compound **5** [Phthalic acid 1-(1, 1-dimethyl-pentyl) ester 2-(2-ethyl-dec-5-enyl) ester] from Solanum surattense*

peak signals, observed in HETCOR and DQF-COSY NMR experiments (Figure 4.25), which suggest the attachment of 1,1-dimethyl-pentyl group to an ester of the phthalic group.

A shielded signal (δ_H 4.21) for the methylene group at (C-1') as a multiplet with integration of two protons in ^{1}H-NMR, showed spin-spin coupling with the hydrogen of methine (δ_H 1.65) at C-2' and methylene (δ_H 1.25) at C-3'. The adjacent shielded methylene to ester oxygen of the phthalyl group is suggested from ^{1}H-^{1}H long range coupling correlations, observed in HMBC-NMR experiments.

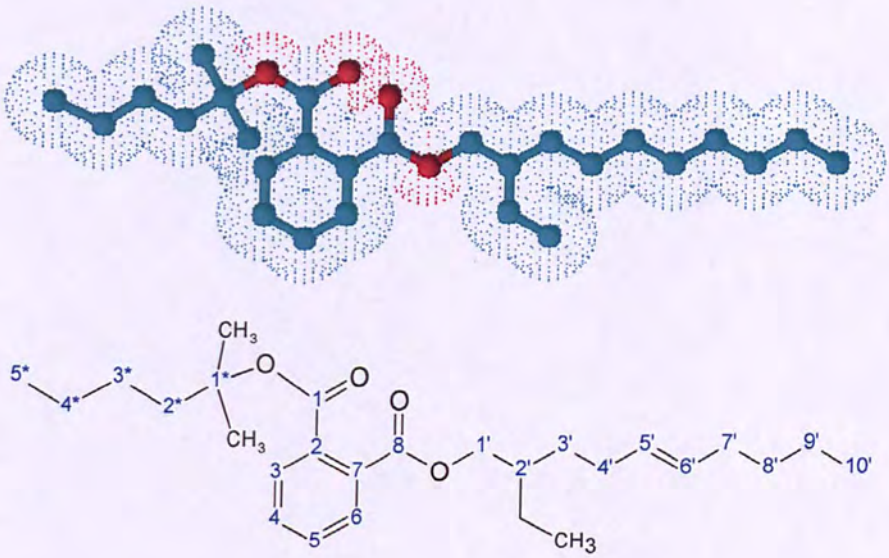

*Figure 4.26: Proposed structure of Compound **5** identified as Phthalic acid 1-(1, 1-dimethyl-pentyl) ester 2-(2-ethyl-dec-5-enyl) ester from the chloroform fraction of Solanum surattense*

The methine groups at position C-5' and C-6' (Figure 4.26) observed as a multiplet at δ_H 5.12 indicated an unsaturated double in the alkyl chain with a terminal methyl group observed as a triplet (J = 6.96 Hz) at δ_H 0.89 and in ^{13}C-NMR at δ_C 14.1. The ethyl group at C-2' is suggested based on the cross peak

signals indicated in DQF-COSY NMR experiments. The observation of 10 peak signals along with signals for the ethyl group in the aliphatic region in ^{13}C-NMR was also an evidence for an alkyl chain as 2-ethyl-dec-5-enyl in the molecular structure of Compound **5**.

The ^{13}C and DEPT-NMR experiments showed a total of 27 carbon signals, of which 5 represents methyl carbons, 10 methylene carbons, 7 methine carbons and 5 quaternary carbons, suggesting that Compound **5** is phthalic acid 1-(1, 1-dimethyl-pentyl) ester 2-(2-ethyl-dec-5-enyl) ester (Figure 4.26) with molecular formula represented as $C_{27}H_{42}O_4$.

4.5.2.3. Liquid Chromatography-Mass Spectrometry (LC-MS)

The molecular weight of the Compound **5** was determined through high resolution (HR) mass spectra (Figure 4.27), recorded on a LCT mass spectrometer with time-of-flight (TOF) using electro spray ionisation positive (ESI +ve) mode.

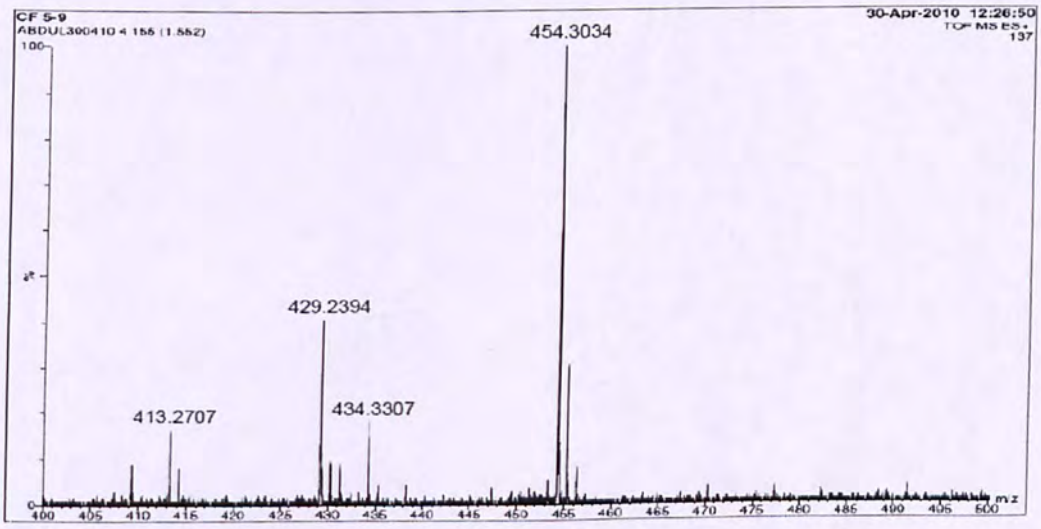

*Figure 4.27: High resolution mass spectrum of Compound **5** on LCT Mass spectrometer with TOF in ESI positive (+ve) mode showing molecular ion as sodium adduct.*

According to the structure elucidation from NMR and IR analysis, the calculated monoisotopic mass for Phthalic acid ester ($C_{27}H_{42}O_4$) should be 430.3083. The mass spectra showed a molecular ion peak m/z 454.3034, indicating the compound is forming a sodium (22.9897) adduct $[M+H+Na]^+$ in ESI (+ve) mode, which determines a molecular mass of 430.3067 for the phthalic acid ester.

A fragmentation pattern can be suggested from the mass spectrum (Figure 4.28), which shows a daughter ion at 391.2857 indicating the loss of (C_3H_4) from the parent molecule $[M+H-40]^+$. Further removal of dimethyl-pentyl (C_7H_{15}) group from this daughter ion $[M+H-40-99]^+$, is shown by a peak at m/z 292.2125. As compared to the mass spectrum (Figure 4.28), a proposed fragmentation pattern with corresponding calculated monoisotopic masses of fragments is described in Figure 4.29.

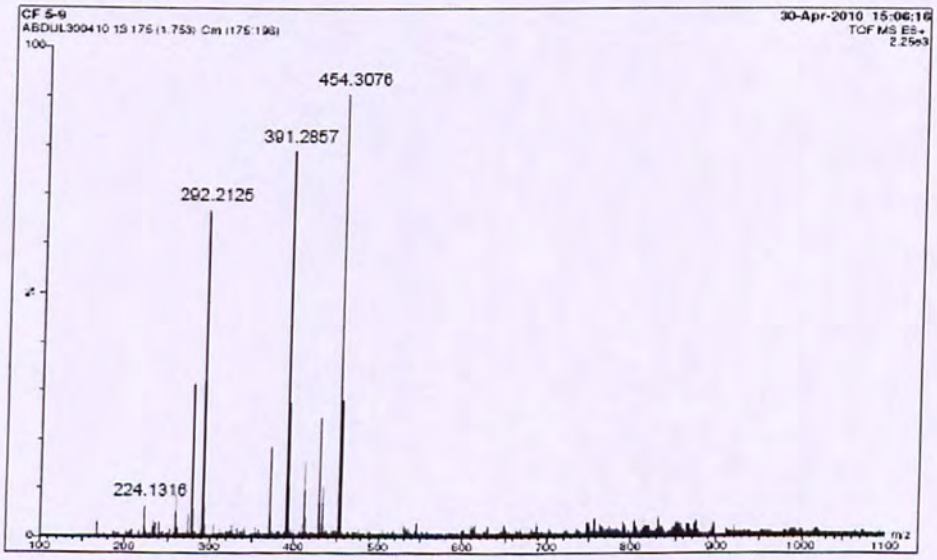

*Figure 4.28: High resolution mass spectrum of Compound **5** on LCT Mass spectrometer with TOF in ESI positive (+ve) modes showing large fragment ions.*

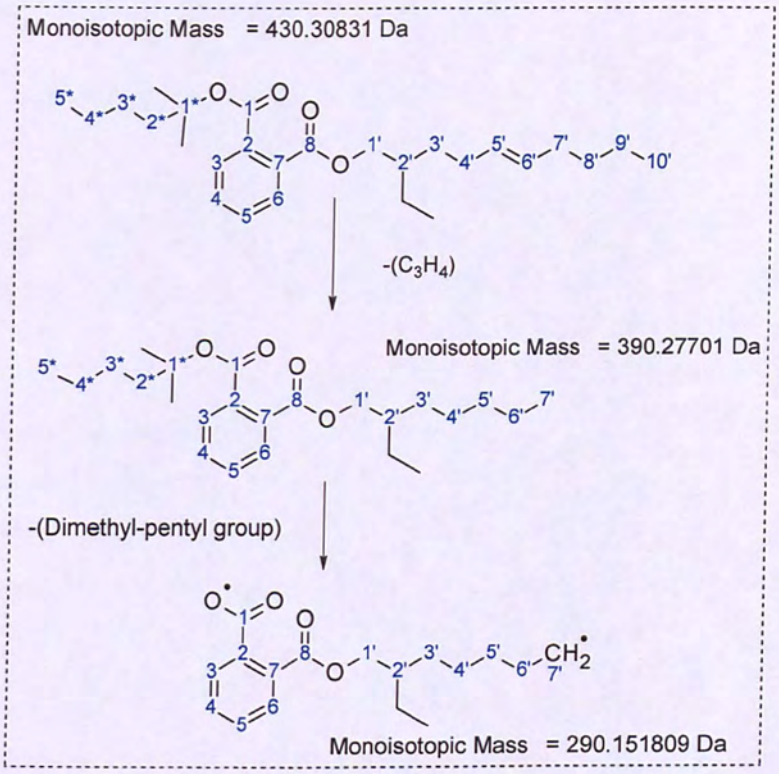

Figure 4.29: Proposed fragmentation pattern of phthalic acid 1-(1, 1-dimethyl-pentyl) ester 2-(2-ethyl-dec-5-enyl) ester with calculated monoisotopic masses of fragments.

4.6. Phytochemical analysis: *Arisaema utile*

Reported phytochemical studies on the family Araceae have shown a series of homologous, phenylalkanoic acids and phenylalkenoic acids isolated from seed lipids of the genus *Arisaema*, e.g. 13-phenyltridecanoic acid (fatty acid) from the seeds of *Arisaema utile* (Meija *et al.*, 2004). Previous studies were mainly focused on investigating the chemical compositions of this poisonous medicinal plant.

In the present study, preliminary screening of crude extracts, organic and aqueous fractions against three cancer cell lines (MCF-7, MDA MB-468, Caco-2) has shown the chloroform fraction to be the most cytotoxic. A series of chromatographic experiments (as described in materials and methods) resulted in the isolation of two compounds (Compounds **6** and **7**). The identification and structure elucidation were carried out on the basis of advanced spectroscopic studies.

4.6.1. Compound 6 (Docosanoic acid methyl ester)

Compound **6** was pale yellow oil at room temperature with a total yield of 68 mg from the chloroform fraction of *Arisaema utile*. Further characterisation for structure elucidation purposes of Compound **6** was attempted through a series of spectroscopic experiments including IR, GC-MS, NMR (^{1}H, ^{13}C, DEPT, HETCOR, DQF-COSY, HMBC) and LC-MS.

4.6.1.1 Infra-Red spectroscopy of Compound 6

The IR spectrum of the Compound **6** (Figure 4.30) showed a typical pattern for ester functional groups. The absorption bands at 1736, 1243 and 1064 cm^{-1} are distinctive functional groups (C=O) and (C-O), represent stretching vibrations for esters in the molecular structure.

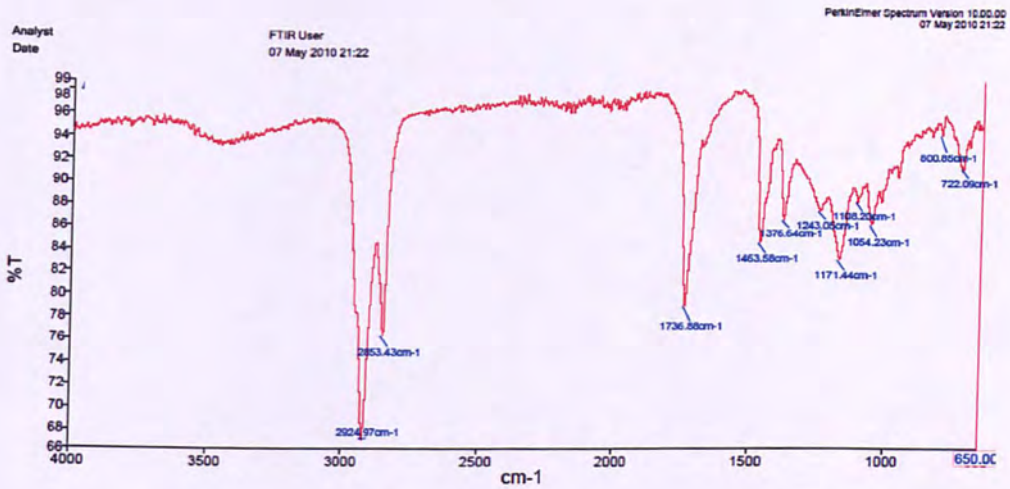

*Figure 4.30: IR spectrum of Compound **6** showing absorption bands of functional groups corresponds to % Transmittance versus Wavenumber (cm^{-1}).*

Furthermore, an absorption band at 1736 cm^{-1} also suggested the presence of (C=O) group as a ketone, (classical example of acetone (2-propanone). As this absorption band (1736 cm^{-1}) is slightly broader than the absorption band for an ester, where the band is much sharper, it may suggest the presence of both ester and ketonic functional groups in the structure. A medium intensity band at 1463 cm^{-1} indicated the antisymmetric ($-CH_3$) deformation and the bending vibrations of ($-CH_2$) groups in aliphatic compounds. The strong intensity absorption bands appeared at 2924, 2852 cm^{-1} and represent the asymmetric and symmetric stretch vibrations of ($-CH_3$) and ($-CH_2$) groups.

4.6.1.2. Gas Chromatography-Mass Spectrometry (GC-MS)

The GC-MS spectra of Compound **6** were recorded by injecting a chloroform solution (1 µl), using temperature programme (as described in material and methods, section: 2.8.3.2.) for 20 min each run. A single peak was observed on the chromatogram (Figure 4.31) at a retention time (RT) 14.83 min. This peak showed a small molecular ion peak at m/z 410, representing the molecular weight of Compound **6**.

The peaks appearing at m/z 284 and 129 on the mass spectrum indicate that the molecule may be split into two major fragments with nominal masses 283 and 128 Da respectively, as shown in Figure 4.32. A further loss of two methylene ($2xCH_2$) groups $[M+H-128-28]^+$ was exhibited at m/z 255 from the major fragment ion (m/z 284). Similarly further one, two or three methylene groups lost from the alkyl chain, appeared on the MS spectra at m/z: 241, 199, 185, 157, 129. The base peak appeared at m/z 88; showed a maximum abundance of 120,000, and represents a loss of a nominal mass 41 Da (corresponding to C_2HO loss) from the fragment ion at m/z 129. The proposed fragmentation pattern of Compound **6** is described in figure 4.32.

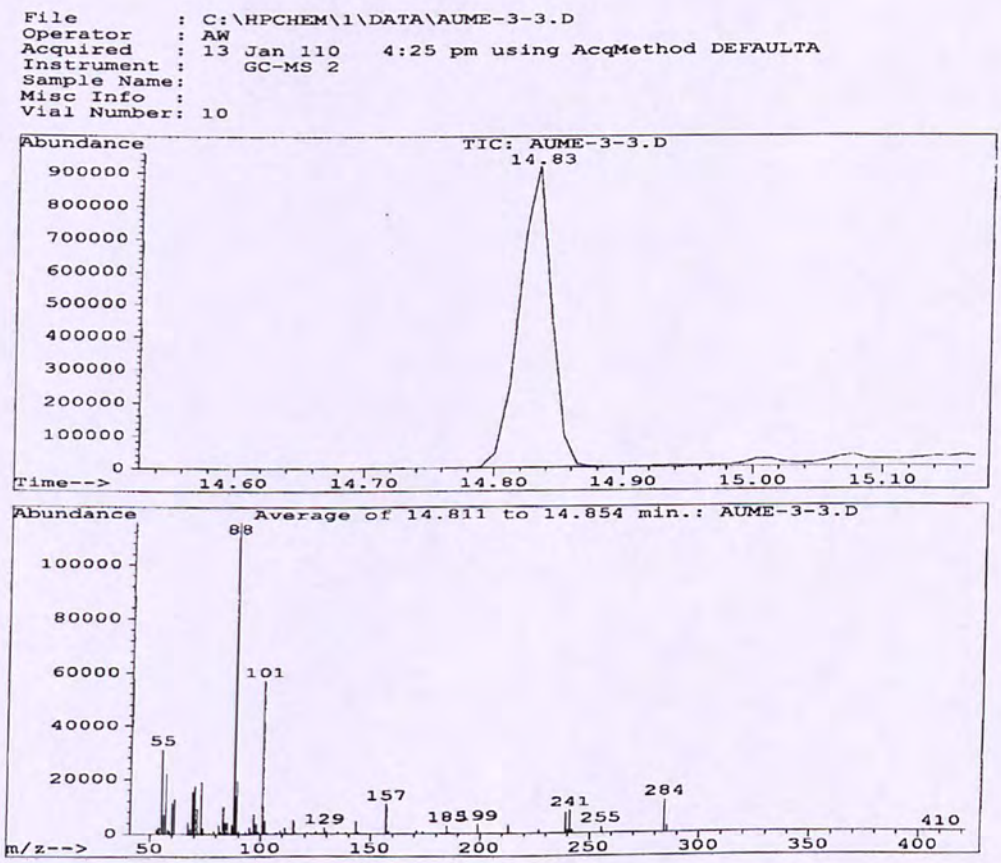

*Figure 4.31: Chromatogram of Compound **6** along with mass spectrum on GC-MS showing retention time (RT 14.83 min) and molecular ion peak (m/z 410).*

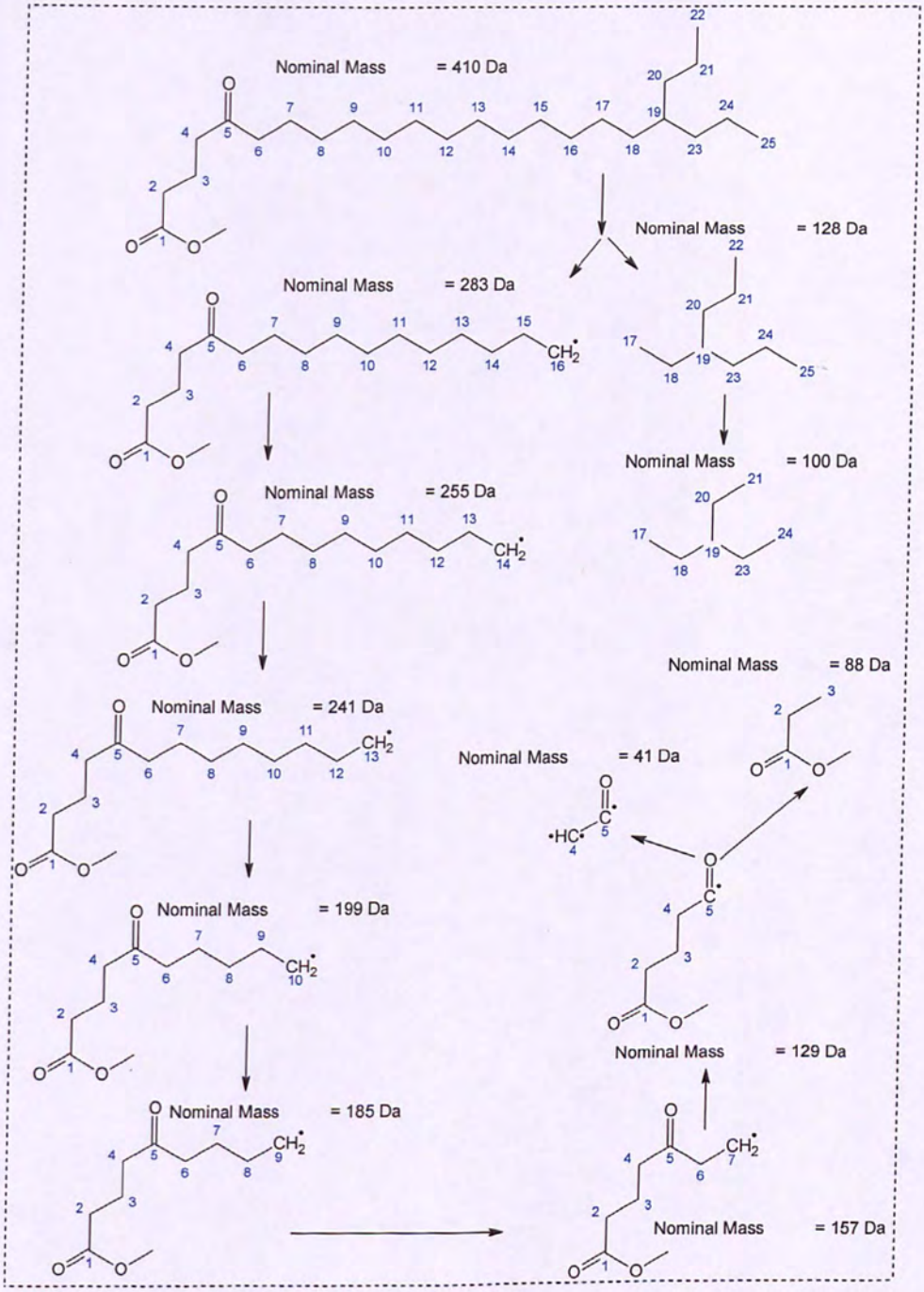

*Figure 4.32: Proposed fragmentation pattern of 5-Oxo-19-propyl-docosanoic acid methyl ester (Compound **6**) with nominal masses of fragments observed in GC-MS spectrum.*

4.6.1.3. Nuclear Magnetic Resonance (NMR) spectroscopy

The data from ^{1}H- and ^{13}C-NMR spectroscopy is summarised in Table 4.14. The analysis of ^{13}C-NMR showed two weak signals for carbonyl groups and appeared at δ_C 188.4 and 174.4. This represents the quaternary carbons of ester and ketone groups, positioned at C-1 and C-5 respectively (Figure 4.33).

No.	δ_H	δ_C	No.	δ_H	δ_C
1	----------	174.4, s	14	1.25(2H, broad m, H-14)	29.2, t
2	4.12(2H, dd, *J* = 7.23,7.23,6.96 Hz,H-2)	60.23, t	15	1.25(2H, broad m, H-15)	29.3, t
3	1.59(2H, m, H-3)	25.0, t	16	1.25(2H, broad m, H-16)	29.4, t
4	2.30(2H, dd, *J* = 7.32, 7.69, 7.14, H-4)	34.4, t	17	1.25(2H, broad m, H-117)	29.5, t
5	----------	188.4, s	18	1.25(2H, broad m, H-18)	32.0, t
6	2.30(2H, dd, *J* = 7.32, 7.69, 7.14, H-6)	34.2, t	19	1.61(1H, m, H-19)	30.2, d
7	1.59(2H, m, H-7)	25.0, t	20	1.25(2H, broad m, H-20)	29.7, t
8	1.25(2H, broad m, H-8)	22.7, t	21	1.28(2H, m, H-21)	29.6, t
9	1.25(2H, broad m, H-9)	29.5, t	22	0.88(3H, t, *J* = 6.96, 6.68 Hz, H-22)	14.2, q
10	1.25(2H, broad m, H-10)	29.4, t	23	1.25(2H, broad m, H-23)	29.7, t
11	1.25(2H, broad m, H-11)	29.3, t	24	1.28(2H, m, H-24)	29.6, t
12	1.25(2H, broad m, H-12)	29.2, t	25	0.88(3H, t, *J* = 6.96, 6.68 Hz, H-25)	14.2, q
13	1.25(2H, broad m, H-13)	29.3, t	1*	3.66(3H, s, H-1*)	51.5, q

*Table 4.14: ^{1}H- and ^{13}C-NMR† data (ppm) of Compound **6** (5-Oxo-19-propyl-docosanoic acid methyl ester).*
†Multiplicity of assigned peaks were determined by edited DEPT experiments (s=quaternary, d = methine, t = methylene, q = methyl), (TMS as internal standard)

The cross peak signals in HMBC experiments as a plot of ^{1}H- and ^{13}C-NMR spectra indicated the ^{1}H-^{1}H long range correlation between the hydrogen of methylene (δ_H 4.12) at C-2 and carbonyl (C=O) at C-1 for the ester moiety and signals of the methylene groups (δ_H 2.30) at C-4 and C-6 to quaternary carbon at C-5. In ^{1}H-NMR, a shielded signal appeared as a singlet at δ_H 3.66 is suggested as the methyl group attached to the oxygen of the ester at position C-1*.

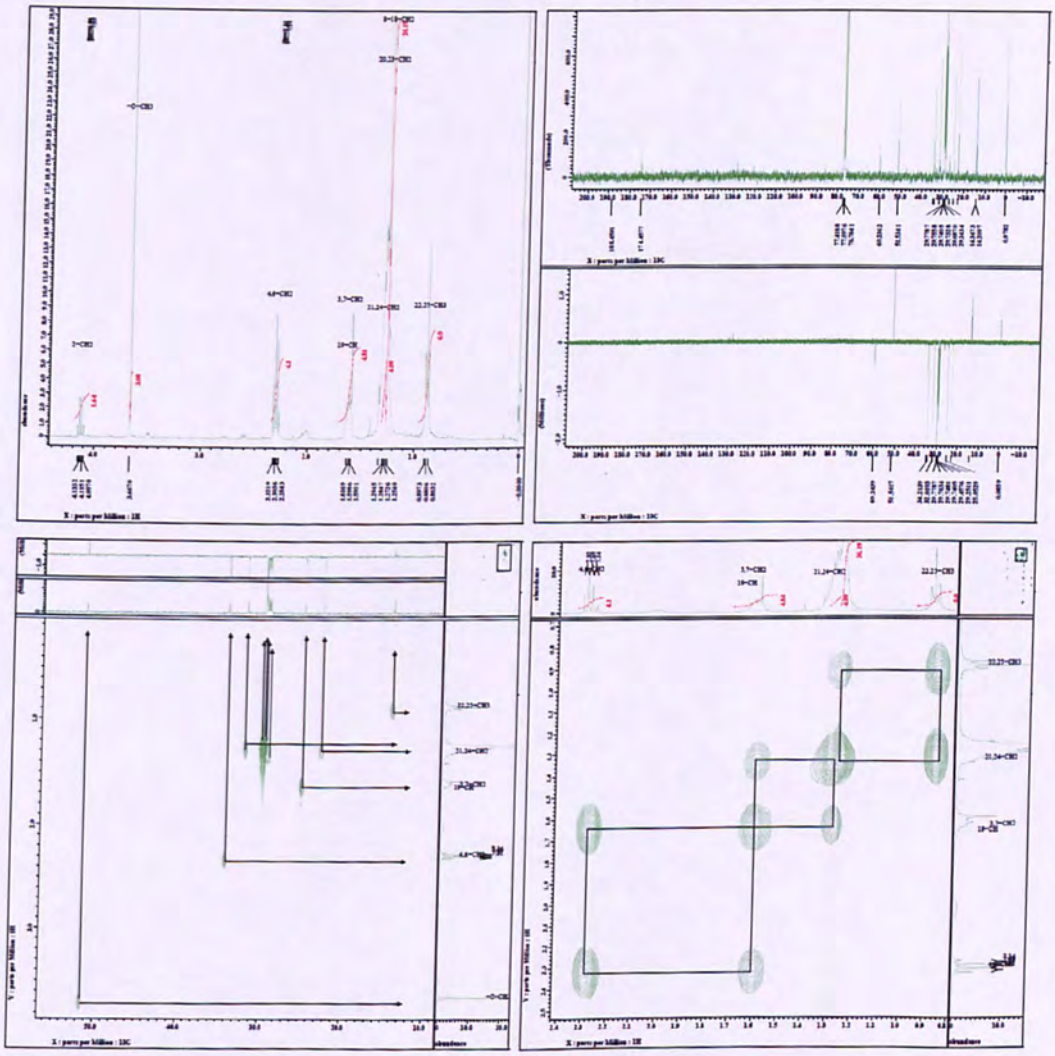

Figure 4.32: 1D (^{1}H, ^{13}C, DEPT) NMR and 2D (HETCOR, DQF-COSY) NMR spectra of Compound 6 (5-Oxo-19-propyl-docosanoic acid methyl ester) from Arisaema utile.

A broad multiplet appeared at δ_H 1.25 and describes the integration of 26 protons of the aliphatic alkyl chain consisting of eleven methylene groups from C-8 to C-18 (δ_c 22.7–32.0) and two methylene groups at C-20 and C-23 (δ_c 29.7) as listed in Table 4.14. The hydrogen (δ_H 1.61) of the methine group positioned at C-19 showed a multiplet signal due to the neighbouring protons of three methylene groups (δ_H 1.25), positioned at C-18, -20, -23. In addition, the methylene groups located at C-3, -7, -21, -24 were also observed as a multiplet. The terminal methyl groups exhibited as a triplet at δ_H 0.88 were positioned at C-22 and C-25 in ^{1}H-NMR. Two dimensional NMR data from HETCOR and DQF-COSY experiments confirmed through cross peak signals, show the ^{13}C's directly bonded to the ^{1}H's and ^{1}H-^{1}H correlation up to one bond length, as illustrated in figure 4.32.

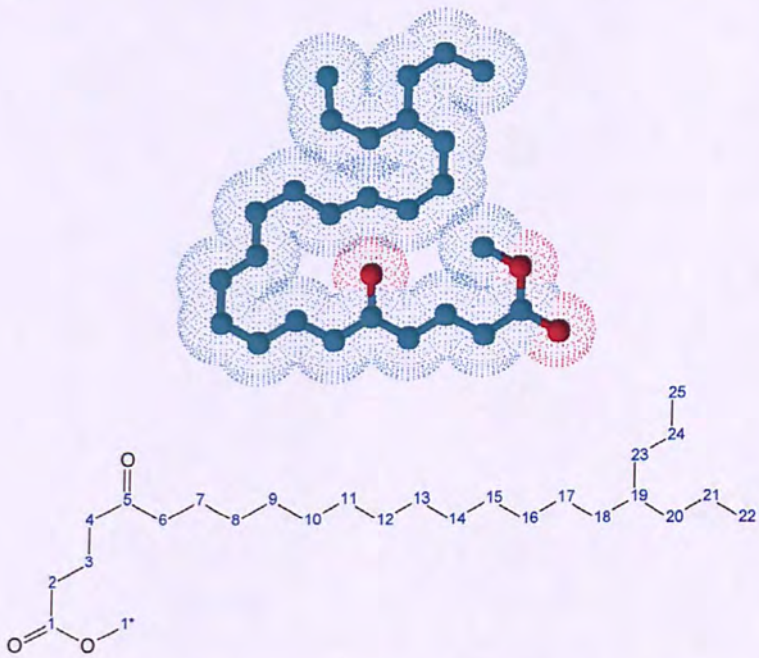

*Figure 4.33: Proposed structure of Compound **6** identified as 5-Oxo-19-propyl-docosanoic acid methyl ester from the chloroform fraction of Arisaema utile.*

The ^{13}C and DEPT-NMR experiments indicated a total of 26 carbon signals, of which three corresponded to methyl carbons, twenty to methylene carbons, one to methine carbon and two to quaternary carbons, suggesting that compound **6** is

5-Oxo-19-propyl-docosanoic acid methyl ester (Figure 4.33) with molecular formula as $C_{26}H_{50}O_3$.

4.6.1.4. Liquid Chromatography-Mass Spectrometry (LC-MS)

The high resolution (HR) mass spectra (Figure 4.34) were recorded on a LCT Mass Spectrometer with Time-of-Flight (TOF) using electro spray ionisation negative (ESI -ve) mode. According to GC-MS data, the molecular weight of the Compound **6** is 410; in addition, NMR and IR data prompted the molecular formula $C_{26}H_{50}O_3$ with calculated monoisotopic mass 410.3759. The mass spectra on LC-MS exhibited a molecular ion peak at 409.3681 $[M-H]^+$, concluded the molecular weight of 5-Oxo-19-propyl-docosanoic acid methyl ester ($C_{26}H_{50}O_3$) is 410.3751. Moreover the fragement ion observed at m/z 264 may be due to the loss of $C_7H_{13}O_3$, which is highlighted at m/z 250 upon further loss of a methylene group (CH_2).

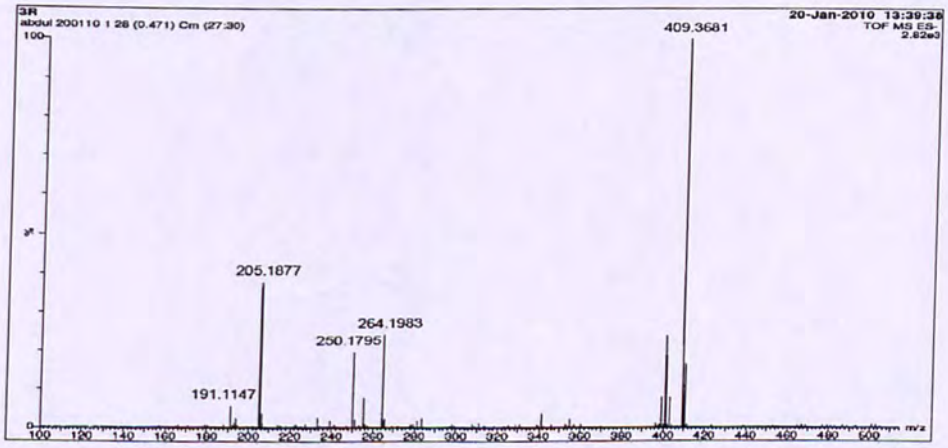

*Figure 4.34: High resolution mass spectrum of Compound **6** on LCT Mass spectrometer with TOF in ESI negative (-ve) mode.*

4.6.2. X-ray crystallography of Compound 7 (3-Hydroxy-20-pentyl-pregnane)

Compound **7** was isolated as colourless, needle-like crystals with a total yield of 4 mg only, from the chloroform fraction of *Arisaema utile* after repeated column

chromatography. Single crystal X-ray crystallography studies, conducted on a Nonius Kappa CCD diffractometer revealed a typical steroidal skeleton. Indexing and unit cell refinement based on all observed reflection from the ten frames, indicated a monoclinic plane lattice. A total of 7359 reflections (λ_{max}=21.11°) were indexed, integrated and corrected for Lorentz polarisation and absorption effects using DENZO-SMN and SCALEPAC (Otwinowski and Minor, 1997). Post refinement of the unit cell gave *a*=69.985(6) Å, *b*=7.6236(7) Å, *c*=9.9555(18) Å, α=90°, β=95.382(3)°, and γ=90°, Volume=10600.10(16) Å^3.

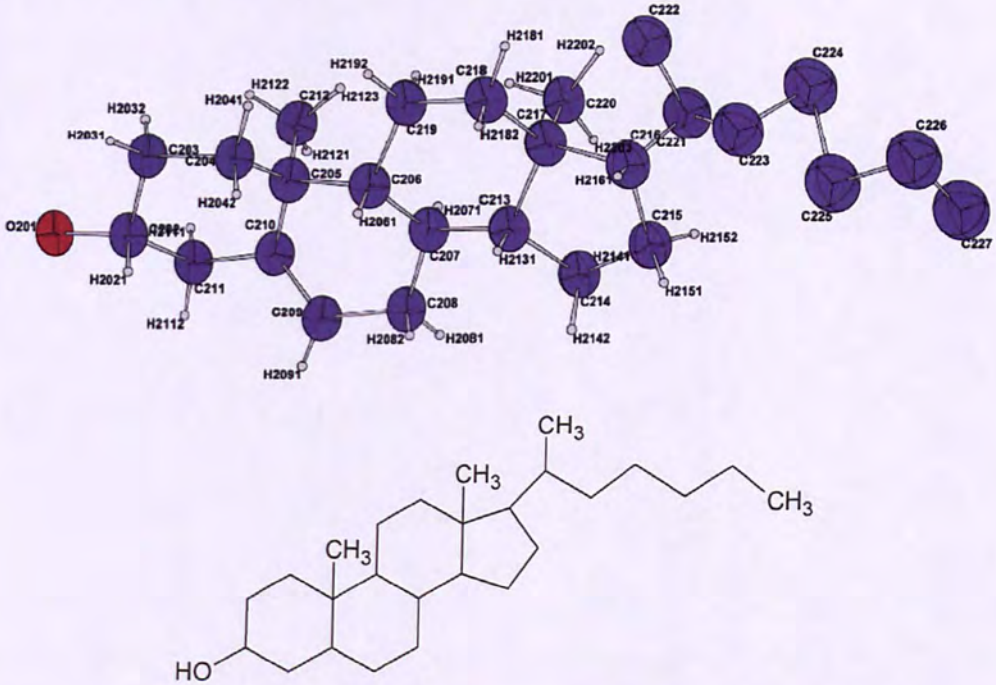

Figure 4.35: Single crystal structure of Compound 7 (3-Hydroxy-20-pentyl-pregnane)

Based on the X-ray crystal structure of Compound **7**, the molecular formula was calculated as $C_{26}H_{46}O$. The molecular structure showed one hydroxyl group and a total of 26 carbons, consisting of 4 methyl, 13 methylene, 7 methine and 2 quaternary carbons. From the aforementioned data, Compound **7** is identified as 3-Hydroxy-20-pentyl-pregnane with formula weight 374.6428.

4.7 Anticancer activity of isolated compounds 1-6

Bioassay systems for anti-cancer activity have been established using the screening process to guide the fractionation and separation of crude extracts. As described earlier (cytotoxicity of crude extracts and fractions, sections: 4.1. and 4.2.), the crude ethanolic extracts and the potent fractions from *Caralluma tuberculata, Fagonia indica, Solanum surattense* and *Arisaema utile* showed highly significant cytotoxicity (up to 95% inhibition) against three cancer cell lines (MCF-7, MDA MB-468, Caco-2). Phytochemical analysis resulted in the isolation of seven compounds (**1–7**) from these four medicinal plants. Unfortunately, the yield for Compound **7** from *Arisaema utile* was very low (4 mg only) and was not enough after phytochemical analysis, to be further investigated for anticancer activity, so only six compounds (**1–6**) were selected for evaluation of antiproliferative activity against three cancer cell lines. The aim was to determine whether these compounds are killing particular tumour cell lines or showing selective growth inhibition and are worth further evaluation for the mode of cell death using established assays of apoptosis and necrosis.

4.7.1. Cytotoxicity and apparent IC_{50} (based on MTT and NRU assays)

A serial dilution of eight concentrations (0.78, 1.56, 3.12, 6.25, 12.5, 25, 50, 100 μM) for each compound (**1–6**) were tested using two cell viability assays (MTT and neutral red uptake assays) for 24 h and 48 h treatments. Three positive controls were used: Actinomycin-D (4 μM, inhibitor of protein synthesis), Tamoxifen (5 μM, oestrogen receptor antagonist) and Anastrozole (5 μM, aromatase inhibitor).

4.7.1.1. Acylated pregnane glycoside (*Caralluma tuberculata*)

Compound **1** was identified as an acylated pregnane glycoside from the ethyl acetate fraction of *Caralluma tuberculata*. The results of MTT and neutral red

Pregnane glycoside Conc. (µM)	Percentage growth inhibition after 24 h treatment						Percentage growth inhibition after 48 h treatment					
	MTT assay			Neutral red uptake assay			MTT assay			Neutral red uptake assay		
	MCF-7 cells	MDA MB-468 cells	Caco-2 cells	MCF-7 cells	MDA MB-468 cells	Caco-2 cells	MCF-7 cells	MDA MB-468 cells	Caco-2 cells	MCF-7 cells	MDA MB-468 cells	Caco-2 cells
0.78	0.87 (±0.49)	3.83 (±5.30)	3.56 (±1.80)	5.21 (±1.44)	4.25 (±3.85)	16.51 (±4.60)	2.71 (±0.54)	5.74 (±4.05)	13.92 (±3.62)	4.43 (±1.41)	3.64 (±0.48)	20.04* (±4.49)
1.56	2.50 (±0.55)	4.10 (±5.12)	2.79 (±1.08)	16.33 (±1.21)	6.08 (±2.01)	27.54* (±3.26)	3.07 (±1.22)	7.42 (±1.72)	28.27* (±3.28)	6.31 (±1.23)	4.46 (±3.06)	45.78** (±5.15)
3.12	4.11 (±0.96)	8.60 (±4.30)	11.22 (±2.64)	12.63 (±3.27)	7.46 (±5.56)	42.25** (±3.49)	3.51 (±1.44)	13.87 (±5.00)	25.76* (±4.12)	9.55 (±0.95)	4.03 (±3.86)	66.05*** (±6.04)
6.25	6.23 (±1.48)	14.21 (±2.01)	26.14* (±5.04)	20.52* (±1.47)	11.18 (±4.08)	46.22** (±4.62)	4.27 (±2.13)	10.18 (±4.14)	52.61*** (±5.63)	28.91* (±5.08)	19.59 (±3.19)	72.23*** (±3.23)
12.5	20.97* (±2.34)	21.05* (±4.45)	35.71** (±4.77)	39.38** (±4.86)	17.28 (±3.99)	74.39*** (±2.82)	34.39** (±2.92)	32.90** (±8.25)	77.43*** (±5.45)	99.36*** (±0.67)	15.85 (±5.17)	83.29*** (±3.69)
25	41.97** (±1.17)	28.56* (±2.39)	54.35*** (±4.69)	68.72*** (±3.09)	23.06* (±3.20)	74.87*** (±3.98)	93.73*** (±2.09)	30.13** (±2.54)	99.04*** (±1.67)	100.40*** (±0.21)	30.98** (±8.44)	92.55*** (±5.89)
50	99.58*** (±0.23)	41.63** (±4.70)	63.77*** (±3.26)	63.56*** (±4.70)	59.21*** (±2.98)	84.24*** (±6.47)	100.71*** (±.013)	56.45*** (±2.61)	100.14*** (±1.31)	100.54*** (±0.37)	66.03*** (±5.40)	98.78*** (±1.25)
100	99.35*** (±0.55)	50.14*** (±3.54)	78.63*** (±4.22)	68.37*** (±2.88)	71.15*** (±2.65)	99.76*** (±0.70)	100.81*** (±0.24)	63.97*** (±3.42)	100.14*** (±0.59)	100.46*** (±0.06)	90.01*** (±3.19)	99.08*** (±1.01)
Actinomycin-D (4µM)	62.04*** (±1.43)	62.87*** (±5.28)	65.40*** (±4.29)	91.84*** (±3.73)	93.94*** (±5.02)	65.97*** (±4.83)	81.81*** (±1.65)	89.86*** (±4.81)	95.15*** (±4.48)	99.97*** (±0.64)	94.64*** (±2.25)	99.38*** (±1.35)
Tamoxifen (5µM)	84.74*** (±4.33)	27.80* (±4.06)	-------	78.19*** (±3.17)	38.36** (±6.26)	-------	99.64*** (±1.14)	45.41** (±4.14)	-------	100.26*** (±0.35)	63.05*** (±3.16)	-------
Anastrozole (5µM)	51.72*** (±3.42)	70.11*** (±1.47)	-------	46.30** (±5.61)	74.11*** (±4.18)	-------	46.39** (±6.43)	86.89*** (±7.04)	-------	36.22** (±4.22)	92.99*** (±6.23)	-------
Vehicle Control	1.57 (±3.61)	1.68 (±5.28)	1.10 (±1.13)	1.76 (±5.12)	1.69 (±4.44)	1.67 (±1.06)	4.41 (±6.22)	1.35 (±3.76)	1.91 (±1.62)	5.21 (±3.02)	-1.81 (±4.96)	1.72 (±1.40)

Table 4.15: Antiproliferative activity of the acylated pregnane glycoside from Caralluma tuberculata against three cancer cell lines using two cytotoxicity assays, after 24 and 48 hours treatment. Where statistically (Dunnett's multiple comparison test)
** = Significant (P<0.05), ** = Highly significant (P<0.01), *** = Very highly significant (P<0.001)*

uptake assays for percentage inhibition of cell growth for the three cancer cell lines after 24 h and 48 h are summarised in Table 4.15, and detailed calculations of absorbance for treated versus untreated cells (n=3, Mean ± STD) are enclosed in appendices (17–20).

The results from the MTT assay showed that statistically significant ($P<0.05$) inhibition (20–21%) of both breast cancer cells (MCF-7 and MDA MB-468) started at a concentration of 12.5 μM, which became highly significant ($P<0.01$) at a concentration of 25 μM for MCF-7 and 50 μM for MDA MB-468 cells after 24h treatment with the acylated pregnane glycoside. In addition, in a prolonged exposure to 48 h, the percentage inhibition was increased to a very highly significant ($P<0.001$) level of 93% for MCF-7 at 25 μM concentration. Here, it is worth mentioning a selective growth inhibition of pregnane glycoside for cancer cells was observed for the oestrogen dependent cancer cell line (MCF-7), while this glycoside could not retard the growth effectively in the oestrogen independent cancer cells (MDA MB-468), where highly significant inhibition of 64% was observed at a very high concentration (100 μM) after 48 h (Table 4.15).

This inhibition can be further justified with the neutral red uptake assay, which represents the healthy uninjured metabolically active cells in the sample. The results showed that significant inhibition started at 6.25 μM for MCF-7 cells after 24 h exposure and exhibited a very highly significant effect (68%) at as little as 25 μM, which further rocketed to 93% after 48 h. In case of oestrogen independent breast cancer cells, the highly significant effect of 59% was observed at 50 μM after 24 h, but this inhibition remained almost constant as 56% inhibition was calculated after 48 h.

Cytotoxicity studies of acylated pregnane glycoside from *Caralluma tuberculata* against Caco-2 indicated that this glycoside possessed more anticancer activity for colorectal carcinoma cells as compared to breast cancer cells (MCF-7 & MDA MB-468). Results showed that a significant inhibition (26%) was achieved at 6.25

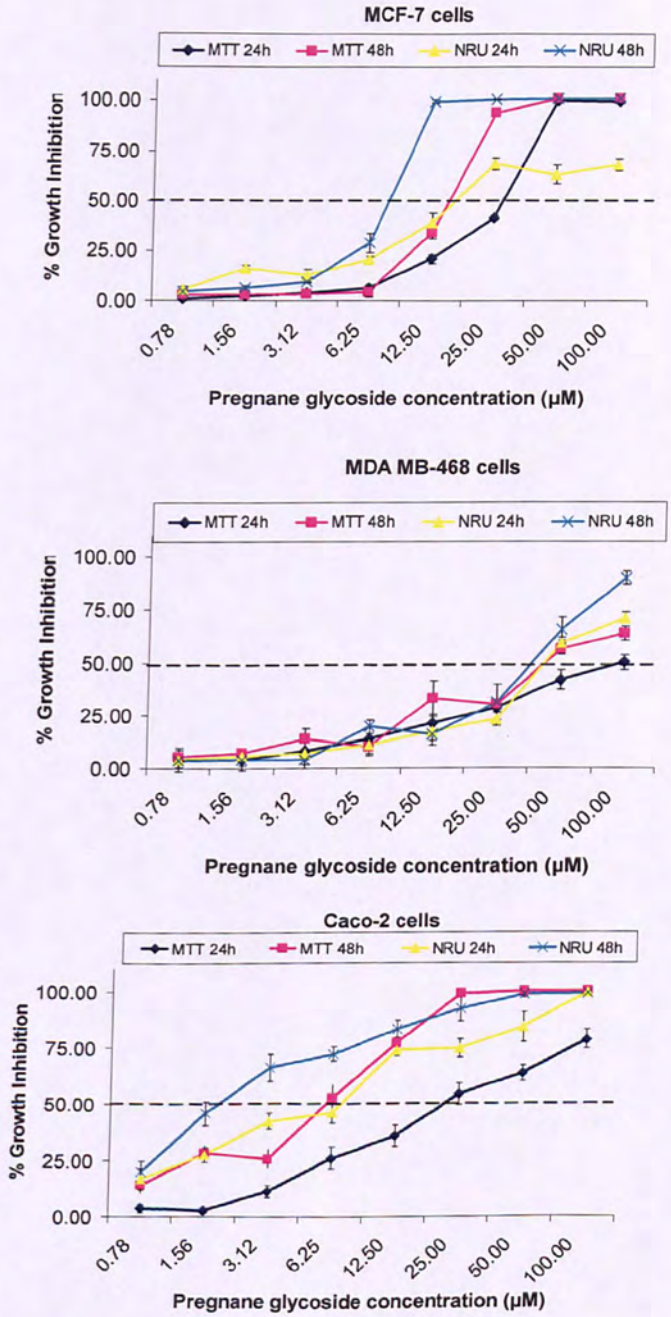

Figure 4.36: Concentration dependent percentage growth inhibition of the acylated pregnane glycoside from Caralluma tuberculata against breast and colon cancer cell lines, showing apparent IC_{50} with MTT and neutral red uptake assays after 24 h and 48 h treatments.

μM corresponding to untreated cells in MTT assay, while this effect was observed at a very low concentration (1.56 μM) with neutral red uptake assay after 24 h treatment (Table 4.15), which is further increased to 74% at 12.5 μM. Both the assays indicated that only 1-8% viable or metabolically active Caco-2 cells could survive at 25 μM after a prolonged exposure of 48 h.

Growth in the three cell lines was inhibited in response to the positive controls as expected. Actinomycin-D inhibited the growth of MCF-7 cells by 62-82% (MTT assay) and 91-100% (NRU assay) after 48 hours. Tamoxifen completely inhibited the growth of MCF-7 after 48 hours, using either MTT or NRU assay, but was less effective, as expected, on the growth of MDA-MB-468 cells (45% MTT assay, 63% NRU assay). Anastrozole was only moderately inhibitory on MCF-7 cells (46% MTT assay, 36% NRU assay), but much more effective on MDA-MB-468 cells (87% MTT assay, 93% NRU assay). Actinomycin-D showed growth inhibition 65-95% with MTT assay after 24-48h, while with NRU assay an increased, almost complete inhibition (99%) was observed after 48 h treatment.

Acylated pregnane glycoside (Compound **1**) inhibited cell growth with the following apparent IC_{50} values, using the NRU assay, after 24 hours: MCF-7 cells 12.5 - 25 μM, MDA-MB-468 cells 25 - 50 μM, Caco-2 cells 6.25 – 12.5 μM (Figure 4.36). Similar data was obtained using the MTT assay, after 48 hours: MCF-7 cells 12.5 - 25.0 μM, MDA-MB-468 cells ~50 μM, Caco-2 cells ~6.25 μM. Inhibition of cell growth, relative to vehicle-treated cells, was statistically significant (by one way ANOVA with Dunnett's post-test) at 6.25 μM and higher for pregnane glycoside in MCF-7 and MDA-MB-468 cells, and at 1.56 μM and higher concentrations tested for Caco-2 cells.

4.7.1.2. Acylated androstane glycoside (*Caralluma tuberculata*)

Compound **2** was identified as an acylated androstane glycoside from the ethyl acetate fraction of *Caralluma tuberculata*. The results of MTT and neutral

Androstane glycoside Conc. (μM)	Percentage growth inhibition after 24 h treatment						Percentage growth inhibition after 48 h treatment					
	MTT assay			Neutral red uptake assay			MTT assay			Neutral red uptake assay		
	MCF-7 cells	MDA MB-468 cells	Caco-2 cells	MCF-7 cells	MDA MB-468 cells	Caco-2 cells	MCF-7 cells	MDA MB-468 cells	Caco-2 cells	MCF-7 cells	MDA MB-468 cells	Caco-2 cells
0.78	4.58 (±1.31)	4.18 (±0.61)	12.46 (±2.29)	3.68 (±1.92)	4.58 (±1.43)	14.56 (±3.79)	4.97 (±1.65)	5.74 (±2.20)	6.35 (±4.20)	11.87 (±3.45)	6.43 (±4.28)	8.47 (±3.48)
1.56	9.81 (±3.29)	5.87 (±1.96)	12.80 (±6.17)	5.68 (±3.01)	5.95 (±2.84)	23.35* (±3.33)	5.29 (±2.93)	13.19 (±3.39)	14.50 (±2.51)	14.72 (±5.64)	11.71 (±6.04)	21.19* (±2.11)
3.12	7.68 (±3.78)	13.18 (±4.85)	20.28* (±1.62)	8.75 (±2.36)	9.21 (±3.37)	40.26** (±4.44)	7.09 (±3.57)	16.46 (±2.68)	45.06** (±4.02)	28.33* (±5.17)	14.76 (±4.67)	55.01*** (±3.32)
6.25	21.56* (±1.57)	12.58 (±4.75)	23.21* (±3.32)	21.98* (±2.35)	13.46 (±3.87)	56.04*** (±5.23)	37.46** (±1.97)	12.32 (±4.88)	59.92*** (±5.10)	55.44*** (±4.77)	25.12* (±2.93)	64.94*** (±3.80)
12.5	34.33** (±2.97)	20.38* (±3.50)	50.30*** (±2.92)	43.37** (±1.80)	16.56 (±4.61)	71.49*** (±5.59)	86.42*** (±4.65)	17.53 (±3.47)	87.67*** (±4.87)	100.47*** (±0.20)	29.21* (±7.74)	97.24*** (±2.47)
25	96.67*** (±0.19)	25.57* (±2.01)	78.86*** (±4.46)	68.08*** (±2.69)	28.23* (±4.10)	81.19*** (±3.80)	100.64*** (±0.29)	29.78* (±3.10)	94.85*** (±2.02)	100.51*** (±0.40)	35.32** (±7.38)	99.82*** (±0.46)
50	99.62*** (±0.28)	52.15*** (±3.37)	79.96*** (±4.95)	70.72*** (±4.07)	52.70*** (±5.10)	84.51*** (±6.25)	100.33*** (±0.48)	66.86*** (±2.54)	96.42*** (±6.03)	100.47*** (±0.11)	66.10*** (±8.14)	99.69*** (±0.70)
100	99.09*** (±0.33)	62.06*** (±6.22)	88.19*** (±3.88)	85.51*** (±3.27)	68.33*** (±3.49)	99.83*** (±0.92)	100.31*** (±0.36)	78.58*** (±5.71)	100.19*** (±1.20)	100.70*** (±0.13)	80.60*** (±5.57)	100.31*** (±0.27)
Actinomycin-D (4μM)	57.42*** (±1.71)	65.30*** (±7.10)	57.61*** (±5.46)	91.35*** (±2.98)	89.11*** (±4.23)	64.41*** (±4.02)	78.48*** (±2.16)	85.94*** (±1.74)	91.78*** (±8.92)	99.91*** (±0.42)	87.89*** (±11.42)	97.47*** (±2.69)
Tamoxifen (5μM)	84.74*** (±4.33)	27.80* (±4.06)	-------	78.19*** (±3.17)	38.36** (±6.26)	-------	99.64*** (±1.14)	45.41** (±4.14)	-------	100.24*** (±0.37)	63.05*** (±3.16)	-------
Anastrozole (5μM)	51.72*** (±3.42)	70.11*** (±1.47)	-------	46.28** (±5.64)	74.11*** (±4.18)	-------	46.39** (±6.43)	86.89*** (±7.04)	-------	36.22** (±4.21)	92.99*** (±6.23)	-------
Vehicle Control	0.55 (±3.97)	4.41 (±2.15)	1.29 (±0.10)	-2.68 (±3.64)	-0.11 (±4.87)	1.25 (±0.56)	4.68 (±2.93)	-2.75 (±2.98)	1.06 (±0.52)	1.50 (±5.11)	4.36 (±1.91)	1.21 (±0.26)

*Table 4.16: Antiproliferative activity of the acylated androstane glycoside from Caralluma tuberculata against three cancer cell lines using two cytotoxicity assays after 24 and 48 hours treatment. The results for anastrozole and tamoxifen were not repeated but are taken from table 4.15 for comparison. Where statistically (Dunnett's multiple comparison test), * = Significant (P<0.05), ** = Highly significant (P<0.01), *** = Very highly significant (P<0.001)*

red uptake assays for percentage inhibition of cell growth for the three cancer cell lines after 24 and 48 h are summarised in Table 4.16, and detailed calculations of absorbance for treated versus untreated cells (n=3, Mean ± STD) are enclosed in appendices (21–24).

In the MTT assay, results showed a significant growth inhibition (22 %) in MCF-7 cells that started at 6.25 μM concentration and gave a very highly significant ($P<0.001$) inhibition (97%) in 24 h treatment with 25 μM. In comparison to MDA MB-468 cells, although cytotoxicity (20 %) was statistically significant at 12.5 μM, the maximum inhibition achieved was only 62% at a very high concentration (100 μM). These results indicated that like pregnane glycoside (as discussed in the previous section: 4.7.1.1.), androstane glycosides also showed a concentration dependent cytotoxic effect in hormone dependent breast cancer cells. Similar results were also shown by the NRU assay, where metabolically inactive cells reached 68% at 25 μM in 24 h.

In a time dependent assay, when the treatment was extended to 48 h, androstane glycoside demonstrated amazing results in MCF-7 cells, where cell survival was 63% initially at 6.25 μM, this further reduced to 14% at 12.5 μM and complete cell death was observed at 25 μM in MTT assay. In comparison, in MDA MB-468 cells percentage inhibition was 29% at 25 μM and the maximum viable cells were about 23% at a higher concentration of 100 μM. It is worth mentioning here that more than half of the population (55%) of MCF-7 cells was observed to be metabolically active at 6.25 μM concentration after 48 h, while such an effect for MDA MB-468 was noted at nearly 50 μM.

Cytotoxic activity of the androstane glycoside from *Caralluma tuberculata* for Caco-2 cells showed that this steroidal glycoside possesses quite good potency, as represented in Table 4.16 from MTT and NRU assays. A significant inhibition of 23% was attained at a very low concentration at 1.56 μM in the NRU assay,

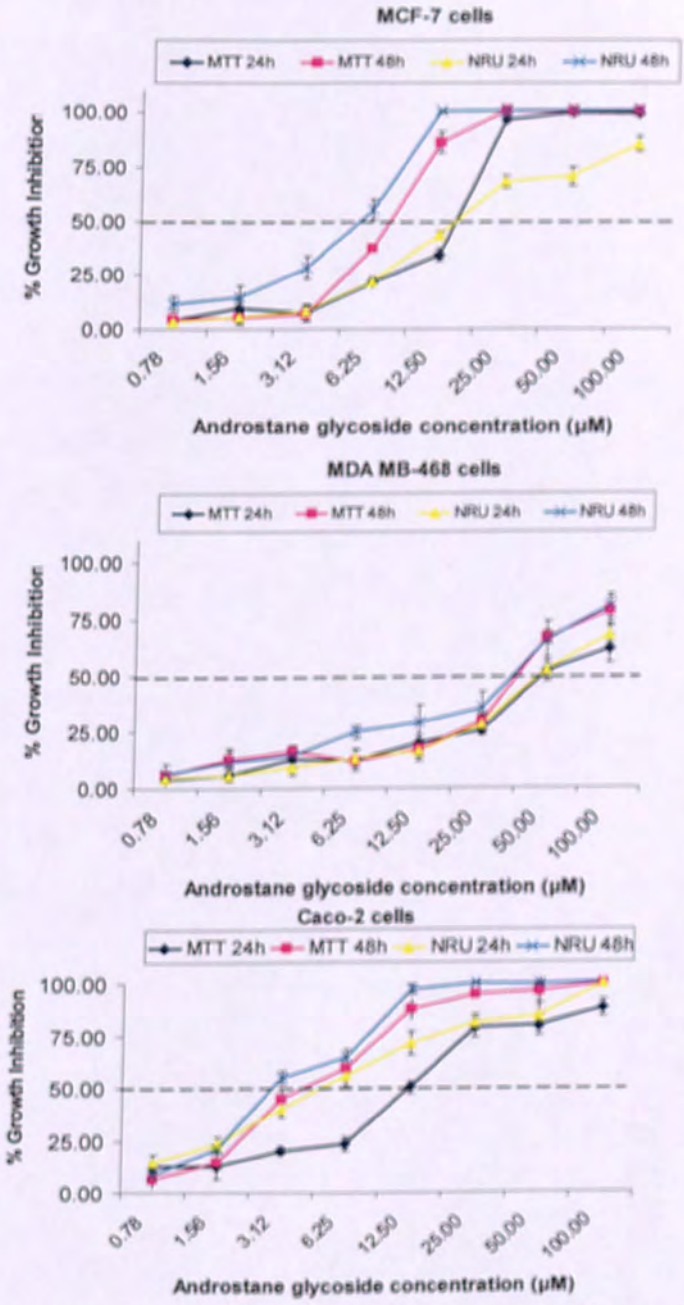

Figure 4.37: Concentration dependent percentage growth inhibition of the acylated androstane glycoside from Caralluma tuberculata against breast and colon cancer cell lines, showing apparent IC_{50} with MTT and neutral red uptake assays after 24 and 48 h treatments.

while in the MTT assay this effect was accomplished at 6.25 μM. The data showed a gradual increase in cell cytotoxicity with respect to concentration dependent effects. Similarly, in a time dependent aspect, the androstane glycoside also gained profound inhibition when treatment was extended from 24 h to 48 h. The MTT assay showed a 50% inhibition in the Caco-2 population after 24 h. This level was increased to 88% ($P<0.001$) after 48 h and in addition 97% ($P<0.001$) cell cytotoxicity was calculated in the NRU assay (Table 4.16).

Compound **2** (acylated androstane glycoside) inhibited cell growth with the following apparent IC_{50} values, using the NRU assay, after 48 hours: MCF-7 cells 6.25- 12.5 μM, MDA-MB-468 cells 25 - 50 μM, Caco-2 cells 1.56 - 3.12 μM (Figure 4.37). Similar data was obtained using the MTT assay, after 48 hours: MCF-7 cells 6.25 - 12.5 μM, MDA-MB-468 cells 25 - 50 μM, Caco-2 cells 3.12 - 6.25 μM. In the NRU assay, inhibition of cell growth by acylated androstane glycoside, relative to vehicle-treated cells, was statistically significant ($P<0.05$) from 1.56 μM and higher concentrations for Caco-2 cells, but from 6.25 μM and higher concentrations in MCF-7 and MDA MB-468 cells after 24h treatment.

4.7.1.3. Pregnane glycoside (*Fagonia indica*)

Compound **3** was isolated from the ethyl acetate fraction of *Fagonia indica.* A serial dilution of eight concentrations (0.78–100 μM) showed a highly significant selective growth inhibition against oestrogen negative breast cancer cells (MDA MB-468) and colorectal carcinoma cells (Caco-2), while in MCF-7 cells, a moderate cytotoxic activity was observed. The results of MTT and neutral red uptake assays for percentage inhibition of cell growth over a concentration range for the three cancer cell lines, after 24 and 48 h are summarised in Table 4.17, and detailed calculations of absorbance for treated versus untreated cells (n=3, Mean ± STD) are enclosed in appendices (25–28).

Pregnane glycoside Conc. (μM)	Percentage growth inhibition after 24 h treatment						Percentage growth inhibition after 48 h treatment					
	MTT assay			Neutral red uptake assay			MTT assay			Neutral red uptake assay		
	MCF-7 cells	MDA MB-468 cells	Caco-2 cells	MCF-7 cells	MDA MB-468 cells	Caco-2 cells	MCF-7 cells	MDA MB-468 cells	Caco-2 cells	MCF-7 cells	MDA MB-468 cells	Caco-2 cells
0.78	4.32 (±2.51)	10.17 (±4.86)	4.93 (±3.29)	6.34 (±2.19)	4.49 (±2.45)	5.73 (±8.05)	4.71 (±2.35)	7.86 (±3.37)	18.69 (±3.49)	6.18 (±2.38)	12.63 (±5.82)	18.04 (±1.63)
1.56	4.85 (±2.62)	14.78 (±5.46)	16.89 (±2.45)	6.91 (±1.82)	4.66 (±2.06)	31.19** (±3.05)	4.53 (±3.07)	21.31* (±2.51)	28.91* (±3.06)	12.93 (±3.87)	17.28 (±3.95)	38.32** (±3.11)
3.12	8.00 (±4.28)	26.12* (±3.15)	20.29* (±4.87)	12.60 (±5.11)	22.88* (±6.86)	37.21** (±6.44)	6.12 (±2.06)	39.94** (±3.63)	33.44** (±1.95)	18.38 (±8.62)	31.54** (±5.07)	38.46** (±3.82)
6.25	7.01 (±5.11)	30.55** (±2.93)	27.98* (±2.15)	16.80 (±4.58)	32.29** (±5.86)	37.03** (±3.60)	9.36 (±2.19)	46.74** (±5.60)	37.24** (±3.62)	18.38 (±5.37)	41.70** (±4.30)	43.82** (±5.13)
12.5	9.37 (±5.16)	37.86** (±4.93)	31.18** (±4.65)	24.17* (±5.62)	52.68*** (±3.46)	41.85** (±5.76)	10.90 (±4.36)	48.33** (±4.68)	43.21** (±4.62)	22.56* (±6.56)	55.51*** (±3.91)	66.00*** (±4.63)
25	13.10 (±5.74)	49.94** (±1.79)	33.97** (±5.17)	29.02* (±4.83)	64.66*** (±5.54)	55.19*** (±5.24)	14.16 (±3.07)	61.66*** (±3.73)	74.15*** (±5.79)	36.76** (±4.62)	68.76*** (±9.32)	75.30*** (±2.33)
50	28.46* (±4.10)	71.07*** (±4.55)	44.76** (±4.10)	36.61** (±4.02)	70.48*** (±4.22)	61.33*** (±2.13)	34.48** (±3.37)	73.03*** (±4.03)	93.76*** (±5.81)	41.16** (±5.47)	87.58*** (±6.24)	96.22*** (±1.67)
100	42.53** (±4.04)	77.05*** (±3.67)	66.36*** (±2.62)	50.22*** (±4.27)	77.73*** (±4.45)	72.14*** (±9.45)	52.77*** (±3.95)	80.72*** (±4.57)	98.93*** (±1.39)	60.06*** (±1.82)	94.95*** (±5.10)	98.67*** (±1.88)
Actinomycin-D (4μM)	53.43*** (±3.24)	63.21*** (±4.93)	54.78*** (±4.51)	74.33*** (±3.64)	77.93*** (±5.52)	71.35*** (±6.49)	75.39*** (±3.90)	75.17*** (±2.53)	90.59*** (±2.28)	97.33*** (±6.19)	94.01*** (±3.65)	87.67*** (±3.69)
Tamoxifen (5μM)	84.74*** (±4.33)	27.80* (±4.06)	-------	78.19*** (±3.17)	38.36** (±6.26)	-------	99.64*** (±1.14)	45.41** (±4.14)	-------	100.24*** (±0.37)	63.05*** (±3.16)	-------
Anastrozole (5μM)	51.72*** (±3.42)	70.11*** (±1.47)	-------	46.28** (±5.64)	74.11*** (±4.18)	-------	46.39** (±6.43)	86.89*** (±7.04)	-------	36.22** (±4.21)	92.99*** (±6.23)	-------
Vehicle Control	2.37 (±1.81)	4.58 (±1.29)	1.51 (±1.19)	2.71 (±2.61)	0.67 (±4.04)	2.07 (±0.98)	1.92 (±2.62)	2.50 (±2.07)	3.03 (±1.68)	1.17 (±2.85)	3.91 (±2.19)	2.64 (±1.35)

*Table 4.17: Antiproliferative activity of the pregnane glycoside from Fagonia indica against three cancer cell lines using two cytotoxicity assays after 24 and 48 hours treatment. The results for anastrozole and tamoxifen were not repeated but are taken from table 4.15 for comparison Where statistically (Dunnett's multiple comparison test), * = Significant (P<0.05), ** = Highly significant (P<0.01), *** = Very highly significant (P<0.001)*

In contrast to the cytotoxicity results of steroidal glycosides from *Caralluma tuberculata,* MDA MB-468 cancer cells were more responsive to Compound **3**.

The results from MTT assay showed that significant ($P<0.05$) inhibition (26%) started at 3.12 μM and reached a highly significant ($P<0.001$) stage where 50% inhibition in the cell population was observed in 24 h. The neutral red uptake assay also exhibited a similar suppression (53%) in cell growth at 12.5 μM. In an extended treatment time (48 h), the percentage of cell death (48-55%) remained almost steady with both MTT and NRU assays at 12.5 μM and maximum inhibition (80-95%) was observed at 100 μM.

A similar extent of cell suppression was also observed for Caco-2 cells, where a statistically significant activity was observed at 3.2 μM and higher concentrations (in MTT assay for 24 h) while in the NRU assay this effect was more pronounced at 1.56 μM and higher concentrations, after 24 h incubation. A prominent enhanced effect in cell cytotoxicity was observed after 48 h incubation, when the NRU assay showed a statistically highly significant ($P<0.001$) inhibition (38%) at a very low concentration (1.56 μM).

The pregnane glycoside (Compound **3**) isolated from *Fagonia indica*, despite the steroidal skeleton in the molecular structure did not demonstrate a cytotoxic response in hormone dependent breast cancer cells. Results from MTT and NRU data (Table 4.17) represented a maximum inhibition of 42-50% at a very high concentration (100 μM) after 24 h in treated cells, where this treatment could not easily increase the antiproliferative effect even after 48h when tested with either assay. This effect may be due to the structure activity relationship, as compared to human body androgens (oestrogen hormone) in the chemical structure. Where the difference in the extended unsaturated aliphatic groups on two esterified positions (C-12 and C-20), as described in section (4.4.2.3.), may not be feasible in order to compete for the enzyme active site to produce a cytotoxic effect.

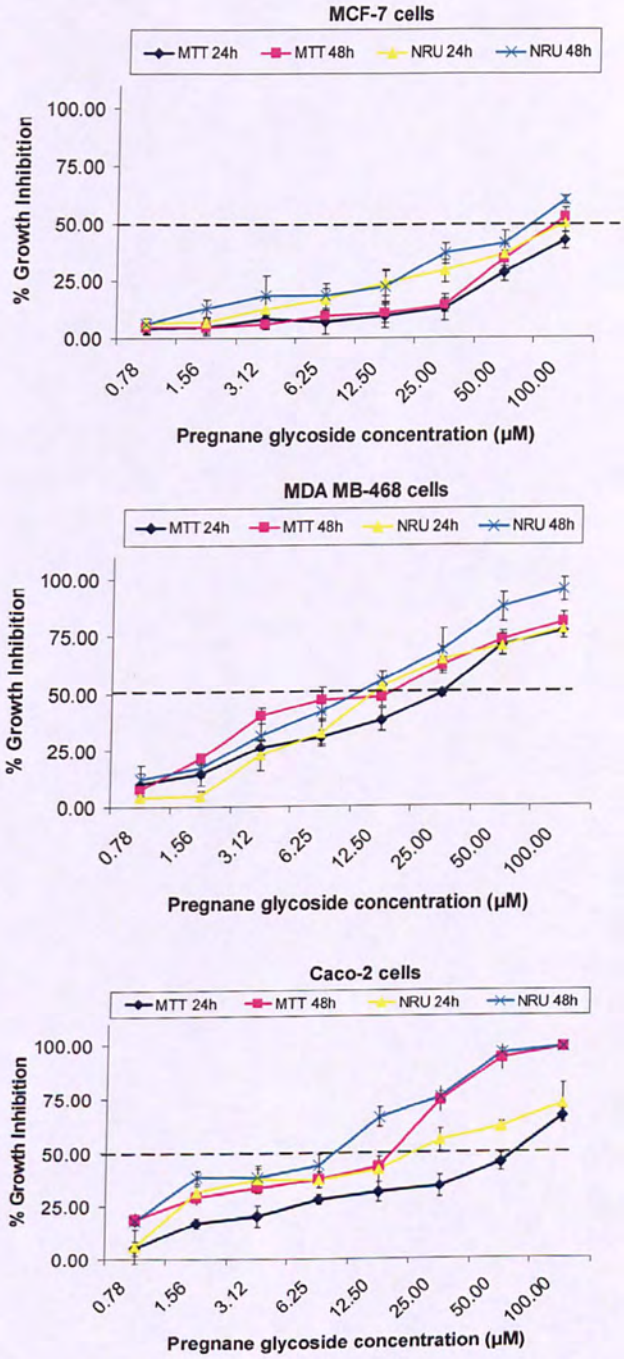

Figure 4.38: Percentage growth inhibition of the pregnane glycoside over concentration range from Fagonia indica against breast and colon cancer cell lines, showing apparent IC_{50} with MTT and neutral red uptake assays after 24 and 48 h treatments.

The apparent IC_{50} values for pregnane glycoside (Compound **3**) were estimated (Figure 4.38) from MTT and NRU assays, after 24 h and 48 h: MDA MB-468 (6.25 – 12.5 μM), Caco-2 (12.5 – 25 μM), where as for MCF-7 cells IC_{50} values range 50 – 100 μM, after 48 h treatment.

4.7.1.4. Hexadecanoic acid ethyl ester (*Solanum surattense*)

Compound **4** (Hexadecanoic acid ethyl ester) was isolated from the chloroform fraction of *Solanum surattense*. Antiproliferative activity was evaluated for concentration and time dependent effects on three cancer cell lines using MTT and neutral red uptake assays. The results for percentage inhibition of cell growth over concentration range, after 24 and 48 hours are summarised in Table 4.18, and detailed calculations of absorbance for treated versus untreated cells (n=3, Mean ± STD) are enclosed in appendices (29–32).

Results from NRU assay after 24 h incubation revealed that Hexadecanoic acid ethyl ester has a moderate to good cytotoxicity against the Caco-2 cell line, as statistically significant ($P<0.01$) cell inhibition (31%) was initiated at 6.25 μM concentration and maximum inhibition (70%) attained at 100 μM while in the MTT assay to some extent lesser inhibition (57%) was accomplished, data shows even a prolonged incubation time up to 48 h could not enhance the antiproliferative effect in both assays and the percentage inhibition was in the range of 67-69%.

On the other hand, the breast cancer cells (MCF-7 and MDA MB-468) were not very responsive to Compound **4** and a mild cytotoxic effect was noted. Highly significant ($P<0.001$) cytotoxic effect was detected at high concentration (100 μM) with both MTT and NRU assays after 24 h, when half of the cell population was found to be dead or metabolically inactive to go through cell division. This percentage inhibition could not extend further (almost 60%), even after 48 h,

Hexadecanoic acid Conc. (µM)	Percentage growth inhibition after 24 h treatment						Percentage growth inhibition after 48 h treatment					
	MTT assay			Neutral red uptake assay			MTT assay			Neutral red uptake assay		
	MCF-7 cells	MDA MB-468 cells	Caco-2 cells	MCF-7 cells	MDA MB-468 cells	Caco-2 cells	MCF-7 cells	MDA MB-468 cells	Caco-2 cells	MCF-7 cells	MDA MB-468 cells	Caco-2 cells
0.78	1.80 (±0.44)	6.29 (±4.24)	9.26 (±2.90)	3.26 (±3.86)	6.97 (±4.75)	8.04 (±5.30)	3.27 (±2.68)	8.67 (±2.79)	7.46 (±0.97)	9.51 (±5.84)	8.90 (±5.27)	16.75 (±8.90)
1.56	2.64 (±0.11)	9.79 (±5.48)	8.80 (±2.05)	6.05 (±1.11)	13.39 (±8.16)	11.93 (±4.19)	5.01 (±1.76)	12.85 (±2.57)	12.45 (±2.51)	10.41 (±6.04)	11.33 (±6.30)	20.58 (±6.69)
3.12	3.05 (±4.22)	9.58 (±7.98)	16.32 (±4.56)	8.63 (±5.36)	14.01 (±7.60)	20.24* (±4.35)	6.24 (±2.29)	11.20 (±2.99)	12.93 (±3.44)	9.98 (±2.59)	14.98 (±3.85)	16.02 (±1.19)
6.25	8.27 (±4.87)	12.29 (±1.89)	17.30 (±6.48)	13.84 (±6.17)	10.20 (±4.51)	31.84** (±6.61)	9.08 (±5.35)	8.17 (±6.27)	17.88 (±2.80)	25.47* (±7.66)	18.48 (±3.06)	23.50* (±9.94)
12.5	14.07 (±7.22)	25.50* (±2.38)	22.31* (±6.24)	23.98* (±2.17)	19.00 (±6.15)	30.17** (±4.02)	15.42 (±3.09)	20.12* (±2.75)	21.66* (±4.79)	26.98* (±5.12)	26.70* (±10.57)	29.66* (±6.94)
25	29.13* (±3.55)	25.14* (±3.89)	35.47** (±5.15)	32.83** (±6.27)	28.04* (±5.57)	37.81** (±6.38)	29.53* (±2.89)	33.75** (±6.04)	41.46** (±5.70)	40.63** (±2.45)	29.78* (±6.65)	25.57* (±5.30)
50	40.64** (±2.18)	32.52** (±3.73)	46.38** (±5.55)	40.74** (±6.31)	40.88** (±4.00)	51.51*** (±2.30)	49.44** (±4.38)	40.35** (±3.15)	53.65*** (±3.48)	43.62** (±4.57)	40.98** (±3.80)	55.96*** (±3.06)
100	56.65*** (±1.76)	47.57** (±4.25)	61.96*** (±6.26)	56.47*** (±4.23)	48.81** (±5.15)	69.97*** (±5.63)	63.17*** (±5.69)	48.22** (±3.77)	66.50*** (±2.91)	57.82*** (±5.54)	51.04*** (±4.98)	69.27*** (±3.84)
Actinomycin-D (4µM)	62.36*** (±6.23)	61.70*** (±7.02)	71.30*** (±2.74)	73.88*** (±2.63)	73.46*** (±5.09)	72.32*** (±5.84)	75.27*** (±2.27)	73.38*** (±3.60)	82.99*** (±3.76)	88.37*** (±5.98)	91.92*** (±5.35)	90.36*** (±5.80)
Tamoxifen (5µM)	84.74*** (±4.33)	27.80* (±4.06)	-------	78.19*** (±3.17)	38.36** (±6.26)	-------	99.64*** (±3.67)	45.41** (±4.14)	-------	100.24*** (±0.37)	63.05*** (±3.16)	-------
Anastrozole (5µM)	51.72*** (±3.42)	70.11*** (±1.47)	-------	46.28*** (±5.64)	74.11*** (±4.18)	-------	46.39** (±1.14)	86.89*** (±7.04)	-------	36.22** (±4.21)	92.99*** (±6.23)	-------
Vehicle Control	2.16 (±1.39)	3.68 (±2.14)	2.85 (±4.63)	5.29 (±1.95)	3.64 (±0.97)	3.39 (±1.90)	4.71 (±6.43)	2.99 (±2.25)	2.62 (±5.57)	2.05 (±3.61)	1.55 (±5.77)	2.17 (±4.43)

Table 4.18: Antiproliferative activity of the hexadecanoic acid from Solanum surattense against three cancer cell lines using two cytotoxicity assays after 24 and 48 hours treatment. The results for anastrozole and tamoxifen were not repeated but are taken from table 4.15 for comparison Where statistically (Dunnett's multiple comparison test), = Significant (P<0.05), ** = Highly significant (P<0.01), *** = Very highly significant (P<0.001)*

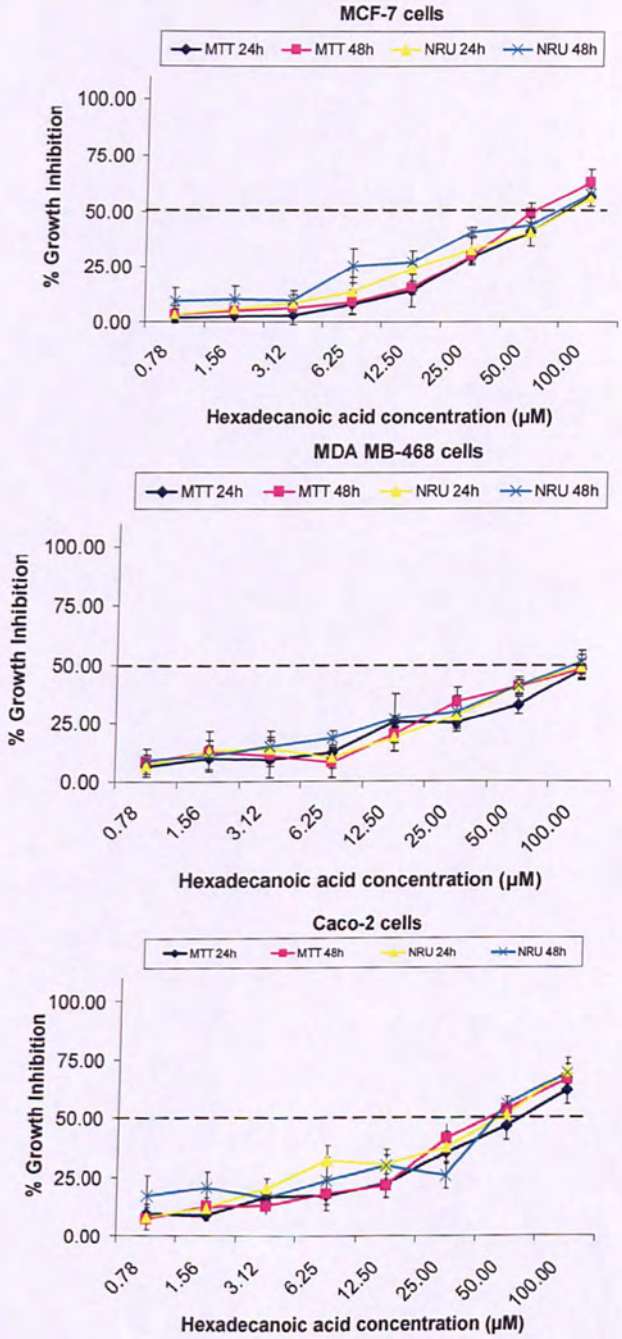

Figure 4.39: Percentage growth inhibition of hexadecanoic acid ethyl ester over concentration range from Solanum surattense against breast and colon cancer cell lines, showing apparent IC_{50} with MTT and neutral red uptake assays after 24 and 48 h treatments.

which indicated that the anticancer activity of hexadecanoic acid ethyl ester was more associated with a concentration-dependent effect as compared to a time dependent response.

The apparent IC_{50} values for hexadecanoic acid ethyl ester (Compound **4**) were estimated (Figure 4.39) from MTT and NRU assays, after 24 h and 48 h: MDA MB-468 and MCF-7 cells (50 – 100 μM) whereas for Caco-2 cells ~50 μM. Inhibition of cell growth, relative to vehicle-treated cells, was statistically significant (by one way ANOVA with Dunnett's multiple comparison test) at 3.12 μM and higher for Compound **4** in Caco-2 cells; similarly in MCF-7 and MDA-MB-468 cells at 25 μM and higher concentrations after 24 h cell treatment.

4.7.1.5. Phthalic acid ester (*Solanum surattense*)

Compound **5** (phthalic acid ester) was purified from the chloroform fraction of *Solanum surattense*. Its anticancer activity was investigated both in a concentration and time dependent manner using two colorimetric assays, MTT and neutral red uptake assays. The eight dilutions ranging from 0.78 to 100 μM were investigated against three cancer cell lines at 24 h and 48 h incubation of treated cells. The results are summarised in Table 4.19, and detailed calculations of absorbance for treated versus untreated cells (n=3, Mean ± STD) are enclosed in appendices (33–36).

The data showed that in Caco-2 cells a statistically significant ($P<0.05$) effect commenced at a very low concentration 1.56 μM, which proceeded to a highly significant ($P<0.001$) cell suppression (52%) at 12.5 μM and maximum inhibition reached 92% at 100 μM concentration after 24 h exposure in NRU assay, whereas the MTT assay showed that 28% treated cells could survive at this concentration. This effect was almost stable for the next 24 h, in a prolonged exposure where half of the cell population was inhibited at 6.25 μM (NRU assay).

Phthalic acid Conc. (µM)	Percentage growth inhibition after 24 h treatment						Percentage growth inhibition after 48 h treatment					
	MTT assay			Neutral red uptake assay			MTT assay			Neutral red uptake assay		
	MCF-7 cells	MDA MB-468 cells	Caco-2 cells	MCF-7 cells	MDA MB-468 cells	Caco-2 cells	MCF-7 cells	MDA MB-468 cells	Caco-2 cells	MCF-7 cells	MDA MB-468 cells	Caco-2 cells
0.78	4.94 (±5.05)	10.58 (±4.41)	8.13 (±3.01)	4.87 (±3.66)	4.35 (±3.36)	14.35 (±3.98)	2.84 (±2.88)	6.98(±3.22)	12.74 (±3.45)	9.71 (±4.33)	5.80 (±7.29)	15.55 (±2.88)
1.56	3.46 (±2.54)	15.59 (±5.72)	7.33 (±3.57)	12.89 (±4.02)	8.29 (±5.41)	20.34* (±7.70)	4.54 (±2.22)	19.58 (±5.92)	20.55* (±4.59)	25.30* (±5.91)	14.33 (±9.66)	17.40 (±3.66)
3.12	6.67 (±2.71)	26.05* (±3.69)	14.03 (±1.77)	15.23 (±5.48)	20.42* (±5.61)	29.19* (±4.53)	7.74 (±1.72)	37.46** (±6.57)	27.77* (±5.80)	32.67** (±5.23)	41.40** (±9.14)	33.64** (±5.26)
6.25	8.35 (±3.71)	29.77* (±3.27)	13.07 (±7.04)	24.88* (±2.69)	31.73** (±7.67)	36.22** (±3.34)	9.05 (±4.05)	44.37** (±8.21)	38.83** (±5.17)	39.96** (±8.53)	47.65** (±1.61)	53.60*** (±7.44)
12.5	20.98* (±8.98)	37.36** (±6.34)	19.70 (±6.60)	32.48** (±7.16)	51.90*** (±9.73)	52.25*** (±7.14)	14.05 (±4.74)	47.86** (±3.12)	60.75*** (±2.89)	51.65*** (±2.19)	62.05*** (±6.10)	68.94*** (±3.47)
25	28.61* (±5.27)	49.78** (±2.32)	43.33** (±4.38)	39.57** (±5.79)	63.79*** (±4.97)	57.62*** (±4.17)	31.04** (±4.57)	61.19*** (±2.43)	72.49*** (±5.89)	56.99*** (±4.37)	72.44*** (±3.78)	79.79*** (±4.53)
50	43.21** (±5.67)	70.96*** (±5.00)	57.74*** (±3.39)	56.84*** (±5.27)	72.94*** (±3.73)	78.78*** (±6.08)	51.65*** (±4.21)	70.13*** (±4.62)	88.80*** (±3.57)	72.79*** (±3.35)	89.52*** (±4.63)	92.60*** (±2.67)
100	58.14** (±3.92)	77.35*** (±4.11)	71.92*** (±5.07)	79.22*** (±4.85)	80.60*** (±5.18)	92.18*** (±4.22)	72.26*** (±3.46)	81.76*** (±6.21)	93.58*** (±3.50)	87.29*** (±7.44)	94.27*** (±4.55)	98.67*** (±1.94)
Actinomycin-D (4µM)	55.51*** (±5.93)	63.74*** (±5.50)	70.26*** (±5.13)	77.62*** (±2.57)	78.96*** (±7.50)	77.15*** (±8.21)	75.39*** (±3.90)	79.90*** (±4.56)	89.79*** (±4.22)	95.13*** (±3.86)	94.31*** (±4.28)	97.51*** (±1.87)
Tamoxifen (5µM)	84.74*** (±4.33)	27.80* (±4.06)	-------	78.19*** (±3.17)	38.36** (±6.26)	-------	99.64*** (±1.14)	45.41** (±4.14)	-------	100.24*** (±0.37)	63.05*** (±3.16)	-------
Anastrozole (5µM)	51.72*** (±3.42)	70.11*** (±1.47)	-------	46.28** (±5.64)	74.11*** (±4.18)	-------	46.39** (±6.43)	86.89*** (±7.04)	-------	36.22** (±4.21)	92.99*** (±6.23)	-------
Vehicle Control	3.00 (±2.16)	5.98 (±1.05)	1.36 (±4.51)	0.53 (±6.15)	3.86 (±1.35)	0.66 (±2.87)	4.58 (±2.64)	0.41 (±2.58)	-0.95 (±2.74)	0.55 (±3.30)	2.12 (±1.69)	-0.12 (±7.82)

Table 4.19: Antiproliferative activity of the phthalic acid ester from Solanum surattense against three cancer cell lines using two cytotoxicity assays after 24 and 48 hours treatment. The results for anastrozole and tamoxifen were not repeated but are taken from table 4.15 for comparison Where statistically (Dunnett's multiple comparison test), = Significant (P<0.05), ** = Highly significant (P<0.01), *** = Very highly significant (P<0.001)*

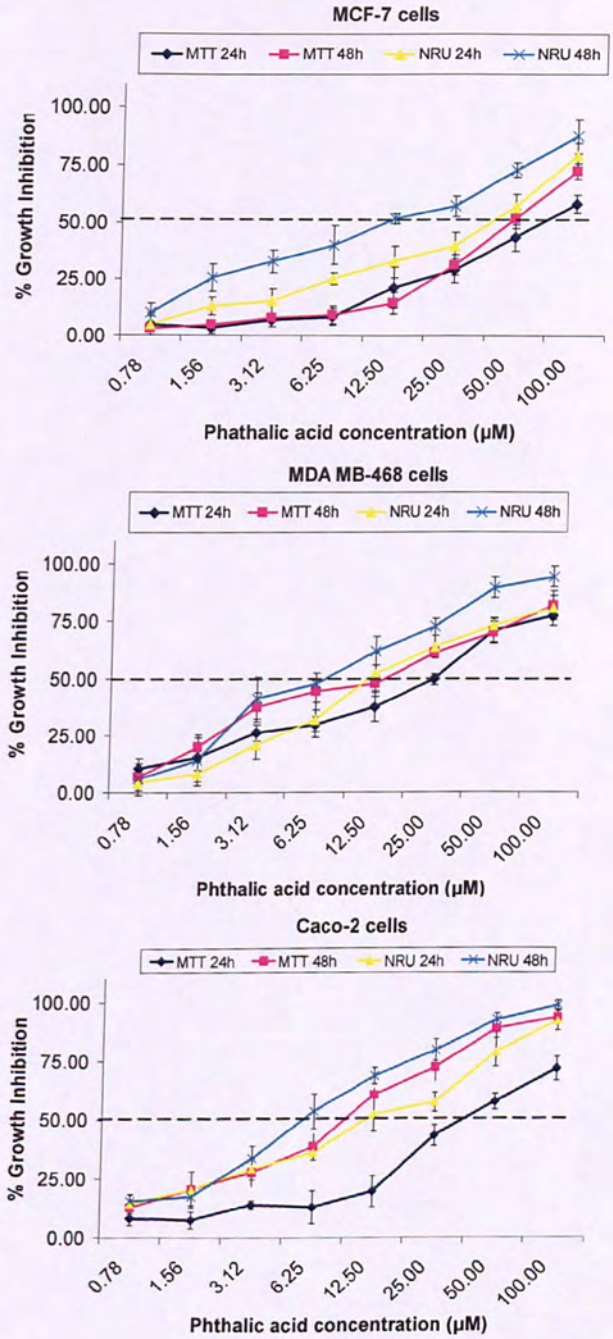

Figure 4.40: Percentage growth inhibition of the phthalic acid ester over concentration range from Solanum surattense against breast and colon cancer cell lines, showing apparent IC_{50} with MTT and neutral red uptake assays after 24 and 48 h treatments.

The second most effective response was observed in MDA MB-468 cells, where initial significant inhibition (26%) was enhanced to 50% at 12.5 μM after 24 h in MTT assay. MCF-7 cells were less responsive to the phthalic acid ester as about 60% inhibition was accomplished at a very high dose 100 μM. The positive control actinomycin-D (4 μM) showed a highly significant ($P<0.001$) inhibition in cell growth (60 – 80%) in all three cancer cell lines, (as mentioned in Table 4.19). tamoxifen (5 μM, oestrogen receptor antagonist) and anastrozole (5 μM, aromatase inhibitor) showed 70 – 80% cell death in MCF-7 and MDA MB-468, respectively.

In a prolonged treatment (48 h), the phthalic acid ester did show enhanced cytotoxicity and 50% inhibition was attained in MCF-7 at 12.5 μM and in MDA MB-468 and Caco-2 cells at concentration ~6.25 μM, in NRU assay.

Inhibition of cell growth, relative to vehicle-treated cells, was statistically significant (by one way ANOVA with Dunnett's multiple comparison test) for Compound **5** at 1.56 μM and higher for Caco-2 cells at 3.12 μM and higher in MDA MB-468 and MCF-7 after 48 h. Overall apparent IC_{50} values (Figure 4.40) estimated for the phthalic acid ester from MTT and NRU assays are as follows: MCF-7 cells ~50 μM, MDA MB-468 and Caco-2 cells ~12.5 μM.

4.7.1.6. Docosanoic acid methyl ester (*Arisaema utile*)

Compound **6** (5-Oxo-19-propyl-docosanoic acid methyl ester) was isolated from the chloroform fraction of *Arisaema utile*. The antiproliferative activity of Compound **6** was evaluated in concentrations ranging from 0.78 to 100 μM, in three cancer cell lines (MCF-7, MDA MB-468 and Caco-2) based on cell viability assays (MTT and neutral red uptake assays). The results of percentage growth inhibition after 24 h and 48 h are summarised in Table 4.20, and detailed calculations of absorbance for treated versus untreated cells (n=3, Mean ± STD) are enclosed in appendices (37–40).

Docosanoic acid Conc. (µM)	Percentage growth inhibition after 24 hr treatment						Percentage growth inhibition after 48 hr treatment					
	MTT assay			Neutral red uptake assay			MTT assay			Neutral red uptake assay		
	MCF-7 cells	MDA MB-468 cells	Caco-2 cells	MCF-7 cells	MDA MB-468 cells	Caco-2 cells	MCF-7 cells	MDA MB-468 cells	Caco-2 cells	MCF-7 cells	MDA MB-468 cells	Caco-2 cells
0.78	7.04 (±0.14)	10.40 (±4.33)	9.23 (±1.60)	10.10 (±6.09)	11.25 (±5.76)	19.64 (±6.36)	5.29 (±2.39)	6.35 (±3.70)	11.99 (±2.32)	15.16 (±3.87)	15.77 (±9.29)	9.84 (±7.45)
1.56	7.98 (±0.99)	14.31 (±7.29)	7.54 (±1.26)	14.85 (±11.66)	15.60 (±9.44)	19.14 (±0.93)	6.83 (±5.70)	19.08 (±4.96)	14.15 (±4.56)	22.03* (±4.64)	19.36 (±7.01)	16.07 (±9.60)
3.12	12.26 (±2.94)	26.26* (±2.95)	16.67 (±6.00)	20.14* (±5.97)	23.19* (±9.54)	30.40** (±7.59)	8.73 (±5.10)	36.13** (±6.51)	29.37* (±6.12)	21.45* (±4.64)	31.34** (±6.09)	27.24* (±9.66)
6.25	11.95 (±6.07)	30.21** (±3.31)	13.43 (±6.68)	23.65* (±7.85)	31.90** (±10.43)	34.48** (±4.13)	13.00 (±6.34)	43.70** (±7.72)	39.64** (±1.29)	31.27** (±5.83)	41.44** (±8.21)	26.71* (±7.57)
12.5	22.26* (±7.79)	38.00** (±5.71)	22.65* (±3.61)	27.25* (±6.94)	53.55*** (±6.71)	47.46** (±8.22)	18.33 (±3.16)	46.33** (±4.04)	59.52*** (±5.62)	45.28** (±6.19)	63.46*** (±6.72)	52.31*** (±7.76)
25	32.18** (±6.48)	49.62** (±2.82)	44.51** (±5.58)	31.26** (±8.04)	69.92*** (±5.53)	53.12*** (±13.32)	41.74** (±8.96)	59.39*** (±1.53)	71.65*** (±7.45)	49.77** (±6.51)	73.34*** (±6.48)	68.49*** (±6.72)
50	44.48** (±4.57)	71.26*** (±3.66)	58.23*** (±4.63)	57.69*** (±5.94)	80.37*** (±4.00)	82.02*** (±8.70)	67.89*** (±6.47)	69.14*** (±6.88)	91.07*** (±5.59)	75.58*** (±5.66)	85.85*** (±6.95)	84.79*** (±2.70)
100	63.04*** (±6.99)	77.20*** (±4.16)	69.01*** (±5.85)	80.39*** (±7.00)	90.91*** (±3.99)	92.89*** (±4.01)	80.14*** (±3.58)	82.39*** (±6.93)	93.68*** (±2.42)	94.70*** (±4.96)	92.64*** (±8.91)	95.89*** (±8.77)
Actinomycin-D (4µM)	65.29*** (±6.25)	64.01** (±4.84)	69.77*** (±0.80)	77.60*** (±7.67)	71.10*** (±4.64)	76.72*** (±1.33)	76.63*** (±4.27)	78.04*** (±4.84)	90.19*** (±6.83)	89.05*** (±4.52)	91.89*** (±5.87)	89.79*** (±6.10)
Tamoxifen (5µM)	84.74*** (±4.33)	27.80* (±4.06)	-------	78.19*** (±3.17)	38.36** (±6.26)	-------	99.64*** (±1.14)	45.41** (±4.14)	-------	100.24*** (±0.37)	63.05*** (±3.16)	-------
Anastrozole (5µM)	51.72*** (±3.42)	70.11*** (±1.47)	-------	46.28** (±5.64)	74.11*** (±4.18)	-------	46.39** (±6.43)	86.89*** (±7.04)	-------	36.22** (±4.21)	92.99*** (±6.23)	-------
Vehicle Control	1.09 (±5.34)	4.70 (±0.63)	3.27 (±4.68)	4.94 (±1.65)	3.29 (±0.63)	5.19 (±5.73)	3.28 (±3.44)	1.83 (±4.56)	0.21 (±5.71)	2.98 (±4.08)	1.84 (±7.12)	-0.15 (±6.60)

Table 4.20: Antiproliferative activity of the docosanoic acid methyl ester from Arisaema utile against three cancer cell lines using two cytotoxicity assays after 24 and 48 hours treatment. The results for anastrozole and tamoxifen were not repeated but are taken from table 4.15 for comparison Where statistically (Dunnett's multiple comparison test), = Significant (P<0.05), ** = Highly significant (P<0.01), *** = Very highly significant (P<0.001)*

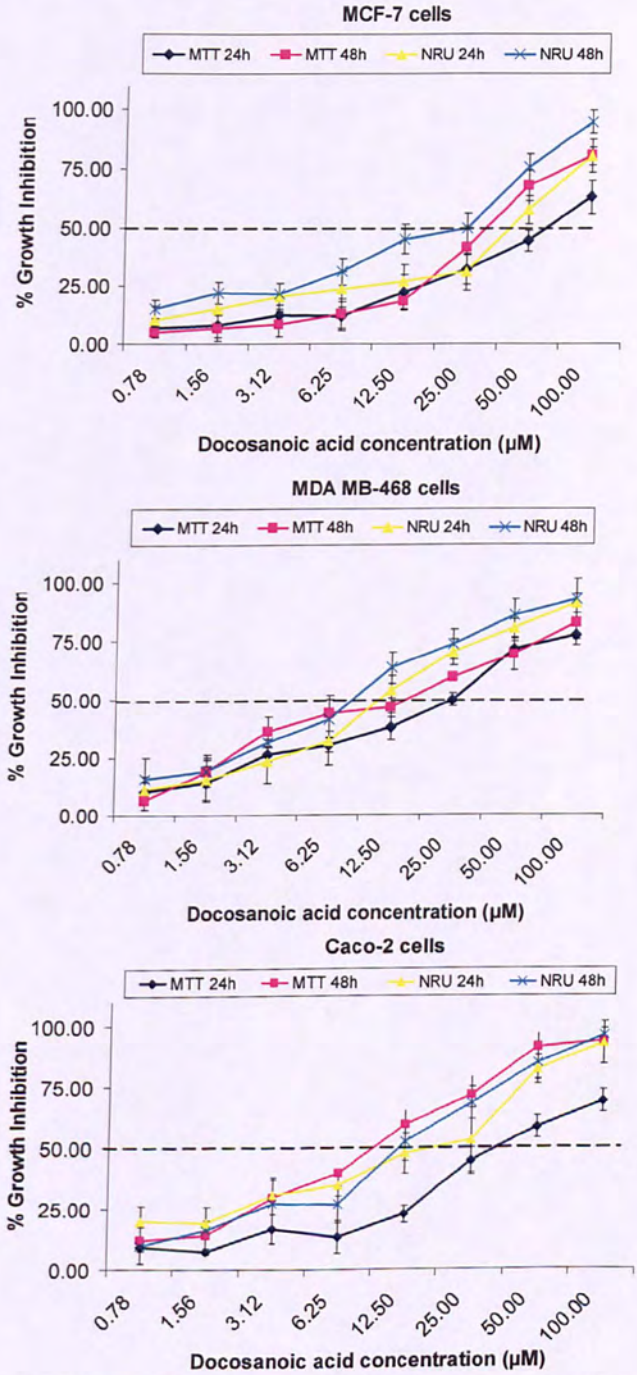

Figure 4.41: Percentage growth inhibition of the docosanoic acid methyl ester over concentration range from Arisaema utile against breast and colon cancer cell lines, showing apparent IC_{50} with MTT and neutral red uptake assays after 24 and 48 h treatments

In hormone independent breast cancer cells (MDA MB-468), the significant ($P<0.05$) growth inhibition (26%) was initiated at 3.12 μM in MTT assay, and half of the suppression in cell population was detected at 25 μM after 24 h. Similarly, the neutral red uptake assay showed a more pronounced effect in this cell line where inhibition reached 50% at 12.5 μM and maximum inhibition 91% was observed at 100 μM. In prolonged incubation time (48 h) after treatment inhibition, was increased to some extent, but a 50% reduction in cell viability was retained in 12.5–25 μM, in MTT and NRU assays.

MCF-7 and Caco-2 cells showed an almost identical response to Compound **6**, and a statistically significant ($P<0.05$) response was observed at 12.5 μM in MTT assay. Inhibitions were 27% and 47% respectively in NRU assays after 24 h. Maximum inhibition was observed at 100 μM, where only 10-20% cells could survive. The positive control Actinomycin-D (4 μM) could exhibit cell suppression in the range 64-77%, when assessed with either assay.

The results from 48 h studies demonstrated that cell growth was reduced to some extent, which is evident from a shift to 50% inhibition at lower concentrations in MCF-7 (decreased to 25 μM) and in Caco-2 (down to 12.5 μM) (Table 4.20).

The apparent IC_{50} values for docosanoic acid methyl ester (Compound **6**) were estimated (Figure 4.41) from MTT and NRU assays, after 24 h and 48 h: MCF-7 cells (25–50 μM), whereas for Caco-2 and MDA MB-468 cells (12.5–25 μM). Inhibition of cell growth, relative to vehicle-treated cells, was statistically significant (by one way ANOVA with Dunnett's multiple comparison test) at 3.12 μM and higher concentrations for docosanoic acid methyl ester in MDA MB-468 and Caco-2 cells and at 12.5 μM and higher in MCF-7 cells.

4.7.2. Cytomorphological alterations (DAPI staining)

A series of experiments were performed to study the changes in the morphology of the cancer cells (MCF-7, MDA MB-468, Caco-2). In order to determine the mode of action in cell death of isolated compounds (1-6), cells were treated for 12 h with concentrations of individual compound (**1-6**) derived from apparent IC_{50} results (from MTT and NRU assays; section 4.7.1.), specific for particular cell line. Fluorescent images were obtained with a Leica confocal fluorescence microscope with excitation at 350 nm and emission at 460 nm under a 40 x oil objective.

Historically, cell death has been distinguished in mammalian cells by morphological criteria. Apoptosis is defined by characteristic changes in the nuclear morphology, including chromatin condensation (pyknosis) and fragmentation (karyorrhexis); minor changes in cytoplasmic organelles; and overall cell shrinkage, blebbing of the plasma membrane and formation of apoptotic bodies that contain nuclear or cytoplasmic material. All of these changes occur before plasma membrane integrity is lost (Edinger *et al.*, 2004).

The alternative to apoptotic cell death is necrosis. A classical, positive definition of necrosis based on morphological criteria is early plasma membrane rupture and dilatation of cytoplasmic organelles in particular mitochondria, where the cell is a passive victim. This follows an energy-independent mode of death (Festjens *et al.*, 2006).

Cell death is an irreversible loss of plasma membrane integrity (Kroemer *et al.*, 2005). In the present study, during observations, these two main phenomena of cell death were both identified in all three cancer cell lines (MCF-7, MDA MB-468 and Caco-2).

MCF-7 Cells

Cytomorphological alterations in MCF-7 cells induced by isolated compounds were observed at a particular dose according to IC_{50} concentration. Cells were treated for 12 h with the pregnane glycoside (20 μM) and the androstane glycoside (10 μM) from *Caralluma tuberculata*; the pregnane glycoside (50 μM) from *Fagonia indica*; hexadecanoic acid ethyl ester (50 μM) and phthalic acid ester (50 μM) from *Solanum surattense*; docosanoic acid methyl ester (50 μM) from *Arisaema utile* and DMSO (0.01%) as vehicle control.

The confocal fluorescence microscopy images (Figure 4.42) showed that all three steroidal glycosides resulted in shrinkage of cells, a reduction in cell number and evidence of nuclear fragmentation, all characteristics of apoptosis, when compared to untreated cells or cells treated with vehicle (0.01% DMSO). Similarly phthalic acid ester also retained the signs of apoptosis as observed with steroidal glycosides, as mentioned previously.

The two fatty acid esters (hexadecanoic and docosanoic) did not exhibit much cytotoxic potential, as no signs of cell shrinkage, or apparent reduction in cell number or nuclear fragmentation were visible. These results were some how in correlation with cell viability (MTT and NRU assays) studies, where 50% cell inhibition was observed at a very high concentration (50-100 μM) after a 24 h treatment, as compared to 12 h exposure time in cytomorphological assay with an objective to detect early signs of apoptosis or necrosis in MCF-7 cells.

The three positive controls used: actinomycin-D (4 μM), tamoxifen (5 μM) and anastrozole (5 μM) also showed clear features of apoptosis, as expected for a reported potential apoptosis-inducer in different cancer cell particularly MCF-7 (Bock *et al.*, 2002; Cheryl *et al.*, 1998; Kijima *et al.*, 2005).

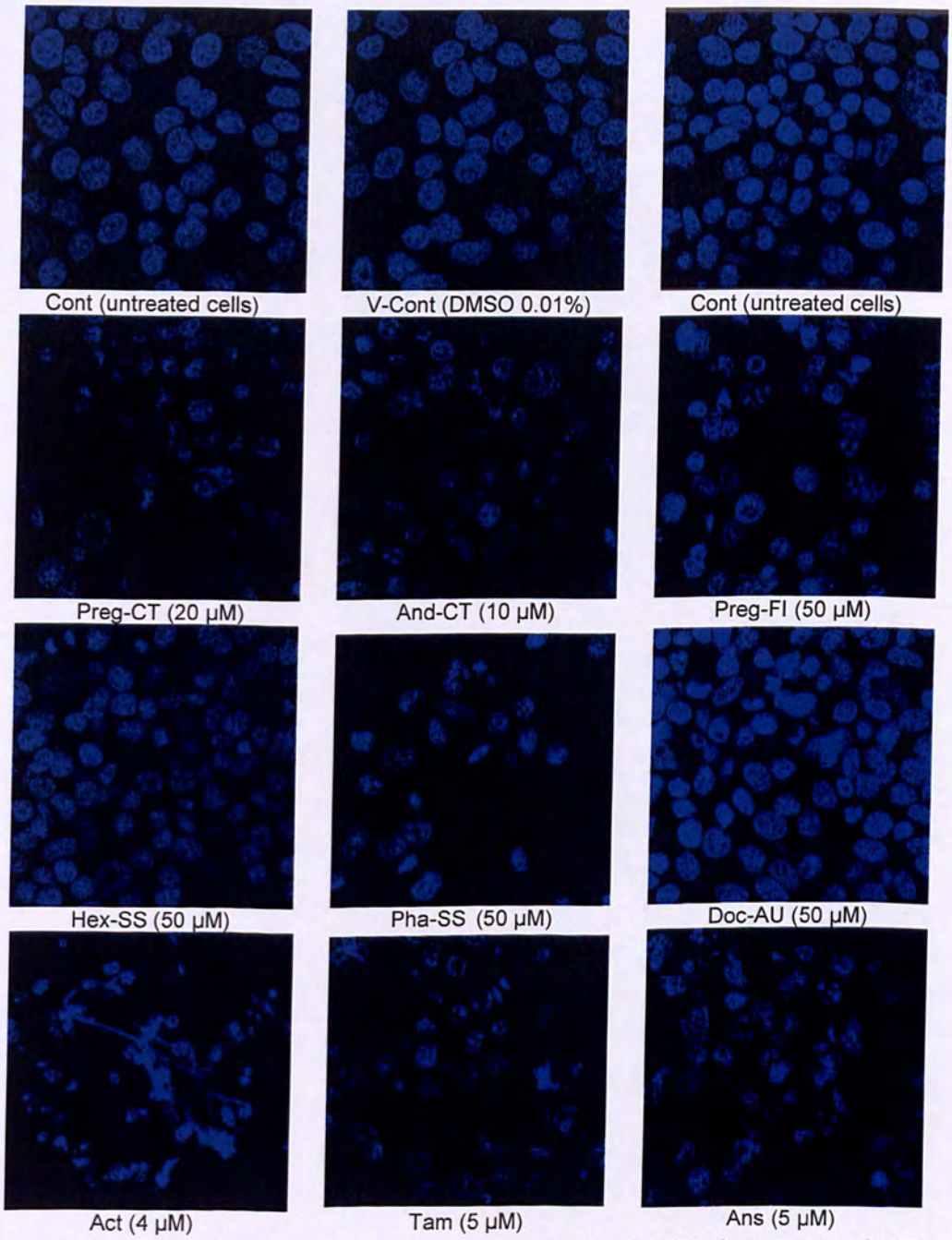

*Figure 4.42: Confocal fluorescence microscopy of nuclei stained with DAPI after treatment of MCF-7 Cells for 24 hours with vehicle (0.01% DMSO) and isolated compounds (**1-6**) at the IC_{50} concentration with positive controls, where Cont: MCF-7 untreated cells, V-Cont: Vehicle control, Preg-CT: Pregnane glycoside (CT), And-CT: Androstane glycoside (CT), Preg-FI: Pregnane glycoside (FI), Hex-SS: Hexadecanoic acid ethyl ester (SS), Pha-SS: Phathalic cid ester (SS), Doc-AU: Docosanoic acid methyl ester (AU), Act: Actinomycin-D, Tam: Tamoxifen, Ans: Anastrozole.*

MDA MB-468 cells

According to IC_{50} values derived from cell cytotoxicity studies using MTT and NRU assays; MDA MB-468 cells received 50 µM each of pregnane and androstane glycosides from *Caralluma tuberculata*, 12.5 µM of pregnane glycosides from *Fagonia indica*, hexadecanoic acid ethyl ester (50 µM) phthalic acid ester and docosanoic acid methyl ester (12.5 µM each). The vehicle control DMSO (0.01%) was also tested along with three positive controls (Figure 4.43).

Results showed that the oestrogen negative cell line (MDA MB-468) exhibited a different response of cell death as was observed in MCF-7 cells. MDA-MB-468 cells, however, appeared fewer in number, after 12 h treatment with the steroidal glycosides, but those remaining cells appeared a little larger than untreated or vehicle-treated cells, suggesting swelling characteristic of necrosis (Figure 4.43). It has been reported that after signalling- or damage-induced lesions, necrosis can include signs of controlled processes such as mitochondrial dysfunction, enhanced generation of reactive oxygen species, ATP depletion, proteolysis by calpains and cathepsins, and early plasma membrane rupture. In addition, the inhibition of specific proteins involved in regulating apoptosis or autophagy can change the type of cell death to necrosis (Golstein and Kroemer 2006).

MDA MB-468 cells treated with esters (hexadecanoic, phthalic acid, and docosanoic) showed a reduction in cell number, shrinkage and more tightly packed nuclei in size as compared to the cell received steroidal glycosides, untreated cells and the cells received vehicle (DMSO 0.01%). It was interesting to note that the MCF-7 cells as described previously, showed no or very little response to hexadecanoic and docosanoic esters, but for MDA MB-468 the cell response was quite significant. On the basis of this current investigation, it may be suggested that hexadecanoic and docosanoic esters are active against hormone independent breast cancer cells as compared to oestrogen dependent

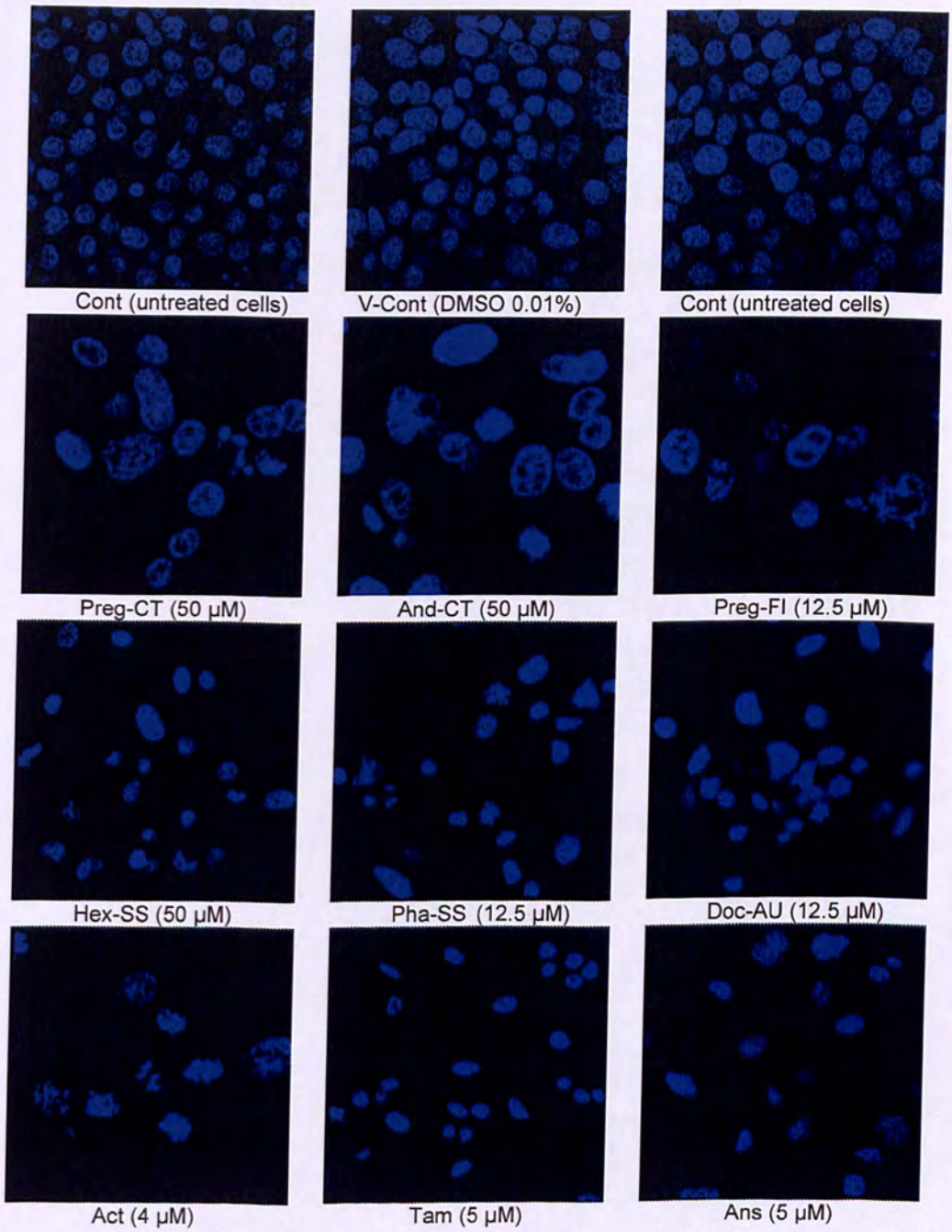

*Figure 4.43: Confocal fluorescence microscopy of nuclei stained with DAPI after treatment of MDA MB-468 Cells for 24 hours with vehicle (0.01% DMSO) and isolated compounds (**1-6**) at the IC_{50} concentration with positive controls, where Cont: MDA MB-468 untreated cells, V-Cont: Vehicle control, Preg-CT: Pregnane glycoside (CT), And-CT: Androstane glycoside (CT), Preg-FI: Pregnane glycoside (FI), Hex-SS: Hexadecanoic acid ethyl ester (SS), Pha-SS: Phathalic cid ester (SS), Doc-AU: Docosanoic acid methyl ester (AU), Act: Actinomycin-D, Tam: Tamoxifen, Ans: Anastrozole.*

breast cancer cells, which is further supported with the evidence from cell cytotoxicity investigation (MTT and NRU assays).

Positive controls actinomycin-D and anastrozole also represented apoptosis characteristics in cell death, while the response from tamoxifen, (as was expected) against oestrogen negative cell line was less significant, with little reduction in cell numbers, but cell shrinkage features were prominent.

Caco-2 cells

IC_{50} concentrations of isolated compounds (**1-6**) used for Caco-2 cells are as follows: 6.25 μM of pregnane and androstane glycosides from *Caralluma tuberculata*; 12.5 μM of pregnane glycoside from *Fagonia indica*; 50 μM of hexadecanoic acid ethyl ester, 12.5 μM each of phthalic acid ester and docosanoic acid methyl ester. Positive control actinomycin-D (4 μM) was also used, whereas the vehicle control was run at 0.01% DMSO.

The confocal fluorescence microscopy results (Figure 4.44) for the colorectal cancer cell line manifest that the mode of cell death is more likely apoptosis (apart from hexadecanoic acid and docosanoic acid esters), indicated by nuclear fragmentation, reduction in cells as compared to untreated and vehicle treated cells. However, in hexadecanoic acid and docosanoic acid esters a mixed response was observed, with cell swellings and fragmented nuclear material. Apart from hexadecanoic acid ethyl ester (50 μM), the other five compounds induced an apoptotic response at quite reasonable concentrations (6–12.5 μM) in 12 h treatment. This effect also corresponded to the results from the cell cytotoxicity activity experiments, where all the compounds were responsive to Caco-2 cells. The apoptotic inducers: actinomycin-D also showed cytotoxic effect (pronounced apoptotic mode) characterised by blebbing and nucleus degradation.

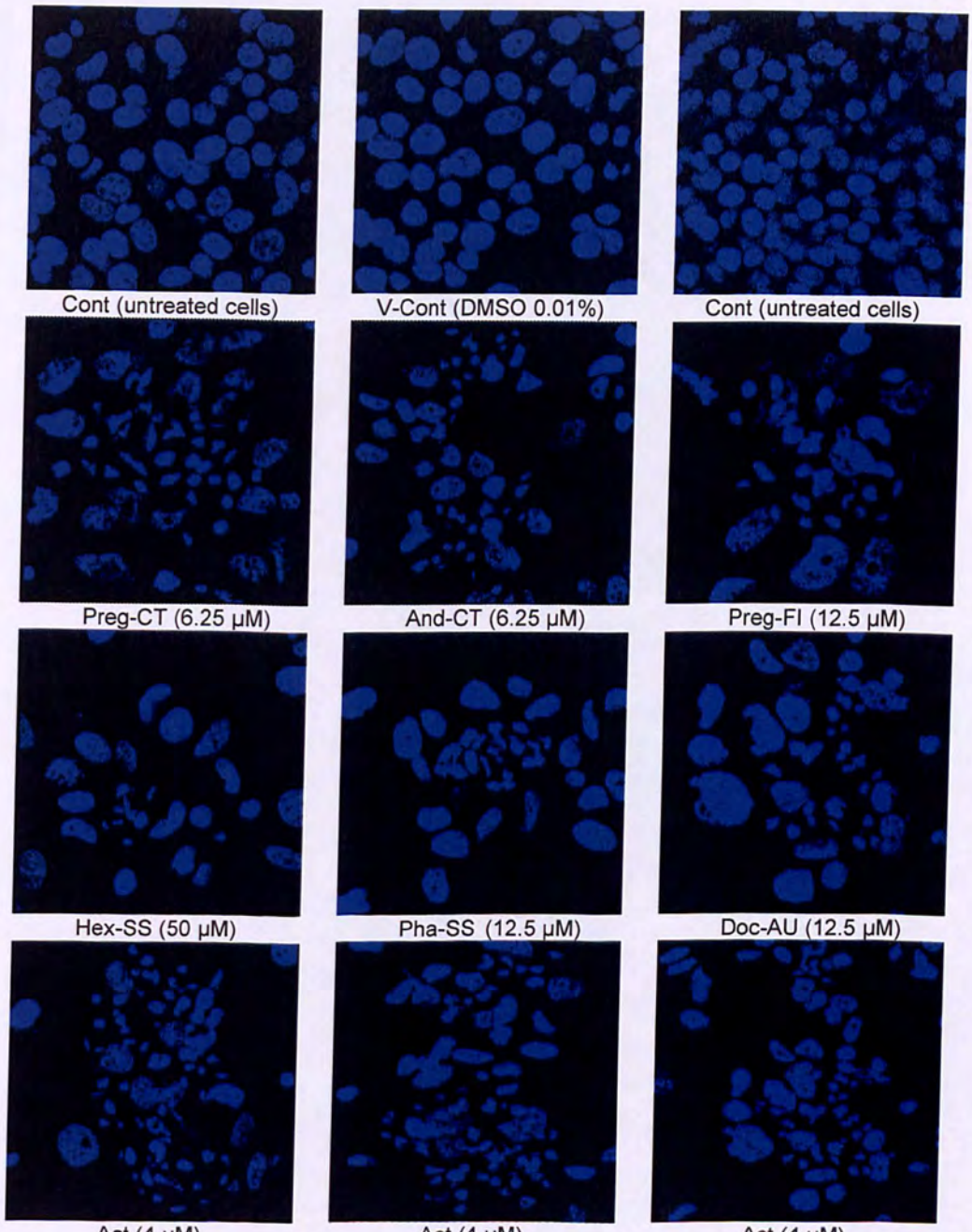

*Figure 4.44: Confocal fluorescence microscopy of nuclei stained with DAPI after treatment of Caco-2 Cells for 24 hours with vehicle (0.01% DMSO) and isolated compounds (**1-6**) at the IC_{50} concentration with positive controls, where Cont: Caco-2 untreated cells, V-Cont: Vehicle control, Preg-CT: Pregnane glycoside (CT), And-CT: Androstane glycoside (CT), Preg-FI: Pregnane glycoside (FI), Hex-SS: Hexadecanoic acid ethyl ester (SS), Pha-SS: Phathalic cid ester (SS), Doc-AU: Docosanoic acid methyl ester (AU), Act: Actinomycin-D.*

4.7.3. Inhibition of apoptosis (Caspase inhibitor Z-VAD-FMK)

Interleukin-1β converting enzyme (ICE)-like proteases, which are synthesised as inactive precursors, play a key role in the induction of apoptosis. Caspases exhibit catalytic and substrate-recognition motifs that have been highly conserved. The characteristic amino acid sequences allow caspases to interact with both positive and negative regulators of their activity (Cryns *et al.,* 1998). Benzyloxycarbonyl- Val-Ala-Asp (OMe) fluoro-methyl ketone (Z-VAD FMK), an ICE-like protease inhibitor, inhibits apoptosis (Zhu *et al.,* 1995).

As previously described, Compounds **1-6** isolated from the four medicinal plants showed highly significant cytotoxic activity in MTT and NRU assays followed by characteristics of apoptosis and necrosis type of cell death, observed in confocal fluorescence microscopy for cell morphology. The next objective was to distinguish between apoptosis and necrosis mode of cell death and to assess the possible involvement of caspases. After 24 h incubation of cell seeding in a 96 well plate, the cancer cells (MCF-7, MDA MB-468 and Caco-2) were pre-treated for one hour with Z-VAD-FMK (50 μM) before receiving the testing dose of isolated compounds (**1-6**). The concentration used for each compound was calculated according to its IC_{50}, each value corresponds to a specific cell line.

MCF-7 Cells

The concentrations of Compounds **1-6** used for MCF-7 are as follows: pregnane (20 μM) and androstane (10 μM) glycosides from *Caralluma tuberculata*; pregnane glycoside (50 μM) from *Fagonia indica*; hexadecanoic ester, phathalic acid and docosanic acid ester 50 μM each from *Solanum surattense* and *Arisaema utile*. The positive control (actinomycin-D) was investigated at 4 μM concentration.

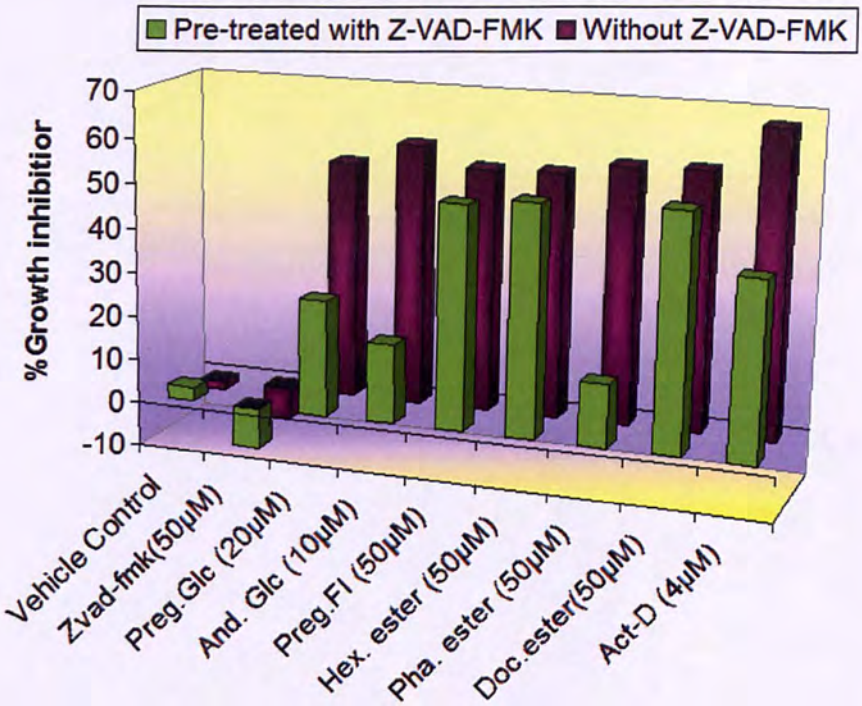

*Figure 4.45: Effect of caspase inhibitor Z-VAD-FMK on percentage growth inhibition of Compounds **1-6** in pre-treated MCF-7 cells as compared to caspase-inhibitor untreated cells which suggested the mode of cell death, either apoptosis or necrosis.*

The results (n=3, Figure 4.45) from the NRU assay revealed that the percentage of growth inhibitions was significantly reduced in MCF-7 cells (pre-treated with caspase inhibitor Z-VAD-FMK) from pregnane (CT; 53 to 26%) and androstane (58 to 17%) glycosides and phthalic acid ester (57 to 14%) as compared to the data calculated in the absence of Z-VAD-FMK. These findings suggest most probably that the mode of cell death is apoptosis, as Z-VAD-FMK has blocked the apoptotic signals to commit the cells to suicide.

However, pregnane (FI) glycoside and both esters (hexadecanoic and docosanoic) were consistent in their cytotoxicity effect, as was observed in the caspase inhibitor treated cells suggesting the mode of cell death was necrosis. Positive control (actinomycin-D) for apoptosis also showed less growth inhibition

(from 67% to 40%) in cells treated with the caspase inhibitor. Vehicle control (DMSO 0.01%) had no effect on cell growth, but Z-VAD-FMK (50 μM) had a slight stimulatory effect, perhaps as a consequence of inhibiting a sub-population of untreated cells in apoptosis. All treatments, including those with Z-VAD-FMK, were statistically significant to vehicle-treated controls (one way ANOVA with Dunnett's post-test).

MDA MB-468 Cells

For MDA MB-468 cells, 50 μM concentrations each of pregnane (CT) and androstane glycosides and hexadecanoic acid ester along with 12.5 μM concentrations each of pregnane (FI) glycoside, phthalic acid and docosanoic acid esters were used as testing doses according to their IC_{50} values.

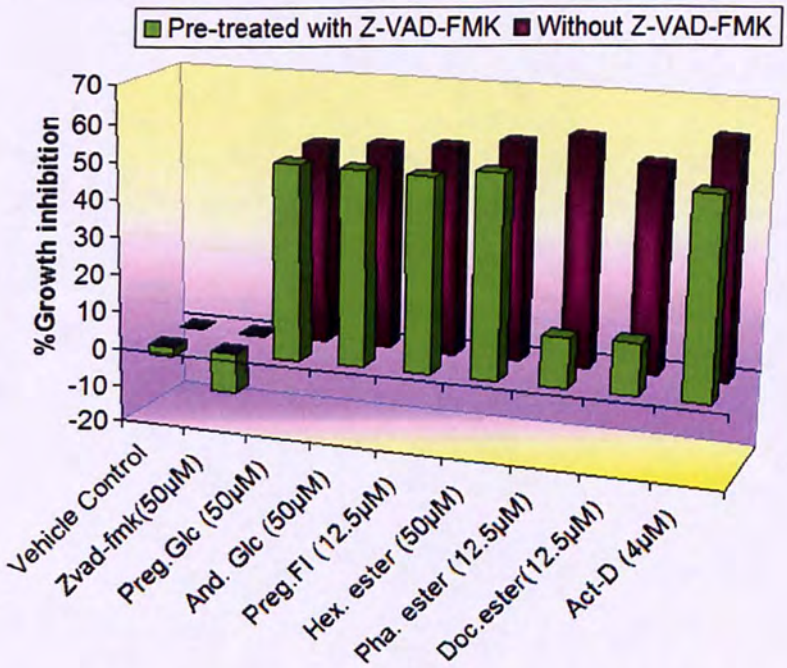

*Figure 4.46: Effect of caspase inhibitor Z-VAD-FMK on percentage growth inhibition of Compounds **1-6** in pre-treated MDA MB-468 cells as compared to caspase-inhibitor untreated cells which suggested the mode of cell death as either apoptosis or necrosis.*

Results were calculated using the NRU assay as percent growth inhibition (Figure 4.46) and a comparison was established between the caspase inhibitor treated and untreated MDA MB-468 cells.

Data showed Z-VAD-FMK could not block the apoptotic response to cell death apart from phthalic acid and docosanoic esters where percentage of growth inhibition was reduced from 59 to 13% and 54 to 13% respectively.

This preventive effect from cell death suggested that proteases enzymes responsible for induction of apoptosis were deprived of their proteolytic action. However, in response to the steroidal glycosides and hexadecanoic acid ester, MDA MB-468 cells pre-treated with Z-VAD-FMK, showed almost same percentage of inhibition as in cells did not receive caspase inhibitor (Z-VAD-FMK) treatment. This effect is in support with the cytomorphological observations (nuclei stained with DAPI), where, the necrosis characteristics of cell death were quite prominent in confocal fluorescence microscopy.

Caco-2 Cells

In Caco-2 cells (Figure 4.47), investigation in response to pre-treatment with caspase inhibitor revealed, that three steroidal glycosides (pregnane (CT) 6.25 μM, androstane 6.25 μM, pregnane (FI) 12.5 μM) caused cytotoxicity through induced apoptosis. This mode of cell death is exhibited as low percentage growth inhibition, which indicated that apoptotic signals were hindered due to the caspase inhibitor (Z-VAD-FMK). However, the esters (hexadecanoic acid and docosanoic acid) demonstrated cytotoxicity for Caco-2 cells at 50 and 12.5 μM respectively; that effect was almost insensitive to Z-VAD-FMK pre-treatment, suggested the necrotic characteristics of cell death. This response is also in line with the morphological features observed in DAPI nuclei staining, where mixed characteristics of apoptosis and necrosis were noted.

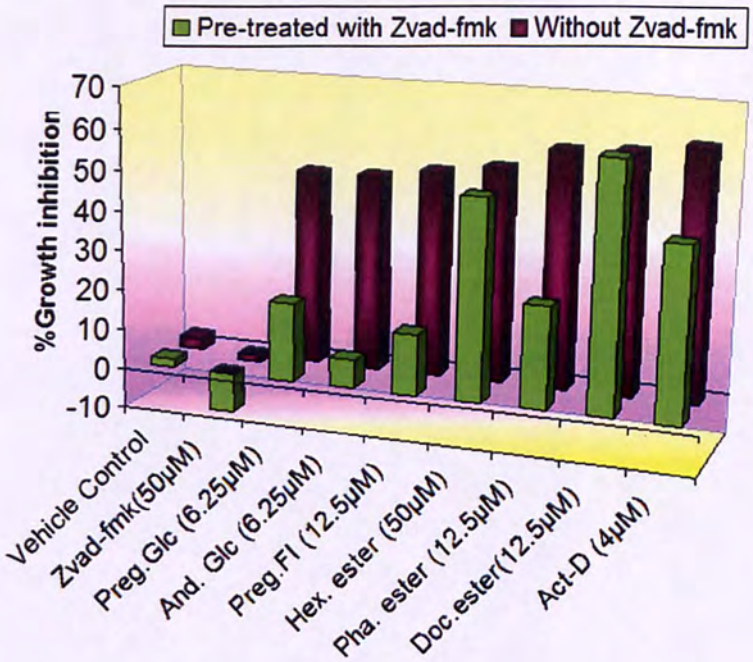

*Figure 4.47: Effect of caspase inhibitor Z-VAD-FMK on percentage growth inhibition of Compounds **1-6** in pre-treated Caco-2 cells as compared to caspase-inhibitor untreated cells which suggested the mode of cell death as either apoptosis or necrosis.*

4.7.4. Poly (ADP-ribose) polymerase (PARP) cleavage (Western blot)

Apoptosis is characterised by a series of distinctive morphological and biochemical changes. Proteolysis of poly (ADP-ribose) polymerase (PARP), an enzyme involved in DNA repair and maintenance of the genome, has been proposed as an early biochemical marker of apoptosis (Kaufmann *et al.,* 1993). This protein can be cleaved by many ICE-like caspases *in vitro* and is one of the main cleavage targets of caspase-3 (Tewari *et al.,* 1995).

In human PARP, the cleavage occurs between Asp214 and Gly215, which separates the PARP amino-terminal DNA binding domain (24 kDa) from the carboxy-terminal catalytic domain (89 kDa) of the enzyme, resulting in the loss of

normal PARP function (Lamarre *et al.*, 1988). It has been proposed that inactivation of PARP directs DNA-damaged cells to undergo apoptosis rather than necrotic degradation, and the presence of the 89 kDa PARP cleavage fraction is considered to be a marker of apoptosis (Kaufmann *et al.*, 1993).

In the present study, the mode of cell death for each isolated compound (**1-6**) was investigated at individual IC_{50} concentrations corresponding to specific cell lines for 24 h on a 10.5% denaturing SDS-polyacrylamide gel using Western blots. The expression of intact-PARP (116 kDa), cleaved-PARP (89 kDa) and β-actin (47 kDa) proteins were detected using specific antibodies (as described in Materials and Methods section: 3.6.3.). The adequate amount (10 µl/well) of the total protein was verified by the intensity of β-actin protein used as an internal loading control. Actinomycin-D (4 µM), Tamoxifen (5 µM) and Anastrozole (5 µM) were used as positive controls and 0.01% DMSO was also tested as a vehicle control for each cell line.

The involvement of caspases in inducing apoptosis by isolated compounds was also detected through Western blots in cancer cells, pre-treated (1 h) with the caspase inhibitor (Z-VAD-FMK, 50 µM).

MCF-7 Cells

In Western blots for MCF-7 cells (Figure 4.48), bands at 116 kDa were observed for untreated cells (Control), vehicle control and cells that received pregnane glycoside (50 µM) from *Fagonia indica,* indicating that the PARP enzyme was intact; thus no signs of apoptosis were detected.

Apart from pregnane (FI) glycoside, the rest of the five isolated compounds: pregnane (20 µM CT) and androstane (10 µM) glycosides, hexadecanoic acid (50 µM), phthalic acid (50 µM) and docosanoic acid (50 µM) esters along with the

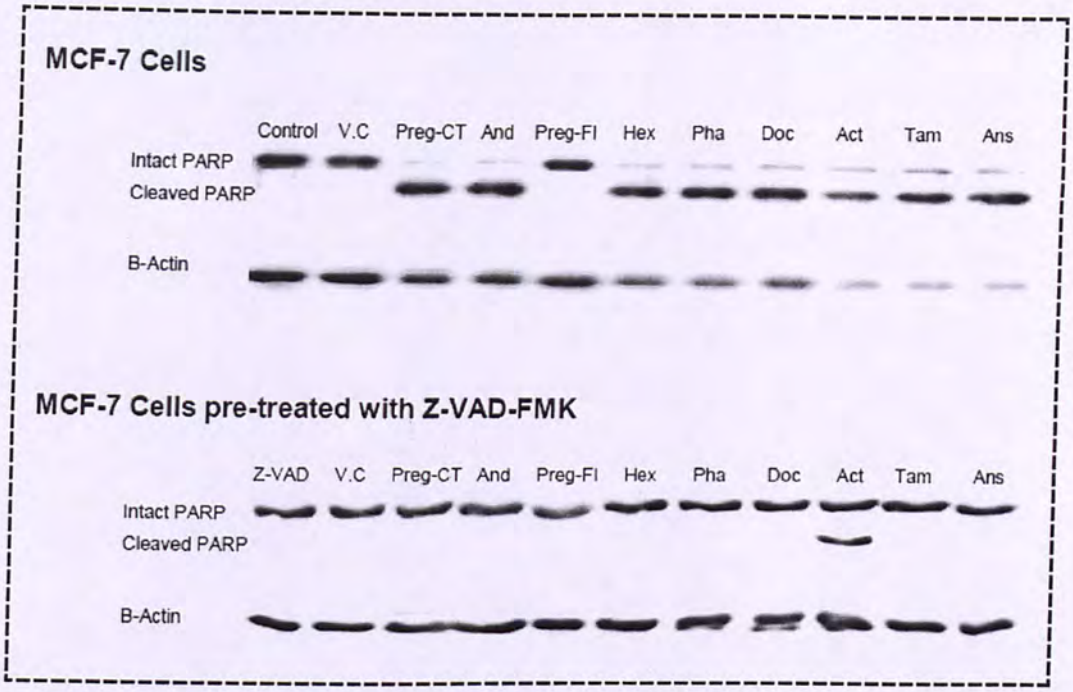

Figure 4.48: Detection of PARP (intact and cleaved) enzyme and β-actin, through Western blotting in lysates of MCF-7 cells treated for 24 hours with Vehicle DMSO 0.01% (V.C.) Pregnane (Preg-CT) and Androstane (And) glycosides from Caralluma tuberculata, Pregnane (Preg-FI)glycoside from Fagonia indica, Hexadecanoic acid ester (Hex), Phthalic acid ester (Pha), Docosanoic acid ester (Doc), Actinomycin- D (Act), Tamoxifen (Tam), Anastrozole (Ans); where (Control) represents untreated MCF-7 cells and (Z-VAD) represents Caspase inhibitor (Z-VAD-FMK) treated only, and combinations thereof . The expression of intact and cleaved PARP, and β-actin was detected at 116 kDa, 89 kDa, and 47 kDa respectively on 10.5% denaturing SDS-polyacrylamide gel using western blot; where β-actin protein was used as the internal control.

three positive controls actinomycin-D (4 μM), tamoxifen (5 μM) and anastrozole (5 μM), each showed an intense band at 89 kDa, pointing to cleaved-PARP. The results suggest apoptosis is the more likely mode of cell death, as exhibited by these anti-cancer compounds. This apoptotic effect was further supported with the second study, where the apoptotic signals were hindered in cancer cells, pre-treated (1 h) with caspase inhibitor (Z-VAD-FMK, 50 μM). Both groups of compounds (steroidal glycosides and fatty acid ester) suppressed the PARP enzyme cleavage, as intense bands at 116 kDa were detected on developed X-ray film (Figure 4.48), corresponding to molecular markers for PARP detection.

The caspase inhibitor also ceased this cleavage in positive controls, although actinomycin-D was more resistant to its effects.

MDA MB-468 Cells

In oestrogen negative cell lines (Figure 4.49), all of the six compounds [pregnane-CT (50 μM), androstane (50 μM), pregnane-FI (12.5 μM), hexadecanoic acid ester (50 μM), phthalic acid ester (12.5 μM), docosanoic acid ester (12.5 μM)], including positive controls actinomycin-D (4 μM), anastrozole (5

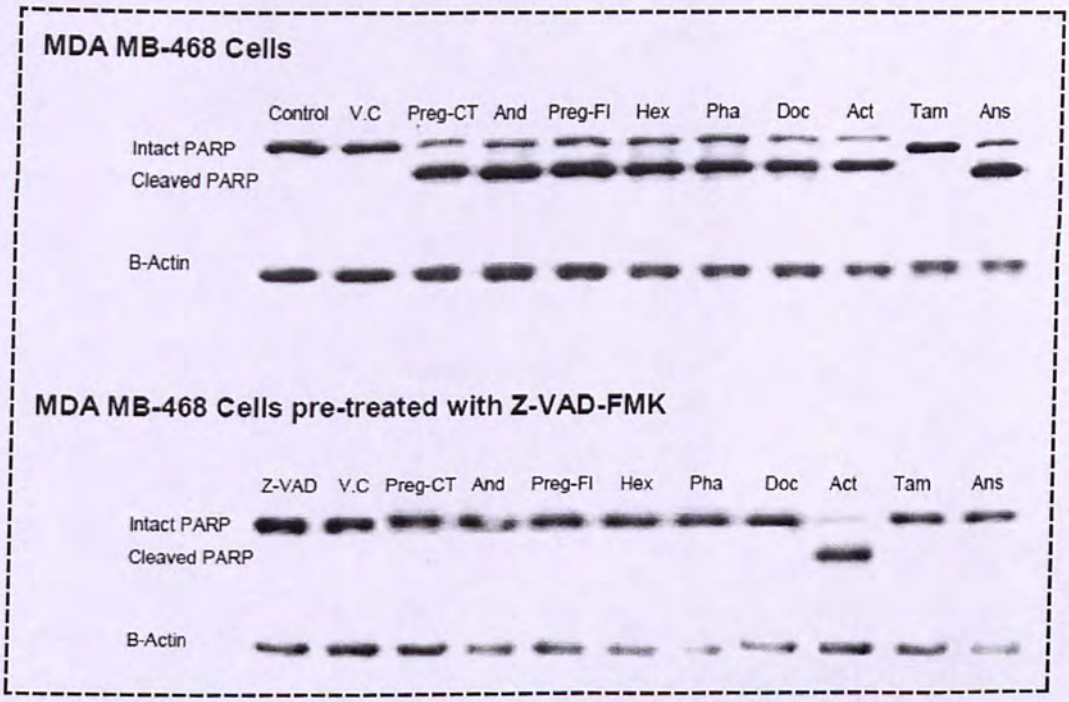

Figure 4.49: Detection of PARP (intact and cleaved) enzyme and β-actin, through Western blotting in lysates of MDA MB-468 cells treated for 24 hours with Vehicle DMSO 0.01% (V.C.) Pregnane (Preg-CT) and Androstane (And) glycosides from Caralluma tuberculata, Pregnane (Preg-FI)glycoside from Fagonia indica, Hexadecanoic acid ester (Hex), Phthalic acid ester (Pha), Docosanoic acid ester (Doc), Actinomycin- D (Act), Tamoxifen (Tam), Anastrozole (Ans); where (Control) represents untreated MDA MB-468 cells and (Z-VAD) represents Caspase inhibitor (Z-VAD-FMK) treated only, and combinations thereof .The β-actin protein was used as the loading control. The expression of intact and cleaved PARP, and β-actin was detected at 116 kDa, 89 kDa, and 47 kDa respectively.

μM) showed a cleaved band at 89 kDa, apart from the oestrogen receptor antagonist (tamoxifen 5 μM), where the PARP enzyme was intact (116 kDa), along with PARP in untreated (control) and vehicle control. Similarly, in pre-treatment with Z-VAD-FMK, the apoptotic signals were completely blocked in all compounds apart from the protein synthesis inhibitor (actinomycin-D). These results focus the characteristics of cell death towards apoptosis, which differ slightly from the observation in confocal fluorescence microscopy that showed the swelling features of necrosis. Although the mechanisms and morphologies of apoptosis and necrosis differ, there is overlap between these two processes. Evidence indicates that necrosis and apoptosis represent morphologic expressions of a shared biochemical network described as the "apoptosis-necrosis continuum" (Zeiss, 2003).

For example, two factors that will convert an ongoing apoptotic process into a necrotic process include a decrease in the availability of caspases and intracellular ATP (Leist *et al.*, 1997; Denecker *et al.*, 2001). Whether a cell dies by necrosis or apoptosis depends in part on the nature of the cell death signal, the cell type, the developmental stage of the cell and the physiologic milieu (Zeiss, 2003).

Caco-2 Cells

Colorectal carcinoma cells (Figure 4.50), treated for 24 h with isolated compounds (pregnane-CT (6.25 μM), androstane (6.25 μM), pregnane-FI (12.5 μM), hexadecanoic acid ester (50 μM), phthalic acid ester (12.5 μM), docosanoic acid ester (12.5 μM)], including positive controls actinomycin-D (4 μM), showed hallmarks of apoptosis, as evident from a cleaved PARP at 89 kDa, as compared to untreated and vehicle control cells (PARP intact 116 kDa). However, in pre-treated (caspase inhibitor Z-VAD-FMK at 50 μM) cancer cells, this action could not be accomplished.

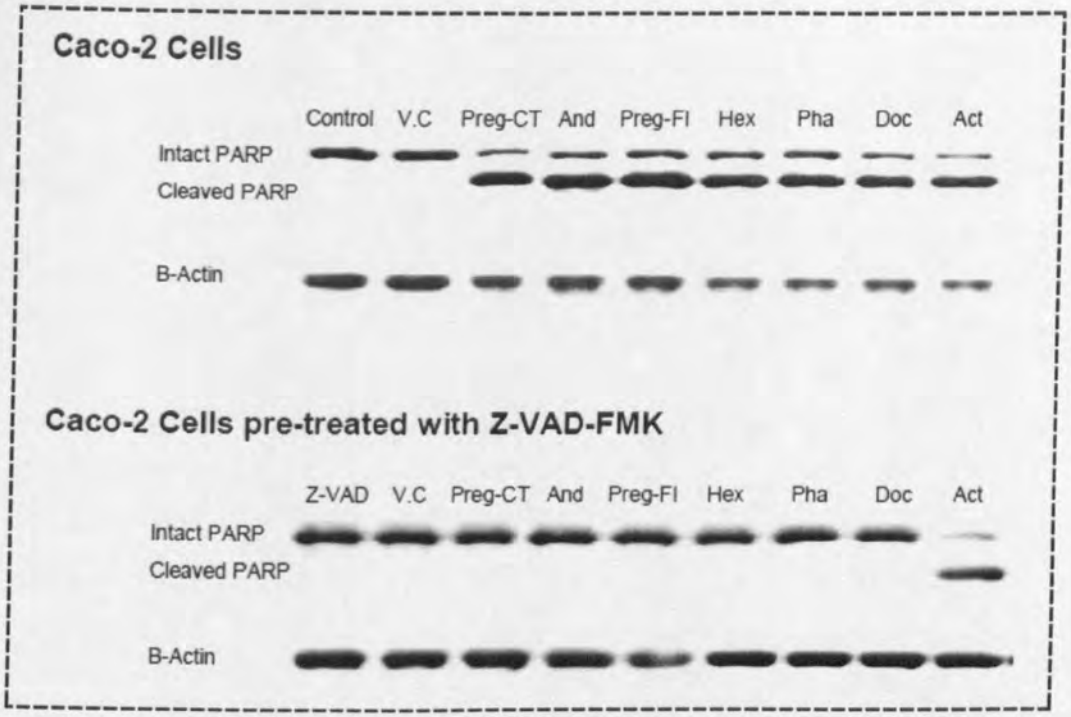

Figure 4.50: Detection of PARP (intact and cleaved) enzyme and β-actin, through Western blotting in lysates of Caco-2 cells treated for 24 hours with Vehicle DMSO 0.01% (V.C.) Pregnane (Preg-CT) and Androstane (And) glycosides from Caralluma tuberculata, Pregnane (Preg-Fl)glycoside from Fagonia indica, Hexadecanoic acid ester (Hex), Phthalic acid ester (Pha), Docosanoic acid ester (Doc), Actinomycin- D (Act); where (Control) represents untreated Caco-2 cells and (Z-VAD) represents Caspase inhibitor (Z-VAD-FMK) treated only, and combinations thereof. The expression of intact and cleaved PARP, and β-actin was detected at 116 kDa, 89 kDa, and 47 kDa respectively. The equal amount of the total protein (10 μl/well) was checked through β-actin protein as an internal loading control.

Moreover, these results are in agreement with the cytomorphological and biochemical studies on this cell line, as described previously in sections 4.7.2. and 4.7.3. that suggested the apoptotic pathway of cell death.

Normal Human cells

The antiproliferative activity of isolated anticancer compounds (**1-6**) was further investigated for cytotoxicity against normal cell lines: HUVEC and U937 cells using Western blot at their individual IC_{50} concentrations. The objective was

whether these compounds are showing selective growth inhibition in tumour cell lines, (as described earlier), or killing normal body cells as well.

HUVEC Cells

The results from the Western blot showed (Figure 4.51) at 12.5 μM concentration that each of steroidal glycosides (pregnane and androstane) from *Caralluma tuberculata* and *Fagonia indica* and at 50 μM concentrations each of hexadecanoic acid, phthalic acid, and docosanoic acid esters from *Solanum surattense* and *Arisaema utile* exhibited no sign of PARP enzyme cleavage, as intense bands were detected at 116 kDa, corresponding to molecular markers for PARP detection. The positive controls actinomycin-D (4 μM), tamoxifen (5 μM), anastrozole (5 μM) showed cleaved PARP at 89 kDa, indicated apoptosis induction in normal human cells.

U937 Cells

Human lymphatic monocytes (U937 cells), were utilised to evaluate the selective cytotoxicity of anticancer compounds (**1-6**) (at concentrations as mentioned above for HUVECs) for 24 h incubation using Western blotting technique. Results (Figure 4.51) indicated feeble, weak bands between 116–90 kDa representing a mixed response of intact and cleaved PARP. The β-actin protein (represented as internal protein loading control) detected at 47 kDa. As the nature of cell death signal depends on the cell type, the developmental stage of the cell and the physiological and biochemical (concentration) surroundings (Zeiss, 2003), it can be suggested that the death process may be concentration dependent in this case. Unfortunately, isolated compounds (**1-6**) were not enough in quantity to repeat this experiment again.

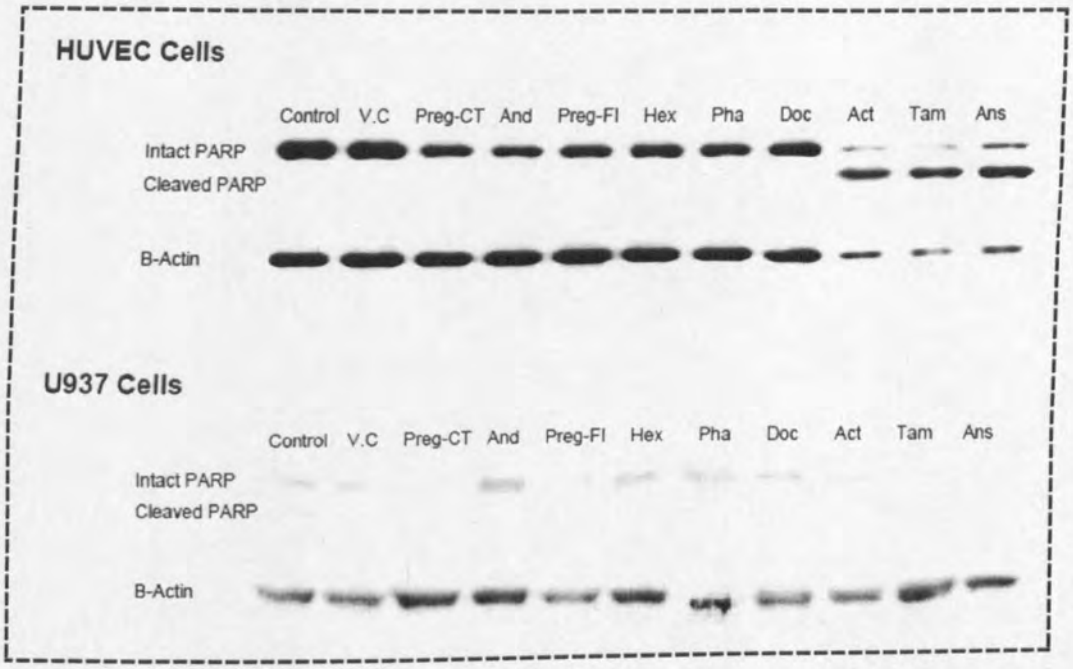

Figure 4.51: Detection of PARP (intact and cleaved) enzyme and β-actin, through Western blotting in lysates of HUVEC and U937 cells treated for 24 hours with Vehicle DMSO 0.01% (V.C.) Pregnane (Preg-CT) and Androstane (And) glycosides from Caralluma tuberculata, Pregnane (Preg-Fl)glycoside from Fagonia indica, Hexadecanoic acid ester (Hex), Phthalic acid ester (Pha), Docosanoic acid ester (Doc), Actinomycin- D (Act), Tamoxifen (Tam), Anastrozole (Ans); where (Control) represents untreated HUVEC or U937 cells. Where, the expression of intact and cleaved-PARP were detected on 10.5% denaturing SDS-polyacrylamide gel using western blot.

Overall, it can be proposed that all six compounds (**1-6**) from four medicinal plants are selective in their antiproliferative activity against human cancer cells as compared to normal human cells. The results from Western blot assay in the presence or absence of caspase inhibitor (Z-VAD-FMK) point towards the apoptotic mode of cell death in cancer cells.

4.7.5. DNA fragmentation (DNA ladder)

DNA fragmentation into high molecular weight fragments is a hallmark of apoptosis (Brown *et al.*, 1992; Huang *et al.*, 1995). During apoptosis, a series of recognition events occur in the cell: chromatin condensations, loss of cell volume and membrane blebbing are some of the most evident morphological changes of apoptotic cells. Chromatins condense and are cleaved initially into large kilobase pair fragments (200–300 and 30–50 Kbp) followed by inter-nucleosomal fragmentation (Oberhammer *et al.*, 1993). The fragmentation of DNA occurs by activation of an endogenous endonuclease that cleaves the DNA in the linker region between histones on the chromosomes. Since the DNA wrapped around the histones comprises 180–200 bp, multiples of this interval are characteristically observed and are commonly referred to as the 'apoptotic ladder'. Such phenomena can be visualised by an agarose gel electrophoresis analysis.

As discussed in previous sections (4.7.2., 4.7.3., 4.7.4), the six compounds (**1-6**) isolated from the four medicinal plants, showed distinct characteristics of apoptosis through cytomorphological alterations, by inhibiting apoptosis in the presence of caspase inhibitors, and through indicative cleaved PARP in cancer cells (MCF-7, MDA MB-469, Caco-2). The next objective was to further explore the mode of action of isolated compounds as apoptosis in cancer cells, through isolation of fragmented DNA from the intact DNA fractions, for their analysis by agarose gel electrophoresis; as a typical ladder pattern due to multiple DNA fragments.

MCF-7 Cells

MCF-7 cells were cultured at a density of $5x10^5$ cells per well in the presence or absence of isolated compounds (compounds **1-6**), according to their estimated IC_{50} [pregnane (20 μM from *Caralluma tuberculata*) and androstane (10 μM) glycosides, hexadecanoic acid (50 μM), phthalic acid (50 μM) and docosanoic

acid (50 μM)] for 48 h. actinomycin-D (4 μM), tamoxifen (5 μM) and anastrozole (5 μM) were used as positive controls. After 24 h treatment, the fragmented DNA

MCF-7 Cells with isolated compounds (**1-6**) and positive controls

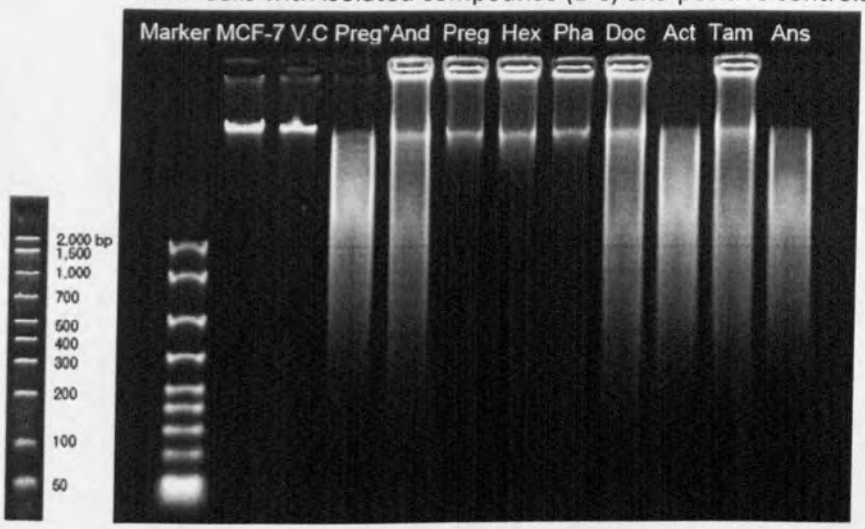

A comparison; MCF-7 Cells (untreated & pre-treated with Z-VAD-FMK)

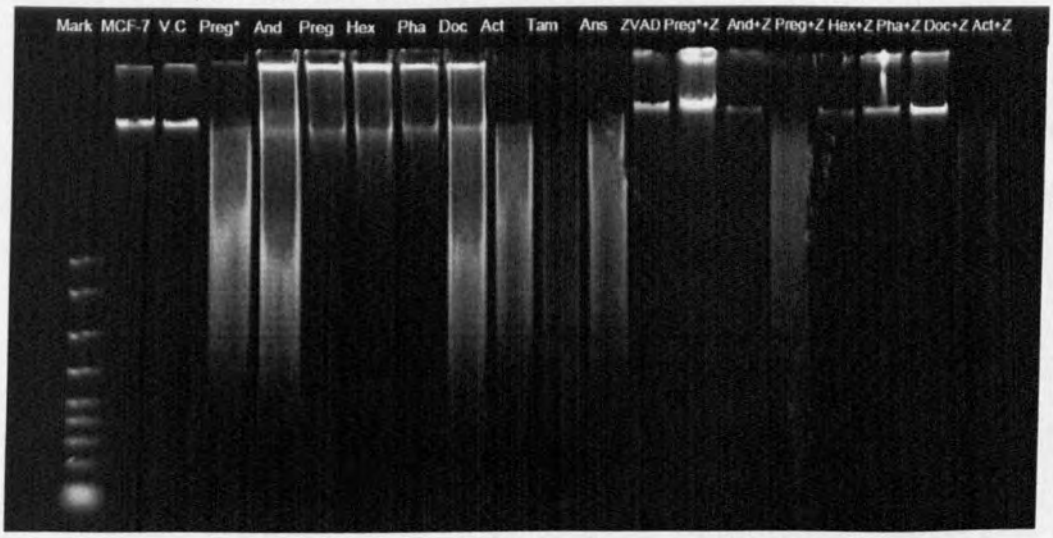

Figure 4.52: DNA fragmentations in MCF-cells after 48 h treatment on agarose gel (1.5%). Where; V.C: Vehicle control (0.01% DMSO), Preg: Pregnane glycoside CT, And: Androstane glycoside, Preg: Pregnane glycoside, Hex: Hexadecanoic acid ester, Pha: Phthalic acid ester, Doc: Docosanoic acid ester, Act: Actinomycin-D, Tam: Tamoxifen, Ans: Anastrozole, ZVAD: Z-VAD-FMK (50 μM) and combinations thereof.*

was isolated from the cell lysates (see Materials and Methods section 3.6.4.) for each compound and resolved by gel (1.5% agarose) electrophoresis.

The photographs (Figure 4.52) on GelDoc system exhibited the fragmentation pattern corresponding to the Amplisize molecular marker (50-2,000 bp) and positive controls. Steroidal glycosides (pregnane and androstane) from *Caralluma tuberculata* and docosanoic acid ester from *Arisaema utile* clearly produce the DNA laddering (200-300 bp) parallel to the molecular marker (50-2,000bp) and the three positive controls; provided further evidence that acylated pregnane and androstane glycosides induce programmed cell death in human oestrogen dependent breast cancer cells (MCF-7). However, from pregnane glycosides (*Fagonia indica*) and the esters (hexadecanoic acid, phthalic acid) the lower molecular weight fragments were absent, which is an added evidence for the results obtained from cytomorphological studies, where features of apoptosis were not very discrete.

In the comparative study, where MCF-7 cells were pre-treated with Z-VAD-FMK (50 μM) for one hour, before they received the IC_{50} concentrations of isolated compounds and positive controls, the results were quite clear as apoptotic signals produced in the presence of steroidal glycosides (pregnane and androstane) from *Caralluma tuberculata* were obstructed by caspase inhibitor. The programmed cell death or "apoptosis" (caspase-dependent PARP cleavage) in response to pregnane and androstane glycosides was confirmed in the hormone dependent human breast cancer cell (MCF-7).

MDA MB-468 Cells

The DNA fragmentation pattern in oestrogen negative human breast cancer cells (MDA MB-468) in response to isolated compounds [pregnane*-CT (50 μM), androstane (50 μM), pregnane-FI (12.5 μM), hexadecanoic acid ester (50 μM),

phthalic acid ester (12.5 μM), docosanoic acid ester (12.5 μM)], along with positive controls: actinomycin-D (4 μM) and anastrozole (5 μM), on 1.5% agarose gel is presented in Figure 4.53.

MDA MB-468 Cells with isolated compounds (**1-6**) and positive controls

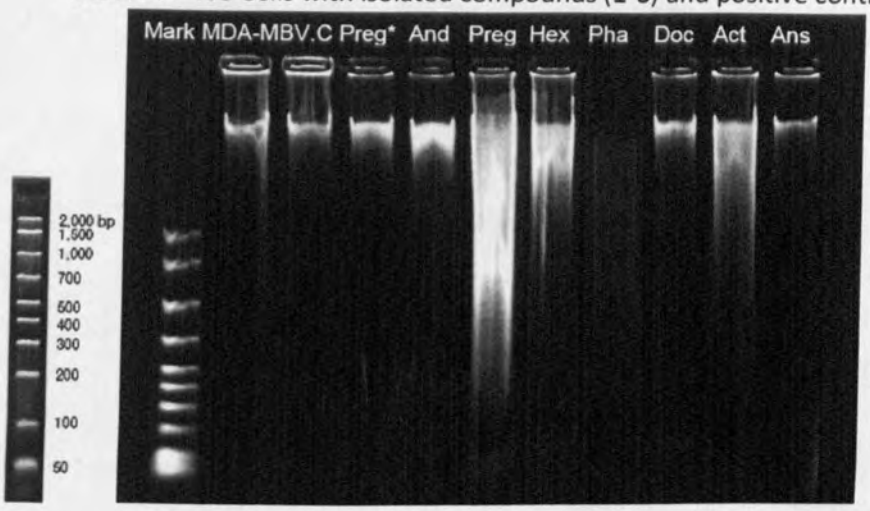

A comparison; MDA MB-468 Cells (untreated & pre-treated with Z-VAD-FMK)

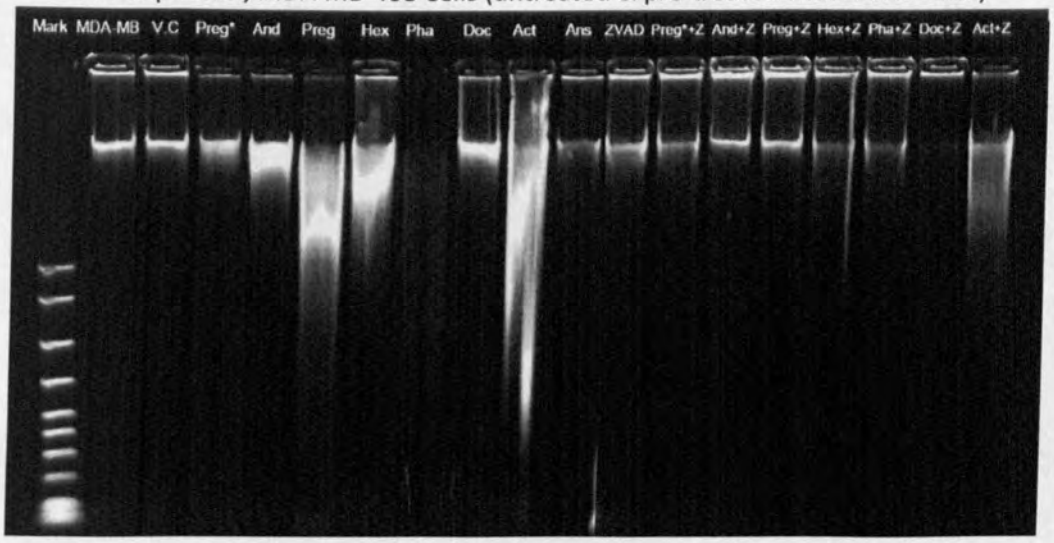

Figure 4.53: Agrose gel stained with GelRed to demonstrate the DNA fragmentations in MDA MB-468 cells after 48 h treatment. Where; V.C: Vehicle control (0.01% DMSO), Preg: Pregnane glycoside CT, And: Androstane glycoside, Preg: Pregnane glycoside, Hex: Hexadecanoic acid ester, Pha: Phthalic acid ester, Doc: Docosanoic acid ester, Act: Actinomycin-D, Tam: Tamoxifen, Ans: Anastrozole, ZVAD: Z-VAD-FMK (50 μM) and combinations thereof.*

The DNA laddering was observed as low molecular weight (200-300 bp) fragments in an apoptotic response from pregnane glycoside from *Fagonia indica* corresponding to the molecular marker and positive control actinomycin-D.

This effect was repetitive as similar induced death characteristics were observed with DAPI nuclei staining and with caspase-dependent PARP cleavage in MDA MB-468 cells. In addition, high molecular weight fragments were visible from androstane glycosides and hexadecanoic acid ester. The formation of high molecular weight DNA is of particular significance as this can occur in cases of apoptosis in which low molecular weight inter-nucleosomal DNA cleavage is absent (Oberhammer, 1993). However, during apoptosis large fragments are thought to be formed initially, and it is from these that the characteristic DNA ladders are derived (Cohen *et al.*, 1994). It may be suggested that the apparent appearances of higher molecular weight fragments are the consequences of prolonged drug exposure (after 24 and 48 h for example).

The programmed cell death response as "apoptosis" from pregnane glycosides (*Fagonia indica*) is further supported from the results (Figure 4.53), as isolated DNA was intact and high or low molecular weight fragments were apparently absent in MDA MB-468 cells; pre-treated with caspase inhibitor Z-VAD-FMK. These findings propose caspase-dependent PARP cleavage, in hormone independent human breast cancer cells from pregnane glycoside; isolated from *Fagonia indica*.

Caco-2 Cells

In colorectal carcinoma cells, treatment for 24 h with isolated compounds at their IC_{50} concentrations [pregnane*-CT (6.25 μM), androstane (6.25 μM), pregnane-FI (12.5 μM), hexadecanoic acid ester (50 μM), phthalic acid ester (12.5 μM), docosanoic acid ester (12.5 μM)], and positive controls actinomycin-D (4 μM)

exhibited DNA laddering in almost all compounds. Although the nuclear fragmentation manifested from steroidal glycosides was substantial, as DNA

Caco-2 Cells with isolated compounds (**1-6**) and positive controls

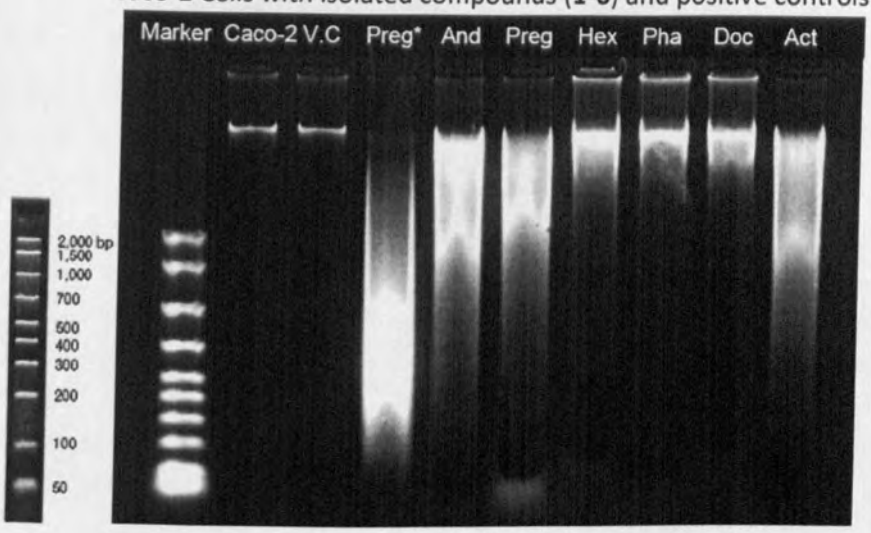

A comparison; Caco-2 Cells (untreated & pre-treated with Z-VAD-FMK)

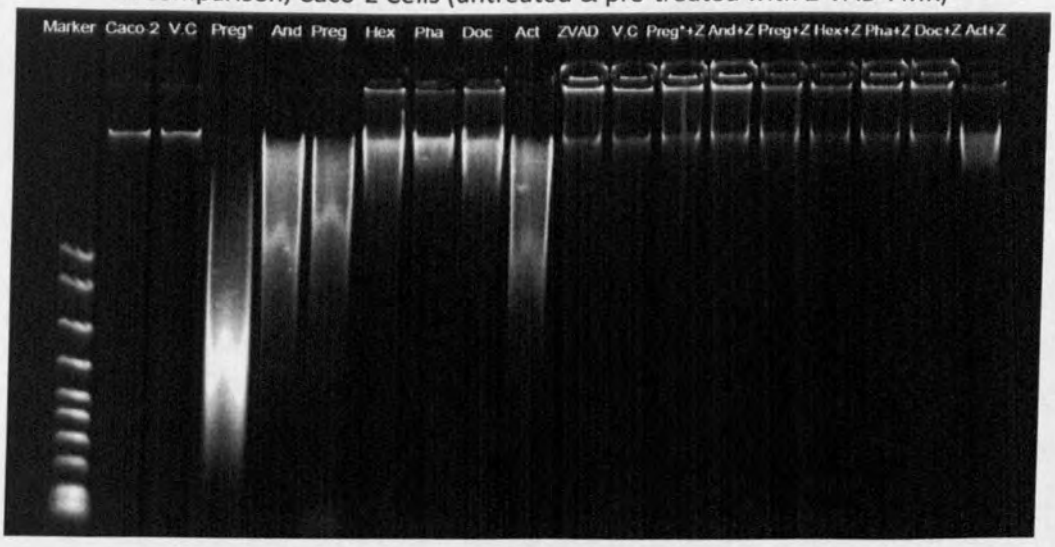

Figure 4.54: DNA fragmentations in Caco-2 cells after 48 h treatment on agarose gel (1.5%). Where; V.C: Vehicle control (0.01% DMSO), Preg: Pregnane glycoside CT, And: Androstane glycoside, Preg: Pregnane glycoside, Hex: Hexadecanoic acid ester, Pha: Phthalic acid ester, Doc: Docosanoic acid ester, Act: Actinomycin-D, ZVAD: Z-VAD-FMK (50 μM) and combinations thereof.*

ladder contained fragments of both high and low molecular fragments; ester compounds (hexadecanoic acid, phthalic acid and docosanoic acid) also showed induction of apoptosis as high molecular base pair fragments (Figure 4.54).

Caspase dependent PARP cleavage (Figure 4.54) was also evident from the comparative study, where Caco-2 cells were pre-treated with caspase inhibitor (Z-VAD-FMK). These results further strengthened the proposed apoptotic mode of cell death in colorectal cancer cells, earlier observed based on morphological and biochemical measurements.

Normal Human Cells

The anticancer activity of isolated compounds (**1-6**) was further investigated through DNA laddering, for its selective cytotoxicity against human cancer cells; with an objective to produce least damage in normal human cells.

In Western blot analysis (see section 4.7.4.) the isolated steroidal glycosides and esters showed signals of intact PARP in human umbilical vein endothelial cells (HUVECs) and in human monocytes U937. Although Compounds (**1-6**) could not exhibit an apoptotic response in normal cells, they can adopt a necrosis mode of cell toxicity. The photographs (Figure 4.55) were taken for isolated DNA in HUVEC and U937 cells on 1.5 % agarose gel using UV GelDoc system. It is apparently clear that at 12.5 μM concentration each of the steroidal glycosides (pregnane and androstane) from *Caralluma tuberculata* and *Fagonia indica* and at 50 μM concentration each of hexadecanoic acid, phthalic acid, and docosanoic acid esters from *Solanum surattense* and *Arisaema utile*; DNA fragmentation is not visible as compared to positive controls: actinomycin-D (4 μM), tamoxifen (5 μM) and anastrozole (5 μM). No smear (random DNA fragmentation) on agarose gel appeared when cells go through necrosis mode of cell death (Walker *et al.*, 1995).

HUVEC cells with isolated compounds (**1-6**) and positive controls

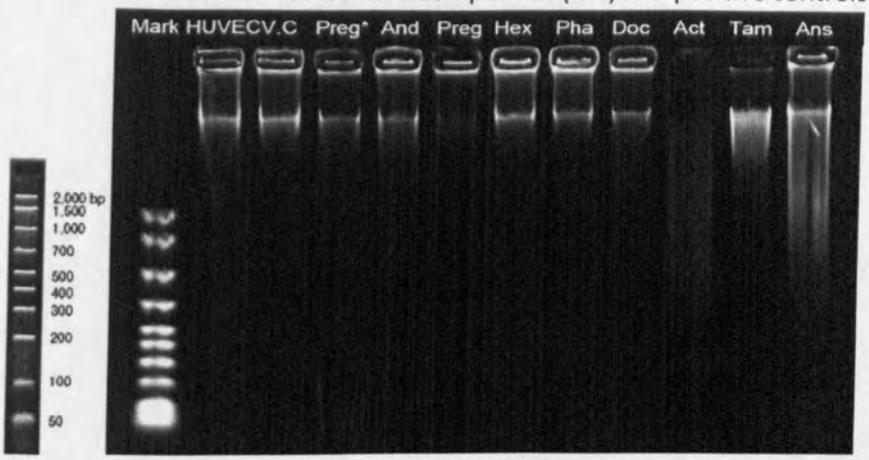

U937 Cells with isolated compounds (**1-6**) and positive controls

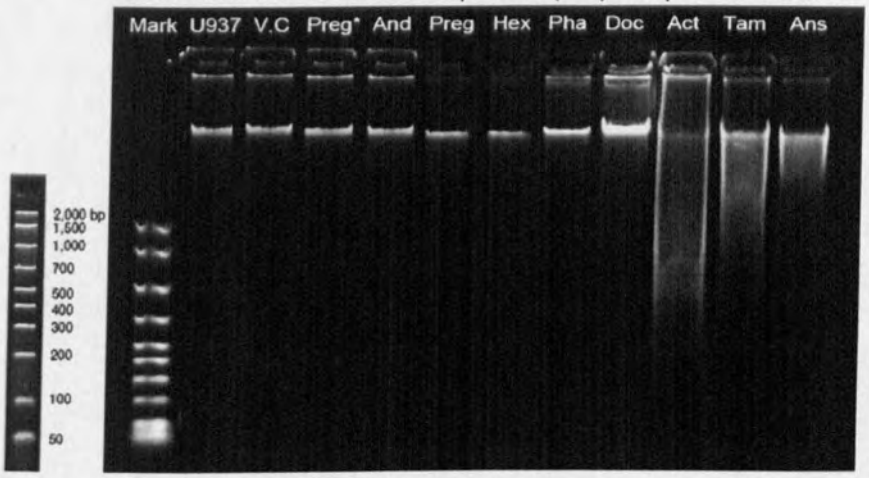

Figure 4.55: Normal human cells (HUVEC and U937 cells) indicated intact DNA as compared to untreated cells after 48 h treatment on agarose gel (1.5%). Where; V.C: Vehicle control (0.01% DMSO), Preg: Pregnane glycoside CT, And: Androstane glycoside, Preg: Pregnane glycoside, Hex: Hexadecanoic acid ester, Pha: Phthalic acid ester, Doc: Docosanoic acid ester, Act: Actinomycin-D, Tam: Tamoxifen, Ans: Anastrozole.*

From the aforementioned results so far, it can be suggested that steroidal glycosides and esters isolated from four medicinal plants are selective in toxicities against rapidly growing human breast and colorectal cancer cells.

5. General Discussion and Conclusion

5.1. General Discussion

The chemotherapy of cancer has undergone substantial improvements since the early years of modern anti-tumour drug research. The identification and development of natural compounds and their derivatives have greatly contributed to this progress and many of these compounds are now being used in clinical practice. Medicinal plants are still a rich source of active constituents against cancer cells. Currently, over 50% of drugs used in clinical trials for anticancer activity are isolated from natural sources or are related to them (Newman and Cragg, 2007).

Ethnobotanical aspect: In the current investigation an attempt was made to explore the anticancer activity of four medicinal plants, mostly from the Himalayan region of Pakistan; *Caralluma tuberculata* (Asclepiadaceae), *Fagonia indica* (Zygophyllaceae), *Solanum surattense* (Solanaceae), *Arisaema utile* (Araceae), against breast cancer (MCF-7, MDA MB-468) and colorectal cancer (Caco-2) cells, based on the traditional or claim to use in folklore medicine in the treatment of different types of tumours and inflammatory conditions. Besides their medicinal properties some of these plants are also a source of food in daily life such as *Caralluma tuberculata*.

Molecular biology becomes essential in medicinal plants drug discovery through the determination and implementation of appropriate screening assays directed towards physiologically relevant molecular targets. In the present study, two cell viability assays, MTT and neutral red uptake (NRU) assays were used to evaluate the cell toxicities based on two different physiological mechanisms; mitochondrial function (MTT assay) and cell metabolic impairment (NRU assay), through differential dye uptake in viable, dead or metabolically inactive cancer cell populations.

The preliminary screening results demonstrated all the four medicinal plants posses substantial cytotoxic activity, which established to some extent, the folklore use of these medicinal plants against cancerous conditions as reported for *Caralluma tuberculata* (Ahmed *et al.*, 1993; Al-Bekairi *et al.*, 1992); *Fagonia indica* (Atta *et al.*, 1982; Qureshi *et al.*, 2008); *Solanum surattense* (Rahman *et al.*, 2003) and *Arisaema utile* (Duke *et al.*, 1985; Zheng *et al.*, 1991). Overall, at that stage, colorectal carcinoma cells were most responsive to the crude extracts, followed by hormone dependent breast cancer cells and then MDA-MB-468 (hormone independent cancer cells). Thus the folklore use is also in agreement with the current investigations. Taking a medicine to treat certain illnesses, is a second or third option in many cases but adopting a healthy life style, where medicinal plants can be used as vegetables, might support the hypothesis "prevention is better than cure".

Phytochemical analysis: In the bioactivity-guided fractionation approach, the ethyl acetate fraction was found to be the most potent fraction in *Caralluma tuberculata* and *Fagonia indica*, while in *Solanum surattense* and *Arisaema utile*, the maximum activity was concentrated in chloroform fractions. Interestingly, like in crude extracts, Caco-2 cells were more sensitive to all the potent fractions (90-97%) as compared to others, whereas the ethyl acetate fractions of *Caralluma* and *Fagonia* were responsible for maximum inhibition (94-95%) in oestrogen positive (ER+ve) and oestrogen negative (ER-ve) cell lines respectively.

Isolation and structure elucidation: The ethyl acetate fraction of *Caralluma tuberculata* resulted in the isolation of two steroidal glycosides (**1**, **2**); an acylated pregnane glycoside ($C_{48}H_{72}O_{20}$) carrying three sugar moieties and an acylated androstan glycoside along with five sugar moieties with a molecular formula represented as ($C_{68}H_{106}O_{26}$). A literature review revealed that the family Asclepiadaceae is a rich source of pregnane glycosides and majority of these steroidal glycosides were isolated mostly from the ethyl acetate fractions of numerous species of plants belonging to genus *Caralluma* (Deepak *et al.*, 1989).

Caralluma umbellate (Lin *et al.*, 1994), *Caralluma retrospiciens* (Halim *et al.*, 1996), *Caralluma russeliana* (Al-Yahya *et al.*, 2000), *Caralluma penicillata* (Abdel-Sattar et al. 2001), *Caralluma negevensis* (Braca *et al.*, 2002) are few examples reported in literature.

According to the reported data so far for steroidal glycosides, the elucidated structures for acylated pregnane and androstane glycosides (Compounds **1**, **2**) from *Caralluma tuberculata* in the present investigation, suggested that these two steroidal glycosides were isolated for the first time from nature. The closest match in structure similarities that could be found was steroidal glycosides, reported by Abdel-Sattar and co-workers as pregnene glycosides from the same plant (Abdel-Sattar *et al.*, 2008). Although the attached groups, benzoyl at C-12 and acetyl at C-20 in a C-21 steroidal skeleton mimic, but differ in the olefinic bond present at C-4 to C-5 and at C-5 to C-6. However, in the isolated glycosides found in the present study, the olefinic bond is absent and compounds were characterised as acylated pregnane and androstane glycosides, according to their skeletal configuration. In addition, these glycosides also differ in the attached sugar moieties and in their configurations. It is also worth mentioning about the cytotoxicity studies of previously reported pregnene glycosides; where these compounds were claimed to posses cytotoxicity against the human diploid embryonic cell line MRC5 (Abdel-Sattar *et al.*, 2008).

The third isolated compound (**3**); a pregnane glycoside carrying two sugar moieties with molecular formula represented as $C_{47}H_{76}O_{12}$ was purified from the ethyl acetate fraction of a second medicinal plant *Fagonia indica*. This is the first report of the isolation and nature of pregnane glycosides from this plant. Previously, reports are available concerning the isolation of triterpenoids saponins (Ansari *et al.*, 1982), steroidal saponins (Graham *et al.*, 2000), betulinic acid (Rizk *et al.*, 1972), phyto–sterol (β-sitosterol), n-triacentanol and ceryl alcohol (Tiwari *et al.*, 1966). NMR spectroscopic data for Compound **3** (pregnane glycoside) showed some resemblance in chemical shift values ^{1}H (δ_H) and ^{13}C

(δ_C) to a steroidal skeleton with the reported data for pregnane glycosides isolated from *Caralluma russeliana* and *Caralluma retrospiciens* (Abdel-Sattar *et al.*, 2007; Halim *et al.*, 1996). From the activity point of view, no biological data is available and research work was limited to the isolation of steroidal glycosides.

Compounds (**4**, **5**) were isolated from the chloroform fraction of *Solanum surattense*. Compound **4** was identified as hexadecanoic acid ethyl ester ($C_{18}H_{36}O_2$). Hexadecanoic acid ethyl ester is the formal name of palmitic acid ethyl ester which has been isolated previously from *Actinidia deliciosa* and is found in China, Hunan, Guangxi, Jiangxi, Shaanxi. Palmitic acid is a common 16-carbon saturated fat that represents 10-20% of the normal human dietary fat intake. Palmitic acid also makes up approximately 25% of the total plasma fatty acids in plasma lipoproteins (Santos *et al.*, 1995).

Compound **5** was identified as phthalic acid 1-(1, 1-dimethyl-pentyl) ester 2-(2-ethyl-dec-5-enyl) ester with molecular formula $C_{27}H_{42}O_4$. A literature search revealed that this compound has not been reported before; however in structural similarities, it has some match with Bis(2-methylheptyl) phthalate isolated from the ethyl acetate fraction extracted from the aerial parts of *Hypericum hyssopifolium* (Cakir *et al.*, 2003).

Compound **6** (5-Oxo-19-propyl-docosanoic acid methyl ester) with molecular formula $C_{26}H_{50}O_3$ and Compound **7**: 3-Hydroxy-20-pentyl-pregnane ($C_{26}H_{46}O$) were isolated from the chloroform fraction of *Arisaema utile*. Phytochemical studies conducted on genus *Arisaema* (family Araceae) have shown a series of homologous, phenylalkanoic acids and phenylalkenoic acids isolated from seed lipids, e.g. 13-phenyltridecanoic acid (fatty acid) from the seeds of *Arisaema utile* (Meija *et al.*, 2004), but Compounds **6** and **7** have not been reported before from any source of the family Araceae. Previous studies were mainly focused on investigating the chemical compositions of *Arisaema utile* and some Lectin-glycoproteins were purified from the rhizome part of the plant, where these

lectins agglutinated rabbit, rat and sheep red blood cells (RBCs), but were inactive towards human ABO erythrocytes (Shangary *et al.*, 1995).

The chemical structure of Compound **7** was elucidated from X-ray crystallography and was searched on chemical databases. Only one hit was found on ChemSpider; where the chemical structure was reported with ID 9934891, but no biological activity data was described.

Cytotoxicity studies: Generally, natural compounds comprise either classical cytotoxic moieties targeting non-specific macromolecules expressed by cancer cells and to lesser extent by normal proliferating cells (e.g. DNA, enzymes) or new compounds targeting macromolecules specifically expressed on cancer cells. Overall, the isolated compounds in the current investigation; steroidal glycosides (Compound **1-3**) and fatty acid esters (Compound **4-6**) showed cytotoxicity subject to cancer cell type. Highly significant ($p<0.001$) percent growth inhibition (80-90%) was observed in colorectal carcinoma cells from all the six isolated compounds in concentration and time dependent cytotoxicity assays (MTT and NRU). However, interestingly, steroidal glycosides (pregnane and androstane) produced a more pronounced cytotoxic effect in breast cancer cells [MCF-7 (IC_{50} 6.25 – 12.5 μM) and MDA MB-468 (IC_{50} 12.5 – 25 μM)], as compared to esterified compounds (hexadecanoic acid ester, phthalic acid ester and docosanoic acid ester), where IC_{50} values ranged 50 – 100 μM after 48 h treatment. Interestingly, in the current study, normal human cells (HUVEC and U937) were less affected by the isolated compounds (steroidal glycosides and fatty acid esters) from *Caralluma tuberculata, Fagonia indica, Solanum surattense* and *Arisaema utile*, at least with regard to DNA fragmentation, the assay used to assess their effect. Possibly, the compounds may show some selectively between malignant and normal cells, but further work is necessary.

Steroidal glycosides and cytotoxicity: It is suggested that the activity of these steroidal glycosides may be related to the structural resemblance of the steroidal

skeleton in body androgens, where they may be competing for the same enzyme active site. Previous studies on the plants of the genus *Caralluma* have reported the isolation of several pregnane glycosides (Ahmed *et al.*, 1998; Tanaka *et al.*, 1990; Lin *et al.*, 1994; Deepak *et al.*, 1997; Qiu *et al.*, 1999; Abdel-Sattar et al. 2008, 2009; Kunert *et al.*, 2009), but there is no data available on breast and colorectal cancer cells for direct comparison, apart from; the pregnane glycosides isolated from *Caralluma tuberculata* (Abdel-Sattar *et al.*, 2009) where IC_{50} values of ~20 µg/ml on the growth of MRC5 cells (human diploid embryonic cells) were reported. Most remarkably, twenty seven pregnane glycosides isolated from *Caralluma dalzielii* had sub-micromolar IC_{50} values, when tested on J774.A1 (murine monocyte/macrophage), WEHI-164 (murine fibrosarcoma), and HEK-293 (human epithelial kidney cells), after 72 hours using the MTT assay (De Leo *et al.*, 2005). At present, it is too early for an explanation for this great difference in potency between pregnane glycosides from that study and steroidal glycosides isolated from *Caralluma* and *Fagonia* in the present study; apart from the difference in cell type and exposure time.

Cell selectivity: Another noteworthy difference observed was in cell-selectivity between steroidal glycosides. The pregnane and androstane glycosides from *Caralluma tuberculata* showed more suppression in cell growth over 48 h treatments with MTT and NRU assays in MCF-7 cells as compared to hormone independent breast cancer cells (MDA MB-468) and *vice versa,* in the case of pregnane glycoside from *Fagonia indica*. This may be a result of structural activity relationship or receptor affinity for attached acetyl and benzoyl moieties at positions C–20 and C-12, present in steroidal glycosides from *Caralluma*, which needs to be determined.

Mode of cell death-apoptosis or necrosis: Since in the current study, cell numbers in MTT, NRU and cytomorphological alteration (DAPI nuclei staining) assays, were decreased with increased time and dose of the treatment, reflecting the cytotoxic effect produced by these six isolated compounds in the corresponding

cancer cell type as compared to untreated cells. Subsequently, it was investigated whether the cytotoxic effect was mediated via an apoptotic mechanism or the necrosis mode of cell death was involved. All of the measures of cytotoxic activity (MTT, NRU, DAPI, PARP cleavage, DNA ladder) on MCF-7, MDA MB-468 and Caco-2 cells were inhibited by pre-treatment with the pan-caspase inhibitor Z-VAD-FMK (50 μM).

Caspases; proteolytic enzymes, widely expressed as pro-enzymes; once activated allow initiation of a protease cascade (Kerr *et al.*, 1994). In caspase–dependent apoptosis, the cell death signals are activated by Ca^{2+} endonucleases via two main pathways: the extrinsic (transmembrane receptor-mediated interactions; death receptor: tumour necrosis factor (TNF) receptor) and the intrinsic (mitochondrial initiated event involving non-receptor mediated stimuli that produce intracellular signals) pathways (Locksley *et al.*, 2001; Igney and Krammer, 2002). The extrinsic and intrinsic pathways converge on the same terminal, or execution phase. It is the activation of the execution caspases (caspase-3) that begins final phase of apoptosis (Slee *et al.*, 2001). Cleaving various substrates including PARP followed by nuclear fragmentation, both of which were end points detected in the present study from the steroidal glycosides and fatty acid esters isolated from four medicinal plants, that ultimately caused the morphological and biochemical changes in cancer cells going through programmed cell death "apoptosis".

These experiments therefore, clearly showed that the pregnane and the androstane glycosides from *Caralluma tuberculata* induced caspase–dependent apoptosis in MCF-7 and Caco-2 cells, while the MDA MB-468 cells were less sensitive. However, in pregnane glycosides from *Fagonia indica* a pronounced effect was observed towards oestrogen negative breast cancer cells and colorectal carcinoma cells. It is presumed that the glycoside is cleaved by cell surface enzymes, such as lactase phlorizin hydrolase, to allow the steroid to cross the plasma membrane and enter the cell (Chen *et al.*, 2005).

Fatty acid esters & cytotoxicity: The isolated compounds from *Solanum surattense* and *Arisaema utile*; phthalic acid ester and docosanoic acid methyl ester respectively, showed a highly significant ($p<0.001$) decrease in cell numbers for MDA MB-468 and Caco-2 cells with apparent IC_{50} range 6.25 – 12.5 μM in cell viability assays (MTT and NRU) after 48 h treatment, while the esterified alkyl hydrocarbon (hexadecanoic acid ethyl ester) was most effective against MCF-7 cells (IC_{50} 25 μM).

Hexadecanoic ethyl ester, which is also known as palmitic acid ethyl ester, showed a positive response towards oestrogen positive breast cancer cells. These results are in agreement with a report where, this compound was isolated from the root extract of *Acitinidia deliciosa*, which has a reputed anti-tumour activity against breast cancer (Zhongzhen *et al.*, 2004; Liang *et al.*, 2006). It is reported that palmitic acid ethyl ester is a neutral, lipid-soluble form of the free acid and is one of the fatty acid ethyl esters that increase cytosolic calcium concentration leading to cell death (Chen *et al.*, 2003).

Possible role of ROS in cytotoxicity: Moreover, it is a possibility that these isolated compounds (hexadecanoic acid ethyl ester, phthalic acid ester and docosanoic acid ester) produce cytotoxicity as a prooxidant in cancer cells, that may be from increased intracellular reactive oxygen species (ROS) production, which inhibited the expression of one of the major constituents (anti-oxidant) of the cellular defence system against ROS, the enzyme Cu/Zn SuperOxide Dismutase (SOD). This decrease could be one of the mechanisms underlying the prooxidant action (Ravid *et al.*, 1999). Evidence from previous studies suggests that cancer cells, compared to normal cells, are under increased oxidative stress associated with oncogenic transformation, alterations in metabolic activity, and increased generation of ROS (Hileman *et al.*, 2001; Behrend *et al.*, 2003).

ROS are broadly defined as oxygen-containing chemical species with reactive chemical properties, and include free radicals such as superoxide ($O_2^{\bullet-}$) and

hydroxyl radicals ($HO^{\bullet}$), which contain an unpaired electron, and non-radical molecules such hydrogen peroxide (H_2O_2). The increased amounts of ROS in cancer cells may have significant consequences, such as stimulation of cellular proliferation, promotion of mutations and genetic instability. Under physiological conditions, the maintenance of an appropriate level of intracellular ROS is important in keeping the redox balance and signaling cellular proliferation (McCord, 1995; Martin and Barrett, 2002). Persistent generation of reactive oxygen species such as superoxide, hydrogen peroxide and hydroxyl radicals is an inevitable consequence of mitochondrial respiration in aerobic organisms, whose ATP requirements are correlated with the level of metabolic activity. Because much of the ($O_2^{\bullet -}$) is generated in the mitochondria, damage to the mitochondrial membrane is likely to cause release of cytochrome *c* and activate the apoptotic cascades (Carmody and Cotter, 2001; Pelicano *et al.*, 2003). Due to their reactive chemical nature, ROS are capable of attacking various components of DNA, leading to the generation of a variety of ROS-mediated modified products including oxidized bases, DNA strand breaks, DNA intra-strand adducts, and DNA–protein crosslinks, which results in apoptosis (Lloyd *et al.*, 1997).

However, because ROS are chemically active and can inflict severe cellular damage, the very fact that cancer cells are under increased intrinsic ROS stress may also provide a unique opportunity to kill the malignant cells based on their vulnerability to further ROS insults. As such, this biochemical characteristic is likely to have significant therapeutic implications. Several anticancer agents (bleomycin, anthracyclines, irradiation) currently used for cancer treatment have been shown to cause increased cellular ROS generation, and are logical candidates for evaluating the strategy of preferentially killing cancer cells with increased ROS stress than in normal cells (Shen *et al.*, 1997).

Bioavailability: The therapeutic efficacy of drugs depends critically on their ability to cross cellular barriers to reach their target and intracellular metabolising

enzymes. However, the extent to which a drug accumulates within a tissue is frequently limited not so much by its ability to enter cells but by its tendency to leave (Evers *et al.*, 1998). This may arise from active efflux mechanisms present in the plasma membrane. These efflux mechanisms play a critical role in limiting the absorption and accumulation of potentially toxic substances and can effectively confer resistance to a diverse range of compounds in tumour cells (Fromm *et al.*, 2000).

The first major obstacle to cross is the intestinal epithelium. Although lipophilic compounds may readily diffuse across the apical plasma membrane, their subsequent passage across the basolateral membrane and into blood is by no means guaranteed. These drug efflux proteins principally comprise the MDR (multidrug resistance)- and MRP (multidrug resistance-associated protein)-type transporters (Hunter *et al.*, 1993a,b; Walgren *et al.*, 2000), located at the apical membrane, may drive compounds from inside the cell back into the intestinal lumen, preventing their absorption into blood.

Drugs may also be modified by intracellular metabolising enzymes. This process may not only render the drug ineffective, but it may also produce metabolites that are themselves substrates for Pgp and/or MRP2. Drugs that reach the blood are then passed to the liver, where they are subject to further metabolism and biliary excretion, often by a similar system of ATP-binding cassette (ABC) transporters and enzymes to that present in the intestine. Thus a synergistic relationship exists between intestinal drug metabolising enzymes and apical efflux transporters, a partnership that proves to be a critical determinant of oral bioavailability (Klein *et al.*, 1999). It has raised the awareness of the importance of ADME (absorption, distribution, metabolism and exrection) and physico-chemical properties for the success of orally bioavailable natural product-based drug discovery, and helped to front-load ADME/toxicity screening in the industrial drug discovery process.

Overview of steroidal glycosides: The steroidal glycosides isolated in this study have some similarity to a glycoside (Bouceroside BNC, $C_{51}H_{78}O_{16}$) isolated from *Boucerosia aucheriana* (Deepak *et al.*, 1991), but no activity on tumour cells has been reported, so a comparison with current data is not possible. Pregnane glycosides are structurally closer to cardiac glycosides such as digoxin and cardiac glycosides from Asclepias Linn; family Asclepiadaceae, which inhibit calcium exchangers, thereby leading to a prolonged increase in intracellular calcium concentration and stimulation of caspases and apoptosis (Deepak *et al.*, 1997). Another possible mechanism of action is the activation of the steroid and xenobiotic receptor (SXR), an orphan steroid receptor, which induces apoptosis in breast cancer cells (Verma *et al.*, 2009). Further studies are required, but the activation of the SXR is an exciting possibility.

Overview of fatty acids: In contrast to isolated steroidal glycosides, hexadecanoic acid ethyl ester and phthalic acid ester from *Solanum surattense* and docosanoic acid ester from *Arisaema utile*, could not restrict the growth inhibition in pre-treated MCF-7 and Caco-2 cells, with Z-VAD-FMK, which indicates less involvement of caspase–dependent apoptosis. As in DAPI staining and in Western blots (cleaved-PARP) characteristics of apoptosis were clear but in the DNA ladder assay, nuclear fragments of high base pairs were detected, so there is a possibility that these compounds are inducing a combined apoptotic-necrotic pathway of cell death in cancer cells. There are reported necrotic-like phenotypic programmed cell deaths (Proskuryakov *et al.*, 2003). These forms of cell death have certain morphological features of both necrosis and apoptosis; have been given the term aponecrosis (Formigli *et al.*, 2000); a type of cell death that shared dynamic, molecular, and morphological features with both apoptosis and necrosis.

5.2. Conclusion

In summary, results from the present study are in agreement with the ethnobotanical or traditional use of these four medicinal plants *Caralluma tuberculata, Fagonia indica, Solanum surattense* and *Arisaema surattense* against cancer growth. The current research work has established that *Caralluma tuberculata* is a rich source of pregnane glycosides and certainly possesses significant anticancer activity against hormone dependent breast cancer cells. Most of the pregnane glycosides induce apoptosis in tumour cells; as evident from the present results, so they are preferable drugs for the treatment of cancer, because the elimination of tumour cells by apoptosis is helpful in lowering the side-effects in patients by avoiding necrosis. Similarly, isolation of pregnane glycoside from *Fagonia indica* has added a new category of "steroidal glycosides" in the list of chemical constituents present in this plant, which was previously limited to saponins, alkaloids and β-sitosterol. In addition, this research work also emphasises the activity of the steroidal glycoside from *Fagonia indica* against hormone independent breast cancer; reported to be more aggressive and difficult to treat due to growing resistance to available chemotherapy. In addition, esters from *Solanum surattense* and *Arisaema utile* also showed more activity towards oestrogen negative breast cancer cells. Interestingly, the crude extracts of four medicinal plants and resultant isolated compounds from the potent fractions, were all responsive to colorectal cancer cells, demonstrating the traditional or folklore use of these plants in gastrointestinal ailments.

Overall, the identification and characterisation of isolated compounds from medicinal plants in the treatment of cancer, the very common "plague" of modern times, justify both the evolutional knowledge coming from pharmacognosy and its historical roots in ancient herbal medicine, as well as the tremendous possibility of a natural product-based drug discovery approach.

5.3. Future Work

In order to further investigate the pharmacokinetic and pharmacodynamic properties of the active compounds either as a parent molecules or their secondary metabolites *in vitro* or *in vivo*, an adequate quantity is compulsory. In this regards the natural product synthesis approach is a quite interesting opportunity for an adequate quantity. This approach also further strengthens the idea of preservation of our natural resources, as biodiversity of many medicinal plants is in danger.

Another exciting aspect this research can be focused on, is to find out what proportion of the active constituents in the plants are actually consumed as vegetables in a routine diet.

Cell selectivity in response to the different steroidal glycosides from the medicinal plants may be a result of structure activity relationship or receptor affinity for a particular functional group, is an interesting aspect of a natural product, which can be investigated through derivatisation of parent compound in order to get biologically more active and physico-chemically more stable molecules.

Further studies on bioavailability of isolated steroidal glycoside would investigate the bio-active form of these molecules, through metabolic pathways in animal models and are the objectives for future investigation from these medicinal plants.

Appendix: 1

Percentage growth inhibition of cancer cells at various concentrations (µg/ml) of crude ethanolic extracts of *Caralluma tuberculata* using MTT assay

Concentration (µg/ml)	Absorbance (cells + extract + media)			Actual Absorbance (cells + extract)- media			% Growth Inhibition (Mean ± STDEV)
Experiments	**1**	**2**	**3**	**1**	**2**	**3**	
MCF-7 Cells							
Media	0.088	0.093	0.087	0.000	0.000	0.000	-------
Media + Cells	0.136	0.146	0.148	0.048	0.053	0.061	-------
10	0.125	0.131	0.138	0.038	0.038	0.051	22.19 (±5.94)
25	0.120	0.136	0.133	0.032	0.043	0.046	24.78 (±7.19)
50	0.115	0.126	0.121	0.027	0.033	0.034	41.65 (±3.87)
100	0.117	0.126	0.121	0.029	0.033	0.034	40.04 (±3.48)
Media	0.083	0.083	0.083	0.000	0.000	0.000	-------
200	0.105	0.110	0.117	0.022	0.027	0.034	48.41 (±4.26)
300	0.099	0.099	0.102	0.016	0.016	0.019	67.65 (±3.00)
400	0.099	0.100	0.096	0.016	0.018	0.014	70.03 (±6.52)
500	0.093	0.091	0.091	0.010	0.009	0.009	82.36 (±3.96)
Vehicle Control	0.128	0.137	0.143	0.045	0.054	0.060	1.11 (±4.43)
MDA MB-468 Cells							
Media	0.095	0.068	0.085	0.000	0.000	0.000	-------
Media + Cells	0.167	0.159	0.159	0.071	0.091	0.074	-------
10	0.166	0.157	0.157	0.070	0.089	0.072	2.25 (±0.73)
25	0.160	0.156	0.156	0.064	0.088	0.070	6.05 (±3.09)
50	0.153	0.149	0.150	0.058	0.081	0.064	14.42 (±4.15)
100	0.142	0.139	0.140	0.046	0.070	0.054	28.14 (±6.32)
Media	0.078	0.078	0.078	0.000	0.000	0.000	-------
200	0.124	0.130	0.121	0.046	0.053	0.043	39.89 (±3.65)
300	0.108	0.116	0.104	0.030	0.038	0.026	60.19 (±3.82)
400	0.103	0.112	0.101	0.025	0.034	0.023	65.60 (±3.48)
500	0.096	0.099	0.095	0.018	0.021	0.017	76.18 (±1.59)
Vehicle Control	0.152	0.166	0.155	0.074	0.088	0.077	-1.39 (±4.05)
Caco-2 Cells							
Media	0.078	0.068	0.079	0.000	0.000	0.000	-------
Media + Cells	0.140	0.138	0.138	0.063	0.070	0.059	-------
10	0.129	0.130	0.133	0.052	0.062	0.054	12.50 (±4.62)
25	0.122	0.122	0.127	0.044	0.054	0.048	23.75 (±5.34)
50	0.118	0.116	0.122	0.040	0.048	0.042	31.79 (±4.23)
100	0.122	0.109	0.113	0.044	0.041	0.034	37.59 (±7.42)
Media	0.078	0.077	0.084	0.000	0.000	0.000	-------
200	0.106	0.107	0.111	0.028	0.030	0.027	55.14 (±7.42)
300	0.098	0.096	0.106	0.020	0.018	0.022	68.23 (±6.07)
400	0.081	0.093	0.093	0.003	0.016	0.009	85.47 (±8.93)
500	0.080	0.089	0.084	0.002	0.012	0.000	93.18 (±9.68)
Vehicle Control	0.145	0.146	0.140	0.067	0.068	0.056	-0.01 (±6.15)

Appendix: 2

Percentage growth inhibition of cancer cells at various concentrations (µg/ml) of crude ethanolic extracts of *Fagonia indica* using MTT assay

Concentration (µg/ml)	Absorbance (cells + extract + media)			Actual Absorbance (cells + extract)- media			% Growth Inhibition
Experiments	**1**	**2**	**3**	**1**	**2**	**3**	*(Mean ± STDEV)*
MCF-7 Cells							
Media	0.084	0.084	0.086	0.000	0.000	0.000	-------
Media + Cells	0.141	0.131	0.152	0.057	0.047	0.066	-------
10	0.128	0.123	0.143	0.044	0.039	0.057	17.46 (±4.41)
25	0.120	0.114	0.127	0.036	0.030	0.041	36.58 (±1.10)
50	0.119	0.112	0.123	0.035	0.028	0.037	40.80 (±3.24)
100	0.121	0.115	0.123	0.037	0.031	0.037	37.18 (±5.75)
Media	0.078	0.079	0.084	0.000	0.000	0.000	-------
200	0.108	0.100	0.118	0.030	0.021	0.034	49.76 (±4.36)
300	0.111	0.106	0.112	0.033	0.027	0.028	47.20 (±8.90)
400	0.103	0.097	0.105	0.025	0.019	0.021	61.23 (±6.45)
500	0.091	0.083	0.093	0.013	0.004	0.009	84.51 (±7.52)
Vehicle Control	0.138	0.131	0.153	0.061	0.052	0.069	-7.51 (±3.03)
MDA MB-468 Cells							
Media	0.086	0.078	0.085	0.000	0.000	0.000	-------
Media + Cells	0.169	0.185	0.149	0.084	0.108	0.064	-------
10	0.155	0.162	0.144	0.069	0.084	0.059	15.96 (±6.82)
25	0.147	0.152	0.132	0.061	0.075	0.047	27.97 (±2.18)
50	0.127	0.128	0.121	0.041	0.050	0.036	49.25 (±5.00)
100	0.126	0.122	0.116	0.040	0.045	0.031	53.93 (±4.00)
Media	0.068	0.084	0.078	0.000	0.000	0.000	-------
200	0.102	0.115	0.102	0.034	0.032	0.024	64.95 (±4.24)
300	0.094	0.099	0.097	0.026	0.015	0.019	75.60 (±8.56)
400	0.072	0.098	0.088	0.004	0.015	0.010	88.90 (±5.88)
500	0.069	0.093	0.082	0.001	0.010	0.005	94.24 (±4.32)
Vehicle Control	0.156	0.188	0.145	0.088	0.105	0.067	-2.10 (±4.26)
Caco-2 Cells							
Media	0.070	0.073	0.074	0.000	0.000	0.000	-------
Media + Cells	0.128	0.139	0.149	0.058	0.066	0.075	-------
10	0.114	0.120	0.136	0.044	0.047	0.062	23.44 (±5.55)
25	0.110	0.119	0.132	0.040	0.045	0.058	28.28 (±4.64)
50	0.102	0.109	0.121	0.032	0.036	0.047	42.04 (±4.14)
100	0.096	0.107	0.116	0.026	0.033	0.042	49.16 (±5.05)
Media	0.090	0.080	0.071	0.000	0.000	0.000	-------
200	0.112	0.102	0.106	0.022	0.022	0.035	60.42 (±7.19)
300	0.102	0.099	0.097	0.012	0.019	0.027	71.65 (±7.12)
400	0.102	0.098	0.088	0.012	0.018	0.017	76.28 (±3.49)
500	0.099	0.093	0.083	0.009	0.013	0.012	82.99 (±2.51)
Vehicle Control	0.145	0.145	0.148	0.055	0.064	0.077	0.88 (±3.69)

Appendix: 3

Percentage growth inhibition of cancer cells at various concentrations (µg/ml) of crude ethanolic extracts of *Solanum surattense* using MTT assay

Concentration (µg/ml)	Absorbance (cells + extract + media)			Actual Absorbance (cells + extract)- media			% Growth Inhibition (Mean ± STDEV)
Experiments	**1**	**2**	**3**	**1**	**2**	**3**	
MCF-7 Cells							
Media	0.074	0.074	0.079	0.000	0.000	0.000	-------
Media + Cells	0.114	0.122	0.139	0.040	0.048	0.060	-------
10	0.106	0.113	0.124	0.032	0.038	0.045	21.58 (±3.27)
25	0.100	0.105	0.114	0.027	0.030	0.035	37.50 (±415)
50	0.101	0.108	0.112	0.027	0.034	0.033	35.45 (±8.67)
100	0.100	0.108	0.115	0.026	0.034	0.036	35.22 (±5.17)
Media	0.085	0.086	0.084	0.000	0.000	0.000	-------
200	0.102	0.105	0.107	0.017	0.019	0.024	58.28 (±4.85)
300	0.100	0.100	0.102	0.016	0.014	0.018	65.74 (±7.85)
400	0.098	0.099	0.094	0.013	0.013	0.010	73.70 (±10.25)
500	0.089	0.086	0.085	0.004	0.000	0.001	95.88 (±6.01)
Vehicle Control	0.121	0.131	0.148	0.037	0.045	0.064	2.87 (±8.63)
MDA MB-468 Cells							
Media	0.083	0.078	0.075	0.000	0.000	0.000	-------
Media + Cells	0.172	0.164	0.176	0.089	0.086	0.101	-------
10	0.166	0.159	0.161	0.083	0.080	0.086	9.47 (±4.95)
25	0.159	0.155	0.154	0.076	0.076	0.079	15.81 (±5.44)
50	0.143	0.132	0.130	0.060	0.053	0.056	38.47 (±6.35)
100	0.131	0.123	0.131	0.048	0.044	0.056	46.25 (±1.87)
Media	0.073	0.073	0.094	0.000	0.000	0.000	-------
200	0.112	0.112	0.123	0.039	0.039	0.029	61.62 (±7.33)
300	0.104	0.102	0.118	0.031	0.029	0.024	70.05 (±4.73)
400	0.100	0.096	0.114	0.027	0.023	0.021	74.82 (±3.74)
500	0.089	0.091	0.101	0.016	0.018	0.008	85.04 (±6.44)
Vehicle Control	0.168	0.162	0.191	0.094	0.089	0.097	-1.63 (±5.20)
Caco-2 Cells							
Media	0.079	0.068	0.073	0.000	0.000	0.000	-------
Media + Cells	0.184	0.164	0.171	0.104	0.096	0.097	-------
10	0.166	0.159	0.161	0.087	0.090	0.087	10.87 (±5.67)
25	0.159	0.155	0.154	0.080	0.086	0.081	16.76 (±6.90)
50	0.143	0.132	0.130	0.064	0.063	0.057	37.98 (±3.83)
100	0.131	0.123	0.131	0.052	0.054	0.058	44.74 (±4.94)
Media	0.084	0.078	0.080	0.000	0.000	0.000	-------
200	0.123	0.116	0.123	0.039	0.039	0.043	56.95 (±3.92)
300	0.104	0.102	0.112	0.020	0.025	0.032	72.32 (±7.44)
400	0.100	0.096	0.096	0.016	0.019	0.016	81.68 (±2.06)
500	0.098	0.091	0.092	0.014	0.014	0.012	85.95 (±1.25)
Vehicle Control	0.183	0.168	0.171	0.099	0.090	0.091	5.67 (±0.89)

Appendix: 4

Percentage growth inhibition of cancer cells at various concentrations (µg/ml) of crude ethanolic extracts of *Arisaema utile* using MTT assay

Concentration (µg/ml)	Absorbance (cells + extract + media)			Actual Absorbance (cells + extract)- media			% Growth Inhibition (Mean ± STDEV)
Experiments	**1**	**2**	**3**	**1**	**2**	**3**	
MCF-7 Cells							
Media	0.075	0.081	0.077	0.000	0.000	0.000	-------
Media + Cells	0.127	0.122	0.138	0.052	0.041	0.061	-------
10	0.118	0.117	0.122	0.043	0.036	0.045	19.26 (±6.66)
25	0.111	0.112	0.115	0.036	0.031	0.038	31.55 (±6.63)
50	0.107	0.109	0.111	0.032	0.028	0.034	38.84 (±6.28)
100	0.099	0.101	0.114	0.024	0.020	0.036	48.60 (±6.94)
Media	0.077	0.078	0.083	0.000	0.000	0.000	-------
200	0.099	0.099	0.107	0.022	0.021	0.025	54.86 (±5.12)
300	0.092	0.088	0.102	0.015	0.009	0.019	72.28 (±4.52)
400	0.088	0.084	0.094	0.011	0.006	0.011	81.72(±4.56)
500	0.078	0.086	0.085	0.001	0.008	0.003	91.32 (±9.70)
Vehicle Control	0.127	0.123	0.142	0.050	0.045	0.059	-0.62 (±6.58)
MDA MB-468 Cells							
Media	0.078	0.078	0.094	0.000	0.000	0.000	-------
Media + Cells	0.182	0.184	0.182	0.104	0.105	0.088	-------
10	0.169	0.176	0.173	0.091	0.098	0.079	10.15 (±2.91)
25	0.172	0.167	0.169	0.094	0.089	0.075	13.32 (±3.24)
50	0.158	0.161	0.158	0.080	0.083	0.064	23.80 (±2.86)
100	0.144	0.142	0.143	0.066	0.063	0.049	40.53 (±3.72)
Media	0.079	0.073	0.079	0.000	0.000	0.000	-------
200	0.119	0.119	0.111	0.040	0.046	0.032	58.86 (±3.76)
300	0.113	0.112	0.106	0.034	0.039	0.027	65.18 (±3.39)
400	0.099	0.095	0.091	0.020	0.021	0.012	81.56 (±4.19)
500	0.086	0.095	0.089	0.007	0.022	0.010	86.89 (±6.62)
Vehicle Control	0.172	0.176	0.174	0.094	0.102	0.095	1.73 (±9.33)
Caco-2 Cells							
Media	0.086	0.084	0.068	0.000	0.000	0.000	-------
Media + Cells	0.182	0.184	0.182	0.097	0.100	0.114	-------
10	0.169	0.176	0.173	0.083	0.092	0.105	9.87 (±3.65)
25	0.172	0.167	0.169	0.087	0.084	0.100	12.72 (±3.08)
50	0.158	0.161	0.158	0.073	0.077	0.090	22.78 (±1.98)
100	0.144	0.142	0.143	0.058	0.058	0.074	38.90 (±3.91)
Media	0.084	0.079	0.078	0.000	0.000	0.000	-------
200	0.119	0.119	0.132	0.035	0.041	0.054	57.26 (±4.48)
300	0.113	0.112	0.106	0.029	0.034	0.028	69.48 (±4.79)
400	0.099	0.095	0.091	0.015	0.016	0.013	85.15 (±2.84)
500	0.086	0.095	0.089	0.002	0.016	0.011	90.54 (±6.86)
Vehicle Control	0.172	0.176	0.194	0.089	0.097	0.116	4.92 (±2.91)

Appendix: 5

Percentage growth inhibition of cancer cells at various concentrations (µg/ml) of crude ethanolic extracts of *Caralluma tuberculata* using neutral red uptake assay

Concentration (µg/ml)	Absorbance (cells + extract + media)			Actual Absorbance (cells + extract)- media			% Growth Inhibition (Mean ± STDEV)
Experiments	**1**	**2**	**3**	**1**	**2**	**3**	
MCF-7 Cells							
Media	0.066	0.065	0.066	0.000	0.000	0.000	-------
Media + Cells	0.126	0.129	0.126	0.060	0.064	0.060	-------
10	0.108	0.107	0.110	0.043	0.042	0.044	30.12 (±3.02)
25	0.097	0.102	0.100	0.032	0.037	0.034	43.92 (±3.02)
50	0.100	0.100	0.096	0.034	0.035	0.030	46.06 (±3.02)
100	0.094	0.096	0.093	0.028	0.031	0.027	53.36 (±3.02)
Media	0.066	0.065	0.065	0.000	0.000	0.000	-------
200	0.096	0.090	0.094	0.030	0.025	0.028	52.69 (±3.02)
300	0.081	0.082	0.079	0.016	0.017	0.014	73.72 (±3.02)
400	0.073	0.073	0.072	0.007	0.009	0.007	87.20 (±3.02)
500	0.068	0.070	0.068	0.003	0.005	0.003	93.87 (±3.02)
Vehicle Control	0.126	0.123	0.124	0.060	0.058	0.058	4.03 (±3.02)
MDA MB-468 Cells							
Media	0.095	0.086	0.073	0.000	0.000	0.000	-------
Media + Cells	0.167	0.186	0.178	0.071	0.100	0.105	-------
10	0.162	0.171	0.154	0.066	0.085	0.081	14.89 (±7.84)
25	0.153	0.153	0.139	0.057	0.067	0.066	29.89 (±9.29)
50	0.132	0.138	0.134	0.037	0.053	0.061	46.06 (±3.57)
100	0.128	0.137	0.131	0.032	0.051	0.058	49.48 (±5.00)
Media	0.078	0.071	0.073	0.000	0.000	0.000	-------
200	0.112	0.115	0.115	0.034	0.044	0.043	56.11 (±3.18)
300	0.103	0.112	0.112	0.025	0.040	0.040	62.32 (±2.72)
400	0.093	0.097	0.109	0.015	0.026	0.037	72.69 (±7.27)
500	0.095	0.092	0.084	0.017	0.021	0.012	81.34 (±6.53)
Vehicle Control	0.152	0.176	0.174	0.074	0.105	0.102	-1.82 (±4.23)
Caco-2 Cells							
Media	0.072	0.087	0.079	0.000	0.000	0.000	-------
Media + Cells	0.147	0.183	0.184	0.075	0.097	0.104	-------
10	0.127	0.156	0.170	0.055	0.070	0.090	22.80 (±8.12)
25	0.119	0.149	0.141	0.046	0.062	0.061	38.42 (±2.65)
50	0.121	0.141	0.136	0.048	0.054	0.056	41.89 (±5.78)
100	0.106	0.130	0.117	0.033	0.043	0.038	58.28 (±4.55)
Media	0.080	0.080	0.073	0.000	0.000	0.000	-------
200	0.107	0.107	0.107	0.027	0.027	0.034	68.74 (±2.70)
300	0.100	0.096	0.102	0.020	0.016	0.029	75.80 (±7.48)
400	0.084	0.091	0.085	0.004	0.011	0.012	92.47 (±3.32)
500	0.082	0.085	0.076	0.002	0.005	0.003	96.52 (±1.33)
Vehicle Control	0.161	0.171	0.183	0.080	0.091	0.110	-2.70 (±6.69)

Appendix: 6

Percentage growth inhibition of cancer cells at various concentrations (µg/ml) of crude ethanolic extracts of *Fagonia indica* using neutral red uptake assay

Concentration (µg/ml)	Absorbance (cells + extract + media)			Actual Absorbance (cells + extract)- media			% Growth Inhibition (Mean ± STDEV)
Experiments	**1**	**2**	**3**	**1**	**2**	**3**	
MCF-7 Cells							
Media	0.071	0.065	0.069	0.000	0.000	0.000	-------
Media + Cells	0.133	0.129	0.139	0.063	0.064	0.070	-------
10	0.120	0.109	0.116	0.049	0.044	0.047	29.00 (±6.12)
25	0.111	0.111	0.114	0.040	0.047	0.045	33.05 (±6.12)
50	0.108	0.100	0.107	0.037	0.035	0.038	44.17 (±6.12)
100	0.100	0.100	0.101	0.030	0.035	0.032	50.76 (±6.12)
Media	0.065	0.068	0.068	0.000	0.000	0.000	-------
200	0.094	0.102	0.100	0.029	0.035	0.032	51.50 (±6.12)
300	0.099	0.091	0.093	0.034	0.023	0.025	58.09 (±6.12)
400	0.083	0.075	0.078	0.018	0.008	0.010	81.68 (±6.12)
500	0.070	0.069	0.069	0.005	0.001	0.001	96.15 (±6.12)
Vehicle Control	0.137	0.133	0.130	0.072	0.066	0.062	-1.61 (±6.12)
MDA MB-468 Cells							
Media	0.079	0.078	0.085	0.000	0.000	0.000	-------
Media + Cells	0.189	0.164	0.165	0.110	0.086	0.081	-------
10	0.163	0.150	0.158	0.084	0.072	0.074	16.02 (±7.56)
25	0.151	0.144	0.144	0.072	0.066	0.060	27.89 (±6.18)
50	0.131	0.124	0.132	0.052	0.046	0.048	46.82 (±6.10)
100	0.128	0.119	0.112	0.050	0.040	0.027	58.08 (±7.16)
Media	0.073	0.073	0.079	0.000	0.000	0.000	-------
200	0.113	0.109	0.118	0.039	0.036	0.039	58.75 (±4.08)
300	0.097	0.101	0.105	0.024	0.028	0.027	71.62 (±4.87)
400	0.099	0.091	0.089	0.026	0.018	0.011	80.89 (±6.24)
500	0.092	0.086	0.086	0.019	0.013	0.008	86.18 (±4.68)
Vehicle Control	0.178	0.162	0.164	0.105	0.089	0.086	-1.49 (±6.05)
Caco-2 Cells							
Media	0.068	0.083	0.071	0.000	0.000	0.000	-------
Media + Cells	0.164	0.176	0.184	0.096	0.093	0.113	-------
10	0.134	0.152	0.146	0.066	0.069	0.076	30.13 (±3.93)
25	0.128	0.138	0.131	0.060	0.055	0.060	41.77 (±4.63)
50	0.113	0.122	0.116	0.045	0.039	0.045	56.89 (±3.73)
100	0.114	0.114	0.113	0.045	0.031	0.043	60.74 (±7.43)
Media	0.078	0.094	0.078	0.000	0.000	0.000	-------
200	0.112	0.128	0.114	0.035	0.035	0.036	65.06 (±2.96)
300	0.102	0.119	0.097	0.025	0.025	0.019	76.97 (±5.61)
400	0.095	0.101	0.085	0.017	0.007	0.007	89.64 (±6.62)
500	0.087	0.097	0.081	0.009	0.003	0.003	94.97 (±3.80)
Vehicle Control	0.168	0.182	0.181	0.090	0.088	0.103	6.93 (±2.10)

Appendix: 7

Percentage growth inhibition of cancer cells at various concentrations (µg/ml) of crude ethanolic extracts of *Solanum surattense* using neutral red uptake assay

Concentration (µg/ml)	Absorbance (cells + extract + media)			Actual Absorbance (cells + extract)- media			% Growth Inhibition (Mean ± STDEV)
Experiments	**1**	**2**	**3**	**1**	**2**	**3**	
MCF-7 Cells							
Media	0.071	0.071	0.067	0.000	0.000	0.000	-------
Media + Cells	0.141	0.139	0.138	0.070	0.068	0.071	-------
10	0.123	0.123	0.118	0.052	0.052	0.051	25.76 (±2.18)
25	0.120	0.124	0.118	0.049	0.053	0.051	26.60 (±4.23)
50	0.117	0.118	0.120	0.046	0.047	0.053	30.52 (±4.32)
100	0.109	0.109	0.110	0.038	0.038	0.043	42.99 (±3.36)
Media	0.073	0.066	0.070	0.000	0.000	0.000	-------
200	0.098	0.102	0.095	0.025	0.037	0.025	59.78 (±6.73)
300	0.089	0.092	0.087	0.017	0.026	0.017	72.47 (±5.63)
400	0.075	0.074	0.076	0.003	0.008	0.007	91.78 (±3.63)
500	0.074	0.071	0.071	0.001	0.005	0.001	96.86 (±2.95)
Vehicle Control	0.141	0.142	0.141	0.068	0.076	0.071	-3.45 (±7.82)
MDA MB-468 Cells							
Media	0.083	0.078	0.0789	0.000	0.000	0.000	-------
Media + Cells	0.172	0.164	0.176	0.089	0.086	0.097	-------
10	0.156	0.152	0.166	0.073	0.074	0.087	13.98 (±3.97)
25	0.141	0.142	0.149	0.058	0.063	0.070	29.60 (±3.97)
50	0.137	0.139	0.128	0.054	0.061	0.050	39.31 (±3.97)
100	0.123	0.131	0.111	0.040	0.053	0.032	53.53 (±3.97)
Media	0.073	0.073	0.094	0.000	0.000	0.000	-------
200	0.115	0.118	0.126	0.042	0.044	0.032	55.75 (±3.97)
300	0.110	0.102	0.118	0.037	0.028	0.024	66.62 (±3.97)
400	0.098	0.1067	0.106	0.024	0.033	0.012	73.72 (±3.97)
500	0.075	0.086	0.096	0.002	0.013	0.003	93.29 (±3.97)
Vehicle Control	0.164	0.158	0.187	0.091	0.085	0.093	1.38 (±3.97)
Caco-2 Cells							
Media	0.072	0.081	0.081	0.000	0.000	0.000	-------
Media + Cells	0.147	0.168	0.180	0.075	0.087	0.099	-------
10	0.131	0.157	0.149	0.059	0.076	0.068	21.58 (±9.58)
25	0.130	0.148	0.139	0.057	0.067	0.058	29.12 (±9.58)
50	0.119	0.144	0.136	0.047	0.063	0.056	36.34 (±9.58)
100	0.115	0.132	0.127	0.043	0.051	0.046	45.72 (±9.58)
Media	0.080	0.090	0.077	0.000	0.000	0.000	-------
200	0.119	0.116	0.107	0.039	0.026	0.030	62.49 (±9.58)
300	0.099	0.102	0.099	0.019	0.012	0.022	79.29 (±9.58)
400	0.091	0.096	0.091	0.011	0.006	0.014	87.80 (±9.58)
500	0.092	0.091	0.087	0.012	0.001	0.010	91.13 (±9.58)
Vehicle Control	0.161	0.173	0.169	0.080	0.083	0.092	1.43 (±9.58)

Appendix: 8

Percentage growth inhibition of cancer cells at various concentrations (µg/ml) of crude ethanolic extracts of *Arisaema utile* using neutral red uptake assay

Concentration (µg/ml)	Absorbance (cells + extract + media)			Actual Absorbance (cells + extract)- media			% Growth Inhibition (Mean ± STDEV)
Experiments	**1**	**2**	**3**	**1**	**2**	**3**	
MCF-7 Cells							
Media	0.085	0.080	0.077	0.000	0.000	0.000	-------
Media + Cells	0.143	0.139	0.143	0.058	0.058	0.067	-------
10	0.135	0.130	0.130	0.050	0.049	0.053	16.76 (±3.49)
25	0.125	0.124	0.121	0.040	0.044	0.045	29.69 (±3.49)
50	0.116	0.118	0.111	0.031	0.038	0.035	43.06 (±3.49)
100	0.108	0.100	0.099	0.023	0.019	0.023	64.51 (±3.49)
Media	0.076	0.075	0.077	0.000	0.000	0.000	-------
200	0.088	0.084	0.086	0.012	0.009	0.009	84.23 (±3.49)
300	0.078	0.081	0.079	0.002	0.006	0.002	94.82 (±3.49)
400	0.076	0.077	0.078	0.001	0.002	0.001	98.39 (±3.49)
500	0.076	0.077	0.078	0.001	0.002	0.001	98.08 (±3.49)
Vehicle Control	0.143	0.140	0.136	0.068	0.065	0.059	-5.51 (±3.49)
MDA MB-468 Cells							
Media	0.080	0.074	0.085	0.000	0.000	0.000	-------
Media + Cells	0.187	0.169	0.165	0.107	0.096	0.081	-------
10	0.176	0.147	0.153	0.096	0.073	0.068	16.30 (±6.52)
25	0.160	0.153	0.145	0.080	0.080	0.061	22.26 (±4.79)
50	0.139	0.136	0.139	0.059	0.063	0.055	37.25 (±7.02)
100	0.132	0.114	0.131	0.052	0.041	0.046	50.59 (±7.39)
Media	0.079	0.077	0.079	0.000	0.000	0.000	-------
200	0.114	0.116	0.102	0.036	0.039	0.023	65.02 (±6.31)
300	0.097	0.117	0.096	0.018	0.039	0.017	73.18 (±12.58)
400	0.091	0.098	0.095	0.012	0.021	0.016	82.10 (±5.11)
500	0.090	0.090	0.091	0.012	0.013	0.012	86.67 (±1.59)
Vehicle Control	0.179	0.167	0.168	0.101	0.089	0.090	0.29 (±10.14)
Caco-2 Cells							
Media	0.071	0.078	0.087	0.000	0.000	0.000	-------
Media + Cells	0.184	0.186	0.145	0.113	0.108	0.059	-------
10	0.151	0.172	0.136	0.081	0.094	0.049	19.43 (±8.35)
25	0.155	0.165	0.127	0.084	0.087	0.040	25.87 (±6.06)
50	0.130	0.152	0.118	0.060	0.074	0.032	41.53 (±8.93)
100	0.127	0.130	0.121	0.056	0.052	0.034	48.11 (±5.05)
Media	0.078	0.073	0.095	0.000	0.000	0.000	-------
200	0.114	0.118	0.110	0.035	0.044	0.015	66.37 (±7.66)
300	0.109	0.109	0.106	0.031	0.036	0.011	72.50 (±7.14)
400	0.087	0.096	0.095	0.009	0.022	0.000	90.14 (±10.00)
500	0.081	0.093	0.094	0.002	0.020	0.000	93.30 (±9.97)
Vehicle Control	0.181	0.187	0.148	0.103	0.114	0.054	4.30 (±8.05)

Appendix: 9

Percentage growth inhibition of cancer cells at 200 µg/ml concentration of fractions from *Caralluma tuberculata* using MTT assay

Concentration (µg/ml)	Absorbance (cells + fraction + media)			Actual Absorbance (cells + fraction)- media			% Growth Inhibition (Mean ± STDEV)
Experiments	**1**	**2**	**3**	**1**	**2**	**3**	
MCF-7 Cells							
Media	0.068	0.071	0.079	0.000	0.000	0.000	-------
Media + Cells	0.171	0.176	0.182	0.102	0.106	0.103	-------
Hexane Frac.	0.124	0.117	0.130	0.056	0.046	0.051	50.62 (±5.38)
Chloroform Frac.	0.087	0.101	0.094	0.019	0.030	0.015	79.69(±7.45)
Ethyl acetate Frac.	0.070	0.077	0.086	0.002	0.007	0.007	95.00(±2.64)
Methanol Frac.	0.094	0.104	0.095	0.026	0.034	0.016	75.88(±8.41)
Aqueous Frac.	0.106	0.116	0.113	0.021	0.021	0.024	54.33(±1.89)
Vehicle Control	0.171	0.176	0.172	0.103	0.105	0.093	3.17(±5.67)
MDA MB-468 Cells							
Media	0.080	0.086	0.085	0.000	0.000	0.000	-------
Media + Cells	0.187	0.179	0.165	0.107	0.094	0.081	-------
Hexane Frac.	0.177	0.175	0.164	0.097	0.089	0.079	5.29 (±3.51)
Chloroform Frac.	0.166	0.154	0.151	0.086	0.068	0.067	21.38 (±5.11)
Ethyl acetate Frac.	0.144	0.139	0.140	0.064	0.053	0.055	38.47 (±6.42)
Methanol Frac.	0.158	0.150	0.147	0.078	0.064	0.063	26.88 (±4.88)
Aqueous Frac.	0.161	0.163	0.161	0.073	0.085	0.076	17.10 (±7.15)
Vehicle Control	0.179	0.186	0.168	0.099	0.100	0.084	-1.31 (±7.44)
Caco-2 Cells							
Media	0.073	0.071	0.073	0.000	0.000	0.000	-------
Media + Cells	0.172	0.184	0.181	0.099	0.113	0.108	-------
Hexane Frac.	0.148	0.166	0.156	0.075	0.095	0.082	21.25 (±4.5)
Chloroform Frac.	0.103	0.117	0.114	0.029	0.047	0.040	63.88 (±5.99)
Ethyl acetate Frac.	0.080	0.074	0.085	0.006	0.003	0.011	93.44 (±3.89)
Methanol Frac.	0.122	0.139	0.127	0.048	0.068	0.054	46.84 (±6.22)
Aqueous Frac.	0.121	0.128	0.115	0.033	0.050	0.031	26.74 (±3.64)
Vehicle Control	0.178	0.181	0.185	0.105	0.110	0.112	-2.51 (±4.57)

Appendix: 10

Percentage growth inhibition of cancer cells at 200 µg/ml concentration of fractions from *Fagonia indica* using MTT assay

Concentration (µg/ml)	Absorbance (cells + fraction + media)			Actual Absorbance (cells + fraction)- media			% Growth Inhibition
Experiments	**1**	**2**	**3**	**1**	**2**	**3**	(Mean ± STDEV)
MCF-7 Cells							
Media	0.078	0.086	0.084	0.000	0.000	0.000	-------
Media + Cells	0.171	0.176	0.182	0.093	0.090	0.098	-------
Hexane Frac.	0.114	0.112	0.107	0.037	0.026	0.023	69.36 (±8.02)
Chloroform Frac.	0.095	0.114	0.103	0.018	0.028	0.019	76.93 (±6.84)
Ethyl acetate Frac.	0.080	0.092	0.093	0.002	0.006	0.009	93.88 (±3.31)
Methanol Frac.	0.139	0.134	0.138	0.061	0.048	0.054	42.01 (±6.67)
Aqueous Frac.	0.102	0.109	0.108	0.017	0.014	0.019	65.37 (±3.34)
Vehicle Control	0.171	0.176	0.172	0.093	0.090	0.088	3.32 (±5.94)
MDA MB-468 Cells							
Media	0.080	0.086	0.085	0.000	0.000	0.000	-------
Media + Cells	0.187	0.179	0.165	0.107	0.094	0.081	-------
Hexane Frac.	0.169	0.171	0.158	0.089	0.085	0.073	11.61 (±4.37)
Chloroform Frac.	0.116	0.114	0.103	0.036	0.028	0.018	71.14 (±5.58)
Ethyl acetate Frac.	0.088	0.086	0.093	0.008	0.000	0.008	94.02 (±5.23)
Methanol Frac.	0.141	0.134	0.125	0.061	0.048	0.041	47.15 (±3.30)
Aqueous Frac.	0.141	0.140	0.134	0.053	0.061	0.050	42.13 (±2.11)
Vehicle Control	0.179	0.186	0.168	0.099	0.100	0.084	-1.31 (±7.44)
Caco-2 Cells							
Media	0.073	0.071	0.070	0.000	0.000	0.000	-------
Media + Cells	0.172	0.184	0.179	0.099	0.113	0.109	-------
Hexane Frac.	0.162	0.159	0.158	0.088	0.089	0.088	17.41 (±5.86)
Chloroform Frac.	0.095	0.114	0.103	0.022	0.043	0.033	69.74 (±7.92)
Ethyl acetate Frac.	0.080	0.086	0.081	0.007	0.015	0.011	89.89 (±3.45)
Methanol Frac.	0.139	0.134	0.126	0.065	0.063	0.056	42.39 (±7.62)
Aqueous Frac.	0.131	0.133	0.122	0.043	0.054	0.037	19.73 (±4.71)
Vehicle Control	0.178	0.181	0.186	0.105	0.110	0.116	-3.28 (±5.13)

Appendix: 11

Percentage growth inhibition of cancer cells at 200 µg/ml concentration of fractions from *Solanum surratense* using MTT assay

Concentration (µg/ml)	Absorbance (cells + fraction + media)			Actual Absorbance (cells + fraction)- media			% Growth Inhibition (Mean ± STDEV)
Experiments	**1**	**2**	**3**	**1**	**2**	**3**	
MCF-7 Cells							
Media	0.073	0.070	0.078	0.000	0.000	0.000	-------
Media + Cells	0.164	0.184	0.167	0.091	0.114	0.089	-------
Hexane Frac.	0.121	0.133	0.118	0.047	0.063	0.040	49.08 (±5.21)
Chloroform Frac.	0.090	0.087	0.088	0.016	0.017	0.010	85.33 (±3.41)
Ethyl acetate Frac.	0.103	0.102	0.107	0.030	0.032	0.029	68.62 (±2.48)
Methanol Frac.	0.115	0.129	0.126	0.041	0.059	0.048	49.20 (±4.76)
Aqueous Frac.	0.124	0.134	0.135	0.039	0.039	0.046	14.09 (±3.76)
Vehicle Control	0.168	0.176	0.160	0.095	0.106	0.082	3.43 (±6.80)
MDA MB-468 Cells							
Media	0.073	0.086	0.074	0.000	0.000	0.000	-------
Media + Cells	0.178	0.186	0.169	0.105	0.100	0.096	-------
Hexane Frac.	0.172	0.173	0.160	0.099	0.087	0.087	9.43 (±3.82)
Chloroform Frac.	0.082	0.088	0.079	0.009	0.002	0.005	94.59 (±3.00)
Ethyl acetate Frac.	0.118	0.123	0.107	0.045	0.037	0.033	61.82 (±4.07)
Methanol Frac.	0.146	0.144	0.136	0.072	0.058	0.062	35.96 (±5.63)
Aqueous Frac.	0.158	0.156	0.147	0.070	0.078	0.062	26.19 (±3.44)
Vehicle Control	0.180	0.186	0.167	0.107	0.101	0.093	0.20 (±2.34)
Caco-2 Cells							
Media	0.078	0.070	0.078	0.000	0.000	0.000	-------
Media + Cells	0.186	0.176	0.167	0.108	0.107	0.089	-------
Hexane Frac.	0.172	0.173	0.160	0.094	0.103	0.082	7.77 (±4.83)
Chloroform Frac.	0.082	0.080	0.079	0.004	0.010	0.001	95.25(±4.35)
Ethyl acetate Frac.	0.118	0.102	0.107	0.040	0.033	0.029	66.43(±3.24)
Methanol Frac.	0.146	0.129	0.126	0.068	0.060	0.048	42.19(±4.27)
Aqueous Frac.	0.140	0.142	0.127	0.052	0.064	0.042	5.85(±2.93)
Vehicle Control	0.187	0.172	0.162	0.109	0.102	0.084	2.92(±3.20)

Appendix: 12

Percentage growth inhibition of cancer cells at 200 µg/ml concentration of fractions from *Arisaema utile* using MTT assay

Concentration (µg/ml)	Absorbance (cells + fraction + media)			Actual Absorbance (cells + fraction)- media			% Growth Inhibition (Mean ± STDEV)
Experiments	**1**	**2**	**3**	**1**	**2**	**3**	
MCF-7 Cells							
Media	0.080	0.090	0.090	0.000	0.000	0.000	-------
Media + Cells	0.164	0.184	0.167	0.084	0.094	0.076	-------
Hexane Frac.	0.130	0.135	0.126	0.050	0.045	0.036	48.58 (±7.36)
Chloroform Frac.	0.105	0.114	0.114	0.025	0.024	0.023	71.19 (±2.76)
Ethyl acetate Frac.	0.135	0.131	0.130	0.055	0.041	0.040	45.96 (±10.67)
Methanol Frac.	0.104	0.101	0.104	0.024	0.011	0.013	80.77 (±8.38)
Aqueous Frac.	0.126	0.138	0.137	0.041	0.042	0.048	9.14 (±3.01)
Vehicle Control	0.168	0.176	0.160	0.088	0.086	0.069	4.23 (±7.80)
MDA MB-468 Cells							
Media	0.073	0.071	0.077	0.000	0.000	0.000	-------
Media + Cells	0.178	0.186	0.169	0.106	0.115	0.092	-------
Hexane Frac.	0.173	0.169	0.164	0.100	0.098	0.086	8.62 (±5.08)
Chloroform Frac.	0.090	0.078	0.088	0.017	0.006	0.011	88.86 (±5.29)
Ethyl acetate Frac.	0.135	0.131	0.131	0.062	0.060	0.054	43.26 (±3.73)
Methanol Frac.	0.107	0.101	0.104	0.035	0.030	0.026	70.86 (±3.61)
Aqueous Frac.	0.158	0.169	0.162	0.070	0.090	0.078	15.96 (±7.66)
Vehicle Control	0.180	0.186	0.167	0.108	0.115	0.089	0.25 (±2.39)
Caco-2 Cells							
Media	0.078	0.070	0.075	0.000	0.000	0.000	-------
Media + Cells	0.186	0.176	0.167	0.108	0.107	0.092	-------
Hexane Frac.	0.173	0.169	0.164	0.095	0.100	0.089	7.40 (±4.74)
Chloroform Frac.	0.090	0.078	0.076	0.012	0.008	0.001	93.59 (±5.00)
Ethyl acetate Frac.	0.135	0.131	0.131	0.057	0.062	0.056	42.62 (±4.42)
Methanol Frac.	0.104	0.101	0.104	0.026	0.032	0.029	71.56 (±3.76)
Aqueous Frac.	0.126	0.124	0.115	0.038	0.045	0.031	31.58 (±3.47)
Vehicle Control	0.187	0.172	0.162	0.109	0.102	0.087	2.86 (±3.14)

Appendix: 13

Percentage growth inhibition of cancer cells at 200 µg/ml concentration of fractions from *Caralluma tuberculata* using neutral red uptake assay

Concentration (µg/ml)	Absorbance (cells + fraction + media)			Actual Absorbance (cells + fraction)- media			% Growth Inhibition (Mean ± STDEV)
Experiments	**1**	**2**	**3**	**1**	**2**	**3**	
MCF-7 Cells							
Media	0.065	0.062	0.068	0.000	0.000	0.000	-------
Media + Cells	0.132	0.130	0.132	0.067	0.068	0.065	-------
Hexane Frac.	0.114	0.111	0.110	0.049	0.049	0.043	29.57 (±3.87)
Chloroform Frac.	0.094	0.092	0.094	0.029	0.030	0.027	57.05 (±1.42)
Ethyl acetate Frac.	0.070	0.069	0.069	0.004	0.006	0.001	94.13 (±4.01)
Methanol Frac.	0.085	0.081	0.079	0.020	0.019	0.011	75.18 (±6.32)
Aqueous Frac.	0.110	0.102	0.100	0.044	0.041	0.038	59.84 (±4.19)
Vehicle Control	0.131	0.132	0.132	0.065	0.070	0.065	-0.19 (±2.68)
MDA MB-468 Cells							
Media	0.081	0.074	0.073	0.000	0.000	0.000	-------
Media + Cells	0.183	0.184	0.173	0.102	0.109	0.100	-------
Hexane Frac.	0.168	0.168	0.161	0.087	0.094	0.088	13.65 (±1.46)
Chloroform Frac.	0.152	0.139	0.127	0.071	0.065	0.053	39.47 (±8.05)
Ethyl acetate Frac.	0.138	0.130	0.129	0.057	0.056	0.056	45.55 (±2.83)
Methanol Frac.	0.147	0.138	0.141	0.066	0.064	0.067	36.37 (±4.64)
Aqueous Frac.	0.155	0.152	0.161	0.081	0.071	0.087	19.82 (±10.85)
Vehicle Control	0.175	0.183	0.165	0.094	0.108	0.091	5.97 (±4.38)
Caco-2 Cells							
Media	0.087	0.086	0.075	0.000	0.000	0.000	-------
Media + Cells	0.183	0.177	0.184	0.097	0.091	0.109	-------
Hexane Frac.	0.147	0.156	0.156	0.060	0.070	0.081	28.79 (±7.77)
Chloroform Frac.	0.126	0.117	0.114	0.040	0.032	0.040	62.68 (±3.33)
Ethyl acetate Frac.	0.086	0.086	0.089	-0.001	0.000	0.014	96.00 (±7.65)
Methanol Frac.	0.123	0.139	0.127	0.036	0.053	0.052	52.14 (±10.53)
Aqueous Frac.	0.113	0.128	0.116	0.036	0.053	0.039	56.59 (±7.02)
Vehicle Control	0.171	0.171	0.190	0.084	0.085	0.115	4.57 (±9.23)

Appendix: 14

Percentage growth inhibition of cancer cells at 200 µg/ml concentration of fractions from *Fagonia indica* using neutral red uptake assay

Concentration (µg/ml)	Absorbance (cells + fraction + media)			Actual Absorbance (cells + fraction)- media			% Growth Inhibition (Mean ± STDEV)
Experiments	**1**	**2**	**3**	**1**	**2**	**3**	
MCF-7 Cells							
Media	0.065	0.062	0.068	0.000	0.000	0.000	-------
Media + Cells	0.132	0.130	0.132	0.067	0.068	0.065	-------
Hexane Frac.	0.097	0.096	0.096	0.032	0.034	0.028	53.16 (±3.31)
Chloroform Frac.	0.076	0.078	0.078	0.011	0.016	0.010	81.67 (±4.15)
Ethyl acetate Frac.	0.070	0.068	0.070	0.004	0.006	0.002	93.81 (±2.32)
Methanol Frac.	0.110	0.104	0.107	0.045	0.042	0.040	36.76 (±3.05)
Aqueous Frac.	0.116	0.121	0.119	0.051	0.059	0.056	46.04 (±2.26)
Vehicle Control	0.131	0.132	0.132	0.065	0.070	0.065	-0.19 (±2.68)
MDA MB-468 Cells							
Media	0.081	0.074	0.073	0.000	0.000	0.000	-------
Media + Cells	0.183	0.184	0.173	0.102	0.109	0.100	-------
Hexane Frac.	0.156	0.160	0.157	0.075	0.086	0.084	21.39 (±5.17)
Chloroform Frac.	0.111	0.101	0.086	0.030	0.026	0.013	77.92 (±8.42)
Ethyl acetate Frac.	0.085	0.084	0.084	0.004	0.010	0.011	92.04 (±3.80)
Methanol Frac.	0.127	0.121	0.117	0.046	0.046	0.044	56.26 (±1.54)
Aqueous Frac.	0.135	0.143	0.127	0.061	0.062	0.053	40.52 (±10.89)
Vehicle Control	0.175	0.183	0.165	0.094	0.108	0.091	5.97 (±4.38)
Caco-2 Cells							
Media	0.087	0.086	0.075	0.000	0.000	0.000	-------
Media + Cells	0.183	0.177	0.184	0.097	0.091	0.109	-------
Hexane Frac.	0.144	0.150	0.157	0.057	0.064	0.083	31.80 (±8.46)
Chloroform Frac.	0.095	0.105	0.104	0.009	0.019	0.029	81.16 (±9.03)
Ethyl acetate Frac.	0.087	0.086	0.080	0.000	0.001	0.006	97.94 (±2.83)
Methanol Frac.	0.142	0.130	0.125	0.055	0.044	0.051	49.35 (±5.57)
Aqueous Frac.	0.130	0.130	0.150	0.053	0.056	0.074	38.25 (±10.11)
Vehicle Control	0.171	0.171	0.190	0.084	0.085	0.115	4.57 (±9.23)

Appendix: 15

Percentage growth inhibition of cancer cells at 200 µg/ml concentration of fractions from *Solanum surattense* using neutral red uptake assay

Concentration (µg/ml)	Absorbance (cells + fraction + media)			Actual Absorbance (cells + fraction)- media			% Growth Inhibition (Mean ± STDEV)
Experiments	**1**	**2**	**3**	**1**	**2**	**3**	
MCF-7 Cells							
Media	0.065	0.061	0.068	0.000	0.000	0.000	-------
Media + Cells	0.156	0.158	0.156	0.091	0.097	0.088	-------
Hexane Frac.	0.135	0.138	0.137	0.070	0.078	0.069	21.44 (±1.54)
Chloroform Frac.	0.070	0.064	0.068	0.005	0.003	-0.001	97.29 (±3.14)
Ethyl acetate Frac.	0.093	0.091	0.085	0.028	0.030	0.016	73.32 (±7.16)
Methanol Frac.	0.124	0.121	0.121	0.059	0.061	0.053	37.47 (±2.49)
Aqueous Frac.	0.145	0.142	0.147	0.079	0.081	0.085	20.31 (±3.42)
Vehicle Control	0.155	0.149	0.155	0.089	0.088	0.087	4.08 (±4.16)
MDA MB-468 Cells							
Media	0.082	0.081	0.081	0.000	0.000	0.000	-------
Media + Cells	0.187	0.186	0.168	0.105	0.105	0.087	-------
Hexane Frac.	0.173	0.155	0.152	0.091	0.074	0.071	20.48 (±8.08)
Chloroform Frac.	0.085	0.085	0.082	0.003	0.004	0.001	97.42 (±1.70)
Ethyl acetate Frac.	0.114	0.102	0.099	0.032	0.021	0.017	76.40 (±5.91)
Methanol Frac.	0.130	0.127	0.131	0.048	0.046	0.050	51.11 (±7.29)
Aqueous Frac.	0.142	0.145	0.135	0.068	0.064	0.061	34.70 (±10.83)
Vehicle Control	0.185	0.186	0.175	0.103	0.106	0.093	-2.01 (±4.79)
Caco-2 Cells							
Media	0.071	0.072	0.071	0.000	0.000	0.000	-------
Media + Cells	0.184	0.183	0.184	0.113	0.112	0.113	-------
Hexane Frac.	0.172	0.173	0.162	0.101	0.101	0.091	13.28 (±5.49)
Chloroform Frac.	0.082	0.077	0.076	0.011	0.006	0.006	93.27 (±2.88)
Ethyl acetate Frac.	0.118	0.100	0.105	0.048	0.028	0.034	67.47 (±8.57)
Methanol Frac.	0.143	0.127	0.131	0.072	0.056	0.060	44.53 (±7.27)
Aqueous Frac.	0.137	0.136	0.140	0.060	0.061	0.063	36.76 (±12.87)
Vehicle Control	0.183	0.180	0.181	0.112	0.109	0.110	2.13 (±0.93)

Appendix: 16

Percentage growth inhibition of cancer cells at 200 µg/ml concentration of fractions from *Arisaema utile* using neutral red uptake assay

Concentration (µg/ml)	Absorbance (cells + fraction + media)			Actual Absorbance (cells + fraction)- media			% Growth Inhibition (Mean ± STDEV)
Experiments	**1**	**2**	**3**	**1**	**2**	**3**	
MCF-7 Cells							
Media	0.065	0.061	0.068	0.000	0.000	0.000	-------
Media + Cells	0.156	0.158	0.156	0.091	0.097	0.088	-------
Hexane Frac.	0.136	0.135	0.135	0.070	0.074	0.067	23.45 (±0.82)
Chloroform Frac.	0.076	0.061	0.069	0.011	0.001	0.001	95.53 (±6.62)
Ethyl acetate Frac.	0.127	0.123	0.126	0.061	0.062	0.058	34.36 (±1.90)
Methanol Frac.	0.094	0.092	0.093	0.028	0.031	0.025	69.58 (±2.17)
Aqueous Frac.	0.140	0.141	0.141	0.074	0.080	0.079	24.45 (±1.00)
Vehicle Control	0.155	0.149	0.155	0.089	0.088	0.087	4.08 (±4.16)
MDA MB-468 Cells							
Media	0.082	0.081	0.081	0.000	0.000	0.000	-------
Media + Cells	0.187	0.186	0.168	0.105	0.105	0.087	-------
Hexane Frac.	0.169	0.152	0.148	0.088	0.071	0.067	23.91 (±7.68)
Chloroform Frac.	0.082	0.081	0.087	0.001	0.001	0.006	97.41 (±3.33)
Ethyl acetate Frac.	0.120	0.107	0.129	0.038	0.026	0.047	61.35 (±14.88)
Methanol Frac.	0.093	0.097	0.091	0.011	0.017	0.010	87.29 (±2.88)
Aqueous Frac.	0.144	0.164	0.156	0.069	0.083	0.082	21.72 (±3.43)
Vehicle Control	0.185	0.186	0.175	0.103	0.106	0.093	-2.01 (±4.79)
Caco-2 Cells							
Media	0.071	0.072	0.071	0.000	0.000	0.000	-------
Media + Cells	0.184	0.183	0.184	0.113	0.112	0.113	-------
Hexane Frac.	0.172	0.163	0.166	0.102	0.092	0.095	14.61 (±3.91)
Chloroform Frac.	0.089	0.079	0.077	0.019	0.007	0.006	90.38 (±6.05)
Ethyl acetate Frac.	0.134	0.137	0.130	0.064	0.066	0.059	44.25 (±3.32)
Methanol Frac.	0.107	0.103	0.115	0.037	0.031	0.044	66.99 (±5.53)
Aqueous Frac.	0.124	0.128	0.119	0.047	0.053	0.043	50.99 (±11.29)
Vehicle Control	0.183	0.180	0.181	0.112	0.109	0.110	2.13 (±0.93)

Appendix: 17

Percentage growth inhibition of cancer cells at various concentrations (μM) of pregnane glycoside from *Caralluma tuberculata* using MTT assay after 24 hours treatment

Concentration (μM)	Absorbance (cells + Pregnane + media)			Actual Absorbance (cells + Pregnane)- media			% Growth Inhibition (Mean ± STDEV)
Experiments	**1**	**2**	**3**	**1**	**2**	**3**	
MCF-7 Cells							
Media	0.218	0.226	0.217	0.000	0.000	0.000	-------
Media + Cells	2.799	2.822	2.746	2.581	2.596	2.529	-------
0.78	2.791	2.789	2.720	2.573	2.562	2.503	0.87 (±0.49)
1.56	2.721	2.770	2.682	2.503	2.544	2.465	2.50 (±0.55)
3.12	2.718	2.690	2.642	2.500	2.464	2.425	4.11 (±0.96)
6.25	2.682	2.631	2.574	2.464	2.405	2.357	6.23 (±1.48)
12.5	2.205	2.344	2.202	1.987	2.117	1.985	20.97 (±2.34)
25	1.725	1.698	1.708	1.508	1.472	1.491	41.97 (±1.17)
50	0.229	0.231	0.233	0.011	0.005	0.016	99.58 (±0.23)
100	0.221	0.258	0.231	0.004	0.032	0.014	99.35 (±0.55)
Actinomycin-D	1.210	1.240	1.136	0.993	1.014	0.919	62.04 (±1.43)
Tamoxifen	1.377	1.364	1.401	0.111	0.062	0.045	84.74 (±4.33)
Anastrozole	1.555	1.486	1.555	0.289	0.185	0.199	51.72 (±3.42)
Vehicle Control	2.723	2.710	2.810	2.506	2.484	2.593	1.57 (±3.61)
MDA MB-468 Cells							
Media	0.523	0.668	0.816	0.000	0.000	0.000	-------
Media + Cells	2.869	3.008	3.024	2.347	2.340	2.209	-------
0.78	2.914	2.808	2.917	2.392	2.140	2.101	3.83 (±5.30)
1.56	2.863	2.958	2.805	2.340	2.290	1.989	4.10 (±5.12)
3.12	2.769	2.806	2.740	2.246	2.138	1.924	8.60 (±4.30)
6.25	2.578	2.684	2.663	2.056	2.016	1.847	14.21 (±2.01)
12.5	2.495	2.471	2.489	1.972	1.803	1.673	21.05 (±4.45)
25	2.163	2.312	2.455	1.640	1.643	1.639	28.56 (±2.39)
50	1.862	1.942	2.220	1.339	1.274	1.405	41.63 (±4.70)
100	1.787	1.801	1.860	1.265	1.133	1.044	50.14 (±3.54)
Actinomycin-D	1.526	1.518	1.529	1.003	0.850	0.713	62.87 (±5.28)
Tamoxifen	1.580	1.634	1.651	0.677	0.727	0.804	27.80 (±4.06)
Anastrozole	1.202	1.220	1.147	0.298	0.313	0.300	70.11 (±1.47)
Vehicle Control	2.779	2.948	3.055	2.256	2.280	2.239	1.68 (±5.28)
Caco-2 Cells							
Media	0.225	0.214	0.232	0.000	0.000	0.000	-------
Media + Cells	0.304	0.324	0.263	0.079	0.110	0.030	-------
0.78	0.303	0.319	0.261	0.078	0.105	0.029	3.56 (±1.80)
1.56	0.301	0.320	0.262	0.076	0.107	0.030	2.79 (±1.08)
3.12	0.294	0.315	0.259	0.069	0.101	0.026	11.22 (±2.64)
6.25	0.279	0.300	0.255	0.054	0.086	0.023	26.14 (±5.04)
12.5	0.275	0.291	0.251	0.049	0.077	0.018	35.71 (±4.77)
25	0.257	0.268	0.247	0.032	0.055	0.014	54.35 (±4.69)
50	0.256	0.254	0.242	0.031	0.040	0.010	63.77 (±3.26)
100	0.245	0.233	0.230	0.020	0.019	-0.002	78.63 (±4.22)
Actinomycin-D	0.256	0.251	0.242	0.031	0.037	0.009	65.40 (±4.29)
Vehicle Control	0.304	0.322	0.262	0.079	0.108	0.030	1.10 (±1.13)

Appendix: 18

Percentage growth inhibition of cancer cells at various concentrations (μM) of pregnane glycoside from *Caralluma tuberculata* using MTT assay after 48 hours treatment

Concentration (μM)	Absorbance (cells + Pregnane + media)			Actual Absorbance (cells + Pregnane)- media			% Growth Inhibition (Mean ± STDEV)
Experiments	**1**	**2**	**3**	**1**	**2**	**3**	
MCF-7 Cells							
Media	0.217	0.245	0.245	0.000	0.000	0.000	-------
Media + Cells	3.176	3.328	3.169	2.960	3.083	2.924	-------
0.78	3.105	3.255	3.072	2.888	3.010	2.827	2.71 (±0.54)
1.56	3.120	3.194	3.081	2.904	2.950	2.836	3.07 (±1.22)
3.12	3.119	3.180	3.059	2.902	2.935	2.814	3.51 (±1.44)
6.25	3.108	3.126	3.054	2.891	2.881	2.809	4.27 (±2.13)
12.5	2.192	2.165	2.228	1.975	1.921	1.982	34.39 (±2.92)
25	0.334	0.455	0.480	0.117	0.211	0.234	93.73 (±2.09)
50	0.196	0.226	0.220	-0.021	-0.018	-0.025	100.71 (±.013)
100	0.201	0.216	0.217	-0.016	-0.029	-0.028	100.81 (±0.24)
Actinomycin-D	0.774	0.748	0.813	0.558	0.503	0.568	81.81 (±1.65)
Tamoxifen	0.284	0.291	0.307	-0.005	0.000	0.007	99.64 (±1.14)
Anastrozole	0.855	0.459	0.503	0.565	0.168	0.203	46.39 (±6.43)
Vehicle Control	2.965	3.056	3.249	2.748	2.812	3.003	4.41 (±6.22)
MDA MB-468 Cells							
Media	0.240	0.292	0.353	0.000	0.000	0.000	-------
Media + Cells	2.988	3.174	2.965	2.748	2.882	2.613	-------
0.78	2.739	2.974	2.933	2.499	2.682	2.581	5.74 (±4.05)
1.56	2.829	2.964	2.725	2.590	2.672	2.372	7.42 (±1.72)
3.12	2.763	2.665	2.553	2.523	2.373	2.201	13.87 (±5.00)
6.25	2.818	2.758	2.706	2.579	2.466	2.353	10.18 (±4.14)
12.5	2.340	2.044	2.027	2.101	1.752	1.674	32.90 (±8.25)
25	2.178	2.225	2.234	1.938	1.933	1.882	30.13 (±2.54)
50	1.484	1.461	1.524	1.244	1.168	1.171	56.45 (±2.61)
100	1.250	1.223	1.372	1.010	0.931	1.020	63.97 (±3.42)
Actinomycin-D	0.664	0.548	0.511	0.425	0.256	0.159	89.86 (±4.81)
Tamoxifen	1.500	1.448	1.457	0.584	0.583	0.499	45.41 (±4.14)
Anastrozole	1.099	1.033	1.009	0.183	0.168	0.051	86.89 (±7.04)
Vehicle Control	2.862	3.109	3.038	2.622	2.817	2.685	1.35 (±3.76)
Caco-2 Cells							
Media	0.227	0.241	0.251	0.000	0.000	0.000	-------
Media + Cells	0.326	0.328	0.300	0.098	0.086	0.049	-------
0.78	0.308	0.317	0.294	0.081	0.076	0.043	13.92 (±3.62)
1.56	0.302	0.301	0.285	0.074	0.060	0.035	28.27 (±3.28)
3.12	0.298	0.310	0.286	0.070	0.068	0.035	25.76 (±4.12)
6.25	0.280	0.279	0.273	0.053	0.038	0.022	52.61 (±5.63)
12.5	0.244	0.265	0.262	0.017	0.024	0.011	77.43 (±5.45)
25	0.229	0.241	0.252	0.002	-0.001	0.001	99.04 (±1.67)
50	0.229	0.243	0.250	0.001	-0.001	0.000	100.14 (±1.31)
100	0.227	0.241	0.251	-0.001	0.000	0.000	100.14 (±0.59)
Actinomycin-D	0.236	0.242	0.253	0.009	0.000	0.003	95.15 (±4.48)
Vehicle Control	0.326	0.325	0.298	0.098	0.084	0.048	1.91 (±1.62)

Appendix: 19

Percentage growth inhibition of cancer cells at various concentrations (μM) of pregnane glycoside from *Caralluma tuberculata* using neutral red uptake assay after 24 hours treatment

Concentration (μM)	Absorbance (cells + Pregnane + media)			Actual Absorbance (cells + Pregnane)- media			% Growth Inhibition (Mean ± STDEV)
Experiments	**1**	**2**	**3**	**1**	**2**	**3**	
MCF-7 Cells							
Media	0.162	0.164	0.164	0.000	0.000	0.000	-------
Media + Cells	0.469	0.497	0.442	0.307	0.333	0.279	-------
0.78	0.452	0.485	0.424	0.290	0.320	0.261	5.21 (±1.44)
1.56	0.422	0.443	0.393	0.260	0.279	0.230	16.33 (±1.21)
3.12	0.418	0.463	0.411	0.256	0.299	0.247	12.63 (±3.27)
6.25	0.411	0.426	0.383	0.249	0.262	0.219	20.52 (±1.47)
12.5	0.359	0.348	0.338	0.197	0.183	0.174	39.38 (±4.86)
25	0.265	0.272	0.241	0.103	0.108	0.078	68.72 (±3.09)
50	0.257	0.287	0.270	0.095	0.123	0.107	63.56 (±4.70)
100	0.260	0.259	0.259	0.098	0.095	0.096	68.37 (±2.88)
Actinomycin-D	0.177	0.189	0.197	0.015	0.025	0.034	91.84 (±3.73)
Tamoxifen	1.377	1.364	1.401	0.111	0.062	0.045	78.19 (±3.17)
Anastrozole	1.555	1.486	1.555	0.289	0.185	0.199	46.30 (±5.61)
Vehicle Control	0.515	0.490	0.424	0.353	0.325	0.260	1.76 (±5.12)
MDA MB-468 Cells							
Media	0.439	0.585	0.618	0.000	0.000	0.000	-------
Media + Cells	0.913	0.975	1.041	0.474	0.390	0.423	-------
0.78	0.891	0.974	1.007	0.452	0.389	0.389	4.25 (±3.85)
1.56	0.889	0.942	1.020	0.450	0.357	0.403	6.08 (±2.01)
3.12	0.866	0.971	0.993	0.427	0.385	0.375	7.46 (±5.56)
6.25	0.862	0.946	0.975	0.424	0.361	0.357	11.18 (±4.08)
12.5	0.843	0.915	0.948	0.404	0.330	0.330	17.28 (±3.99)
25	0.820	0.882	0.932	0.381	0.297	0.314	23.06 (±3.20)
50	0.620	0.741	0.804	0.182	0.156	0.187	59.21 (±2.98)
100	0.561	0.706	0.744	0.122	0.120	0.126	71.15 (±2.65)
Actinomycin-D	0.457	0.631	0.629	0.018	0.046	0.011	93.94 (±5.02)
Tamoxifen	1.651	1.578	1.545	0.764	0.640	0.553	38.36 (±6.26)
Anastrozole	1.132	1.205	1.292	0.245	0.267	0.301	74.11 (±4.18)
Vehicle Control	0.901	0.953	1.054	0.462	0.368	0.436	1.69 (±4.44)
Caco-2 Cells							
Media	0.214	0.234	0.228	0.000	0.000	0.000	-------
Media + Cells	0.278	0.333	0.328	0.064	0.099	0.100	-------
0.78	0.265	0.316	0.316	0.051	0.082	0.088	16.51 (±4.60)
1.56	0.259	0.307	0.303	0.044	0.073	0.075	27.54 (±3.26)
3.12	0.254	0.288	0.285	0.039	0.054	0.057	42.25 (±3.49)
6.25	0.250	0.291	0.276	0.036	0.057	0.049	46.22 (±4.62)
12.5	0.232	0.257	0.254	0.018	0.022	0.026	74.39 (±2.82)
25	0.233	0.258	0.249	0.019	0.024	0.022	74.87 (±3.98)
50	0.229	0.247	0.239	0.015	0.013	0.011	84.24 (±6.47)
100	0.215	0.234	0.229	0.000	0.000	0.001	99.76 (±0.70)
Actinomycin-D	0.237	0.263	0.266	0.022	0.029	0.038	65.97 (±4.83)
Vehicle Control	0.277	0.332	0.327	0.062	0.098	0.099	1.67 (±1.06)

Appendix: 20

Percentage growth inhibition of cancer cells at various concentrations (μM) of pregnane glycoside from *Caralluma tuberculata* using neutral red uptake assay after 48 hours treatment

Concentration (μM)	Absorbance (cells + Pregnane + media)			Actual Absorbance (cells + Pregnane)- media			% Growth Inhibition
Experiments	**1**	**2**	**3**	**1**	**2**	**3**	(Mean ± STDEV)
MCF-7 Cells							
Media	0.439	0.441	0.506	0.000	0.000	0.000	-------
Media + Cells	0.913	0.964	0.940	0.474	0.523	0.435	-------
0.78	0.891	0.934	0.927	0.452	0.493	0.422	4.43 (±1.41)
1.56	0.889	0.930	0.908	0.450	0.489	0.402	6.31 (±1.23)
3.12	0.866	0.910	0.903	0.427	0.469	0.398	9.55 (±0.95)
6.25	0.796	0.783	0.821	0.357	0.343	0.315	28.91 (±5.08)
12.5	0.443	0.447	0.505	0.004	0.006	-0.001	99.36 (±0.67)
25	0.437	0.438	0.505	-0.002	-0.003	-0.001	100.40 (±0.21)
50	0.437	0.436	0.504	-0.002	-0.005	-0.001	100.54 (±0.37)
100	0.436	0.439	0.504	-0.003	-0.002	-0.002	100.46 (±0.06)
Actinomycin-D	0.440	0.437	0.508	0.001	-0.004	0.002	99.97 (±0.64)
Tamoxifen	0.284	0.291	0.307	-0.005	0.000	0.007	100.26 (±0.35)
Anastrozole	0.855	0.459	0.503	0.565	0.168	0.203	36.22 (±4.22)
Vehicle Control	0.901	0.920	0.920	0.462	0.479	0.414	5.21 (±3.02)
MDA MB-468 Cells							
Media	0.733	0.783	0.776	0.000	0.000	0.000	-------
Media + Cells	1.017	1.005	1.045	0.284	0.223	0.268	-------
0.78	1.007	0.996	1.036	0.274	0.213	0.259	3.64 (±0.48)
1.56	0.994	1.000	1.036	0.261	0.218	0.259	4.46 (±3.06)
3.12	0.993	1.003	1.038	0.260	0.220	0.262	4.03 (±3.86)
6.25	0.951	0.964	0.999	0.218	0.181	0.223	19.59 (±3.19)
12.5	0.960	0.983	0.998	0.227	0.200	0.221	15.85 (±5.17)
25	0.956	0.930	0.944	0.223	0.147	0.167	30.98 (±8.44)
50	0.846	0.856	0.854	0.113	0.074	0.078	66.03 (±5.40)
100	0.770	0.805	0.794	0.037	0.023	0.018	90.01 (±3.19)
Actinomycin-D	0.741	0.796	0.796	0.008	0.013	0.020	94.64 (±2.25)
Tamoxifen	1.346	1.300	1.359	0.403	0.297	0.318	63.05 (±3.16)
Anastrozole	1.087	1.024	1.079	0.144	0.021	0.038	92.99 (±6.23)
Vehicle Control	1.034	1.012	1.035	0.301	0.230	0.259	-1.81 (±4.96)
Caco-2 Cells							
Media	0.279	0.234	0.247	0.000	0.000	0.000	-------
Media + Cells	0.347	0.311	0.360	0.068	0.077	0.112	-------
0.78	0.330	0.299	0.337	0.001	0.065	0.089	20.04 (±4.49)
1.56	0.317	0.279	0.302	0.051	0.045	0.054	45.78 (±5.15)
3.12	0.307	0.259	0.280	0.038	0.024	0.033	66.05 (±6.04)
6.25	0.300	0.254	0.276	0.028	0.020	0.029	72.23 (±3.23)
12.5	0.288	0.250	0.266	0.021	0.016	0.019	83.29 (±3.69)
25	0.280	0.240	0.262	0.009	0.006	0.015	92.55 (±5.89)
50	0.279	0.234	0.250	0.001	0.000	0.003	98.78 (±1.25)
100	0.280	0.234	0.248	0.001	0.000	0.000	99.08 (±1.01)
Actinomycin-D	0.280	0.235	0.247	0.001	0.001	-0.001	99.38 (±1.35)
Vehicle Control	0.347	0.309	0.357	0.068	0.075	0.109	1.72 (±1.40)

Appendix: 21

Percentage growth inhibition of cancer cells at various concentrations (µM) of androstane glycoside from *Caralluma tuberculata* using MTT assay after 24 hours treatment

Concentration (µM)	Absorbance (cells + Pregnane + media)			Actual Absorbance (cells + Pregnane)- media			% Growth Inhibition (Mean ± STDEV)
Experiments	**1**	**2**	**3**	**1**	**2**	**3**	
MCF-7 Cells							
Media	0.201	0.211	0.204	0.000	0.000	0.000	-------
Media + Cells	2.856	2.907	2.829	2.655	2.696	2.626	-------
0.78	2.694	2.804	2.729	2.493	2.593	2.525	4.58 (±1.31)
1.56	2.687	2.633	2.490	2.486	2.423	2.287	9.81 (±3.29)
3.12	2.660	2.594	2.723	2.458	2.384	2.519	7.68 (±3.78)
6.25	2.237	2.339	2.296	2.036	2.128	2.093	21.56 (±1.57)
12.5	1.869	1.975	2.009	1.667	1.765	1.805	34.33 (±2.97)
25	0.285	0.300	0.296	0.084	0.089	0.093	96.67 (±0.19)
50	0.213	0.228	0.206	0.012	0.017	0.002	99.62 (±0.28)
100	0.229	0.242	0.218	0.027	0.032	0.014	99.09 (±0.33)
Actinomycin-D	1.339	1.310	1.363	1.137	1.099	1.159	57.42 (±1.71)
Tamoxifen	1.377	1.364	1.401	0.111	0.062	0.045	84.74 (±4.33)
Anastrozole	1.555	1.486	1.555	0.289	0.185	0.199	51.72 (±3.42)
Vehicle Control	2.738	2.888	2.921	2.537	2.677	2.718	0.55 (±3.97)
MDA MB-468 Cells							
Media	0.664	0.746	0.773	0.000	0.000	0.000	-------
Media + Cells	2.580	2.561	2.772	1.916	1.815	1.999	-------
0.78	2.498	2.497	2.677	1.834	1.751	1.905	4.18 (±0.61)
1.56	2.464	2.492	2.617	1.800	1.746	1.844	5.87(±1.96)
3.12	2.342	2.403	2.405	1.678	1.656	1.632	13.18(±4.85)
6.25	2.237	2.403	2.550	1.573	1.656	1.777	12.58(±4.75)
12.5	2.114	2.213	2.419	1.450	1.467	1.647	20.38(±3.50)
25	2.074	2.071	2.306	1.410	1.324	1.534	25.57(±2.01)
50	1.648	1.610	1.665	0.984	0.863	0.892	52.15(±3.37)
100	1.496	1.458	1.396	0.832	0.712	0.623	62.06(±6.22)
Actinomycin-D	1.482	1.331	1.356	0.818	0.585	0.583	65.30(±7.10)
Tamoxifen	1.580	1.634	1.651	0.677	0.727	0.804	27.80(±4.06)
Anastrozole	1.202	1.220	1.147	0.298	0.313	0.300	70.11(±1.47)
Vehicle Control	2.542	2.464	2.653	1.878	1.718	1.881	4.41(±2.15)
Caco-2 Cells							
Media	0.240	0.231	0.235	0.000	0.000	0.000	-------
Media + Cells	0.283	0.320	0.281	0.043	0.090	0.046	-------
0.78	0.277	0.311	0.275	0.038	0.081	0.040	12.46 (±2.29)
1.56	0.277	0.314	0.273	0.037	0.084	0.038	12.80 (±6.17)
3.12	0.274	0.303	0.271	0.034	0.073	0.036	20.28 (±1.62)
6.25	0.273	0.302	0.269	0.033	0.072	0.034	23.21 (±3.32)
12.5	0.261	0.277	0.256	0.022	0.047	0.022	50.30 (±2.92)
25	0.247	0.251	0.246	0.007	0.020	0.012	78.86 (±4.46)
50	0.246	0.247	0.247	0.007	0.017	0.012	79.96 (±4.95)
100	0.243	0.245	0.240	0.003	0.014	0.005	88.19 (±3.88)
Actinomycin-D	0.259	0.263	0.257	0.019	0.032	0.022	57.61 (±5.46)
Vehicle Control	0.282	0.319	0.281	0.043	0.089	0.046	1.29 (±0.10)

Appendix: 22

Percentage growth inhibition of cancer cells at various concentrations (μM) of androstane glycoside from *Caralluma tuberculata* using MTT assay after 48 hours treatment

Concentration (μM)	Absorbance (cells + Pregnane + media)			Actual Absorbance (cells + Pregnane)- media			% Growth Inhibition (Mean ± STDEV)
Experiments	**1**	**2**	**3**	**1**	**2**	**3**	
MCF-7 Cells							
Media	0.200	0.226	0.213	0.000	0.000	0.000	-------
Media + Cells	3.105	3.229	3.055	2.905	3.003	2.843	-------
0.78	3.010	3.032	2.911	2.810	2.807	2.699	4.97 (±1.65)
1.56	3.013	2.970	2.940	2.813	2.744	2.727	5.29 (±2.93)
3.12	3.010	2.918	2.839	2.810	2.692	2.626	7.09 (±3.57)
6.25	1.957	2.110	2.043	1.757	1.884	1.831	37.46 (±1.97)
12.5	0.536	0.535	0.750	0.335	0.309	0.537	86.42 (±4.65)
25	0.190	0.206	0.186	-0.010	-0.020	-0.026	100.64 (±0.29)
50	0.195	0.200	0.214	-0.005	-0.026	0.002	100.33 (±0.48)
100	0.196	0.204	0.211	-0.004	-0.022	-0.002	100.31 (±0.36)
Actinomycin-D	0.891	0.812	0.817	0.691	0.586	0.605	78.48 (±2.16)
Tamoxifen	0.284	0.291	0.307	-0.005	0.000	0.007	99.64 (±1.14)
Anastrozole	0.855	0.459	0.503	0.565	0.168	0.203	46.39 (±6.43)
Vehicle Control	2.891	3.147	2.943	2.691	2.921	2.731	4.68 (±2.93)
MDA MB-468 Cells							
Media	0.785	0.787	0.724	0.000	0.000	0.000	-------
Media + Cells	2.854	2.793	2.910	2.069	2.006	2.185	-------
0.78	2.683	2.710	2.804	1.898	1.923	2.080	5.74 (±2.20)
1.56	2.578	2.462	2.697	1.793	1.675	1.973	13.19 (±3.39)
3.12	2.505	2.413	2.612	1.720	1.626	1.888	16.46 (±2.68)
6.25	2.495	2.552	2.743	1.710	1.764	2.019	12.32 (±4.88)
12.5	2.427	2.516	2.512	1.642	1.729	1.788	17.53 (±3.47)
25	2.171	2.200	2.324	1.386	1.413	1.600	29.78 (±3.10)
50	1.512	1.469	1.386	0.727	0.681	0.662	66.86 (±2.54)
100	1.169	1.142	1.336	0.384	0.355	0.612	78.58 (±5.71)
Actinomycin-D	1.054	1.109	1.011	0.269	0.322	0.286	85.94 (±1.74)
Tamoxifen	1.500	1.448	1.457	0.584	0.583	0.499	45.41 (±4.14)
Anastrozole	1.099	1.033	1.009	0.183	0.168	0.051	86.89 (±7.04)
Vehicle Control	2.970	2.852	2.902	2.185	2.065	2.178	-2.75 (±2.98)
Caco-2 Cells							
Media	0.222	0.237	0.235	0.000	0.000	0.000	-------
Media + Cells	0.340	0.326	0.281	0.118	0.089	0.046	-------
0.78	0.329	0.325	0.277	0.107	0.088	0.042	6.35 (±4.20)
1.56	0.322	0.312	0.276	0.100	0.075	0.041	14.50 (±2.51)
3.12	0.286	0.290	0.259	0.064	0.053	0.024	45.06 (±4.02)
6.25	0.263	0.273	0.256	0.041	0.036	0.021	59.92 (±5.10)
12.5	0.231	0.248	0.243	0.009	0.010	0.008	87.67 (±4.87)
25	0.228	0.244	0.236	0.006	0.006	0.001	94.85 (±2.02)
50	0.221	0.238	0.240	-0.001	0.001	0.005	96.42 (±6.03)
100	0.222	0.236	0.235	0.000	-0.001	0.000	100.19 (±1.20)
Actinomycin-D	0.230	0.253	0.235	0.008	0.016	0.000	91.78 (±8.92)
Vehicle Control	0.338	0.326	0.281	0.116	0.089	0.046	1.06 (±0.52)

Appendix: 23

Percentage growth inhibition of cancer cells at various concentrations (μM) of androstane glycoside from *Caralluma tuberculata* using neutral red uptake assay after 24 hours treatment

Concentration (μM)	Absorbance (cells + Pregnane + media)			Actual Absorbance (cells + Pregnane)- media			% Growth Inhibition (Mean ± STDEV)
Experiments	**1**	**2**	**3**	**1**	**2**	**3**	
MCF-7 Cells							
Media	0.171	0.157	0.168	0.000	0.000	0.000	-------
Media + Cells	0.398	0.390	0.374	0.227	0.233	0.206	-------
0.78	0.393	0.382	0.362	0.223	0.226	0.194	3.68 (±1.92)
1.56	0.391	0.378	0.355	0.220	0.222	0.188	5.68 (±3.01)
3.12	0.376	0.376	0.353	0.205	0.219	0.185	8.75 (±2.36)
6.25	0.354	0.337	0.325	0.183	0.180	0.157	21.98 (±2.35)
12.5	0.296	0.293	0.283	0.125	0.137	0.116	43.37 (±1.80)
25	0.248	0.234	0.227	0.077	0.077	0.060	68.08 (±2.69)
50	0.238	0.234	0.219	0.067	0.078	0.052	70.72 (±4.07)
100	0.211	0.191	0.190	0.040	0.035	0.023	85.51 (±3.27)
Actinomycin-D	0.184	0.184	0.185	0.013	0.027	0.017	91.35 (±2.98)
Tamoxifen	1.377	1.364	1.401	0.111	0.062	0.045	78.19 (±3.17)
Anastrozole	1.555	1.486	1.555	0.289	0.185	0.199	46.28 (±5.64)
Vehicle Control	0.411	0.387	0.381	0.241	0.230	0.214	-2.68 (±3.64)
MDA MB-468 Cells							
Media	0.564	0.711	0.714	0.000	0.000	0.000	-------
Media + Cells	1.006	1.087	1.064	0.443	0.375	0.350	-------
0.78	0.993	1.069	1.043	0.429	0.358	0.329	4.58 (±1.43)
1.56	0.976	1.056	1.054	0.412	0.345	0.340	5.95 (±2.84)
3.12	0.965	1.065	1.020	0.401	0.354	0.306	9.21 (±3.37)
6.25	0.932	1.033	1.031	0.368	0.322	0.317	13.46 (±3.87)
12.5	0.916	1.019	1.024	0.353	0.308	0.310	16.56 (±4.61)
25	0.900	0.980	0.951	0.336	0.269	0.237	28.23 (±4.10)
50	0.777	0.906	0.860	0.213	0.195	0.146	52.70 (±5.10)
100	0.716	0.815	0.829	0.152	0.104	0.115	68.33 (±3.49)
Actinomycin-D	0.595	0.769	0.750	0.031	0.058	0.036	89.11 (±4.23)
Tamoxifen	1.651	1.578	1.545	0.764	0.640	0.553	38.36 (±6.26)
Anastrozole	1.132	1.205	1.292	0.245	0.267	0.301	74.11 (±4.18)
Vehicle Control	0.997	1.075	1.084	0.433	0.364	0.369	-0.11 (±4.87)
Caco-2 Cells							
Media	0.256	0.260	0.228	0.000	0.000	0.000	-------
Media + Cells	0.349	0.329	0.328	0.093	0.068	0.100	-------
0.78	0.331	0.320	0.316	0.076	0.059	0.088	14.56 (±3.79)
1.56	0.330	0.311	0.303	0.075	0.051	0.075	23.35 (±3.33)
3.12	0.316	0.300	0.285	0.060	0.039	0.057	40.26 (±4.44)
6.25	0.298	0.286	0.276	0.042	0.026	0.049	56.04 (±5.23)
12.5	0.278	0.284	0.254	0.023	0.024	0.026	71.49 (±5.59)
25	0.269	0.274	0.249	0.013	0.014	0.022	81.19 (±3.80)
50	0.267	0.276	0.239	0.012	0.016	0.011	84.51 (±6.25)
100	0.255	0.261	0.229	-0.001	0.000	0.001	99.83 (±0.92)
Actinomycin-D	0.290	0.281	0.266	0.035	0.021	0.038	64.41 (±4.02)
Vehicle Control	0.348	0.327	0.327	0.092	0.067	0.099	1.25 (±0.56)

Appendix: 24

Percentage growth inhibition of cancer cells at various concentrations (μM) of androstane glycoside from *Caralluma tuberculata* using neutral red uptake assay after 48 hours treatment

Concentration (μM)	Absorbance (cells + Pregnane + media)			Actual Absorbance (cells + Pregnane)- media			% Growth Inhibition (Mean ± STDEV)
Experiments	**1**	**2**	**3**	**1**	**2**	**3**	
MCF-7 Cells							
Media	0.392	0.431	0.506	0.000	0.000	0.000	-------
Media + Cells	0.950	1.032	0.940	0.558	0.601	0.435	-------
0.78	0.905	0.942	0.927	0.513	0.511	0.422	11.87 (±3.45)
1.56	0.904	0.929	0.908	0.512	0.498	0.402	14.72 (±5.64)
3.12	0.811	0.826	0.903	0.420	0.395	0.398	28.33 (±5.17)
6.25	0.668	0.696	0.821	0.277	0.265	0.315	55.44 (±4.77)
12.5	0.390	0.428	0.505	-0.002	-0.002	-0.001	100.47 (±0.20)
25	0.389	0.426	0.505	-0.003	-0.005	-0.001	100.51 (±0.40)
50	0.388	0.428	0.504	-0.003	-0.003	-0.001	100.47 (±0.11)
100	0.388	0.427	0.504	-0.004	-0.004	-0.002	100.70 (±0.13)
Actinomycin-D	0.393	0.429	0.508	0.001	-0.002	0.002	99.91 (±0.42)
Tamoxifen	0.284	0.291	0.307	-0.005	0.000	0.007	100.24 (±0.37)
Anastrozole	0.855	0.459	0.503	0.565	0.168	0.203	36.22 (±4.21)
Vehicle Control	0.922	1.009	0.959	0.530	0.578	0.454	1.50 (±5.11)
MDA MB-468 Cells							
Media	0.786	0.818	0.751	0.000	0.000	0.000	-------
Media + Cells	1.204	1.194	1.199	0.417	0.376	0.447	-------
0.78	1.159	1.186	1.170	0.372	0.368	0.419	6.43 (±4.28)
1.56	1.132	1.175	1.141	0.346	0.357	0.390	11.71 (±6.04)
3.12	1.138	1.158	1.114	0.352	0.340	0.363	14.76 (±4.67)
6.25	1.092	1.093	1.101	0.306	0.275	0.350	25.12 (±2.93)
12.5	1.045	1.098	1.091	0.258	0.281	0.340	29.21 (±7.74)
25	1.022	1.083	1.052	0.235	0.265	0.301	35.32 (±7.38)
50	0.889	0.958	0.929	0.103	0.140	0.178	66.10 (±8.14)
100	0.842	0.909	0.844	0.055	0.091	0.093	80.60 (±5.57)
Actinomycin-D	0.799	0.849	0.863	0.013	0.031	0.112	87.89 (±11.42)
Tamoxifen	1.346	1.300	1.359	0.403	0.297	0.318	63.05 (±3.16)
Anastrozole	1.087	1.024	1.079	0.144	0.021	0.038	92.99 (±6.23)
Vehicle Control	1.179	1.176	1.189	0.393	0.358	0.437	4.36 (±1.91)
Caco-2 Cells							
Media	0.215	0.247	0.239	0.000	0.000	0.000	-------
Media + Cells	0.343	0.351	0.369	0.128	0.105	0.130	-------
0.78	0.337	0.342	0.354	0.122	0.095	0.115	8.47 (±3.48)
1.56	0.314	0.329	0.345	0.099	0.082	0.106	21.19 (±2.11)
3.12	0.276	0.295	0.293	0.061	0.048	0.054	55.01 (±3.32)
6.25	0.259	0.280	0.290	0.044	0.033	0.051	64.94 (±3.80)
12.5	0.222	0.248	0.242	0.007	0.001	0.003	97.24 (±2.47)
25	0.216	0.247	0.239	0.001	0.000	0.000	99.82 (±0.46)
50	0.215	0.247	0.241	0.000	0.000	0.001	99.69 (±0.70)
100	0.215	0.247	0.238	0.000	0.000	-0.001	100.31 (±0.27)
Actinomycin-D	0.219	0.247	0.246	0.004	0.000	0.007	97.47 (±2.69)
Vehicle Control	0.341	0.351	0.367	0.126	0.104	0.128	1.21 (±0.26)

Appendix: 25

Percentage growth inhibition of cancer cells at various concentrations (μM) of pregnane glycoside from *Fagonia indica* using MTT assay after 24 hours treatment

Concentration (μM)	Absorbance (cells + Pregnane + media)			Actual Absorbance (cells + Pregnane)- media			% Growth Inhibition (Mean ± STDEV)
Experiments	**1**	**2**	**3**	**1**	**2**	**3**	
MCF-7 Cells							
Media	0.659	0.655	0.766	0.000	0.000	0.000	-------
Media + Cells	2.750	2.776	2.719	2.091	2.122	1.953	-------
0.78	2.600	2.708	2.669	1.941	2.054	1.903	4.32 (±2.51)
1.56	2.594	2.673	2.675	1.935	2.018	1.909	4.85 (±2.62)
3.12	2.491	2.613	2.643	1.832	1.958	1.877	8.00 (±4.28)
6.25	2.543	2.564	2.697	1.884	1.909	1.931	7.01 (±5.11)
12.5	2.468	2.542	2.649	1.809	1.887	1.883	9.37 (±5.16)
25	2.350	2.512	2.568	1.691	1.858	1.802	13.10 (±5.74)
50	2.173	2.078	2.233	1.514	1.423	1.467	28.46 (±4.10)
100	1.949	1.867	1.813	1.289	1.212	1.047	42.53 (±4.04)
Actinomycin-D	1.567	1.641	1.740	0.907	0.986	0.974	53.43 (±3.24)
Tamoxifen	1.377	1.364	1.401	0.111	0.062	0.045	84.74 (±4.33)
Anastrozole	1.555	1.486	1.555	0.289	0.185	0.199	51.72 (±3.42)
Vehicle Control	2.657	2.751	2.690	1.998	2.096	1.924	2.37 (±1.81)
MDA MB-468 Cells							
Media	0.874	0.864	0.883	0.000	0.000	0.000	-------
Media + Cells	2.944	2.921	3.059	2.069	2.056	2.176	-------
0.78	2.636	2.815	2.831	1.762	1.951	1.947	10.17 (±4.86)
1.56	2.508	2.672	2.816	1.634	1.807	1.933	14.78 (±5.46)
3.12	2.416	2.314	2.552	1.541	1.449	1.669	26.12 (±3.15)
6.25	2.252	2.290	2.460	1.378	1.425	1.577	30.55 (±2.93)
12.5	2.061	2.136	2.346	1.187	1.272	1.463	37.86 (±4.93)
25	1.884	1.936	1.955	1.010	1.072	1.072	49.94 (±1.79)
50	1.367	1.534	1.544	0.493	0.670	0.661	71.07 (±4.55)
100	1.264	1.359	1.447	0.390	0.495	0.564	77.05 (±3.67)
Actinomycin-D	1.518	1.690	1.734	0.644	0.825	0.851	63.21 (±4.93)
Tamoxifen	1.580	1.634	1.651	0.677	0.727	0.804	27.80 (±4.06)
Anastrozole	1.202	1.220	1.147	0.298	0.313	0.300	70.11 (±1.47)
Vehicle Control	2.842	2.856	2.936	1.967	1.991	2.053	4.58 (±1.29)
Caco-2 Cells							
Media	0.271	0.256	0.211	0.000	0.000	0.000	-------
Media + Cells	0.323	0.336	0.280	0.053	0.080	0.069	-------
0.78	0.319	0.333	0.279	0.048	0.077	0.068	4.93 (±3.29)
1.56	0.316	0.320	0.269	0.045	0.064	0.058	16.89 (±2.45)
3.12	0.310	0.324	0.266	0.040	0.068	0.055	20.29 (±4.87)
6.25	0.307	0.313	0.263	0.037	0.057	0.052	27.98 (±2.15)
12.5	0.309	0.308	0.258	0.039	0.051	0.047	31.18 (±4.65)
25	0.302	0.312	0.257	0.032	0.056	0.047	33.97 (±5.17)
50	0.301	0.297	0.250	0.031	0.040	0.039	44.76 (±4.10)
100	0.289	0.281	0.235	0.019	0.025	0.024	66.36 (±2.62)
Actinomycin-D	0.297	0.289	0.242	0.026	0.033	0.031	54.78 (±4.51)
Vehicle Control	0.323	0.334	0.280	0.052	0.077	0.069	1.51 (±1.19)

Appendix: 26

Percentage growth inhibition of cancer cells at various concentrations (µM) of pregnane glycoside from *Fagonia indica* using MTT assay after 48 hours treatment

Concentration (µM)	Absorbance (cells + Pregnane + media)			Actual Absorbance (cells + Pregnane)- media			% Growth Inhibition (Mean ± STDEV)
Experiments	**1**	**2**	**3**	**1**	**2**	**3**	
MCF-7 Cells							
Media	0.821	0.849	0.857	0.000	0.000	0.000	-------
Media + Cells	2.753	2.818	2.864	1.931	1.969	2.007	-------
0.78	2.620	2.720	2.819	1.798	1.871	1.963	4.71 (±2.35)
1.56	2.685	2.776	2.704	1.864	1.927	1.847	4.53 (±3.07)
3.12	2.590	2.732	2.752	1.769	1.883	1.895	6.12 (±2.06)
6.25	2.600	2.585	2.698	1.779	1.735	1.841	9.36 (±2.19)
12.5	2.634	2.585	2.569	1.813	1.736	1.712	10.90 (±4.36)
25	2.468	2.485	2.646	1.647	1.636	1.789	14.16 (±3.07)
50	2.035	2.118	2.248	1.214	1.269	1.391	34.48 (±3.37)
100	1.735	1.701	1.883	0.914	0.852	1.027	52.77 (±3.95)
Actinomycin-D	1.378	1.320	1.281	0.557	0.471	0.424	75.39 (±3.90)
Tamoxifen	0.284	0.291	0.307	-0.005	0.000	0.007	99.64 (±1.14)
Anastrozole	0.855	0.459	0.503	0.565	0.168	0.203	46.39 (±6.43)
Vehicle Control	2.681	2.840	2.801	1.860	1.991	1.944	1.92 (±2.62)
MDA MB-468 Cells							
Media	0.843	0.871	0.907	0.000	0.000	0.000	-------
Media + Cells	2.905	2.903	2.855	2.061	2.032	1.948	-------
0.78	2.771	2.665	2.750	1.928	1.794	1.843	7.86 (±3.37)
1.56	2.522	2.459	2.397	1.678	1.588	1.490	21.31 (±2.51)
3.12	2.104	2.151	1.998	1.261	1.281	1.091	39.94 (±3.63)
6.25	2.018	2.008	1.820	1.175	1.137	0.912	46.74 (±5.60)
12.5	1.806	1.934	1.998	0.963	1.063	1.091	48.33 (±4.68)
25	1.547	1.674	1.712	0.704	0.803	0.805	61.66 (±3.73)
50	1.318	1.415	1.513	0.475	0.544	0.606	73.03 (±4.03)
100	1.208	1.190	1.383	0.365	0.319	0.476	80.72 (±4.57)
Actinomycin-D	1.412	1.365	1.347	0.568	0.494	0.440	75.17 (±2.53)
Tamoxifen	1.500	1.448	1.457	0.584	0.583	0.499	45.41 (±4.14)
Anastrozole	1.099	1.033	1.009	0.183	0.168	0.051	86.89 (±7.04)
Vehicle Control	2.805	2.883	2.824	1.961	2.012	1.916	2.50 (±2.07)
Caco-2 Cells							
Media	0.211	0.238	0.229	0.000	0.000	0.000	-------
Media + Cells	0.320	0.364	0.307	0.109	0.125	0.077	-------
0.78	0.299	0.345	0.290	0.088	0.107	0.060	18.69 (±3.49)
1.56	0.285	0.327	0.287	0.074	0.089	0.057	28.91 (±3.06)
3.12	0.281	0.322	0.282	0.070	0.084	0.053	33.44 (±1.95)
6.25	0.276	0.316	0.281	0.065	0.078	0.051	37.24 (±3.62)
12.5	0.275	0.303	0.276	0.064	0.065	0.047	43.21 (±4.62)
25	0.247	0.267	0.246	0.035	0.029	0.017	74.15 (±5.79)
50	0.217	0.254	0.230	0.006	0.015	0.001	93.76 (±5.81)
100	0.214	0.238	0.230	0.003	0.000	0.001	98.93 (±1.39)
Actinomycin-D	0.222	0.253	0.235	0.011	0.014	0.005	90.59 (±2.28)
Vehicle Control	0.319	0.359	0.303	0.108	0.120	0.074	3.03 (±1.68)

Appendix: 27

Percentage growth inhibition of cancer cells at various concentrations (μM) of pregnane glycoside from *Fagonia indica* using neutral red uptake assay after 24 hours treatment

Concentration (μM)	Absorbance (cells + Pregnane + media)			Actual Absorbance (cells + Pregnane)- media			% Growth Inhibition (Mean ± STDEV)
Experiments	**1**	**2**	**3**	**1**	**2**	**3**	
MCF-7 Cells							
Media	0.148	0.175	0.206	0.000	0.000	0.000	-------
Media + Cells	0.618	0.640	0.740	0.470	0.465	0.534	-------
0.78	0.597	0.599	0.709	0.448	0.424	0.248	6.34 (±2.19)
1.56	0.576	0.615	0.706	0.428	0.440	0.504	6.91 (±1.82)
3.12	0.575	0.554	0.685	0.427	0.379	0.500	12.60 (±5.11)
6.25	0.548	0.578	0.622	0.399	0.403	0.479	16.80 (±4.58)
12.5	0.534	0.507	0.600	0.386	0.332	0.416	24.17 (±5.62)
25	0.505	0.504	0.559	0.356	0.329	0.394	29.02 (±4.83)
50	0.468	0.462	0.529	0.319	0.287	0.354	36.61 (±4.02)
100	0.405	0.399	0.454	0.256	0.224	0.323	50.22 (±4.27)
Actinomycin-D	0.255	0.313	0.337	0.107	0.138	0.131	74.33 (±3.64)
Tamoxifen	1.377	1.364	1.401	0.111	0.062	0.045	78.19 (±3.17)
Anastrozole	1.555	1.486	1.555	0.289	0.185	0.199	46.28 (±5.64)
Vehicle Control	0.603	0.640	0.713	0.455	0.465	0.507	2.71 (±2.61)
MDA MB-468 Cells							
Media	0.672	0.684	0.754	0.000	0.000	0.000	-------
Media + Cells	1.202	1.209	1.250	0.530	0.525	0.496	-------
0.78	1.187	1.192	1.214	0.515	0.508	0.460	4.49 (±2.45)
1.56	1.169	1.197	1.224	0.496	0.513	0.470	4.66 (±2.06)
3.12	1.052	1.129	1.126	0.380	0.445	0.371	22.88 (±6.86)
6.25	1.033	1.069	1.060	0.360	0.386	0.306	32.29 (±5.86)
12.5	0.902	0.946	0.995	0.230	0.263	0.241	52.68 (±3.46)
25	0.880	0.882	0.898	0.208	0.198	0.144	64.66 (±5.54)
50	0.834	0.858	0.878	0.161	0.174	0.124	70.48 (±4.22)
100	0.771	0.827	0.858	0.099	0.143	0.104	77.73 (±4.45)
Actinomycin-D	0.765	0.832	0.856	0.093	0.148	0.102	77.93 (±5.52)
Tamoxifen	1.651	1.578	1.545	0.764	0.640	0.553	38.36 (±6.26)
Anastrozole	1.132	1.205	1.292	0.245	0.267	0.301	74.11 (±4.18)
Vehicle Control	1.178	1.203	1.268	0.506	0.519	0.514	0.67 (±4.04)
Caco-2 Cells							
Media	0.216	0.237	0.190	0.000	0.000	0.000	-------
Media + Cells	0.347	0.348	0.287	0.131	0.111	0.097	-------
0.78	0.330	0.341	0.289	0.114	0.103	0.100	5.73 (±8.05)
1.56	0.310	0.311	0.256	0.094	0.073	0.066	31.19 (±3.05)
3.12	0.297	0.314	0.245	0.081	0.077	0.055	37.21 (±6.44)
6.25	0.297	0.312	0.248	0.081	0.074	0.058	37.03 (±3.60)
12.5	0.297	0.294	0.249	0.081	0.057	0.059	41.85 (±5.76)
25	0.283	0.284	0.230	0.067	0.046	0.040	55.19 (±5.24)
50	0.269	0.278	0.227	0.053	0.041	0.037	61.33 (±2.13)
100	0.244	0.263	0.227	0.028	0.026	0.038	72.14 (±9.45)
Actinomycin-D	0.260	0.261	0.220	0.044	0.024	0.031	71.35 (±6.49)
Vehicle Control	0.345	0.345	0.286	0.129	0.107	0.096	2.07 (±0.98)

Appendix: 28

Percentage growth inhibition of cancer cells at various concentrations (μM) of pregnane glycoside from *Fagonia indica* using neutral red uptake assay after 48 hours treatment

Concentration (μM)	Absorbance (cells + Pregnane + media)			Actual Absorbance (cells + Pregnane)- media			% Growth Inhibition (Mean ± STDEV)
Experiments	**1**	**2**	**3**	**1**	**2**	**3**	
MCF-7 Cells							
Media	0.212	0.239	0.237	0.000	0.000	0.000	-------
Media + Cells	0.824	0.895	0.869	0.611	0.656	0.631	-------
0.78	0.801	0.840	0.828	0.589	0.601	0.591	6.18 (±2.38)
1.56	0.764	0.817	0.760	0.552	0.578	0.523	12.93 (±3.87)
3.12	0.751	0.710	0.774	0.539	0.471	0.536	18.38 (±8.62)
6.25	0.744	0.740	0.752	0.532	0.501	0.515	18.38 (±5.37)
12.5	0.713	0.767	0.679	0.501	0.528	0.442	22.56 (±6.56)
25	0.631	0.634	0.623	0.419	0.394	0.385	36.76 (±4.62)
50	0.609	0.616	0.580	0.397	0.377	0.342	41.16 (±5.47)
100	0.466	0.488	0.493	0.254	0.249	0.255	60.06 (±1.82)
Actinomycin-D	0.271	0.243	0.223	0.059	0.004	-0.014	97.33 (±6.19)
Tamoxifen	0.284	0.291	0.307	-0.005	0.000	0.007	100.24 (±0.37)
Anastrozole	0.855	0.459	0.503	0.565	0.168	0.203	36.22 (±4.21)
Vehicle Control	0.800	0.907	0.859	0.588	0.668	0.622	1.17 (±2.85)
MDA MB-468 Cells							
Media	0.875	0.888	0.876	0.000	0.000	0.000	-------
Media + Cells	1.301	1.269	1.255	0.426	0.381	0.379	-------
0.78	1.270	1.224	1.184	0.394	0.336	0.308	12.63 (±5.82)
1.56	1.245	1.202	1.175	0.369	0.314	0.299	17.28 (±3.95)
3.12	1.165	1.169	1.117	0.289	0.281	0.241	31.54 (±5.07)
6.25	1.103	1.124	1.102	0.228	0.236	0.225	41.70 (±4.30)
12.5	1.051	1.054	1.061	0.175	0.166	0.185	55.51 (±3.91)
25	0.963	1.031	1.012	0.087	0.143	0.135	68.76 (±9.32)
50	0.956	0.932	0.901	0.081	0.045	0.025	87.58 (±6.24)
100	0.918	0.909	0.875	0.042	0.021	-0.001	94.95 (±5.10)
Actinomycin-D	0.915	0.913	0.884	0.039	0.025	0.008	94.01 (±3.65)
Tamoxifen	1.346	1.300	1.359	0.403	0.297	0.318	63.05 (±3.16)
Anastrozole	1.087	1.024	1.079	0.144	0.021	0.038	92.99 (±6.23)
Vehicle Control	1.292	1.256	1.231	0.417	0.368	0.355	3.91 (±2.19)
Caco-2 Cells							
Media	0.219	0.253	0.253	0.000	0.000	0.000	-------
Media + Cells	0.297	0.356	0.338	0.079	0.103	0.085	-------
0.78	0.282	0.337	0.324	0.063	0.084	0.071	18.04 (±1.63)
1.56	0.266	0.320	0.303	0.048	0.067	0.050	38.32 (±3.11)
3.12	0.264	0.319	0.306	0.045	0.066	0.053	38.46 (±3.82)
6.25	0.259	0.316	0.300	0.040	0.063	0.047	43.82 (±5.13)
12.5	0.250	0.284	0.280	0.031	0.031	0.028	66.00 (±4.63)
25	0.238	0.276	0.276	0.020	0.023	0.023	75.30 (±2.33)
50	0.223	0.256	0.255	0.004	0.003	0.002	96.22 (±1.67)
100	0.221	0.254	0.252	0.002	0.002	-0.001	98.67 (±1.88)
Actinomycin-D	0.229	0.269	0.260	0.010	0.016	0.007	87.67 (±3.69)
Vehicle Control	0.294	0.353	0.337	0.075	0.100	0.084	2.64 (±1.35)

Appendix: 29

Percentage growth inhibition of cancer cells at various concentrations (µM) of hexadecanoic acid from *Solanum surattense* using MTT assay after 24 hours treatment

Concentration (µM)	Absorbance (cells + Pregnane + media)			Actual Absorbance (cells + Pregnane)- media			% Growth Inhibition (Mean ± STDEV)
Experiments	**1**	**2**	**3**	**1**	**2**	**3**	
MCF-7 Cells							
Media	0.810	0.707	0.826	0.000	0.000	0.000	-------
Media + Cells	2.768	2.728	2.715	1.958	2.021	1.889	-------
0.78	2.738	2.697	2.671	1.928	1.990	1.845	1.80 (±0.44)
1.56	2.718	2.672	2.665	1.908	1.965	1.839	2.64 (±0.11)
3.12	2.746	2.725	2.566	1.936	2.018	1.740	3.05 (±4.22)
6.25	2.614	2.656	2.463	1.804	1.949	1.637	8.27 (±4.87)
12.5	2.576	2.526	2.291	1.766	1.819	1.465	14.07 (±7.22)
25	2.118	2.184	2.200	1.308	1.477	1.374	29.13 (±3.55)
50	1.988	1.857	1.978	1.178	1.150	1.152	40.64 (±2.18)
100	1.693	1.547	1.646	0.883	0.840	0.820	56.65 (±1.76)
Actinomycin-D	1.410	1.510	1.630	0.600	0.803	0.804	62.36 (±6.23)
Tamoxifen	1.377	1.364	1.401	0.111	0.062	0.045	84.74 (±4.33)
Anastrozole	1.555	1.486	1.555	0.289	0.185	0.199	51.72 (±3.42)
Vehicle Control	2.698	2.712	2.675	1.888	2.005	1.849	2.16 (±1.39)
MDA MB-468 Cells							
Media	0.863	0.864	0.862	0.000	0.000	0.000	-------
Media + Cells	2.982	2.871	3.046	2.118	2.007	2.183	-------
0.78	2.781	2.842	2.873	1.917	1.977	2.011	6.29 (±4.24)
1.56	2.665	2.790	2.819	1.802	1.926	1.957	9.79 (±5.48)
3.12	2.601	2.829	2.856	1.738	1.965	1.994	9.58 (±7.98)
6.25	2.685	2.665	2.771	1.821	1.801	1.909	12.29 (±1.89)
12.5	2.436	2.315	2.544	1.572	1.450	1.681	25.50 (±2.38)
25	2.539	2.298	2.479	1.676	1.434	1.617	25.14 (±3.89)
50	2.273	2.155	2.425	1.409	1.291	1.563	32.52 (±3.73)
100	2.048	1.941	1.904	1.185	1.077	1.041	47.57 (±4.25)
Actinomycin-D	1.511	1.754	1.736	0.648	0.889	0.873	61.70 (±7.02)
Tamoxifen	1.580	1.634	1.651	0.677	0.727	0.804	27.80 (±4.06)
Anastrozole	1.202	1.220	1.147	0.298	0.313	0.300	70.11 (±1.47)
Vehicle Control	2.880	2.847	2.936	2.017	1.982	2.074	3.68 (±2.14)
Caco-2 Cells							
Media	0.834	0.828	0.892	0.000	0.000	0.000	-------
Media + Cells	2.873	2.767	2.939	2.039	1.939	2.048	-------
0.78	2.738	2.597	2.686	1.904	1.769	1.794	9.26 (±2.90)
1.56	2.740	2.586	2.723	1.906	1.758	1.832	8.80 (±2.05)
3.12	2.441	2.531	2.620	1.607	1.703	1.728	16.32 (±4.56)
6.25	2.370	2.481	2.683	1.536	1.653	1.792	17.30 (±6.48)
12.5	2.366	2.472	2.389	1.532	1.644	1.497	22.31 (±6.24)
25	2.057	2.187	2.192	1.223	1.359	1.300	35.47 (±5.15)
50	1.825	1.850	2.111	0.991	1.022	1.220	46.38 (±5.55)
100	1.473	1.585	1.787	0.639	0.757	0.895	61.96 (±6.26)
Actinomycin-D	1.361	1.390	1.532	0.527	0.562	0.641	71.30 (±2.74)
Vehicle Control	2.795	2.809	2.798	1.961	1.981	1.906	2.85 (±4.63)

Appendix: 30

Percentage growth inhibition of cancer cells at various concentrations (µM) of hexadecanoic acid from *Solanum surattense* using MTT assay after 48 hours treatment

Concentration (µM)	Absorbance (cells + Pregnane + media)			Actual Absorbance (cells + Pregnane)- media			% Growth Inhibition (Mean ± STDEV)
Experiments	**1**	**2**	**3**	**1**	**2**	**3**	
MCF-7 Cells							
Media	0.811	0.850	0.862	0.000	0.000	0.000	-------
Media + Cells	2.683	2.756	2.885	1.872	1.906	2.023	-------
0.78	2.671	2.696	2.764	1.860	1.846	1.902	3.27 (±2.68)
1.56	2.626	2.652	2.754	1.815	1.803	1.892	5.01 (±1.76)
3.12	2.532	2.623	2.811	1.721	1.773	1.949	6.24 (±2.29)
6.25	2.623	2.560	2.608	1.812	1.710	1.746	9.08 (±5.35)
12.5	2.375	2.415	2.644	1.564	1.566	1.782	15.42 (±3.09)
25	2.070	2.239	2.305	1.259	1.389	1.443	29.53 (±2.89)
50	1.801	1.717	1.940	0.990	0.868	1.078	49.44 (±4.38)
100	1.612	1.540	1.499	0.802	0.690	0.637	63.17 (±5.69)
Actinomycin-D	1.336	1.332	1.283	0.526	0.482	0.421	75.27 (±2.27)
Tamoxifen	0.284	0.291	0.307	-0.005	0.000	0.007	99.64 (±3.67)
Anastrozole	0.855	0.459	0.503	0.565	0.168	0.203	46.39 (±1.14)
Vehicle Control	2.637	2.623	2.791	1.826	1.773	1.929	4.71 (±6.43)
MDA MB-468 Cells							
Media	0.855	0.882	0.899	0.000	0.000	0.000	-------
Media + Cells	2.790	2.877	2.865	1.935	1.995	1.966	-------
0.78	2.560	2.742	2.719	1.705	1.861	1.821	8.67 (±2.79)
1.56	2.489	2.668	2.618	1.634	1.787	1.719	12.85 (±2.57)
3.12	2.509	2.703	2.661	1.654	1.821	1.762	11.20 (±2.99)
6.25	2.717	2.570	2.759	1.862	1.689	1.860	8.17 (±6.27)
12.5	2.462	2.441	2.441	1.607	1.560	1.542	20.12 (±2.75)
25	2.197	2.280	2.064	1.343	1.398	1.166	33.75 (±6.04)
50	2.062	2.086	2.004	1.207	1.205	1.105	40.35 (±3.15)
100	1.793	1.898	1.998	0.938	1.017	1.099	48.22 (±3.77)
Actinomycin-D	1.300	1.413	1.492	0.445	0.532	0.594	73.38 (±3.60)
Tamoxifen	1.500	1.448	1.457	0.584	0.583	0.499	45.41 (±4.14)
Anastrozole	1.099	1.033	1.009	0.183	0.168	0.051	86.89 (±7.04)
Vehicle Control	2.773	2.821	2.760	1.919	1.939	1.862	2.99 (±2.25)
Caco-2 Cells							
Media	0.861	0.901	0.787	0.000	0.000	0.000	-------
Media + Cells	2.891	2.625	2.449	2.030	1.724	1.662	-------
0.78	2.737	2.515	2.310	1.875	1.613	1.523	7.46 (±0.97)
1.56	2.621	2.377	2.289	1.760	1.475	1.502	12.45 (±2.51)
3.12	2.562	2.398	2.293	1.700	1.496	1.506	12.93 (±3.44)
6.25	2.514	2.276	2.203	1.652	1.375	1.416	17.88 (±2.80)
12.5	2.342	2.316	2.117	1.480	1.415	1.330	21.66 (±4.79)
25	1.970	1.866	1.869	1.109	0.964	1.082	41.46 (±5.70)
50	1.721	1.743	1.582	0.860	0.841	0.796	53.65 (±3.48)
100	1.481	1.528	1.346	0.619	0.626	0.560	66.50 (±2.91)
Actinomycin-D	1.151	1.269	1.044	0.289	0.367	0.257	82.99 (±3.76)
Vehicle Control	2.784	2.515	2.512	1.923	1.614	1.725	2.62 (±5.57)

Appendix: 31

Percentage growth inhibition of cancer cells at various concentrations (µM) of hexadecanoic acid from *Solanum surattense* using neutral red uptake assay after 24 hours treatment

Concentration (µM)	Absorbance (cells + Pregnane + media)			Actual Absorbance (cells + Pregnane)- media			% Growth Inhibition (Mean ± STDEV)
Experiments	**1**	**2**	**3**	**1**	**2**	**3**	
MCF-7 Cells							
Media	0.193	0.173	0.216	0.000	0.000	0.000	-------
Media + Cells	0.622	0.635	0.734	0.429	0.463	0.518	-------
0.78	0.611	0.601	0.735	0.419	0.428	0.519	3.26 (±3.86)
1.56	0.595	0.603	0.709	0.402	0.430	0.493	6.05 (±1.11)
3.12	0.603	0.568	0.698	0.410	0.395	0.482	8.63 (±5.36)
6.25	0.589	0.543	0.663	0.396	0.370	0.447	13.84 (±6.17)
12.5	0.524	0.513	0.616	0.331	0.340	0.400	23.98 (±2.17)
25	0.494	0.450	0.585	0.302	0.277	0.369	32.83 (±6.27)
50	0.468	0.414	0.534	0.275	0.241	0.318	40.74 (±6.31)
100	0.378	0.355	0.464	0.185	0.183	0.248	56.47 (±4.23)
Actinomycin-D	0.292	0.303	0.355	0.099	0.131	0.140	73.88 (±2.63)
Tamoxifen	1.377	1.364	1.401	0.111	0.062	0.045	78.19 (±3.17)
Anastrozole	1.555	1.486	1.555	0.289	0.185	0.199	46.28 (±5.64)
Vehicle Control	0.608	0.603	0.704	0.415	0.431	0.488	5.29 (±1.95)
MDA MB-468 Cells							
Media	0.689	0.735	0.815	0.000	0.000	0.000	-------
Media + Cells	1.175	1.205	1.321	0.487	0.470	0.506	-------
0.78	1.166	1.169	1.264	0.477	0.434	0.449	6.97 (±4.75)
1.56	1.142	1.154	1.207	0.454	0.419	0.392	13.39 (±8.16)
3.12	1.139	1.148	1.208	0.450	0.413	0.393	14.01 (±7.60)
6.25	1.109	1.149	1.295	0.421	0.414	0.480	10.20 (±4.51)
12.5	1.112	1.117	1.193	0.424	0.382	0.378	19.00 (±6.15)
25	1.068	1.070	1.153	0.379	0.335	0.338	28.04 (±5.57)
50	0.993	1.017	1.092	0.305	0.282	0.277	40.88 (±4.00)
100	0.922	1.004	1.060	0.233	0.269	0.245	48.81 (±5.15)
Actinomycin-D	0.842	0.861	0.923	0.153	0.126	0.108	73.46 (±5.09)
Tamoxifen	1.651	1.578	1.545	0.764	0.640	0.553	38.36 (±6.26)
Anastrozole	1.132	1.205	1.292	0.245	0.267	0.301	74.11 (±4.18)
Vehicle Control	1.157	1.193	1.298	0.468	0.458	0.483	3.64 (±0.97)
Caco-2 Cells							
Media	0.227	0.212	0.250	0.000	0.000	0.000	-------
Media + Cells	0.409	0.423	0.406	0.183	0.211	0.156	-------
0.78	0.398	0.393	0.400	0.171	0.182	0.150	8.04 (±5.30)
1.56	0.395	0.388	0.388	0.168	0.177	0.138	11.93 (±4.19)
3.12	0.364	0.381	0.381	0.137	0.169	0.131	20.24 (±4.35)
6.25	0.337	0.365	0.361	0.111	0.154	0.111	31.84 (±6.61)
12.5	0.353	0.368	0.353	0.126	0.157	0.103	30.17 (±4.02)
25	0.327	0.349	0.354	0.100	0.137	0.104	37.81 (±6.38)
50	0.310	0.316	0.328	0.084	0.105	0.078	51.51 (±2.30)
100	0.273	0.288	0.295	0.046	0.077	0.045	69.97 (±5.63)
Actinomycin-D	0.288	0.269	0.284	0.061	0.058	0.034	72.32 (±5.84)
Vehicle Control	0.403	0.420	0.398	0.176	0.208	0.148	3.39 (±1.90)

Appendix: 32

Percentage growth inhibition of cancer cells at various concentrations (μM) of hexadecanoic acid from *Solanum surattense* using neutral red uptake assay after 48 hours treatment

Concentration (μM)	Absorbance (cells + Pregnane + media)			Actual Absorbance (cells + Pregnane)- media			% Growth Inhibition (Mean ± STDEV)
Experiments	**1**	**2**	**3**	**1**	**2**	**3**	
MCF-7 Cells							
Media	0.240	0.273	0.276	0.000	0.000	0.000	-------
Media + Cells	0.757	0.752	0.777	0.517	0.479	0.501	-------
0.78	0.737	0.708	0.699	0.497	0.435	0.423	9.51 (±5.84)
1.56	0.739	0.682	0.711	0.499	0.409	0.435	10.41 (±6.04)
3.12	0.692	0.704	0.740	0.452	0.431	0.464	9.98 (±2.59)
6.25	0.616	0.598	0.691	0.376	0.325	0.415	25.47 (±7.66)
12.5	0.642	0.597	0.646	0.402	0.324	0.369	26.98 (±5.12)
25	0.548	0.569	0.561	0.308	0.296	0.284	40.63 (±2.45)
50	0.539	0.519	0.577	0.298	0.246	0.301	43.62 (±4.57)
100	0.452	0.452	0.518	0.211	0.179	0.242	57.82 (±5.54)
Actinomycin-D	0.330	0.331	0.303	0.090	0.058	0.027	88.37 (±5.98)
Tamoxifen	0.284	0.291	0.307	-0.005	0.000	0.007	100.24 (±0.37)
Anastrozole	0.855	0.459	0.503	0.565	0.168	0.203	36.22 (±4.21)
Vehicle Control	0.745	0.761	0.749	0.504	0.487	0.473	2.05 (±3.61)
MDA MB-468 Cells							
Media	0.857	0.874	0.906	0.000	0.000	0.000	-------
Media + Cells	1.327	1.295	1.271	0.470	0.420	0.365	-------
0.78	1.294	1.274	1.217	0.437	0.400	0.311	8.90 (±5.27)
1.56	1.306	1.241	1.210	0.449	0.367	0.303	11.33 (±6.30)
3.12	1.267	1.241	1.200	0.410	0.366	0.294	14.98 (±3.85)
6.25	1.254	1.204	1.204	0.397	0.329	0.298	18.48 (±3.06)
12.5	1.148	1.222	1.181	0.291	0.348	0.274	26.70 (±10.57)
25	1.162	1.201	1.154	0.305	0.326	0.248	29.78 (±6.65)
50	1.137	1.137	1.107	0.280	0.263	0.201	40.98 (±3.80)
100	1.061	1.088	1.098	0.204	0.214	0.192	51.04 (±4.98)
Actinomycin-D	0.887	0.891	0.958	0.030	0.016	0.051	91.92 (±5.35)
Tamoxifen	1.346	1.300	1.359	0.403	0.297	0.318	63.05 (±3.16)
Anastrozole	1.087	1.024	1.079	0.144	0.021	0.038	92.99 (±6.23)
Vehicle Control	1.313	1.267	1.289	0.456	0.393	0.383	1.55 (±5.77)
Caco-2 Cells							
Media	0.247	0.237	0.257	0.000	0.000	0.000	-------
Media + Cells	0.413	0.429	0.422	0.166	0.192	0.166	-------
0.78	0.292	0.378	0.407	0.142	0.141	0.151	16.75 (±8.90)
1.56	0.389	0.377	0.399	0.132	0.139	0.143	20.58 (±6.69)
3.12	0.379	0.398	0.394	0.141	0.161	0.137	16.02 (±1.19)
6.25	0.389	0.379	0.402	0.113	0.142	0.145	23.50 (±9.94)
12.5	0.360	0.367	0.386	0.108	0.130	0.130	29.66 (±6.94)
25	0.356	0.379	0.389	0.115	0.142	0.133	25.57 (±5.30)
50	0.363	0.329	0.326	0.071	0.091	0.069	55.96 (±3.06)
100	0.318	0.297	0.314	0.044	0.060	0.057	69.27 (±3.84)
Actinomycin-D	0.255	0.268	0.270	0.008	0.031	0.014	90.36 (±5.80)
Vehicle Control	0.418	0.423	0.412	0.170	0.186	0.156	2.17 (±4.43)

Appendix: 33

Percentage growth inhibition of cancer cells at various concentrations (μM) of phthalic acid from *Solanum surattense* using MTT assay after 24 hours treatment

Concentration (μM)	Absorbance (cells + Pregnane + media)			Actual Absorbance (cells + Pregnane)- media			% Growth Inhibition (Mean ± STDEV)
Experiments	**1**	**2**	**3**	**1**	**2**	**3**	
MCF-7 Cells							
Media	0.588	0.653	0.766	0.000	0.000	0.000	-------
Media + Cells	2.631	2.770	2.719	2.043	2.117	1.953	-------
0.78	2.600	2.543	2.669	2.012	1.890	1.903	4.94 (±5.05)
1.56	2.594	2.635	2.675	2.006	1.982	1.909	3.46 (±2.54)
3.12	2.491	2.574	2.643	1.903	1.921	1.877	6.67 (±2.71)
6.25	2.543	2.576	2.493	1.955	1.923	1.726	8.35 (±3.71)
12.5	2.023	2.520	2.301	1.435	1.867	1.535	20.98 (±8.98)
25	1.925	2.251	2.197	1.337	1.598	1.430	28.61 (±5.27)
50	1.641	1.839	1.993	1.053	1.186	1.227	43.21 (±5.67)
100	1.380	1.512	1.670	0.792	0.859	0.903	58.14 (±3.92)
Actinomycin-D	1.367	1.616	1.740	0.779	0.963	0.974	55.51 (±5.93)
Tamoxifen	1.377	1.364	1.401	0.111	0.062	0.045	84.74 (±4.33)
Anastrozole	1.555	1.486	1.555	0.289	0.185	0.199	51.72 (±3.42)
Vehicle Control	2.519	2.726	2.690	1.931	2.073	1.924	3.00 (±2.16)
MDA MB-468 Cells							
Media	0.873	0.862	0.858	0.000	0.000	0.000	-------
Media + Cells	2.945	2.934	3.036	2.072	2.072	2.178	-------
0.78	2.642	2.812	2.792	1.769	1.950	1.934	10.58 (±4.41)
1.56	2.490	2.647	2.798	1.617	1.785	1.939	15.59 (±5.72)
3.12	2.401	2.320	2.552	1.528	1.458	1.693	26.05 (±3.69)
6.25	2.257	2.324	2.455	1.384	1.462	1.597	29.77 (±3.27)
12.5	2.046	2.149	2.366	1.172	1.287	1.508	37.36 (±6.34)
25	1.858	1.930	1.981	0.985	1.068	1.123	49.78 (±2.32)
50	1.355	1.522	1.556	0.482	0.659	0.698	70.96 (±5.00)
100	1.246	1.361	1.422	0.373	0.499	0.563	77.35 (±4.11)
Actinomycin-D	1.494	1.691	1.705	0.621	0.829	0.846	63.74 (±5.50)
Tamoxifen	1.580	1.634	1.651	0.677	0.727	0.804	27.80 (±4.06)
Anastrozole	1.202	1.220	1.147	0.298	0.313	0.300	70.11 (±1.47)
Vehicle Control	2.802	2.834	2.901	1.929	1.972	2.043	5.98 (±1.05)
Caco-2 Cells							
Media	0.883	0.836	0.837	0.000	0.000	0.000	-------
Media + Cells	2.803	2.813	2.898	1.920	1.978	2.061	-------
0.78	2.711	2.636	2.679	1.828	1.800	1.842	8.13 (±3.01)
1.56	2.728	2.595	2.752	1.845	1.760	1.915	7.33 (±3.57)
3.12	2.495	2.564	2.620	1.612	1.728	1.783	14.03 (±1.77)
6.25	2.396	2.642	2.705	1.513	1.806	1.868	13.07 (±7.04)
12.5	2.429	2.552	2.353	1.546	1.716	1.517	19.70 (±6.60)
25	1.906	1.926	2.106	1.022	1.090	1.270	43.33 (±4.38)
50	1.643	1.650	1.786	0.759	0.814	0.949	57.74 (±3.39)
100	1.349	1.352	1.534	0.466	0.517	0.697	71.92 (±5.07)
Actinomycin-D	1.349	1.438	1.547	0.466	0.603	0.710	70.26 (±5.13)
Vehicle Control	2.754	2.885	2.792	1.870	2.050	1.955	1.36 (±4.51)

Appendix: 34

Percentage growth inhibition of cancer cells at various concentrations (μM) of phthalic acid from *Solanum surattense* using MTT assay after 48 hours treatment

Concentration (μM)	Absorbance (cells + Pregnane + media)			Actual Absorbance (cells + Pregnane)- media			% Growth Inhibition (Mean ± STDEV)
Experiments	**1**	**2**	**3**	**1**	**2**	**3**	
MCF-7 Cells							
Media	0.824	0.831	0.811	0.000	0.000	0.000	-------
Media + Cells	2.724	2.772	2.822	1.900	1.941	2.011	-------
0.78	2.685	2.763	2.700	1.861	1.932	1.890	2.84 (±2.88)
1.56	2.590	2.718	2.745	1.766	1.887	1.934	4.54 (±2.22)
3.12	2.600	2.583	2.681	1.776	1.752	1.871	7.74 (±1.72)
6.25	2.634	2.585	2.564	1.810	1.754	1.754	9.05 (±4.05)
12.5	2.468	2.402	2.628	1.644	1.571	1.817	14.05 (±4.74)
25	2.035	2.232	2.238	1.211	1.400	1.427	31.04 (±4.57)
50	1.735	1.692	1.872	0.911	0.861	1.061	51.65 (±4.21)
100	1.326	1.446	1.316	0.502	0.615	0.505	72.26 (±3.46)
Actinomycin-D	1.378	1.320	1.279	0.554	0.489	0.468	75.39 (±3.90)
Tamoxifen	0.284	0.291	0.307	-0.005	0.000	0.007	99.64 (±1.14)
Anastrozole	0.855	0.459	0.503	0.565	0.168	0.203	46.39 (±6.43)
Vehicle Control	2.664	2.624	2.762	1.840	1.792	1.951	4.58 (±2.64)
MDA MB-468 Cells							
Media	0.853	0.892	0.906	0.000	0.000	0.000	-------
Media + Cells	2.718	2.886	2.856	1.865	1.993	1.950	-------
0.78	2.626	2.672	2.752	1.773	1.780	1.846	6.98(±3.22)
1.56	2.480	2.423	2.412	1.627	1.530	1.506	19.58 (±5.92)
3.12	2.147	2.126	2.005	1.294	1.233	1.098	37.46 (±6.57)
6.25	2.050	1.987	1.838	1.197	1.094	0.932	44.37 (±8.21)
12.5	1.779	1.911	1.991	0.926	1.019	1.085	47.86 (±3.12)
25	1.529	1.673	1.707	0.675	0.781	0.801	61.19 (±2.43)
50	1.316	1.566	1.511	0.462	0.674	0.605	70.13 (±4.62)
100	1.198	1.130	1.381	0.344	0.238	0.475	81.76 (±6.21)
Actinomycin-D	1.292	1.190	1.332	0.439	0.298	0.426	79.90 (±4.56)
Tamoxifen	1.500	1.448	1.457	0.584	0.583	0.499	45.41 (±4.14)
Anastrozole	1.099	1.033	1.009	0.183	0.168	0.051	86.89 (±7.04)
Vehicle Control	2.765	2.857	2.811	1.912	1.965	1.904	0.41 (±2.58)
Caco-2 Cells							
Media	0.842	0.788	0.749	0.000	0.000	0.000	-------
Media + Cells	2.813	2.573	2.494	1.971	1.785	1.745	-------
0.78	2.582	2.277	2.321	1.740	1.489	1.572	12.74 (±3.45)
1.56	2.306	2.235	2.198	1.464	1.447	1.449	20.55 (±4.59)
3.12	2.138	2.109	2.092	1.296	1.320	1.343	27.77 (±5.80)
6.25	1.941	1.888	1.902	1.100	1.100	1.153	38.83 (±5.17)
12.5	1.674	1.439	1.431	0.833	0.651	0.682	60.75 (±2.89)
25	1.515	1.242	1.149	0.673	0.454	0.400	72.49 (±5.89)
50	1.135	0.926	0.941	0.293	0.138	0.192	88.80 (±3.57)
100	1.027	0.834	0.876	0.185	0.046	0.127	93.58 (±3.50)
Actinomycin-D	1.134	0.955	0.862	0.292	0.166	0.113	89.79 (±4.22)
Vehicle Control	2.834	2.540	2.558	1.992	1.752	1.809	-0.95 (±2.74)

Appendix: 35

Percentage growth inhibition of cancer cells at various concentrations (μM) of phthalic acid from *Solanum surattense* using neutral red uptake assay after 24 hours treatment

Concentration (μM)	Absorbance (cells + Pregnane + media)			Actual Absorbance (cells + Pregnane)- media			% Growth Inhibition (Mean ± STDEV)
Experiments	**1**	**2**	**3**	**1**	**2**	**3**	
MCF-7 Cells							
Media	0.160	0.175	0.205	0.000	0.000	0.000	-------
Media + Cells	0.621	0.640	0.729	0.461	0.465	0.524	-------
0.78	0.615	0.599	0.706	0.455	0.424	0.500	4.87 (±3.66)
1.56	0.554	0.566	0.685	0.394	0.391	0.480	12.89 (±4.02)
3.12	0.578	0.566	0.622	0.418	0.391	0.417	15.23 (±5.48)
6.25	0.507	0.536	0.584	0.347	0.361	0.379	24.88 (±2.69)
12.5	0.504	0.455	0.559	0.344	0.280	0.354	32.48 (±7.16)
25	0.462	0.426	0.529	0.302	0.251	0.324	39.57 (±5.79)
50	0.366	0.348	0.454	0.206	0.173	0.249	56.84 (±5.27)
100	0.281	0.265	0.293	0.121	0.090	0.088	79.22 (±4.85)
Actinomycin-D	0.261	0.268	0.337	0.101	0.094	0.132	77.62 (±2.57)
Tamoxifen	1.377	1.364	1.401	0.111	0.062	0.045	78.19 (±3.17)
Anastrozole	1.555	1.486	1.555	0.289	0.185	0.199	46.28 (±5.64)
Vehicle Control	0.616	0.667	0.695	0.456	0.492	0.490	0.53 (±6.15)
MDA MB-468 Cells							
Media	0.716	0.696	0.827	0.000	0.000	0.000	-------
Media + Cells	1.196	1.197	1.268	0.480	0.502	0.441	-------
0.78	1.174	1.159	1.264	0.458	0.464	0.437	4.35 (±3.36)
1.56	1.161	1.180	1.206	0.445	0.485	0.379	8.29 (±5.41)
3.12	1.088	1.127	1.159	0.372	0.431	0.332	20.42 (±5.61)
6.25	1.019	1.083	1.111	0.303	0.387	0.285	31.73 (±7.67)
12.5	0.933	0.991	1.004	0.217	0.296	0.177	51.90 (±9.73)
25	0.873	0.906	0.977	0.157	0.210	0.150	63.79 (±4.97)
50	0.861	0.836	0.928	0.145	0.140	0.101	72.94 (±3.73)
100	0.815	0.816	0.887	0.099	0.120	0.061	80.60 (±5.18)
Actinomycin-D	0.787	0.843	0.910	0.071	0.148	0.083	78.96 (±7.50)
Tamoxifen	1.651	1.578	1.545	0.764	0.640	0.553	38.36 (±6.26)
Anastrozole	1.132	1.205	1.292	0.245	0.267	0.301	74.11 (±4.18)
Vehicle Control	1.184	1.177	1.245	0.468	0.481	0.419	3.86 (±1.35)
Caco-2 Cells							
Media	0.228	0.228	0.245	0.000	0.000	0.000	-------
Media + Cells	0.394	0.393	0.411	0.166	0.165	0.166	-------
0.78	0.377	0.370	0.380	0.149	0.142	0.135	14.35 (±3.98)
1.56	0.351	0.374	0.372	0.123	0.146	0.127	20.34 (±7.70)
3.12	0.348	0.351	0.354	0.120	0.123	0.109	29.19 (±4.53)
6.25	0.339	0.334	0.345	0.111	0.106	0.100	36.22 (±3.34)
12.5	0.319	0.306	0.312	0.091	0.079	0.068	52.25 (±7.14)
25	0.305	0.299	0.308	0.077	0.071	0.063	57.62 (±4.17)
50	0.252	0.271	0.283	0.024	0.043	0.038	78.78 (±6.08)
100	0.235	0.239	0.265	0.007	0.011	0.021	92.18 (±4.22)
Actinomycin-D	0.272	0.250	0.292	0.044	0.022	0.047	77.15 (±8.21)
Vehicle Control	0.388	0.393	0.414	0.160	0.165	0.169	0.66 (±2.87)

Appendix: 36

Percentage growth inhibition of cancer cells at various concentrations (μM) of phthalic acid from *Solanum surattense* using neutral red uptake assay after 48 hours treatment

Concentration (μM)	Absorbance (cells + Pregnane + media)			Actual Absorbance (cells + Pregnane)- media			% Growth Inhibition (Mean ± STDEV)
Experiments	**1**	**2**	**3**	**1**	**2**	**3**	
MCF-7 Cells							
Media	0.218	0.232	0.255	0.000	0.000	0.000	-------
Media + Cells	0.825	0.751	0.803	0.607	0.519	0.548	-------
0.78	0.794	0.698	0.728	0.576	0.466	0.472	9.71 (±4.33)
1.56	0.681	0.586	0.692	0.463	0.354	0.436	25.30 (±5.91)
3.12	0.601	0.573	0.656	0.383	0.341	0.401	32.67 (±5.23)
6.25	0.570	0.592	0.544	0.353	0.360	0.288	39.96 (±8.53)
12.5	0.522	0.470	0.524	0.304	0.238	0.269	51.65 (±2.19)
25	0.455	0.480	0.486	0.238	0.248	0.231	56.99 (±4.37)
50	0.383	0.356	0.423	0.165	0.124	0.168	72.79 (±3.35)
100	0.337	0.303	0.282	0.119	0.071	0.026	87.29 (±7.44)
Actinomycin-D	0.271	0.237	0.282	0.053	0.005	0.027	95.13 (±3.86)
Tamoxifen	0.284	0.291	0.307	-0.005	0.000	0.007	100.24 (±0.37)
Anastrozole	0.855	0.459	0.503	0.565	0.168	0.203	36.22 (±4.21)
Vehicle Control	0.799	0.761	0.807	0.581	0.529	0.552	0.55 (±3.30)
MDA MB-468 Cells							
Media	0.912	0.944	0.885	0.000	0.000	0.000	-------
Media + Cells	1.260	1.255	1.259	0.348	0.311	0.373	-------
0.78	1.264	1.240	1.208	0.351	0.296	0.323	5.80 (±7.29)
1.56	1.247	1.203	1.175	0.335	0.259	0.289	14.33 (±9.66)
3.12	1.135	1.142	1.065	0.223	0.198	0.179	41.40 (±9.14)
6.25	1.099	1.101	1.083	0.187	0.157	0.197	47.65 (±1.61)
12.5	1.028	1.055	1.053	0.116	0.111	0.167	62.05 (±6.10)
25	0.995	1.030	1.002	0.082	0.087	0.116	72.44 (±3.78)
50	0.956	0.960	0.937	0.044	0.016	0.051	89.52 (±4.63)
100	0.925	0.978	0.895	0.013	0.034	0.009	94.27 (±4.55)
Actinomycin-D	0.929	0.950	0.924	0.017	0.006	0.039	94.31 (±4.28)
Tamoxifen	1.346	1.300	1.359	0.403	0.297	0.318	63.05 (±3.16)
Anastrozole	1.087	1.024	1.079	0.144	0.021	0.038	92.99 (±6.23)
Vehicle Control	1.248	1.254	1.249	0.335	0.311	0.364	2.12 (±1.69)
Caco-2 Cells							
Media	0.213	0.203	0.216	0.000	0.000	0.000	-------
Media + Cells	0.371	0.358	0.394	0.158	0.155	0.178	-------
0.78	0.345	0.330	0.372	0.132	0.127	0.156	15.55 (±2.88)
1.56	0.342	0.337	0.357	0.130	0.134	0.141	17.40 (±3.66)
3.12	0.323	0.310	0.323	0.111	0.107	0.108	33.64 (±5.26)
6.25	0.278	0.288	0.292	0.066	0.085	0.076	53.60 (±7.44)
12.5	0.257	0.257	0.269	0.044	0.054	0.054	68.94 (±3.47)
25	0.237	0.234	0.260	0.025	0.031	0.044	79.79 (±4.53)
50	0.228	0.210	0.231	0.015	0.007	0.015	92.60 (±2.67)
100	0.217	0.206	0.214	0.005	0.003	-0.001	98.67 (±1.94)
Actinomycin-D	0.219	0.207	0.216	0.007	0.004	0.001	97.51 (±1.87)
Vehicle Control	0.385	0.350	0.388	0.172	0.147	0.173	-0.12 (±7.82)

Appendix: 37

Percentage growth inhibition of cancer cells at various concentrations (μM) of docosanoic acid from *Arisaema utile* using MTT assay after 24 hours treatment

Concentration (μM)	Absorbance (cells + Pregnane + media)			Actual Absorbance (cells + Pregnane)- media			% Growth Inhibition (Mean ± STDEV)
Experiments	**1**	**2**	**3**	**1**	**2**	**3**	
MCF-7 Cells							
Media	0.674	0.723	0.781	0.000	0.000	0.000	-------
Media + Cells	2.603	2.721	2.808	1.929	1.998	2.027	-------
0.78	2.470	2.582	2.662	1.795	1.859	1.881	7.04 (±0.14)
1.56	2.434	2.584	2.639	1.760	1.861	1.858	7.98 (±0.99)
3.12	2.302	2.512	2.592	1.627	1.789	1.811	12.26 (±2.94)
6.25	2.316	2.622	2.484	1.641	1.899	1.703	11.95 (±6.07)
12.5	2.030	2.438	2.344	1.356	1.715	1.563	22.26 (±7.79)
25	1.843	2.184	2.196	1.169	1.461	1.415	32.18 (±6.48)
50	1.677	1.800	2.011	1.003	1.077	1.230	44.48 (±4.57)
100	1.389	1.601	1.388	0.714	0.877	0.607	63.04 (±6.99)
Actinomycin-D	1.366	1.529	1.348	0.691	0.806	0.567	65.29 (±6.25)
Tamoxifen	1.377	1.364	1.401	0.111	0.062	0.045	84.74 (±4.33)
Anastrozole	1.555	1.486	1.555	0.289	0.185	0.199	51.72 (±3.42)
Vehicle Control	2.528	2.823	2.718	1.854	2.100	1.937	1.09 (±5.34)
MDA MB-468 Cells							
Media	0.865	0.886	0.877	0.000	0.000	0.000	-------
Media + Cells	2.947	2.920	3.069	2.081	2.034	2.191	-------
0.78	2.653	2.805	2.817	1.788	1.920	1.939	10.40 (±4.33)
1.56	2.476	2.690	2.871	1.611	1.804	1.994	14.31 (±7.29)
3.12	2.408	2.322	2.553	1.543	1.437	1.676	26.26 (±2.95)
6.25	2.249	2.305	2.479	1.384	1.419	1.602	30.21 (±3.31)
12.5	2.056	2.116	2.374	1.191	1.230	1.497	38.00 (±5.71)
25	1.849	1.958	1.998	0.983	1.073	1.121	49.62 (±2.82)
50	1.376	1.507	1.560	0.511	0.621	0.683	71.26 (±3.66)
100	1.240	1.391	1.437	0.375	0.505	0.559	77.20 (±4.16)
Actinomycin-D	1.501	1.697	1.700	0.636	0.811	0.823	64.01 (±4.84)
Tamoxifen	1.580	1.634	1.651	0.677	0.727	0.804	27.80 (±4.06)
Anastrozole	1.202	1.220	1.147	0.298	0.313	0.300	70.11 (±1.47)
Vehicle Control	2.834	2.830	2.976	1.969	1.944	2.098	4.70 (±0.63)
Caco-2 Cells							
Media	0.859	0.902	0.840	0.000	0.000	0.000	-------
Media + Cells	2.869	2.906	2.855	2.010	2.004	2.015	-------
0.78	2.694	2.685	2.695	1.835	1.783	1.855	9.23 (±1.60)
1.56	2.695	2.749	2.731	1.836	1.848	1.890	7.54 (±1.26)
3.12	2.403	2.596	2.626	1.544	1.695	1.785	16.67 (±6.00)
6.25	2.458	2.652	2.711	1.599	1.750	1.871	13.43 (±6.68)
12.5	2.494	2.432	2.338	1.636	1.530	1.498	22.65 (±3.61)
25	1.944	1.920	2.083	1.085	1.018	1.243	44.51 (±5.58)
50	1.696	1.646	1.778	0.837	0.745	0.937	58.23 (±4.63)
100	1.385	1.530	1.554	0.526	0.629	0.714	69.01 (±5.85)
Actinomycin-D	1.357	1.492	1.574	0.499	0.590	0.734	69.77 (±0.80)
Vehicle Control	2.786	2.855	2.792	1.927	1.953	1.951	3.27 (±4.68)

Appendix: 38

Percentage growth inhibition of cancer cells at various concentrations (μM) of docosanoic acid from *Arisaema utile* using MTT assay after 48 hours treatment

Concentration (μM)	Absorbance (cells + Pregnane + media)			Actual Absorbance (cells + Pregnane)- media			% Growth Inhibition (Mean ± STDEV)
Experiments	**1**	**2**	**3**	**1**	**2**	**3**	
MCF-7 Cells							
Media	0.839	0.805	0.803	0.000	0.000	0.000	-------
Media + Cells	2.774	2.773	2.816	1.934	1.969	2.013	-------
0.78	2.721	2.628	2.699	1.882	1.823	1.896	5.29 (±2.39)
1.56	2.689	2.511	2.760	1.850	1.706	1.957	6.83 (±5.70)
3.12	2.656	2.486	2.705	1.816	1.681	1.902	8.73 (±5.10)
6.25	2.481	2.658	2.454	1.641	1.853	1.650	13.00 (±6.34)
12.5	2.485	2.402	2.390	1.645	1.597	1.586	18.33 (±3.16)
25	2.008	1.758	2.131	1.168	0.953	1.327	41.74 (±8.96)
50	1.576	1.455	1.311	0.737	0.650	0.508	67.89 (±6.47)
100	1.205	1.274	1.143	0.365	0.469	0.339	80.14 (±3.58)
Actinomycin-D	1.386	1.208	1.233	0.547	0.403	0.430	76.63 (±4.27)
Tamoxifen	0.284	0.291	0.307	-0.005	0.000	0.007	99.64 (±1.14)
Anastrozole	0.855	0.459	0.503	0.565	0.168	0.203	46.39 (±6.43)
Vehicle Control	2.680	2.662	2.829	1.841	1.857	2.026	3.28 (±3.44)
MDA MB-468 Cells							
Media	0.865	0.906	0.913	0.000	0.000	0.000	-------
Media + Cells	2.713	2.905	2.825	1.848	1.999	1.911	-------
0.78	2.640	2.693	2.740	1.775	1.787	1.826	6.35 (±3.70)
1.56	2.465	2.451	2.421	1.600	1.545	1.508	19.08 (±4.96)
3.12	2.171	2.172	2.015	1.305	1.266	1.102	36.13 (±6.51)
6.25	2.052	2.024	1.845	1.186	1.119	0.932	43.70 (±7.72)
12.5	1.789	1.966	2.022	0.924	1.060	1.109	46.33 (±4.04)
25	1.585	1.723	1.716	0.720	0.817	0.803	59.39 (±1.53)
50	1.292	1.570	1.606	0.427	0.664	0.693	69.14 (±6.88)
100	1.168	1.133	1.393	0.302	0.228	0.479	82.39 (±6.93)
Actinomycin-D	1.306	1.234	1.402	0.441	0.329	0.489	78.04 (±4.84)
Tamoxifen	1.500	1.448	1.457	0.584	0.583	0.499	45.41 (±4.14)
Anastrozole	1.099	1.033	1.009	0.183	0.168	0.051	86.89 (±7.04)
Vehicle Control	2.773	2.841	2.719	1.908	1.935	1.805	1.83 (±4.56)
Caco-2 Cells							
Media	0.843	0.787	0.774	0.000	0.000	0.000	-------
Media + Cells	2.761	2.670	2.545	1.918	1.883	1.771	-------
0.78	2.582	2.414	2.314	1.739	1.627	1.540	11.99 (±2.32)
1.56	2.568	2.311	2.310	1.724	1.524	1.536	14.15 (±4.56)
3.12	2.219	1.993	2.122	1.375	1.206	1.348	29.37 (±6.12)
6.25	2.015	1.895	1.857	1.171	1.109	1.083	39.64 (±1.29)
12.5	1.738	1.524	1.405	0.895	0.737	0.631	59.52 (±5.62)
25	1.551	1.259	1.183	0.707	0.472	0.409	71.65 (±7.45)
50	1.138	0.888	0.881	0.295	0.101	0.107	91.07 (±5.59)
100	0.997	0.854	0.904	0.154	0.067	0.131	93.68 (±2.42)
Actinomycin-D	1.150	0.993	0.818	0.307	0.206	0.044	90.19 (±6.83)
Vehicle Control	2.854	2.549	2.561	2.011	1.763	1.787	0.21 (±5.71)

Appendix: 39

Percentage growth inhibition of cancer cells at various concentrations (µM) of docosanoic acid from *Arisaema utile* using neutral red uptake assay after 24 hours treatment

Concentration (µM)	Absorbance (cells + Pregnane + media)			Actual Absorbance (cells + Pregnane)- media			% Growth Inhibition (Mean ± STDEV)
Experiments	**1**	**2**	**3**	**1**	**2**	**3**	
MCF-7 Cells							
Media	0.161	0.197	0.221	0.000	0.000	0.000	-------
Media + Cells	0.652	0.649	0.789	0.491	0.453	0.569	-------
0.78	0.613	0.625	0.693	0.452	0.428	0.472	10.10 (±6.09)
1.56	0.609	0.521	0.746	0.448	0.325	0.525	14.85(±11.66)
3.12	0.565	0.578	0.636	0.404	0.381	0.415	20.14(±5.97)
6.25	0.521	0.583	0.621	0.360	0.386	0.400	23.65(±7.85)
12.5	0.501	0.562	0.609	0.340	0.366	0.388	27.25(±6.94)
25	0.461	0.546	0.606	0.300	0.350	0.386	31.26(±8.04)
50	0.366	0.416	0.429	0.205	0.219	0.208	57.69(±5.94)
100	0.293	0.282	0.295	0.133	0.085	0.074	80.39(±7.00)
Actinomycin-D	0.313	0.270	0.335	0.152	0.073	0.114	77.60(±7.67)
Tamoxifen	1.377	1.364	1.401	0.111	0.062	0.045	78.19(±3.17)
Anastrozole	1.555	1.486	1.555	0.289	0.185	0.199	46.28(±5.64)
Vehicle Control	0.634	0.619	0.764	0.473	0.422	0.543	4.94(±1.65)
MDA MB-468 Cells							
Media	0.759	0.782	0.889	0.000	0.000	0.000	-------
Media + Cells	1.183	1.195	1.296	0.424	0.413	0.407	-------
0.78	1.141	1.169	1.225	0.382	0.387	0.336	11.25 (±5.76)
1.56	1.132	1.160	1.189	0.373	0.378	0.300	15.60 (±9.44)
3.12	1.100	1.129	1.158	0.341	0.347	0.269	23.19 (±9.54)
6.25	1.032	1.112	1.134	0.273	0.330	0.245	31.90 (±10.43)
12.5	0.945	1.005	1.058	0.186	0.223	0.169	53.55 (±6.71)
25	0.876	0.932	0.996	0.117	0.150	0.107	69.92 (±5.53)
50	0.861	0.857	0.957	0.102	0.075	0.067	80.37 (±4.00)
100	0.813	0.822	0.909	0.054	0.040	0.020	90.91 (±3.99)
Actinomycin-D	0.904	0.894	0.992	0.145	0.112	0.103	71.10 (±4.64)
Tamoxifen	1.651	1.578	1.545	0.764	0.640	0.553	38.36 (±6.26)
Anastrozole	1.132	1.205	1.292	0.245	0.267	0.301	74.11 (±4.18)
Vehicle Control	1.171	1.182	1.280	0.412	0.400	0.391	3.29 (±0.63)
Caco-2 Cells							
Media	0.232	0.238	0.245	0.000	0.000	0.000	-------
Media + Cells	0.426	0.407	0.399	0.194	0.169	0.154	-------
0.78	0.381	0.368	0.380	0.148	0.130	0.135	19.64 (±6.36)
1.56	0.388	0.376	0.369	0.156	0.138	0.124	19.14 (±0.93)
3.12	0.382	0.356	0.340	0.149	0.118	0.095	30.40 (±7.59)
6.25	0.351	0.355	0.347	0.118	0.117	0.102	34.48 (±4.13)
12.5	0.317	0.339	0.328	0.085	0.101	0.083	47.46 (±8.22)
25	0.299	0.315	0.339	0.067	0.076	0.094	53.12 (±13.32)
50	0.260	0.280	0.268	0.028	0.041	0.023	82.02 (±8.70)
100	0.241	0.238	0.271	0.009	0.000	0.026	92.89 (±4.01)
Actinomycin-D	0.278	0.284	0.274	0.046	0.046	0.029	76.72 (±1.33)
Vehicle Control	0.419	0.396	0.391	0.186	0.158	0.146	5.19 (±5.73)

Appendix: 40

Percentage growth inhibition of cancer cells at various concentrations (μM) of docosanoic acid from *Arisaema utile* using neutral red uptake assay after 48 hours treatment

Concentration (μM)	Absorbance (cells + Pregnane + media)			Actual Absorbance (cells + Pregnane)- media			% Growth Inhibition (Mean ± STDEV)
Experiments	**1**	**2**	**3**	**1**	**2**	**3**	
MCF-7 Cells							
Media	0.224	0.236	0.293	0.000	0.000	0.000	-------
Media + Cells	0.843	0.802	0.793	0.620	0.566	0.500	-------
0.78	0.761	0.691	0.730	0.537	0.455	0.437	15.16 (±3.87)
1.56	0.682	0.671	0.708	0.458	0.435	0.415	22.03 (±4.64)
3.12	0.690	0.711	0.676	0.466	0.475	0.383	21.45 (±4.64)
6.25	0.666	0.648	0.603	0.442	0.412	0.310	31.27 (±5.83)
12.5	0.607	0.532	0.544	0.383	0.296	0.251	45.28 (±6.19)
25	0.539	0.555	0.510	0.315	0.319	0.217	49.77 (±6.51)
50	0.401	0.387	0.383	0.177	0.151	0.090	75.58 (±5.66)
100	0.268	0.234	0.339	0.044	-0.002	0.046	94.70 (±4.96)
Actinomycin-D	0.264	0.298	0.371	0.040	0.062	0.077	89.05 (±4.52)
Tamoxifen	0.284	0.291	0.307	-0.005	0.000	0.007	100.24 (±0.37)
Anastrozole	0.855	0.459	0.503	0.565	0.168	0.203	36.22 (±4.21)
Vehicle Control	0.812	0.771	0.802	0.588	0.535	0.508	2.98 (±4.08)
MDA MB-468 Cells							
Media	0.926	0.950	0.910	0.000	0.000	0.000	-------
Media + Cells	1.259	1.283	1.253	0.333	0.333	0.343	-------
0.78	1.206	1.200	1.232	0.280	0.250	0.321	15.77 (±9.29)
1.56	1.214	1.193	1.194	0.288	0.243	0.284	19.36 (±7.01)
3.12	1.169	1.155	1.155	0.243	0.206	0.245	31.34 (±6.09)
6.25	1.100	1.136	1.143	0.173	0.186	0.233	41.44 (±8.21)
12.5	1.036	1.098	1.021	0.110	0.148	0.111	63.46 (±6.72)
25	0.991	1.047	1.018	0.064	0.097	0.108	73.34 (±6.48)
50	0.965	0.979	0.986	0.039	0.030	0.076	85.85 (±6.95)
100	0.931	0.960	0.971	0.005	0.010	0.060	92.64 (±8.91)
Actinomycin-D	0.944	0.964	0.961	0.018	0.014	0.051	91.89 (±5.87)
Tamoxifen	1.346	1.300	1.359	0.403	0.297	0.318	63.05 (±3.16)
Anastrozole	1.087	1.024	1.079	0.144	0.021	0.038	92.99 (±6.23)
Vehicle Control	1.241	1.262	1.275	0.314	0.313	0.365	1.84 (±7.12)
Caco-2 Cells							
Media	0.222	0.256	0.243	0.000	0.000	0.000	-------
Media + Cells	0.362	0.345	0.379	0.141	0.089	0.137	-------
0.78	0.352	0.341	0.355	0.130	0.086	0.112	9.84 (±7.45)
1.56	0.342	0.338	0.343	0.120	0.083	0.101	16.07 (±9.60)
3.12	0.326	0.329	0.328	0.104	0.073	0.086	27.24 (±9.66)
6.25	0.330	0.326	0.331	0.108	0.070	0.088	26.71 (±7.57)
12.5	0.300	0.291	0.307	0.078	0.036	0.064	52.31 (±7.76)
25	0.264	0.290	0.278	0.042	0.035	0.035	68.49 (±6.72)
50	0.242	0.264	0.273	0.021	0.008	0.030	84.79 (±2.70)
100	0.224	0.262	0.247	0.002	0.006	0.005	95.89 (±8.77)
Actinomycin-D	0.250	0.263	0.246	0.028	0.007	0.004	89.79 (±6.10)
Vehicle Control	0.365	0.339	0.387	0.143	0.083	0.144	-0.15 (±6.60)

REFERENCES

Abdel-Sattar, E., Fathalla, M., Harraz, Al-ansari, S.M.A., El-Mekkawy, S., Ichino, C., Kiyohara, H., Ishiyama, A., Otoguro, K., Omura, S., Yamada, H., (2008). Acylated pregnane glycosides from *Caralluma tuberculata* and their antiparasitic activity. Phytochemistry 69: 2180–2186.

Abdullaev, G., Mejia, E.G., (1997). Antitumor effect of plant lectins. Natural Toxins 5: 157–163.

Abe, I., Rohmer, M., Prestwich, G.C., (1993). Enzymatic cyclization of squalene and oxidosqualene to sterols and triterpenes. Chemical Reviews 93: 2189–2206.

Adriana, B., Rafael, M., (2001). Current Opinion in Pharmacology 10: 364–369.

Agrawal, P.K., (1992). NMR spectroscopy in the structural elucidation of oligosaccharides and glycosides. Phytochemistry 31: 3307–3330.

Ahmad, M.M., Shaikh, M.M., (1989). Improvement in glucose tolerance by *Caralluma tuberculata*, Acacia nilotica and Papaver somniferum. Pakistan Journal of Zoology 21: 325–332.

Ahmad, V., Khan, U., Rizwani, G., (1988). New Pregnane glycosides from *Caralluma tuberculata*. Journal of Natural Products 51(6): 1092–1097.

Ahmad, V.U., Basha, A., (2006). Spectroscopic Data of Steroid Glycosides: Cardenolides and Pregnanes; Asclepias Fruticosa Saponin, 16α– hydroxy–5,6–dehydroasclepin 4(1): 2664–2716.

Ahmed, M.M., Qureshi, S., Shah, A., Qazi, N.S., Khan, Z.A., Shah, A.H., (1993). Anti-inflammatory activity of *Caralluma tuberculata* alcoholic extract. Fitoterapia 64: 357–360.

Al-Bekairi, A.M., Qureshi, S., Ahmed, M.M., Afzal, M., Shah, A.H., (1992). Effect of Caralluma tuberculata on the cytological and biochemical changes induced by cyclophosphamide in mice. Food Chemistry & Toxicology 30: 719–722.

Ali, S.I., (1983). Flora of Pakistan, Asclepiadaceae No: 150 (Eds) Nasir, E., pp: 44–48

Altomare, A., Burla, M.C., Camalli, M., Cascarano, G., Giacovazzo, C., Guagliardi, A., Moliteni, G., Polidori, G., Spagna, R., (1997). SIR97 (Release 1.02)-A Program for Automatic Solution and Refinement of Crystal Structure.

Al-Yahya, M., Al-Meshal, M., (1978). Flora of Saudi Arabia 2: 406–407.

REFERENCES

Anand, P., Kunnumakkara, A.B., Kunnumakara, A.B., (2008). "Cancer is a preventable disease that requires major lifestyle changes". Pharmaceutical. Research, 25 (9): 2097–116.

Ansari, A.A., Kenne, L., Atta, U.R., (1982). Isolation procedure and structure of new saponins from *Fagonia indica*. Planta Medica 45:143.

Ansari, A.A., Kenne, L., Atta, U.R., Wehler, T., (1987). Isolation and characterization of two saponins from *Fagonia indica*. Phytochemistry 26:1487–1490.

Ansari, A.A., Kenne, L., Atta, U.R., Wehler, T., (1988). Isolation and characterization of a saponin from *Fagonia indica*. Phytochemistry 27:3979–3982.

Arditti, J., Rodriguez, E., (1982). Dieffenbachia: uses, abuses and toxic constituents: a review, Journal of Ethnopharmacology 5: 293–302.

Arends, M.J., Morris, R.G., Wyllie, A.H., (1990). Apoptosis: The role of endonuclease. American Journal of Pathology 136: 593–608.

Ashkenazi, A., Dixit, V.M., (1998). Death receptors: signalling and modulation. Science 8: 1281–1305.

Atta, U.R., (1982). Some approaches to the study of indigenous medicinal plants. Bulletin Islamic Medicine 2: 562–568.

Atta, U.R., Ansari, A.A., Drexlex, S.A., Clardy, J., (1982). The isolation and structure of nahagenin. Heterocycles 19: 217–220.

Atta, U.R., Ansari, A.A., Kenne, L., (1984). Hederagenin, ursolic acid, and pinatol from *Fagonia indica*. Journal of Natural Products 47: 186–18.

Behrend, L., Henderson, G., Zwacka, R.M., (2003). Reactive oxygen species in oncogenic transformation. Biochemical Society Transactions 31: 1441–1444.

Bertino, J.R., (1997). Irinotecan for colorectal cancer. Seminars in Oncology 24: S18–S23.

Bock, J., Szabó, I., Jekle, A., Gulbins, E., (2002). Actinomycin–D induced apoptosis involves the potassium channel K. Biochemical and Biophysical Research Communications, 295, Issue 2, 12 July 2002: 526–531.

Borenfreund, E., Babich, H., Martin–Alguacil, N., (1988). Comparison of two in vitro cytotoxicity assays: the neutral red (NR) and tetrazolium (MTT) tests. Toxicology *in Vitro* 2: 1–6.

Borenfreund, E., Puerner, J.A., (1985). Toxicity determined *in vitro* by morphological alterations and neutral red absorption. Toxicology Letters 24: 119–124.

Brock, T.A., Brugnara, C., Canessa, M., (1986). Bradykinin and vasopressin stimulate Na*–K+–C1– cotransport in cultured endothelial cells. American Journal of Physiology 250: C888–C894.

Broudy, V.C., Kaushansky, K., Segal, G.M., (1986). Tumor necrosis factor type a stimulates human endothelial cells to produce granuloeyte / macrophage colony–stimulating factor. Proceedings of National Academy of Science. USA 83:7467–7471.

Brown, D.G., Sun, X.M., Cohen, G.M., (1992). Dexamethasone–induced apoptosis involves cleavage of DNA to large fragments prior to internucleosomal fragmentation. Journal of Biological Chemistry 268: 3037–3039.

Buchman, D.D., (1980). Herbal Medicine, the natural ways to get well and stay well, Germany: 8–13.

Burke, R.W., Diamondstone, B.I., Velapoldi, R.A., Menis, O., (1974). Mechanism of the Liebermann–Burchard and Zak color reactions for cholesterol. Clinical Chemistry 20: 794–801.

Cailleau, R., Olive, M., Cruciger, Q.V., (1978). Long–term human breast carcinoma cell lines of metastatic origin: preliminary characterization. *In* vitro 14: 911–915.

Cakir, A., Mavi, A., Yıldırım, A., Duru, M.E., Harmandar, M., Kazaz, C., (2003). Isolation and characterization of antioxidant phenolic compounds from the aerial parts of *Hypericum hyssopifolium* by activity–guided fractionation. Journal of Ethnopharmacology 87: 73–83.

Cakir, A., Mavi, A., Yıldırım, A., Duru, M.E., Harmandar, M., Kazaz, C., (2003). Isolation and characterization of antioxidant phenolic compounds from the aerial parts of *Hypericum hyssopifolium* by activity-guided fractionation. Journal of Ethnopharmacology 87: 73–83

Carmody, R.J., Cotter, T.G., 2001. Signalling apoptosis: a radical approach. Redox Reports 6: 77–90.

Chabner, B.A., (1991). Anticancer drugs in Cancer: Principles and Practice, edn 4. Edited by DeVita V.T., Hellman, S., Rosenberg, A.S., Philadelphia: Lippincott: 325–417.

Chabner, B.A., Roberts, T.G., (2005). Timeline—chemotherapy and the war on cancer. Nature Reviews on Cancer 5: 65–72.

Chakre, O.J., (2000). The Wealth of India – A Dictionary of Information Resource on Plants, Animals and Minerals, C.S.I.R., New Delhi, India, 4: 1-2.

Chandra, R., Deepak, D., Khare, A., (1994). Pregnane glycosides from Hemidesmus indicus. Phytochemistry 35: 1545.

Chang, H.M., But, P.P.H., (1986). Pharmacology and Applications of Chinese Materia Medica. World Scientific Publishing, Singapore, pp: 521.

Chen, A., Berhow, M.A., Tappenden, K.A., Donovan, S.M., (2005). Genistein Inhibits Intestinal Cell Proliferation in Piglets. Paediatric Research 57(2): 192–200

Chen, N., Appell, M., Berfield, J.L., (2003). Inhibition by arachidonic acid and other fatty acids of dopamine uptake at the human dopamine transporter. Eurpeon Journal of Pharmacology 478: 89–95.

Chen, N., Appell, M., Berfield, J.L., (2003). Inhibition by arachidonic acid and other fatty acids of dopamine uptake at the human dopamine transporter. Eurpeon Journal of Pharmacology 478: 89–95.

Chen, X., Shu, Y., Li, W., Yin, Y., (2008). TNF–alpha–induced metastasis gene changes in MCF–7 cells. Journal of Nanjing Medical University 22(6): 366–371.

Cheryl, L., Fattman, B.A., Lachelle, S., Dou, P.Q., (1998). P53–independent dephosphorylation and cleavage of retinoblastoma protein during Tamoxifen–induced apoptosis in human breast carcinoma cells. Cancer Letters, 130(1–2): 103–113.

Chi, S., (1980). "Encyclopaedia of Contemporary Chinese Medicinal Plants," Kogyo Chosakai, Tokyo, pp: 79–87.

Choo, C.Y., Chan, K.L., Itokawa, H., (2001). Cytotoxic activity of Typhonium flagelliforme (Araceae). Phytotherapy Research 15(3): 260–262.

Chopra, I.C., Handa, K.L., Kapur, L.D. (1982). Sir R.N.Chopra's Indigenous drugs of India. 2nd Ed., Academic Publishers; Calcutta, India, pp: 92–93.

Chopra, R.N., Nayar, S.L., Chopra, I.C., (1956). Glossary of Indian Medicinal Plants. C.S.I.R., New Delhi, India, pp: 116.

Clardy, J., Walsh, C., (2004). Lessons from natural molecules. Nature 432: 829–837.

Clarke, C.B., (1885). Solanaceae. In: Flora of British India, (Eds.): Hooker HD Vol. IV. Bishen Singh Mahendra Pal Singh, New Connaught Place, London, UK, pp: 229–237.

Clegg, W., (1998). Crystal Structure Determination. Oxford Science Publications UK. ISBN–978–0–19–855901–6.

Cocco, R.E., Ucker D.S., (2001). Department of Microbiology and Immunology, Molecular Biology of the Cell 12: 919–930.

Cohen GM, (1997). Caspases: the executioners of apoptosis. Biochemistry Journal 326: 1–16.

Cohen, G.M., Sun, X.M., Fearnhead, H., Macfarlane, M., Brown, D.G., Snowden, R.T., Dinsdale, D., (1994). Formation of large molecular weight fragments of DNA is a key committed step of apoptosis in thymocytes. Journal of Immunology 153: 507–516.

Compton, M.M., (1992). A biochemical hallmark of apoptosis: internucleosomal degradation of the genome. Cancer Metastasis Review 11: 105–19.

Copra, R.N., Nayar, S.L., Chopra, I.C., (1956). Glossary of Indian medicinal Plants, Council of Scientific and Industrial Research, New Delhi. pp: 5–5.

Cortes, J.E., Pazdur, R., (1995). Docetaxel. Journal of Clinical Oncology 13: 2643–2655.

Cragg, G., Newmann, D.J., (2005). Biodiversity: A continuing source or novel drug leads. Pure and Applied Chemistry 77: 7–24.

Cragg, G., Suffness, M., (1988). Metabolism of plant–derived anticancer agents. Pharmacology and Therapeutics 37: 425–432.

Cragg, G.M., Newman, D.J., Snader, K.M., (1997). Natural products in drug discovery and development. Journal of Natural Product 60: 52–60.

Cryns, V., Yuan, J., (1998). Proteases to die for. Genes and development 12: 1551–1570.

D' Arcy, W.G., (1991). The Solanaceae since 1976, with the Review of its Biogeography. In: Solanaceae III; Taxonomy, Chemistry and Evolution. (Eds.): Hawkes JG, Lester RN, Nee M and Estrada N. Academic press, London, UK, pp: 75–137.

David, J., McConkey, Zhivotovsky, B., Orrenius, S., (1996). Apoptosis – Molecular mechanism and biomedical implications. Molecular Aspects of Medicine 17(1): 1–110.

De Leo, M., De Tommasi, N., Sanogo, R., Autore, G., Marzocco, S., Pizza, C., Morelli, I., Braca, A., (2005). New pregnane glycosides from *Caralluma dalzielii*. Steroids 70(9): 573–585.

De Leo, M., De Tommasi, N., Sanogo, R., Autore, G., Marzocco, S., Pizza, C., Morelli, I., Braca, A., (2005). New pregnane glycosides from *Caralluma dalzielii*. Steroids 70(9): 573–585.

Deepak, D., Khare, A., Khare, M.P., (1989). Plant Pregnanes. Phytochemistry 28: 3255–3263.

Deepak, D., Srivastav, S., Khare, A., (1997). Pregnane glycosides. Progress in the Chemistry of Organic Natural Products 71:169–325.

Deepak, D., Srivastav, S., Khare, A., (1997). Pregnane glycosides. Progress in the Chemistry of Organic Natural Products 71:169–325.

Deepak, D., Srivastava, S., Khare, A., (1997). Pregnane glycosides from *Hemidesmus indicus*. Phytochemistry 44(1):145–151.

Defacque, H., Piquemal, D., Basset, A., Marti, J., Commes, T., (1999). Transforming growth factor–beta1 is an autocrine mediator of U937 cell growth arrest and differentiation induced by vitamin D3 and retinoids. Journal of Cellular Physiology 178(1): 109–119.

Degterev, A., Boyce, M., Yuan, J., (2003). A decade of caspases. Oncogene 22: 8543– 8567.

Denecker, G., Vercammen, D., Declercq, W., Vandenabeele, P., (2001). Apoptotic and necrotic cell death induced by death domain receptors. Cellular and Molecular Life Sciences, 58: 356–370.

Devi, P.R., Laxmi, V., Charulata, C., Rajyalakshmi, A., (2004). "Alternative medicine" – A right choice for male infertility management. International Congress series 1271: 67–70.

Dhuna, V., Dhuna, K., Singh, J., Saxena, A.K., Agrawal, S.K., Kamboj, S.S., (2010). Isolation, purification and characterization of an N–acetyl–D–lactosamine binding mitogenic and anti–proliferative lectin from tubers of a cobra lily *Arisaema utile* Schott. Advances in Bioscience and Biotechnology 1: 79–90.

Dixon, H.B.F., (1981). Defining a lectin, Nature, 292: 192.

Duke, J.A., Ayensu, E.S., (1985). Medicinal plants of China, vol. 1. Reference Publications, Inc, Algonac, Michigan, USA, pp: 52–361.

Dulberger, R., Levy, A., Palevitch, A.D., (1981). Andromonoecy in Solanum marginatum. Botanical Gazette, 142(2): 259–266.

Edinger, A.L., Thompson, C.B., (2004). Death by design: apoptosis, necrosis and autophagy. Current Opinons on Cell Biology 16: 663–669.

Edward, E.S., (1990). The black nightshades (*Solanum* section *Solanum*) of the Indian subcontinents. Botanical Journal of the Linnean Society 102: 253–259.

Eguchi, Y., Shimizu, S., Tsujimoto, Y., (1997). Intracellular ATP Levels Determine Cell Death Fate by Apoptosis or Necrosis.Cancer Research 57:1835–1840.

El–Hadidi, M.N., Al–Wakeel, S.A.M., El–Garf, I.A., (1988). Systematic significance of the flavonoid constituents in *Fagonia indica* complex. Biochemical Systematic Ecology, 16: 293–297.

El-Kheir, Y.M., Salih, M.H., (1979). Investigation of the alkaloidal content of *Solanum dubium* L. growing in Sudan. Fitoterapia 50: 255–258.

Elledge, S.J., (1996). Cell cycle checkpoints: preventing an identity crisis. Science 274:1664–1671.

Ellis, H.M., Horvitz, H.R., Ellis, H.M., Horvitz, H.R., (1986). Genetic control of programmed cell death in the nematode C. elegans. Cell 44: 817–829.

Endress, M.E., Bruyns, P.V., (2000). A revised classification of the Apocynaceae. Botanical Review 66: 1–56.

Ennis, B.W., Valverius, E.M., Bates, S.E., Lippman, M.E., Bellot, F., Kris, R., Schlessinger, J., Masui, H., Goldenberg, A., Mendelsohn, J., Dickson, R.B., (1989). Anti–epidermal growth factor receptor antibodies inhibit the autocrine-stimulated growth of MDA–468 human breast cancer cells. Molecular Endocrinology 3: 1830–1838.

Evers, R., de Haas, M., Sparidans, R., Beijnen, J., Wielinga, P.R., Lankelma, J., Borst, P., (2000). Vinblastine and sulfinpyrazone export by the multidrug resistance protein MRP2 is associated with glutathione export. British Journal of Cancer 83: 375–383.

Farnsworth, N.R., (1966). Biological and phytochemical screening of plants. Journal of Pharmaceutical Sciences 55: 225–276.

Farnsworth, N.R., Akerele, O., Bingel, A.S., Soejarto, D.D., Guo, Z., (1985). Medicinal plants in therapy. Bulletin of World Health Organisation 63: 965–981.

Farnsworth, N.R., Bingel, A.S., (1997). Problems and prospects of discovery new drugs from higher plants by pharmacological screening. In: H.Wagner and P.Wolff (eds.), New Natural products and plant drugs with pharmacological, biological and therapeutical activity, Springer Verlag, Berlin: 1–22.

Farrugia, L.J., (1997). ORTEP–3 for windows – A version of ORTEP–III with a graphical user interface. Journal of Applied Crystallography 30: 565.

Feher, M., Schmidt, J.M., (2003). Property distributions: differences between drugs, natural products, and molecules from combinatorial chemistry. Journal of Chemical Information and Computer Sciences: 43 (1): 218–227.

Ferlay, J., Shin, H.R., Bray, F., Forman, D., Mathers, C., Parkin, D.M., (2010). "GLOBOCAN 2008", Cancer Incidence and Mortality Worldwide: IARC CancerBase No. 10.

Fernandez, A., Crespo, A., Tiwari, A., (2009). Is there a case for selectively promiscuous anticancer drugs? Drug Discovery Today 14: 1–5.

Festjens, N., Vanden, T., Vandenabeele, P., (2006). Necrosis, a well–orchestrated form of cell demise: signalling cascades, important mediators and concomitant immune response. Biochimistry & Biophysics Acta 1757: 1371–1387.

Filmus, L., Pollak, M.N., Cailleau, R., Buick, R.N., (1985). MDA–468, a human breast cancer cell line with a high number of epidermal growth factor (EGF) receptors, has an amplified EGF receptor gene and is growth inhibited by EGF. Biochemical Biophysics Research communication 128: 898–905.

Fitzpatrick, S.L., LaChance, M.P., Schultz, G.S., (1984). Characterization of epidermal growth factor receptor and action on human breast cancer cells in culture. Cancer Research 44: 3442–3447.

Fogh, J., Fogh, J.M., Orfeo, T., (1977). One hundred and twenty seven cultured human tumour cell lines producing tumour in nude mice. Journal of National Cancer Institute 59: 221–226.

Folkman, J., (1983). How is blood vessel growth regulated in normal and neoplastic tissue? Cancer Research 46: 467–473.

Formigli, L., Papucci, L., Tani, A., Schiavone, N., Tempestini, A., Orlandini, G.E., Capaccioli, S., Orlandini, S.Z., (2000). Aponecrosis: morphological and biochemical exploration of a syncretic process of cell death sharing apoptosis and necrosis. Journal of Cell Physiology 182: 41–9.

Fromm, M.F., Kauffman, H.M., Fritz, P., Burk, O., Kroemer, H.K., Warzok, R.W., Eichelbaum, M., Siegmund, W., Schrenk, D., (2000). The effect of rifampin treatment on intestinal expression of human MRP transporters. American Journal of Pathology 157: 1575–1580.

Fulda, S., (2008). Betulinic Acid for Cancer Treatment and Prevention. International Journal of Molecular Sciences 9: 1096–1107.

Furie, B., Furie, B.C.,(1988). The molecular basis of blood coagulation. Cell 53: 505–518.

Garcia-Calvo, M., Thornberry, N.A., Lazebnik, Y., (1998). Inhibition of human caspases by peptide–based and macromolecular inhibitors. Journal of Biological Chemistry. 273: 32608–32613.

Gastman, B.R., Yin, X.M., Johnson, D.E., (1999). Caspase–mediated degradation of T–cell receptor zeta–chain. Cancer Research 59:1422–1427.

Ghafoor, A., (1974). Zygophyllaceae. In: Flora of Pakistan. (Eds.) E. Nasir and S.I. Ali. Karachi University, Karachi, Pakistan, 76: 1–35.

Gilbert, M.T., Haselkorn, T., Bunce, M., Sanchez, J.J., Lucas, S.B., Jewell, L.D., Van-Marck, E., Worobey, M., (2007). The isolation of nucleic acids from fixed, paraffin embedded tissues, which methods are useful when? PloS ONE 20 2 (6), e537.

Golstein, P., Kroemer, G., (2006). Cell death by necrosis: towards a molecular definition. Trends in Biomedical Sciences 32(1): 37–43.

Good, R., (1952). An Atlas of the Asclepiadaceae, Blackwell Publishing, Ltd. 108 Cowley Road, Oxford UK, 51(2): 98–209.

Graham, J.G., Quinn, M.L., Fabricant, D.S., Farnsworth, N.R., (2000). Plants used against cancer – an extension of the work of Jonathan Hartwell. Journal of Ethnopharmacology 73: 347–377.

Green, D.R., Kroemer, G., (2004). The pathophysiology of mitochondrial cell death. Science 305: 626–629.

Gromkowski, S.H., Brown, T.C., Cerutti, P.A., Cerottini, J.C., (1986). DNA of human Raji target cells is damaged upon lymphocyte–mediated lysis. Journal of Immunology 136: 752–756.

Guerrero, J.M., Pozo, D., Garcia–Maurino, S., (2000). Nuclear receptors are involved in the enhanced IL–6 production by melatonin in U937 cells. Biological Signals and Receptors 9(3–4): 197–202.

Halim, A.F., Khalil, A.T., (1996). Pregnane glycosides from *Caralluma retrospiciens*. Phytochemistry 42: 1135–1139.

Hall, M., Johnson, R.T., (1996). The role of DNA repair in the prevention of cancer.Molecular Aspects of Medicine 17(3): 235–383.

Halliwell, B., (2000). "A super way to kill cancer cell"?. Nature Medicine 6(10): 1105–1106.

Halliwell, B., Gutteridge, J.M.C., (1988). Free radicals in biology and medicine 2nd edn. Oxford, Charendon Press UK, pp: 481.

Hamayun, M., (2007). Traditional uses of some medicinal plants of Swat Valley, Pakistan. Indian journal of traditional knowledge 6(4): 636–641.

Hammond, C., (2001). The Basics of Crystallography and Diffraction. Oxford University Press, New York USA. ISBN–10: 0198–50–552–3.

Haralampidis, K., Trojanowska, M., Osbourn, A., (2002). Biosynthesis of triterpenoids saponins in plants. Advances in Biochemical Engineering 75: 31–49.

Harbour, J.W., Dean, D.C., (2000). The Rb/E2F pathway: expanding roles and emerging paradigms. Genes Review 14: 2393–2409.

Harmon, A.D., Weiss, U., Silverton, J.V., (1979). The structure of rohutukine, the main alkaloid of Amoora rohituka (syn. Aphanamixis polystachya). Tetrahydron 20: 721–724.

Hartwell, J.L., (1967). Plants used against cancer. A survey, Lloydia 30: 379–436.

Hartwell, J.L., (1982). Plants Used Against Cancer. Quarterman Publications, Lawrence, Massachusetts pp: 438–439.

Harvey, A.L., (1999). Medicines from nature: are natural products still relevant to drug discovery? Trends in Pharmacological Sciences 20: 196–198.

Hatfield, G., (2004). Encyclopedia of folk medicine old world and new world traditions. Santa Barbara, Library of Congress Cataloging–in–Publication Data California USA, pp: 134–154.

Hatse, S., Clercq, E.D., Balzarini, J., (1999). Role of Antimetabolites of purine and pyrimidine nucleotide metabolism in tumour cell differentiation. Biochemical Pharmacology 58(4): 539–555.

Hawkes, J.G. (1992). Biosystematics of the potato. In: The Potato crop, (Ed.): P.M. Harris. Chapman and Hall, London, pp: 909.

Heiser, C.B., (1969). The Wonder berry. In: Nightshades–Paradoxical Plants. (Ed.): W.H. Freeman. Freeman and Co, San Francisco, pp: 62–105.

Hengartner, M.O., (2000). The biochemistry of apoptosis. Nature 6: 407–770.
Heo, K.S., Lee, S.J., Ko, J.H., Lim, K., Lim, K.T., (2004). Glycoprotein isolated from Solanum nigrum L. inhibits the DNA–binding activities of NF–jB and AP–1, and increases the production of nitric oxide in TPA–stimulated MCF–7 cells. Toxicology *in Vitro* 18: 755–763.

Hileman, E.O., Achanta, G., Huang, P., (2001). Superoxide dismutase: an emerging target for cancer therapeutics. Expert Opinions on Therapeutic Targets 5: 679–710.

Hirsch, T., Marchetti, P., Susin, S.A., (1997). The apoptosis-necrosis paradox. Apoptogenic proteases activated after mitochondrial permeability transition determine the mode of cell death. Oncogene 15: 1573–1581.

Hooker, J.D., (1975). Flora of British India. Reeva, London, UK, pp: 425.
Hostettmann, K., Marston, A., (2005). Saponins, chemistry and pharmacology on natural products. Cambridge University Press, Cambridge. ISBN–10: 0521020174.

Hu, S.L., (1993). A comment on two medicinal aroids huzhang and "tiannanxing", Journal of Chinese Traditional Drugs 18(4): 239, 253.

Huang, P., Robertson, L.E., Wright, S., Plunkett, W., (1995). High molecular weight DNA fragmentation: A critical event in nucleotide analogue–induced apoptosis in leukaemia cells. Clinical Cancer Research 1: 1005–1013.

Hunter, J., Hirst, B.H., Simmons, N.L., (1993b). Drug absorption limited by P-glycoprotein-mediated secretory drug transport in human intestinal epithelial Caco-2 cell layers. Pharmaceutical Research 10: 743–749.

Hunter, J., Jepson, M., Tsuruo, T., Simmons, N.L., Hirst, B.H., (1993a). Functional expression of P-glycoprotein in apical membranes of human intestinal Caco-2 cells. Kinetics of vinblastine secretion and interaction with modulators. Journal of Biological Chemistry 268: 14991–14997.

Igney, F.H., Krammer, P.H., (2002). Death and anti–death: tumour resistance to apoptosis. Nature Reviews Cancer 2: 277–288.

Ikeda, T., Tsumagari, H., Honbu, T., Nohara, T., (2003). Cytotoxic Activity of Steroidal Glycosides from Solanum Plants, Biological & Pharmaceutical Bulletin 26(8): 1198–1201.

Jain, S.P., Puri, H.S., (1984). Ethnomedicinal plants of Jaunsar –Bawar Hills, Uttar Pradesh, India. Journal of Ethnopharmacol 12: 213–222.

Jennifer, M.E., James, A.C., (1997). Black nightshades, *Solanum nigrumL* and related species. International Plant Genetic and Research institute (IPGRI), Italy, pp:113.

Ji, Y.B., Gao, S.Y., Ji, C.F., Zou, X., (2008). Induction of apoptosis in HepG2 cells by solanine and Bcl–2 protein Journal of Ethnopharmacology 115: 194–202.
Johnson, I.S., Armstrong, J.G., Gorman, M., Burnett, P., (1963). The Vinca Alkaloids: A New Class of Oncolytic Agents Journal of Cancer Research 23: 1390–1427.

Jordan, M.A., (2002). Mechanism of action of antitumour drugs that interact with microtubules and tubulin. Current Medicinal Chemistry 2: 1–17.

Julian, M.M., (2008). Foundations of crystallography with computer applications. CRC press USA, ISBN–978–1–4200–6075–1.

Jung, J.H., Lee, C.O., Kim, Y.C., Kang, S.S., (1996b) New Bioactive Cerebrosides from *Arisaema amurense*. Journal of Natural Product 59: 319–322.

Jung, J.H., Lee, H., Kang, S.S., (1996a) Diacylglycerylgalactosides from *arisaema amurense*. Phytochemistry 42(2): 447–452.

Kaina, B., Van, Zeeland, A.A., De-Groot, A., Natarajan, A.T., (1990). DNA repair and chromosomal stability in the alkylating agent–hypersensitive Chinese hamster cell line 27–1. Mutation Reseach 243: 219–224.

Kane, D.J., Sarafian, T.A., Anton, R.,(1993). Bcl–2 inhibition of neural death: Decreased generation of reactive oxygen species. Science 262: 1274–1277.

Kang, S.J., Wang, S., Kuida, K., Yuan, J., (2002). Distinct downstream pathways of caspase–11 in regulating apoptosis and cytokine maturation during septic shock response. Cell Death Differences 9:1115–1125.

Kapoor, L.D., (1990). CRC Handbook or Ayurvedic Medicinal Plants. CRC Press, Boca Raton, USA, pp: 416 – 417.

Kapuscinski, J., (1995). DAPI: a DNA–specific fluorescent probe. Biotechnic and Histochemistry 70(5): 220–233.

Kashman, Y.D., Green, C., Garcia, C., Arevalos, D.G., (1991). Verrucoside, a new cytotoxic pregnane glycoside from a Gorgonian Eunicella verrucosa. Journal of Natural Products 54: 1651.

Kaufmann, S.H., Desnoyers, S., Ottaviano, Y., Davidson, N.E., Poirier, G.G., (1993). Specific proteolytic cleavage of poly(ADP–ribose) polymerase: an early marker of chemotherapy–induced apoptosis. Cancer Research 53(17): 3976–3985.

Kaur, G., Stetler–Stevenson, M., Sebers, S., Worland, P., Sedlacek, H., Myers, C., Czech, J., Naik, R., Sausville, E., (1992). Growth inhibition with reversible cell cycle arrest of carcinoma cells by flavone L86–8275. Journal of National Cancer Institute 84:1736–1740.

Kaur, M., Singh, K., Rup, R.J., Saxena, A.K., Khan, R.H., Ashraf, M.T., Kamboj, S.S., Singh, J., (2006). A tuber lectin from *Arisaema helleborifolium* Schott with anti–insect activity against melon fruit fly, *Bactrocera cucurbitae* (Coquillett) and anti–cancer eVect on human cancer cell lines. Archives of Biochemistry and Biophysics 445:156–165.

Kelland, L.R., (2000). Flavopiridol, the first cyclin–dependent kinase inhibitor to enter the clinic: current status. Expert Opinion on Investigational Drugs 9: 2903–2911.

Kerr, J.F., Winterford, C.M., Harmon, B.V., (1994). Apoptosis; Its significance in cancer and cancer therapy. Cancer 73: 2013–26.

Kerr, J.F., Wyllie, A.H., Currie, A.R., (1972). Apoptosis: a basic biological phenomenon with wide–ranging implications in tissue kinetics. British journal of cancer 26: 239–257.

Khan, U., Rizwani, G.H., Ahmad, M., (1987). Chemical investigation of medicinal herb *Caralluma tuberculata*. Jornal of Pharmacy University of Karachi 5(2): 133–137.

Kijima, I., Itoh, T., Chen, S., (2005). Growth inhibition of estrogen receptor positive and aromatase–positive human breast cancer cells in monolayer and spheroid cultures by letrozole, Anastrozole and Tamoxifen. The Journal of Steroid Biochemistry and Molecular Biology, 97 (4): 360–368.

Kim, H.G., Song, H., Yoon, D.H., Song, B.W., Park, S.M., Sung, G.H., Cho, J.Y., Park, H., Choi, S., Song, W.O., Hwangi, K.C., Kima, T.W., (2010). Cordyceps pruinosa extracts induce apoptosis of HeLa cells by a caspases dependent pathway. Journal of Ethnopharmacology 128: 342–351.

Kim, J.S., Qian. T., Lemasters, J.J., (2003). Mitochondrial permeability transition in the switch from necrotic to apoptotic cell death in ischemic rat hepatocytes. Gastroenterology 124: 494–503.

King, G.L., Johnson, S.H., (1985). Receptor–mediated transport of insulin across endothelial cells. Science 227: 1583–1586.

Kirtikar, K.R., Basu, B.D., (1987). "Indian Medicinal Plants", 2nd edn. Vol II, International Book Distributors, Dehradun, pp: 1638–1640.

Klein, I., Sarkadi, B., Váradi, A., (1999). An inventory of the human ABC proteins. Biochimica Biophysica Acta 1461: 237–262.

Koehn, F.E., Carter, G.T., (2005). The evolving role of natural products in drug discovery. Nature Reviews Drug Discovery 4 (3): 206– 220.

Koenig, U., Eckhart, L., Tschachler, E., (2001). Evidence that caspase–13 is not a human but a bovine gene. Biochemistry and Biophysics Research Communications 285:1150–1154.

Kraus, W.L., (2008). Transcriptional control by PARP–1: chromatin modulation, enhancer–binding, coregulation, and insulation. Current Opinion in Cell Biology 20: 294–302.

Kroemer, G., El–Deiry, W.S., Golstein, P., (2005). Classification of cell death: recommendations of the nomenclature committee on cell death. Cell Death Differences 12:1463–1467.

Kumagai, A., Guo, Z., Emami, K.H., Wang, S.X., Dunphy, W.G., (1998). The Xenopus Chk1 protein kinase mediates a caffeine–sensitive pathway of checkpoint control in cell free extracts. Journal of Cell Biology 142: 1559–1569.

Lacroix, M., Leclercq, G., (2004). "Relevance of breast cancer cell lines as models for breast tumours: an update". Breast Research and Treatment 83 (3): 249–289.

Lamarre, D., Talbot, B., de-Murcia, G., (1988). Structural and functional analysis of poly(ADP ribose) polymerase: an immunological study. Biochimica et Biophysica Acta 950(2): 147–160.

Lampe, K.F., McCann, M.A., (1985). AMA Handbook of poisonous and injurious plants. American Medical Assoc. Chicago, Ill., USA, pp: 432.

Lazebnik, Y.A., Kafmann, S.H., Desnoyers, S., Poirier, G.G., Earnshaw, W.C., (1994). Cleavage of poly(ADP–ribose) polymerase by a proteinase with properties like ICE. Nature 371(6495):346–747.

Lee, M.L., Schneider, G., (2001). Scaffold architecture and pharmacophoric properties of natural products and trade drugs: application in the design of natural product–based combinatorial libraries. Journal of Combinatorial Chemistry, 3 (3): 284– 289.

Lee, S.J., Lim, K.T., (2006). 150 kDa glycoprotein isolated from Solanum nigrum Linne stimulates caspase–3 activation and reduces inducible nitric oxide production in HCT–116 cells. Toxicology *in Vitro* 20: 1088–1097.

Lee, Y.Y., Hsu, F.L., Nohara, T., (1997). Two new soladulcidine glycosides from *Solanum lyratum*. Chemical and Pharmaceutical Bulletin 45: 1381–1382.

Leist, M., Single, B., Castoldi, A.F., Kuhnle, S., Nicotera, P., (1997). Intracellular adenosine triphosphate (ATP) concentration: a switch in the decision between apoptosis and necrosis. Journal of Experimental medicine, 185: 1481–1486.

Lenartz, D., Stoffel, B., Menzel, J., Beuth, J., (1996). Immunoprotective activity of the galactoside–specific lectin from mistletoe after tumor destructive therapy in glioma patients, Anticancer Research 16: 3799–3802.

Levenson, A.S., Jordan, V.C., (1997). "MCF–7: the first hormone–responsive breast cancer cell line". Cancer Research 57 (15): 3071–3078.

Li, J., Li, X.Q., Du, Y.J., Ge, L.P., Dai, C.H., Chen, P., (2010). Cisplatin – based chemotherapy in elderly patients with non–small cell lung cancer. International Journal of Gerontology 4(1): 30–36.

Liang, J.L., Zhen, H., (2006). Deliciosa root extract on CCl4 induced acute liver injury in rats. Guangxi Traditional Chinese Medicine 29 (4): 50–52.

Liang, J.L., Zhen, H.,(2006). Deliciosa root extract on CCl4 induced acute liver injury in rats. Guangxi Traditional Chinese Medicine 29 (4): 50–52.

Lin, L.J., Lin, L.Z., Gil, R.R., Cordell, G.A., Ramesh, M., Srilatha, B. (1994). Pregnaneglycosides from *Caralluma umbellata*. Phytochemistry 35:1549–1553.

Lin, Y., Yang, Q., Wang, X., Liu, Zg., (2004). Tumor Necrosis Factor–induced Nonapoptotic Cell Death Requires. Journal of biology and chemistry 279: 10822–10828.

Liu, L.F., (1989). DNA topoisomerase poisons as antitumor drugs. Annual Review of Biochemistry 58: 351–375.

Liu, L.F., Desai, S.D., Li, T.K., Mao, Y., Sun, M., Sim, S.P., (2000). Mechanism of action of camptothecin. Annals of New York Acadmey of Science 922: 1–10.

Liu, L.F., Liang, C.H., Shiu, L.I., Lin, W.L., Lin, C.C., Kuo, K.W., (2004). Action of solamargine on human lung cancer cells – enhancement of the susceptibility of cancer cells to TNFs. FEBS Letters 577: 67–74.

Lloyd, D.R., Phillips, D.H., Carmichael, P.L., 1997. Generation of putative intrastrand cross-links and strand breaks in DNA by transition metal ion-mediated oxygen radical attack. Chemical Research in Toxicology 10: 393–400.

Lockshin, R.A., William, C.M., (1965)."Programmed cell death. V. Cytoloytic enzymes in relation to the breakdown of the intersegmental muscles of silkmoths". Journal of insect physiology 11(7): 831–844.

Locksley, R.M., Killeen, N., Lenardo, M.J. (2001). The TNF and TNF receptor superfamilies: integrating mammalian biology. Cell 104: 487–501.

Locksley, R.M., Killeen, N., Lenardo, M.J., (2001). The TNF and TNF receptor superfamilies: integrating mammalian biology. Cell 104: 487–501.

Losiewicz, M.D., Carlson, B.A., Kaur, G., Sausville, E.A., Worland, P.J., (1994). Potent inhibition of cdc2 kinase activity by the flavonoid L86–8275. Biochemical & Biophysical Research Communications 20: 589–595.

Mabberley, D.I., (1987). The Plant Book. Cambridge University UK. Press Cambridge, New York.

Madine, M.A., Khoo, C.Y., Mills, A.D., Laskey, R.A., (1995). MCM3 complex required for cell cycle regulation of DNA replication in vertebrate cells. Nature 375: 421–424.

Manandhar, N.P., Manandhar, S., (2002). Plants and People of Nepal, ISBN 0–88192–527–6, pp: 599.

Mann, J. D., (1978). Production of solasodine for pharmaceutical industry, in Advances in Agronomy edited by N.C. Brady, Academic Press, London, UK, pp: 207.

Marks, W.H., Fong, H.H.S., Tina–Wa, M., Farnsworth, N.R., (1975). Cytotoxic principles of *Parquetina nigrescens* (Afzel.) bullock (asclepiadaceae). Journal of Pharmaceutical sciences 64(10): 1674–1676.

Martin, K.R., Barrett, J.C., (2002). Reactive oxygen species as double-edged swords in cellular processes: low-dose cell signaling versus high-dose toxicity. Human and Experimental Toxicology 21: 71–75.

Martinvalet, D., Zhu, P., Lieberman, J., (2005). Granzyme A induces caspases independent mitochondrial damage, a required first step for apoptosis. Immunity 22: 355–370.

McCord, J.M., (1995). Superoxide radical: controversies, contradictions, and paradoxes. Proceedings of the Society for Experimental Biology and Medicine. Society for Experimental Biology and Medicine. 209: 112–117.

McKinnell, R.G., Parchment, R.E., Perantoni, A.O., Pierce, G.B., (1998). The biological basis of cancer, Cambridge University Press, New York, USA, pp: 2–4.
Meija, J., Soukup, V.G., (2004). Phenyl–terminated fatty acids in seeds of various aroids. Phytochemistry 65: 2229–2237.

Mendelsohn, J., (2002). Targeting the epidermal growth factor receptor for cancer therapy. Journal of Clinical Oncology 18:1–13.

Minshull, J., Sun, H., Tonks, N.K., Murray, A.W., (1994). A MAP kinase dependent spindle assembly checkpoint in Xenopus egg extract.Cell 79: 475–486.

Mohan, H., (2002). Textbook of Pathology, IVth Ed.,Jaypee Brothers Medical Publishers Pvt. Ltd., New Delhi, pp: 262–268.

Moreno, S., Nurse, P., (1994). Regulation of progression through the G1 phase of thecell cycle by the rum1+ gene. Nature 367: 236–242.

Morgan, D.O., (1997). Cyclin–Dependent Kinases: Engines, Clocks, and Microprocessors. Annual Review of Cell and Developmental Biology 13: 261–291.

Mulligan, G.A., Munro, D.B., (1990). Poisonous plants of Canada. Agriculture Canadian Research Board Technical Bulletin 1842/E: 96.

Munday, N.A., Vaillancourt, J.P., Ali, A., Casano, F.J., Miller, D.K., Molineaux, S.M., Yamin, T.T., Nicholson, D.W., (1995). Molecular cloning of ICErelII and ICErelIII, members of the ICE/CED–3 family of cysteine proteases. Journal of Biological Chemistry 270(26): 15870–15876.

Murcia, G., Murica, M., (1994). Poly (AdP–ribose) polymerase: a molecular nick–sensor. Trends in Biochemical Sciences 19: 172–176.

Nakanishi, T., Kobayashi, M., Murata, H., Inada, A., (1988). Phytochemical studies on Meliaceous Plants. IV. Structure of new pregnane glycoside, Toosendanoside, from Leaves pf Melia toosendan Sieb, et. Zucc. Chemical & Pharmaceutical Bulletin 36: 4148.

Nasir, J.Y. (1985). Solanaceae. In: Flora of Pakistan. (Eds.): Ali, S.I., Nasir, E., Pakistan Agricultural Research council, Islamabad. Fascicle 168: 1–61.

Natarajan, D., Balaguru, B., Nagamurugan, Soosairaj, S., Natarajan, E., (2010). Ethno–medico–botanical survey in the Malligainatham village, Kandarvakottai Taluk, Pudukottai District,Tamil Nadu. Indian Journal of Traditional knowledge, 9(4): 768–774.

Nayak, B.S., Jena, P.K., Sahu, N.P., Nayak, U.K., Patro, K.B., (2009). Comparative study of anthelmintic activity between aqueous and ethanolic extract of Solanum surattense linn. International Journal of Pharmacy and Pharmaceutical Sciences 1(1): 103–107.

Newman, D.J., Cragg, G.M., (2007). Natural products as sources of new drugs over the last 25 years. Journal of Natural Products 70: 461–477.

Nicolaou, K.C., Snyder, S.A., (2004). The essence of total synthesis. Proceedings of the National Academy of Sciences of the United States of America 101 (33): 11929–11936.

Nikaido, H., Yuzuru, S., Mitsushashi, H., (1967). Components of *Boucerosia aucheriana* Decne. Chemical & Pharmaceutical Bulletin 15(5): 725–726.

Noble, R.L., (1990). The discovery of the vinca alkaloids–chemotherapeutic agents against cancer. Biochemistry & Cell Biology 68: 1344–1351.

Nonius, B.V., (1998). "COLLECT" Data Collection Software.

Norman, R.I., Lodwick, D., (2007). Flesh and Bones of Medical Cell Biology. MOSBY Elsevier, Philadelphia, USA, pp: 106–107.

Nowell, P.C., (1960). *Phytohemagglutinin: an inhibitor of mitosis in cultures of* normal human leucocytes. Cancer Research 20: 462–464.

Oberhammer, F., Wilson, J.W., Dive, C., Morris, I.D., Hickman, J.A., Wakeling, A.E., Walker, P.R., Sikorska, M., (1993). Apoptotic death in epithelial cells: cleavage of DNA to 300 and/ or 50 kb fragments prior to or in the absence of inter–nucleosomal fragmentation. The EMBO Journal 12: 3679–3684.

Okouneva, T., Hill, B.T., Wilson, L., Jordan, M.A., (2003). The effects of vinflunine, vinorelbine, and vinblastine on centromere dynamics. Molecular Cancer Therapeutics 2 (5): 427–436.

Okuma, E., Saeki, K., Shimura, M., Ishizaka, Y., Yasugi, E., You, A., (2000). Induction of apoptosis in human hematopoietic U937 cells by granulocyte–macrophage colony–stimulating factor: possible existence of caspase 3–like pathway. Leukemia 14(4): 612–619.

Oleszek, W.A., (2002). Chromatographic determination of plant saponins. Journal of Chromatography A, 967:147–162.

Otwinowski, Z., Minor, W., (1997). Processing of X-ray diffraction data collected in oscillation mode. Methods in Enzymology 276: 307–326.

Paschka, A.G., Butler, R., Young, C.Y.F., (1998). Induction of apoptosis in prostate cancer cell lines by the green tea component epigallocatechin–3–gallate. Cancer Letters 130: 1–7.

Paulo, A., Jimeno, M.L., Gomes, E.T., Houghton, P.J., (2000). Steroidal alkaloids from Cryptolepis obtuse. Phytochemistry 53(3): 417–422.

Pawar, P.K., Borse, T.P., Pinjari, R.Z., Maheshwari, V.L., (2008). A simple technique for rapid quantitative determination of solasodine from cultured hairy roots of *Solanum surattense*. Journal of Herbal Medicine and Toxicology 2(1): 7–10.

Pelicano, H., Feng, L., Zhou, Y., Carew, J.S., Hileman, E.O., Plunkett, W., Keating, M.J., Huang, P., (2003). Inhibition of mitochondrial respiration: a novel strategy to enhance drug-induced apoptosis in human leukaemia cells by a reactive oxygen species-mediated mechanism. *Journal of Biological Chemistry* 278: 37832–37839.

Peterson, E.A., Overman, L.E., (2004). Contiguous stereogenic quaternary carbons: a daunting challenge in natural products synthesis. Proceedings of the National Academy of Sciences of the United States of America 101 (33): 11943–11948.

Peumans, W.J., Damme, E.J.M., (1995). Lectins as plant defense proteins. Plant Physiology 109: 347–352.

Pezzuto, J.M., (1997). Plant–derived anticancer agents. Biochemical Pharmacology 53:121–133.

Pinto, M., Robine–Leon, S., Appay, M.D., Kedinger, M., Triadou, N., Dussaulx, E., Lacroix, B., Simon–Assmann, P., Haffen, K., Fogh, J., (1983). "Enterocyte-like differentiation and polarization of the human colon carcinoma cell line Caco-2 in culture". Biology of Cell 47: 323–30.

Plater, R., Haddon, W.f., Lundin, R.E., (1972). Structure of safflower steroid Cellobioside. Phytochemistry 11: 2327.

Plinsky, K.R., (2007). "Tumour Suppressor Genes" Nova Science Publishers, New York,USA, pp: 1–4.

Plowman, T., (1969). Folk uses of New World aroids. Economic Botany 23: 97–122.

Proskuryakov, S.Y., Konoplyannikov, A.G., Gabai, V.L., (2003). Necrosis: a specific form of programmed cell death? Experimental Cell Research 283: 1–16.

Proskuryakov, S.Y., Konoplyannikov, A.G., Gabai, V.L., (2003). Necrosis: a specific form of programmed cell death? Experimental Cell Research 283: 1–16.

Prychid, C.J., Jabaily, R.S., Rudall, P., (2008). Cellular Ultrastructure and Crystal Development in *Amorphophallus* (Araceae). Annals of Botany 101(7): 983–995.

Qiu, S.X., Cordell, G.A., Kumar, B.R., Rao, Y.N., Ramesh, M., Kokate, C., (1999). Studies on the C–21 steroids from asclepiadaceous plants bisdesmosidic pregnane glycosides from *Caralluma lasiantha*. Phytochemistry 50: 485–491.

Qiua, S.X., Cordell, G.A., Kumarb, B.R., Raoc, Y.N., Rameshc, M., Kokateb, C., Rao, A.V.N.A., (1999). Bisdesmosidic pregnane glycosides from *Caralluma lasianthap* Phytochemistry 50: 485–491.

Qureshi, R., Bhatti, G.R., (2008). Ethnobotany of plants used by the Thari people of Nara Desert, Pakistan. Fitoterapia 79: 468–473.

Raff, M.C., (1996). Size control: the regulation of cell numbers in animal development. Cell 86: 173–175.

Rahman, A.U., (2008). Antitumor agents 248, chemistry and antitumor activity of tylophorine–related alkaloids. Studies in Natural product chemistry, Elsevier, the Boulevard, Langford lane, Kidlington, Oxford, UK, pp: 3–7.

Rahman, M.T., Ahmed, M., Alimuzzaman, M., Shilpi, J.A., (2003). Antinociceptive activity of the aerial parts of *Solanum xanthocarpum*. Fitoterapia 74: 119–21.

Ramazani, A., Zakeri, S., Sardari, S., Khodakarim, N., Djadidt, N.D., (2010). *In vitro* and *in vivo* anti–malarial activity of *Boerhavia elegans* and *Solanum surattense*. Malaria Journal 9:124–132.

Ravid, A., Rocker, D., Machlenkin, A., Rotem, C., Hochman, A., Kessler-Icekson, G., Liberman, U.A., Koren, R., (1999). 1,25-Dihydroxyvitamin D3 enhances the susceptibility of breast cancer cells to doxorubicin-induced oxidative damage. Cancer Research 59: 862–867

Ravid, A., Rocker, D., Machlenkin, A., Rotem, C., Hochman, A., Kessler–Icekson, G., Liberman, U.A., Koren, R., (1999). 1,25–Dihydroxyvitamin D3 enhances the susceptibility of breast cancer cells to doxorubicin–induced oxidative damage. Cancer Research 59: 862–867.

Reddivari, L., Vanamala, J., Chintharlapalli, S., Safe, S.H. Creighton, J., (2007). Anthocyanin fraction from potato extracts is cytotoxic to prostate cancer cells through activation of caspase–dependent and caspase–independent pathways. Carcinogenesis (28)10: 2227–2235.

Reichestein, T., (1967). Cardenolid– un Pregnanglykoside. Naturwissenschaften, 54: 53.

Renner, S.S., Zhang, L.B., Murata, J., (2004). A chloroplast phylogeny of *Arisaema* (Araceae) illustrates Tertiary floristic links between Asia, North America, and East Africa. American Journal of Botany 91: 881.

Rimpler, H., Rizk, A.M., (1969). Isolation of oleanolic acid from Fagonia cretica. Phytochemistry 8(11): 2269.

Rios, J.L., Waterman, P.G., (1998). A review of the pharmacology and toxicology of *Astragalus*. Phytotherapy Research 11: 411–418.

Rizk, A.M., Hammouda, F.M., Abdel–Gawad, M.M., (1972). The triterpenoid sapogenins of Fagonia indica Brum. Pharmazie 27(8): 534–535.

Rizwani, G.H., Khan, U., Ahmad, M., (1992). Pregnane glycosides from *Caralluma tuberculata*. Natural Product Letters 2(2): 97–104.

Rizwani, G.H., Khan, U., Ahmad, M., Ahmad, V.U. (1990). Flavone glycosides of *Caralluma tuberculata* N.E. Brown. Pakistan journal of pharmaceutical sciences 3(2): 27–32.

Rizwani, G.H., Khan, U., Ahmad, M., Ahmad, V.U., (1993).Caratuberoside A2: A new pregnane from Caralluma tuberculata. Spectroscopy Letters 26(8): 1427–1434.

Rubio–Moscardo, F., Blesa, D., Mestre, C., Siebert, R., Balasas, T., Benito, A., Rosenwald, A., Climent, J., Martinez, J.I., Schilhabel, M., Karran, E.L., Gesk, S., Esteller, M., DeLeeuw, R., Staudt, L.M., Fernandez–Luna, J.L., Pinkel, D., Dyer, M.J., Martinez–Climent, J.A., (2005). Characterization of 8p21.3 chromosomal deletions in B–cell lymphoma: TRAIL–R1 and TRAIL–R2 as candidate dosage–dependent tumor suppressor genes. Blood 106: 3214–3222.

Saeed, M.A., (1969). Hamdard Pharmacopoeia of Eastern Medicine. Hamdard Academy, Karachi, Pakistan, pp: 41–43.

Saelens, X., Festjens, N., Vande, L., Van-Gurp, M., Van-Loo, G., Vandenabeele, P., (2004). Toxic proteins released from mitochondria in cell death. Oncogene 23: 2861–2874.

Saijo, R., Murakami, K., Nohara, T., Tomimatsa, A., Saito, A., Matsuoka, K., (1982). Studies on *the* constituents of *Solanum* plants II. Constituents of the immature fruits of *Solanum nigrum*. Yakugaku Zasshi 102 (3): 300–305.

Saived, I.Z., (1963). Fruits of *Solanum xanthocarpum*. The Proceedings of the Indian Academy of Sciences Series A4: 255–260.

Santos, M.J., López-Jurado, M., Llopis, J., (1995). Influence of dietary supplementation with fish oil on plasma fatty acid composition in coronary heart disease patients. Annals of Nutrition and Metabolism, 39: 52–62

Santos, M.J., López–Jurado, M., Llopis, J., (1995). Influence of dietary supplementation with fish oil on plasma fatty acid composition in coronary heart disease patients. Annals of Nutrition and Metabolism, 39: 52–62.

Sawyers, C., (2004). Targeted cancer therapy. Nature 432: 294–297.

Schilling, E.E., Ma Q.S., Anderson, R.N., (1992). Common names and species identification in blacknightshades, *Solanum* sect. *Solanum* (Solanaceae). Economic Botany 46(2): 223–225.

Secko, D., (2009). The Cell Cycle: A Universal Cellular Division Program. The science creative quarterly, 4. http://www.scq.ubc.ca/the-cell-cycle-a-universal-cellular-division-program/ (Date: 12/08/2010).

Senderowicz, A.M., Headlee, D., Stinson, S.F., Lush, R.M., Kalil, N., Villalba, L., Hill, K., Steinberg, S.M., Figg, W.D., Tompkins, A., (1998). Phase I trial of continuous infusion flavopiridol, a novel cyclin-dependent kinase inhibitor, in patients with refractory neoplasms. Journal of Clinical Oncology 16: 2986–2999.

Shaker, K.H., Bernhardt, M., Elgamal, H.A., Seifert, K., (1999). Triterpenoid saponins from *Fagonia indica*. Phytochemistry 51: 1049–1053.

Shangary, S., Singh, J., Kamboj, S., Kamboj, K.K., Sandhu, R.S., (1995). Purification and properties of four monocot lectins from the family Araceae. Phytochemistry 40(2): 449–455.

Sharma, S., Gupta, V., Sharma, G., (2010). Phytopharmacology of *Fagonia Indica* (L): A Review. Journal of Natura Conscientia, 1(1): 143–147.

Sheeba, E., (2009). Antibacterial activity of *Solanum surattense* burm. Kathmandu University journal of science, engineering and technology 6: 1–4.

Sheldrick, G.M., (1997). SHELX97 [Includes SHELXS97, SHELXL97, CIFTAB] Programs for Crystal Structure Analysis (Release 97–2). University of Gottingen, Germany.

Shen, Z.X., Chen, G.Q., Ni, J.H., Li, X.S., Xiong, S.M., Qiu, Q.Y., Zhu, J., Tang, W., Sun, G.L., Yang, K.Q., Chen, Y., Zhou, L., Fang, Z.W., Wang, Y.T., Ma, J., Zhang, P., Zhang, T.D., Chen, S.J., Chen, J., Wang, Z.Y., 1997. Use of arsenic trioxide (As2O3) in the treatment of acute promyelocytic leukemia (APL): II. Clinical efficacy and pharmacokinetics in relapsed patients. Blood 89: 3354–3360.

Singh, J., Kamboj, S.S., (2004). A novel mitogenic and antiproliferative lectin from a wild cobra lily. *Arisaema* flavum. Biochemical and Biophysical Research Communications 318: 1057–1065.

Singh, V., Pandey, R.P., (1998). Ethnobotany of Rajasthan, India. ISBN: 81–7233–182–7. Scientific Publisher, Jodhpur, India, pp: 79–81.

Slee, E.A., Adrain, C., Martin, S.J., (2001). Executioner caspase–3, –6, and –7 perform distinct, non–redundant roles during the demolition phase of apoptosis. Journal of Biological Chemistry 276: 7320–7326.

Slee, E.A., Adrain. C., Martin, S.J., (2001). Executioner caspase-3, -6, and -7 perform distinct, non-redundant roles during the demolition phase of apoptosis. Journal of Biological Chemistry 276: 7320–7326.

Smets, L.A., (1994). Programmed cell death (apoptosis) and response to anti–cancer drugs. Anti-Cancer Drugs 5: 3–9.

Smith, S., (2001). The world according to PARP. Trend s in Biochemical Science 26: 174–179.

Smulson, M.E., Smulson, M.E., Simbulan–Rosenthal, C.M., Boulares, A.H., Yakovlev, A., Stoica, B., Iyer, S., (2000). Roles of poly(ADP–ribosyl)ation and PARP in apoptosis, DNA repair, genomic stability and function of p35 and E2F–1. Advances in Enzyme Regulation 40: 183–215.

Son, Y.O., Kim, J., Lim, J.C., Chung, Y., Chung, G.H., Lee, J.C., (2003). Ripe fruits of *Solanum nigrum* L. inhibits cell growth and induces apoptosis in MCF–7 cells. Food and Chemical Toxicology 41: 1421–1428.

Soule, H.D., Vazquez, J., Long, A., Albert, S., Brennan, M., (1973). "A human cell line from a pleural effusion derived from a breast carcinoma". Journal of the National Cancer Institute 51 (5): 1409–1416.

Spano, J.P., Lagorce, C., Atlan, D., (2005). Impact of EGFR expression on colorectal cancer patient prognosis and survival. Annals of Oncology 16: 102–108.

Sridevi, M., Chandramohan, G., Pugalendi, K.V., (2007). Protective effect of *Solanum surattense* leaf–extract on blood glucose, oxidative stress and hepatic marker enzymes in STZ-diabetic rats. Asian journal of Biochemistry 2(4): 247–255.

Steller, H., (1995). Mechanisms and genes of cellular suicide. Science 267: 1445–1449.

Stewart, R.R., (1972). An Annotated Catalogue of Vascular Plants from West Pakistan and Kashmir. In: Flora of West Pakistan. (Eds.): Nasir, E., Ali, S.I., Karachi University, Karachi, Pakistan pp: 638–645.

Stewart, R.R., (1972). Annotated Catalogue of vascular plants of West Pakistan and Kashmir, Ed. Nasir, E. and Ali, S.I., The Flora of West Pakistan pp: 566.

Strasser, A., Harris, A.W., Bath, M.L., Cory, S., (1990). Novel primitive lymphoid tumours induced in transgenic mice by cooperation between myc and bcl–2. Nature 348(6299): 331–333.

Sundell, E., (1994). Vascular Plants of Arizona, Asclepiadaceae Milkweed Family. Journal of the Arizona–Nevada Academy of Science 27(2): 169–187.

Sundstrom, C., Nilsson, K., (1976). Establishment and characterization of a human histiocytic lymphoma cell line (U–937). International Journal of Cancer 17: 565–577.

Swamy, N., Ugandhar, T., Praveen, M., Rambabu, M., Upender, M., (2005). Induction of streptomycin–resistent plantlets in solanum surattense through in vitro mutagenesis. Plant cell, tissue and organic culture, 80 (2): 201–207.

Symon, D.E., (1981). A revision of genus *Solanum* in Australia. Journal of Adelaide Botanical Gardens 4: 361–367.

Taketani, Y., Oka, T., (1983). Biological action of epidermal growth factor and its Functional receptors in normal mammary epitheial cells. Proceedings of the National Academy of Sciences of the United States of America, 80: 2647–2650.

Tan, X.G., Peng, S.L., Liao, X., Liang, J., Ding, L.S., (2003). A Novel Pregnane Glycoside from *Biondia chinensis*. Chinese Chemical Letters 14(10): 1027 – 1028.

Tanaka, T., Tsukamoto, S., Hayashi, K., (1990). Pregnane glycosides from *Boucerosia aucherian*. Phytochemistry 29: 229–237.

Taya, Y., (1997). Kinases RB and RB–binding proteins: new points of view. Trends Biochemical Science 22(1):14–17.

Tewari, M., Quan, L.T., O'Rourke, K., (1995). Yama/CPP32 beta, a mammalian homolog of CED–3, is a CrmA–inhibitable protease that cleaves the death substrate poly(ADP–ribose) polymerase. Cell 81(5): 801–809.

Thornberry, N., Lazebnik, Y., (1998). Caspases: Enemies Within. Science 281(5381): 1312–1316.

Tiwari, K.P., Gupta, A.P., Tandon, S.P., (1966). Vijnana Parisshad Anusandhan Patrika (Hindi) 9: 87.

Tong, W.M., Yang, Y.G., Cao, W.H., Galendo, D., Frappart, L., Shen, Y., Wang, Z.Q., (2007). Poly(ADP–ribose) polymerase–1 plays a role in suppressing mammary tumourigenesis in mice. Oncogene, 26: 3857–3867.

Trichopoulos, D., Li, F.P., Hunter, D.J., (1996). What causes cancer? Scientific American 275(3): 80.

Troyano, A., Fernandez, P., Sancho, E., Aller, P., (2001). The Role Of Intracellular Oxidation. Journal of Biology and Chemistry 276: 47107–47115.

Troyano, A., Sancho, P., Fernández, C., De-Blas, E., Bernardi, P., Aller, P., (2003). The selection between apoptosis and necrosis is differentially regulated in hydrogen peroxide–treated and glutathione–depleted human promonocytic cells. Cell Death and Differentiation 10: 889–898.

Twentyman, P.R., Luscombe, M., (1987). A study of some variables in a tetrazolium dye (MTT) based assay for cell growth and chemosensitivity. Bristish Journal of Cancer 56(3): 279–285.

Unal–Cevik, I., Kilinc, M., Can, A., Gursoy–Ozdemir, Y., Dalkara, T., (2004). Apoptotic and necrotic death mechanisms are concomitantly activated in the same cell after cerebral ischemia. Stroke 35: 2189–2194.

Vaidyaratnam, P.S.V., (1994). Indian medicinal plants - A compendium of 500 species. Vol. IV. Orient Longman Private Ltd., Hyderabad, India, pp: 164.

Vainsthein, B.K., (1996). Fundamentals of crystals, symmetry and methods of structural crystallography, 2nd Edition. Springer–Verlag New York USA. ISBN–3–540–56558–2.

Van, C., Den, S., Broeck, W., (2002). "Morphological and biochemical aspects of apoptosis, oncosis and necrosis." Anatomia Histologia Embryologia 31(4): 214–23.

Van, D., Heijden, R., Jacobs, D.I., Snoeijer, W., Hallard, D., Verpoorte, R., (2004). The Catharanthus alkaloids: pharmacognosy and biotechnology. Current Medicinal Chemistry 11 (5): 607–628.

Vaux, D.L., Cory, S., Adams, J.M., (1988). Bcl–2 gene promotes haemopoietic cell survival and cooperates with c–myc to immortalize pre–B cells. Nature 335:440–442.

Verma, S., Tabb, M.M., Blumberg, B., (2009). Activation of the steroid and xenobiotic receptor, SXR, induces apoptosis in breast cancer cells. BMC Cancer 9, 3–4.

Vetter, J., (2000). Plant cyanogenic glycosides. Toxicon, 38: 11–36.

Vincent, T., De, V., Hellman, S., Steven, A., (2005). Cancer: principles & practice of oncology. Philadelphia: Lippincott–Raven. ISBN 0–7817–4865–4868.

Virag, L., Szabo, C., (2002). The therapeutic potential of poly(ADP–Ribose) polymerase inhibitors. Pharmacological Reviews 54: 375–429.

Vogelstein, B., Kinzler, K.W., (1998). The genetic basis of cancer. New York: McGraw Hill USA.

Walgren, R.A., Karnaky, K.J., Lindenmayer, G.E., Walle, T., (2000). Efflux of dietary flavonoid quercetin 4-β-glucoside across human intestinal Caco-2 cell monolayers by apical multidrug resistance-associated protein-2a. Journal of Pharmacology and Experimental Therapeutics 294: 830–836.

Walker, P.R., Pandey, S., Sikorska, M., (1995). Degradation Of Chromatin In Apoptotic Cells. Cell Death And Differentiation 2 (2): 97–104.

Wani, M.C., Taylor, H.L., Wall, M.E., Coggon, P., McPhail, A.T., (1971). Plant antitumor agents. VI. The isolation and structure of taxol, a novel antileukemic and antitumor agent from *Taxus brevifolia*. Journal of American Chemical 93: 2325–2327.

Weiss, T.L., Selleck, S.E., Reusch, M., Wintroub, B.U., (1990). Serial subculture and relative transport of human endothelial cells in serum–free, defined conditions In Vitro Cellular and Development Biology 26: 759–768.

Werner, U., Kissel, T., (1996). In–vitro cell culture models of nasal epithelium: a comparative histochemical investigation of their suitability for drug transport studies. Pharmacy Research 13: 978–988.

Williams, S.D., Birch, R., Einhorn, L.H., Irwin, L., Greco, F.A., Loehrer, P.J., (1987). Treatment of disseminated germ–cell tumors with cisplatin, bleomycin, and either vinblastine or etoposide. New england Journal of Medicine 316:1435–1440.

Winckler, J., (1974). Vital staining of lysosomes and other organelles of the rat with neutral red. Progress in Histochemistry and Cytochemistry 6: 1–89.

Worland, P.J., Kaur, G., Stetler–Stevenson, M., Sebers, S., Sartor, O., Sausville, E.A., (1993). Alteration of the phosphorylation state of p32cdc2 kinase by the flavone L86–8275 in breast carcinoma cells. Biochemistry & Pharmacology 46:1831–1836.

Wright, J., Blatner, G.L., Cheson, B.D., (1998). Clinical trials referral resource. Clinical trials of flavopiridol. Oncology 12:1023–1024.

Wu, B., Ootani, A., Iwakiri, R., Sakata, Y., Fujise, T., Amemori, S., Yokoyama, F., Tsunada, S., Fujimoto, K., (2005). T cell deficiency leads to liver carcinogenesis in Azoxymethane–treated rats. Experimental Biology and Medicine 231: 91–98.

Wyllie, A.H., (1992). Apoptosis and the regulation of cell numbers in normal and neoplastic tissue: an overview. Cancer Metastasis Review. 11: 95–103.

Wyllie, A.H., Kerr, J.F., Currie, A.R., (1980). Cell death: the significance of apoptosis. International review of cytology 68: 251–306.

Yamanaka, T., Okamoto, T., Ichinose, Y., Oda, S., Maehara, Y., (2006). Methodological aspects of current problems in target based anticancer drug development. International Journal of Clinical Oncology 11: 167–175.

Ye, Y.P., Sun, H.X., Li, X.Y., (2005). Four new C_{21} steroidal glycosides from the roots of *Stephanotis mucronata* and their immunological activities. Steroids 70 (12): 791–797.

Yousaf, Z., Khan, M.A., Shinwari, Z.K., (2009). A new variety of Solanum surattense burm. from Pakistan. Pakistan Journal of Botany 41(5): 2097–2103.

Yu, S.M., Kim, H.J., Woo, E.R., Park, H.K., (1994). Some sesquiterpenoids and 5–alpha, 8–alpha–epidioxysterols from *Solanum lyratum*. Archives of Pharmaceutical Research 17: 1–4.

Zeiss, C.J., (2003). The apoptosis–necrosis continuum: insights from genetically altered mice. Veterinary Pathology 40: 481–95.

Zeng, Y., Forbes, K.C., Wu, Z., Moreno, S., Piwnica–Worms, H., Enoch, T., (1998). Replication checkpoint requires phosphorylation of the phosphatase Cdc25 by Cds1 or Chk1. Nature 395: 507–510.

Zhang, Jiaqing, (1988). Treatment of 40 cases of epilepsy with Manan Tang, Shanxi. Journal of Traditional Chinese Medicine 4(6): 14.

Zheng, B., Zhou, L., (1991). Status of Yunnan drug banxia and its botanical origin. Journal of Chinese Traditional Drugs 16(3): 135–136.

Zhongzhen, G., Zhang, F., Zhen, H., (2004). Deliciosa root extract anti–tumor effects of the experimental study. Journal of Traditional Chinese Medicine 9 (22): 70–73.

Zhou, D.C., Zittoun, R., Marie, J.P., (1995). Homoharringtonine: an effective new natural product in cancer chemotherapy. Bulletin du Cancer 82: 987–995.

Zhu, H., Fearnhead, H.O., Cohen, G.M., (1995). An ICE like protease is a common mediator of apoptosis induced by diverse stimuli in human monocytic THP–1 cells. FEBS Letters 374: 303–308.

Zimmermann, G.R., Leha, J.R., Keith, C.T., (2007). Multi-target therapeutics: when the whole is greater than the sum of the parts. Drug Discovery Today 12: 34–42.